UNIVERSITY OF SOUTHAMPTON

The investigation of the properties and behaviour of superficial bladder cancer by an *in vitro* explant tumour system, and its use in the response to conventional and novel intravesical cytotoxic agents.

Timothy John Crook BSc(HONS) MBBS FRCS

A thesis submitted in consideration for the degree of

Doctor of Medicine

Professorial Surgical Unit

Faculty of Medicine, Health and Biological Sciences

March 2004

UNIVERSITY OF SOUTHAMPTON

ABSTRACT

FACULTY OF MEDICINE, HEALTH AND BIOLOGICAL SCIENCES
PROFESSORIAL SURGICAL UNIT

Doctor of Medicine

The investigation of the properties and behaviour of superficial bladder cancer by an *in vitro* explant tumour system, and its use in the response to conventional and novel intravesical cytotoxic agents.

Timothy John Crook

Aim: To produce a four-dimensional model of superficial transitional cell carcinoma of the bladder *in vitro* for the assessment of therapeutic agents used as intravesical therapy, and which is consistent and amenable to rationalised experiments.
Introduction: Superficial transitional cell carcinoma of the bladder is more common compared to the invasive type, but has a high probability of recurrence. The various modalities of control include cystoscopic resection or diathermy ablation, as well as intravesical chemotherapeutic adjuncts such as the anthracyclines, Mitomycin C and immunotherapy with BCG.

The laboratory investigation of these intravesical agents is by assays on monolayers of tumour cell lines. However, the cells in this setting are exquisitely sensitive to the effects of cytotoxic agents, and as such do not provide a satisfactory reflection of the *in vivo* results. Animal models are able to give more accurate representations of clinical tumours in certain cancer types. However, there is no reliable animal model of superficial transitional cell carcinoma because of the difficulty in keeping the tumour both non-invasive and consistent in size and tumour grade.
Methods: The MGH-U1 cell line was transfected with green fluorescent protein in its parental and resistant forms. Rat bladder explant cultures were established, and the explants seeded with the transfected cell lines. Visualisation of the resulting colonies was by fluorescent confocal microscopy. Fluorescence intensity and area of the colonies were recorded for each time point. Cytotoxic drugs were applied to the tumour colonies for 1 hour and the effects observed over several days.
Results: The MGH-U1 cell line stably expressed Green Fluorescent Protein, and maintained its characteristics. Tumour colonies were successfully established on the explants, and visualised for up to 11 days after seeding. Mean area of the colony was used as a measure of colony growth. Experiments with cytotoxic agents showed that high concentrations of drugs similar to those in use clinically could be applied to the model, with continuing growth of the colonies.
Conclusion: An *in vitro* model has been developed that allows tumour colonies to be followed over time. High concentrations of drugs may be used in the system allowing better comparison with clinical use.

Table of Contents.

List of Figures 6

Abbreviations. 14

Acknowledgements 16

1. Introduction 18

1.1 Bladder Cancer *18*
1.1.1 The History of Bladder Cancer 18
1.1.2 Epidemiology 22
1.1.3 Aetiology 22
1.1.4 Molecular Biology and Genetics 24
1.1.5 Multi-Drug Resistance 26
1.1.6 Clinical Presentation. 28
1.1.7 Investigation 29
1.1.8 Staging and Grading 30
1.1.9 Natural History 31
1.1.10 Carcinoma *in situ.* 31
1.1.11 Theories of Recurrence. 32
1.1.12 Treatment. 33

1.2 Intravesical Treatment. *36*
1.2.1 General and pharmacokinetic considerations. 36
1.2.2 Intravesical Chemotherapy 38
1.2.3 Intravesical Immunotherapy 43

1.3 Novel chemotherapeutic Agents *45*
1.3.1 Meglumine Gamma Linolenic Acid (MeGLA) 45
1.3.2 Indole-3-Carbinol. 48

1.4 Estramustine *50*

1.5 In Vitro Models of Bladder Cancer. *53*
1.5.1 Immortalised tumour cell lines. 53
1.5.2 Methods for assessing monolayer cultures 55
1.5.3 Spheroids 59
1.5.4 Organ Culture 62

1.6 Animal Models. *65*
1.6.1 Induction of Bladder Tumours 65
1.6.2 Inoculated Bladder Tumours. 68

2. Materials and Methods. 74

2.1 GFP Transfection of MGH-U1 ..... *74*
2.1.1 Tumour Cell Lines 74
2.1.2 Production of Green Fluorescent Protein transfected cell lines 74

2.2 Explant Characteristics. *77*
2.2.1 Explantation. 77
2.2.2 Staining and cytotoxic agents on the skirts and urothelium. 79

2.2.3 Bromodeoxyuridine (BrDU) Staining. 80
2.2.4 Confocal Microscopy. 81
2.2.5 Scanning Electron Microscopy (SEM) 83
2.2.6 Production of MGH-U1 Tumour Explants. 84

2.3 MTT assays using 96-well plates. 85
2.3.1 General principles 85
2.3.2 Cytotoxic Drugs 86

2.4 Explant Drug Experiments. 87
2.4.1 General Principles 87
2.4.2 Controls 89
2.4.3 Classical MDR Drugs 89
2.4.4 Estramustine 89
2.4.5 MeGLA 90
2.4.6 Indole-3-Carbinol 90

3. Results. 92

3.1 GFP Transfection. 92

3.1 GFP Transfection. 93
3.1.1 Antibiotic Selection 93
3.1.2 Fluorescence activated cell sorting 94
3.1.3 Lateral transfer of GFP 97
3.1.4 Stability of transfection 97
3.1.5 Fixation 98
3.1.6 Epirubicin handling by parental and MDR transfectants. 98

3.2 Explant Characteristics. 101
3.2.1 Skirts 101
3.2.2 Urothelial surface 106
3.2.3 Tumour Explants 109
3.2.4 Control Experiments with superglue. 116
3.2.5 Lateral Transfer Insert Experiments with Explants and Tumour Cells. 117
3.2.6 BrDU Staining 119

3.3 MTT Assays 120
3.3.1 Conventional Cytotoxic Agents 120
3.3.2 Estramustine. 122
3.3.3 MeGLA 123
3.3.4 Indole-3-Carbinol 124

3.4 Explant Cytotoxicity Experiments. 126
3.4.1 Control Experiments. 126
3.4.2 Classical MDR Drugs. 132
3.4.3 Non-MDR drug Experiments 156
3.4.4 MeGLA 163
3.4.5 MeGLA in albumin. 172
3.4.6 Indole-3-Carbinol 177

4. Discussion 183

4.1 GFP Transfection. 183

4.2 Explant Characteristics. 184
4.2.1 Skirts. 184
4.2.2 Explant surface 185

4.2.3 Use of Cyanoacrylate Glue 186
4.2.4 Tumour Colonies 186
4.2.5 BrDU Staining 188

4.3 Cytotoxic agents *188*
4.3.1 MTT assays 188
4.3.2 Classical MDR drugs 188
4.3.3 Estramustine 189
4.3.4 MeGLA 190
4.3.5 MeGLA in Albumin 190
4.3.6 Indole-3-Carbinol 190

4.4 Limitations of the Model. *191*

4.5 Advantages of the model. *197*

4.6 Suggestions for future work. *199*

4.7. Conclusions. *200*

Appendix I: Bladder Cancer TNM Staging. **201**

Appendix II: Confocal Microscopy **202**

Appendix II: Fluorescence Activated Cell Sorting. **207**

References **214**

Index **226**

List of Figures.

1.1 Bladder Tumour, Ruysch, 1691

1.2 Bladder Tumour, Thompson, 1884

1.3 Epirubicin, molecular structure.

1.4 Chemical formula of the essential fatty acid γ-Linolenic acid (GLA)

1.5 Chemical structure of Indole-3-Carbinol

1.6 Chemical Structure of Estramustine

2.1 $25cm^2$ flasks, laminar flow hood and incubator

2.2 The Beckton-Dickinson FAC Sorting machine.

2.3 Schematic diagram showing method of obtaining confocal slices through the tumour colony, in transverse section.

3.1.1 FACSort histogram fluorescence analysis of the initial transfection of GFP within MMC–MGH-U1 cells (cell passage number 0) and the stability of the FACSorted transfections over time 24 cell passages (three months growth).

3.1.2 Sub-cellular distribution of GFP within MMC-MGH-U1 cells and drug sensitive cells pre- and post- FACSort detected using the confocal microscope.

3.1.3 Patterns of intracellular Epirubicin (10μg/ml) in GFP transfected cells, detected using the confocal microscope.

3.1.4 Co-localisation of the intracellular distribution of epirubicin and GFP within (a) MGH-U1 and (b) MMC-MGH-U1 cells.

3.2.1 Schematic diagram showing the different elements of the explant model

3.2.2 Combined transmission and FITC filter images of an FDA stained explant urothelial skirt.

3.2.3 FITC filter image of FDA stained explant urothelial skirt

3.2.4 Combined transmission and FITC filter image of explant skirt after 6 hour incubation with BrDU. The green BrDU labelled cells are those in S-phase.

3.2.5 Sequence of images showing the interaction between explant urothelial skirt and tumour cells over several days.

3.2.6 Urothelial surface stained with AO at day 3. Note prominent mucosal folds and viable urothelium.

3.2.7 Urothelial surface stained with acridine orange at day 14. Note less prominent mucosal folds and viable urothelium.

3.2.8 Low power SEM view of urothelial surface at 14 days, X1000

3.2.9 A gallery of confocal images showing a typical explant colony at different levels

3.2.10 A typical explant colony viewed with the confocal microscope

3.2.11 SEM image of the same explant colony as shown in fig 3.2.10

3.2.12 Low power SEM image of another explant colony day 7 after explant establishment, and day 3 after tumour cell seeding.

3.4.13 SEM Close-up view of MGH-U1 cells on urothelial surface. X1500

3.2.14 Reconstructed transverse confocal view of an explant colony

3.2.15 Schematic transverse section derived from the above image

3.2.16 Chart showing the effects of cyanoacrylate glue on MGH-U1 cells at 5 days

3.2.17 Chart showing the results of inserts experiments

3.2.18 BrDU labelled MHG-U1 colony cells in S phase.

3.3.1 The effects of a 1 hour exposure to Epirubicin assessed at 5 days by MTT assay

3.3.2 The effects of a 1 hour exposure to MMC assessed at 5 days by MTT assay

3.3.3 The effects of a 1-hour exposure to MeGLA on parental and resistant MGH-U1 cells assessed at 5 days by MTT assay

3.3.4 The effects of continuous exposure to I-3-C for 5 days on MGH-U1 cells

3.3.5 Graph showing the effects of a 1-hour exposure to I-3-C on MGH-U1 cells assessed at 5 days by MTT assay

3.4.1 Graph showing the progress of an explant colony exposed to PBS for 1 hour after 7 days of colony culture, and followed over 7 days

3.4.2 Graph showing the progress of an explant colony exposed to PBS for 1 hour after 2 days of colony culture, and followed over 8 days

3.4.3 Graph showing the average change in relative area of several parental explant colonies

3.4.4 Graph showing the progress of a resistant explant colony exposed to PBS for 1 hour after 7 days of colony culture, and followed over 6 days

3.4.5 Graph showing the progress of a resistant explant colony exposed to PBS for 1 hour after 2 days of colony culture, and followed over 7 days

3.4.6 Graph showing the average change in relative area of several resistant explant colonies

3.4.7 Chart showing the change in area of parental and resistant MGH-U1 colonies at 1 day and 5 days after exposure to 10μg/ml Epirubicin

3.4.8 Chart showing the change in area of parental and resistant MGH-U1 colonies at 1 day and 5 days after exposure to 100μg/ml Epirubicin

3.4.9 Graph showing the progress of a parental MGH-U1 colony over 5 days after exposure to Epirubicin at 10μg/ml

3.4.10 Graph showing the progress of a parental MGH-U1 colony over 5 days after exposure to Epirubicin at 1μg/ml

3.4.11 Graph showing the progress of an MMC-MGH-U1 colony over 8 days after exposure to Epirubicin 10μg/ml

3.4.12a Graph showing the areas of figs 3.4.9-3.4.11 colonies for comparison

3.4.12b Combined FITC and TRITC filters confocal image at low power of an MMC-MGH-U1 GFP tumour colony (green) 1 day after exposure to Epirubicin at 1mg/ml

3.4.13 Graph showing a parental MGH-U1 colony exposed to 1μg/ml of Epirubicin for 1 hour, over a period of 6 days

3.4.14 Graph showing a parental MGH-U1 colony exposed to 10μg/ml of Epirubicin for 1 hour, over a period of 10 days

3.4.15 Graph showing a parental MGH-U1 colony exposed to 100μg/ml of Epirubicin for 1 hour, over a period of 7 days

3.4.16 Graph showing a parental MGH-U1 colony exposed to 1mg/ml of Epirubicin for 1 hour, over a period of 7 days

3.4.17 Graph showing the areas of each parental MGH-U1 colony exposed to the above concentrations of Epirubicin for 1 hour

3.4.18 Graph showing the average area of the above colonies exposed to Epirubicin

3.4.19 Graph showing an MMC-MGH-U1 colony exposed to 1μg/ml of Epirubicin for 1 hour, over a period of 7 days

3.4.20 Graph showing an MMC-MGH-U1 colony exposed to 10μg/ml of Epirubicin for 1 hour, over a period of 7 days

3.4.21 Graph showing an MMC-MGH-U1 colony exposed to 100μg/ml of Epirubicin for 1 hour, over a period of 7 days

3.4.22 Graph showing an MMC-MGH-U1 colony exposed to 1mg/ml of Epirubicin for 1 hour, over a period of 7 days

3.4.23 Graph showing the areas of each MMC-MGH-U1 colony exposed to the above concentrations of Epirubicin for 1 hour, over 7 and 9 days

3.4.24 Graph showing the average area of MMC-MGH-U1 colonies exposed to Epirubicin for 1 hour, over 9 days

3.4.25 Graph showing the overall mean of all 4 resistant explant colonies exposed to Epirubicin at various concentrations

3.4.26 Confocal Images of the Resistant colony exposed to Epirubicin for 1 hour at 1mg/ml

3.4.27 The effects of a 1 hour exposure to MMC at 10 and 100μg/ml on parental and resistant colonies, 2 days after exposure

3.4.28 The effects of a 1 hour exposure to 100μg/ml MMC at 1 and 3 days

3.4.29 Graph showing the progress of a parental MGH-U1 colony over 11 days after exposure to Mitomycin C at 1μg/ml

3.4.30 Graph showing the progress of a parental MGH-U1 colony over 11 days after exposure to Mitomycin C at 10μg/ml

3.4.31 Graph showing the progress of a parental MGH-U1 colony over 11 days after exposure to Mitomycin C at 100μg/ml

3.4.32 Graph showing the progress of a parental MGH-U1 colony over 11 days after exposure to Mitomycin C at 1mg/ml

3.4.33 Graph showing the areas of each parental MGH-U1 colony exposed to the above concentrations of Mitomycin C for 1 hour

3.4.34 Graph showing the average area of the colonies exposed to the above concentrations of MMC

3.4.35 Graph showing the progress of an MMC-MGH-U1 colony over 11 days after exposure to Mitomycin C at 1 μg/ml

3.4.36 Graph showing the progress of an MMC-MGH-U1 colony over 11 days after exposure to Mitomycin C at 10 μg/ml

3.4.37 Graph showing the progress of an MMC-MGH-U1 colony over 11 days after exposure to Mitomycin C at 100 μg/ml

3.4.38 Graph showing the progress of an MMC-MGHU-1 colony over 11 days after exposure to Mitomycin C at 1 mg/ml

3.4.39 Graph showing the areas of each MMC-MGH-U1 colony exposed to the above concentrations of Mitomycin C for 1 hour

3.4.40a Graph showing the average area of the colonies exposed to the above concentrations of MMC

3.4.40b Confocal images of the MMC-MGH-U1 colony exposed to 1mg/ml of Mitomycin C at days 5,6,9 and 10, showing gradual deterioration of the colony.

3.4.41 Graph showing the progress of a parental MGH-U1 colony over 3 days after exposure to Estramustine at 1 μg/ml

3.4.42 Graph showing the progress of a parental MGH-U1 colony over 3 days after exposure to Estramustine at 10 μg/ml

3.4.43 Graph showing the progress of a parental MGH-U1 colony over 3 days after exposure to Estramustine at 100 μg/ml

3.4.44 Graph showing the progress of a parental MGH-U1 colony over 3 days after exposure to Estramustine at 500 μg/ml

3.4.45 Graph showing the areas of each MGH-U1 colony exposed to the above concentrations of Estramustine for 1 hour

3.4.46 Graph showing the average area of each parental colony exposed to Estramustine over 3 days

3.4.47 Graph showing the progress of an MMC-MGH-U1 colony over 3 days after exposure to Estramustine at 1 μg/ml

3.4.48 Graph showing the progress of an MMC-MGH-U1 colony over 3 days after exposure to Estramustine at 10 μg/ml

3.4.49 Graph showing the progress of an MMC-MGH-U1 colony over 3 days after exposure to Estramustine at 100 μg/ml

3.4.50 Graph showing the progress of an MMC-MGH-U1 colony over 3 days after exposure to Estramustine at 500 μg/ml

3.4.51 Graph showing the areas of each MMC-MGH-U1 colony exposed to the above concentrations of Estramustine for 1 hour

3.4.52 Graph showing the average area of each parental colony exposed to Estramustine over 3 days

3.4.53 Graph showing the areas of each parental MGH-U1 colony exposed to various concentrations of MeGLA for 1 hour, after 7 days of colony culture

3.4.54 Graph showing the areas of each resistant MGH-U1 colony exposed to various concentrations of MeGLA for 1 hour, after 7 days of culture

3.4.55 Graph showing the progress of a parental MGH-U1 colony over 6 days after exposure to MeGLA at 1 μg/ml

3.4.56 Graph showing the progress of a parental MGH-U1 colony over 6 days after exposure to MeGLA at 10 μg/ml

3.4.57 Graph showing the progress of a parental MGH-U1 colony over 6 days after exposure to MeGLA at 100 μg/ml

3.4.58 Graph showing the progress of a parental MGH-U1 colony over 6 days after exposure to MeGLA at 1 mg/ml

3.4.59 Graph showing the progress of the above parental MGH-U1 colonies over 3 days after exposure to 1 hour of MeGLA

3.4.60 Graph showing the average areas of each parental colony exposed to MeGLA over 3 days

3.4.61 Graph showing the progress of an MMC-MGH-U1 colony over 6 days after exposure to MeGLA for 1 hour at 1 μg/ml

3.4.62 Graph showing the progress of an MMC-MGH-U1 colony over 6 days after exposure to MeGLA for 1 hour at 10 μg/ml

3.4.63 Graph showing the progress of an MMC-MGH-U1 colony over 6 days after exposure to MeGLA for 1 hour at 100 μg/ml

3.4.64 Graph showing the progress of an MMC-MGH-U1 colony over 6 days after exposure to MeGLA for 1 hour at 1 mg/ml

3.4.65 Graph showing the average areas of each resistant colony exposed to MeGLA over 3 days

3.4.66 Graph showing the progress of an MMC-MGH-U1 colony over 7 days after exposure to MeGLA in 10%FCS at 1 μg/ml

3.4.67 Graph showing the progress of an MMC-MGH-U1 colony over 6 days after exposure to MeGLA in 10%FCS at 10 μg/ml

3.4.68 Graph showing the progress of an MMC-MGH-U1 colony over 6 days after exposure to MeGLA in 10%FCS at 100 μg/ml

3.4.69 Graph showing the progress of an MMC-MGH-U1 colony over 6 days after exposure to MeGLA in 10%FCS at 500 μg/ml

3.4.70 Graph showing the progress of an MMC-MGH-U1 colony over 12 days after exposure to MeGLA in 10%FCS at 1 mg/ml

3.4.71 Graph showing the progress of the above MMC-MGH-U1 colonies over 7 days after exposure to MeGLA in 10% FCS

3.4.72 Graph showing the average areas of MMC-MGH-U1 colonies exposed to various concentrations of MeGLA in FCS

3.4.73 Graph showing the progress of parental MGH-U1 colonies over 6 days, after exposure to I-3-C at various concentrations

3.4.74 Graph showing the average areas of each parental colony exposed to a different concentration of I-3-C

3.4.75 Graph showing the progress of an MMC-MGH-U1 colony over 9 days after exposure to I-3-C at 10 μg/ml

3.4.76 Graph showing the progress of an MMC-MGH-U1 colony over 9 days after exposure to I-3-C at 25 μg/ml

3.4.77 Graph showing the progress of an MMC-MGH-U1 colony over 9 days after exposure to I-3-C at 50 μg/ml

3.4.78 Graph showing the progress of an MMC-MGH-U1 colony over 9 days after exposure to I-3-C at 100 μg/ml

3.4.79 Graph showing the progress of an MMC –MGH-U1 colony over 9 days after exposure to I-3-C at 1 mg/ml

3.4.80 Graph showing the progress of MMC-MGH-U1 colonies over 9 days, after exposure to I-3-C at various concentrations

3.4.81 Graph showing the mean areas of resistant colonies exposed to various concentrations of I-3-C over 9 days

4.1 Diagram showing possible reason for variability in area measurement of the explant colony

4.2 Diagram showing the schematic progress of an explant colony in transverse section

4.3 Schematic diagram showing the proposed behaviour of a control compared to a colony exposed to a high drug concentration

Abbreviations.

AA	Antibiotic antimycotic solution
AO	Acridine Orange
BCG	Bacille Calmette Guerin
BrDU	Bromodeoxyuridine
CA	Cyanoacrylate ("superglue")
Cis	carcinoma in situ
CMV	Cisplatin, Vinblastine and Methotrexate
DMEM	Dulbecco's modification of Eagle's medium
DMSO	Dimethyl Sulphoxide
DNA	deoxyribonucleic acid
DXT	deep X-ray therapy - syn. radiotherapy
Epi	epirubicin
Epo	epodyl
EDTA	Ethylene Diamine Tetracetic Acid
EORTC	European Organisation for Research and Treatment of Cancer
FACS	Fluorescence Activated Cell Sorter
FBS/FCS	foetal bovine/calf serum
FITC	Fluorescein IsoThioCyanate
FDA	Fluorescein Diacetate
GFP	Green Fluorescent Protein
HEPES	N-2-hydroxyethylpiperazine-N'-2-ethanesulphonic acid
I-3-C	Indole-3-Carbinol
IC50	inhibitory concentration (50%)

IgG	Immunoglobulin G
kDa	kiloDalton
MB	Methylene Blue
MDR	multidrug resistance
MeGLA	Meglumine Gamma Linolenic Acid
MMC	Mitomycin C
MRC	Medical Research Council
MRP	multidrug resistance-related protein
MTT	3-[4,5-dimethylthiazol-2-yl]-2,5-diphenyltetrazolium bromide
PBS	phosphate buffered saline
PGP	P-glycoprotein
Rpm	revolutions per minute
SEM	Scanning Electron Microscopy
MGH-U1	"Massachusetts General Hospital – Urothelial cell line
MMC-MGH-U1	MMC resistant form of MGH-U1 cell line
TCC(B)	Transitional Cell Carcinoma (bladder)
TNM	Tumour Nodes Metastases (classification)
TP	Trypan Blue
TRITC	Tetramethyl Rhodamine IsoThioCyanate
TURBT	Transurethral Resection of Bladder Tumour
WAY	Waymouth's Medium

Acknowledgements.

I am most grateful to Dr Alan Cooper (below). My thanks to him for being there for questions and ideas.

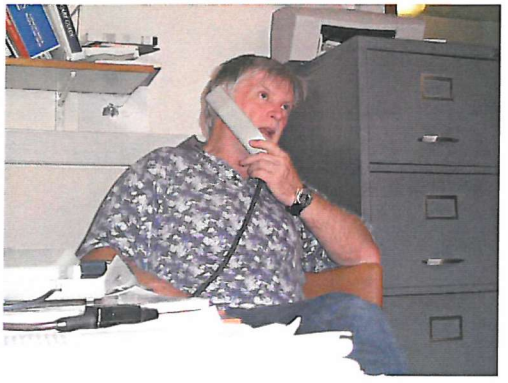

Thanks also to Mr Brian Birch, for his advice, ideas and feedback, Mr John Cumming and Mr Chris Smart for their support and financial facilitation.

I am also grateful to the following for their direct assistance:

Professor Jon Primrose and Mr Colin Johnson FRCS who provided facilities and invaluable feedback during the project, and all the staff in the PSU including Matt, and Jeremy.

Mr Roger Alston in the Biomedical Imaging Unit for his patience and availability for help on the confocal microscope. I am also grateful to Anton and Nick for their help in preparing the explants for scanning electron microscopy.

Dr Ruth French of Tenovus for her assistance with the FACS machine.

Dr Claire Davies for her initial work with GFP transfection and her guiding influence in the laboratory, which helped me throughout the project. Specifically, Claire performed the transfections for the MGH-U1 and MMC-MGH-U1 cell lines, some of which were used in the explant experiments, either from her frozen samples, or my own transfectants.

Dr Rob McCormick for his help with the BrDU staining.

Mr Andrew Jennings FRCS for providing the data for Estramustine MTT assays on GFP transfected cell lines, which had become lost to infection in my own experiments.

I am also most grateful to my examiners, Mr Colin Johnson FRCS, and Dr Janina Chowaniec, for their meticulous attention to detail and suggestions for improvement.

This work was made possible by the support, encouragement and patience of my wife Tina. She at many times became a thesis widow, and single mother, making great sacrifices so that I could complete this work.

The light of her soul shines on this work and all who read it.

Dedication.

To Emily and Charles.

Gloria Filiorum Patres

This thesis is the result of original work carried out by myself (except where stated) in the Professorial Surgical Unit of Southampton University Hospital whilst in registered postgraduate candidature between July 1999 and June 2001.

1. Introduction

1.1 Bladder Cancer

1.1.1 The History of Bladder Cancer

Haematuria has long been recognised as a sinister sign of urinary tract pathology. However, it is only in the last four centuries that there has been a gradual realisation of this symptom's association with tumours of the bladder. Undoubtedly the existence of bladder tumours was known in the 16th Century, but reports are difficult to find. Jean Riolan is said to have reported cases in the latter part of the 1500s. The first well-recorded observations occurred during lithotomy for extraction of bladder stones, when the tumour was coincidentally removed. Covillard and Fabricius Hildanus both removed tumours in this manner in the early 17th Century. Other reports came from post-mortem examinations at this time. The first recorded illustration came in 1691 by Ruysch (Figure 1), which showed a large pedunculated tumour close to the bladder neck, and which he supposed had caused acute retention in the patient, necessitating catheterisation. Many early operators, including Colot, Henckel, and Sandifort probably removed fragments of tumours unintentionally. The first deliberate attempt to remove a bladder neoplasm using forceps introduced along the urethra is thought to have been by Le Cat on a lady(113).

In the 18th Century little further progress occurred with further reports, including those of Warner in 1750 and Desault (1744-1795), who removed a calculus at the same time as two bladder growths. Desault's avulsion was reported by Chopart, an early pioneer in the study of bladder neoplasms around 1800. He noted the difference between papillary and invasive neoplasms, and was also instrumental in realising the significance of haematuria. Other surgeons continued in their observations, including for example Petit in 1820 and Nicod in 1827. The removal of tumours was still by the same

instruments that were used for lithotomy, and examples are recorded by Civiale in 1827, and Leroy d'Etoilles in 1833. Operations in women could be more easily achieved by dilatation or incision of the urethra(113).

Excision of tumours continued in this fashion until the latter half of the 19th Century, when improved anaesthesia allowed previously unthinkable procedures to be performed. In 1874, Billroth, the leading surgeon of his day, carried out the first suprapubic operation for a bladder growth. Another pioneer of bladder tumour study, Sir Henry Thompson, proved well ahead of his time when in the 1870s he described the presence of tumour cells and fragments in the urine, and also used lavage to obtain specimens for histological inspection. His landmark book "Tumours of the Bladder" published in 1884, was the first text to deal specifically with this subject. In it he also laid out his pathological classification based on histological examination, which formed the basis of future systems of categorisation. He also described his digital exploration of the bladder via a perineal urethrotomy, although this operation did not gain wide acceptance. Adding to this formidable contribution was his revolutionary "treatment by injections" using perchloride of iron or nitrate of silver(160). This represents the birth of intravesical therapy, and the method seems to have enjoyed some success according to Thompson, and later his pupil Herbert Herring, who documented a series of 12 cases over 10 years(67;68). Perhaps less well known is the work of David Jones, who also described a bladder treatment that employed an alcohol spray administered via a catheter in 1883(90). However, this treatment modality remained dormant for over half a century while cystoscopic fulguration took over as the dominant option.

Cystoscopy changed the way that bladder cancer was diagnosed and treated. The ability to apply electrocautery to a tumour was such an effective method for dealing with the regularly recurring papillary growths that other methods of therapy almost disappeared. The earliest attempt at some form of internal examination without recourse to cutting is generally attributed to Bozzini's "Lichtleiter", known to have been tested at the Austrian military medical academy in 1805. Subsequent inventions by Segalas, Desormeaux and Grunfeld all suffered with the problem of delivering enough light to the area to be examined. The only available methods were either sunlight, oil or gas illumination; not really a practical solution. Nitze initially found the answer in the form of a white-hot platinum wire mounted at the tip of the instrument. This proved to be the crucial step in the development of the cystoscope, and within a few years the instrument was using an electric bulb, further improving its practicality (Fig.2). Nitze is thus hailed as the father of modern cystoscopy(41).

Whilst endoscopy allowed superficial bladder cancer to be treated adequately, it was still unable to remove invasive cancer. The first partial cystectomy was by Sonnenburg in 1884 and total cystectomy by Bardenheuer in 1887, although Pawlick is credited with the first long-term survivor of total cystectomy a year later. It was also at this time that observation was made of possible aetiology. Harrison suggested Bilharzial infestation as a cause of vesical neoplasm in 1887. Rehn had noted the increased incidence of tumours in those working in the aniline dye industry by 1895.

Figure 1.1 Drawing of bladder tumour by Ruysch 1691.

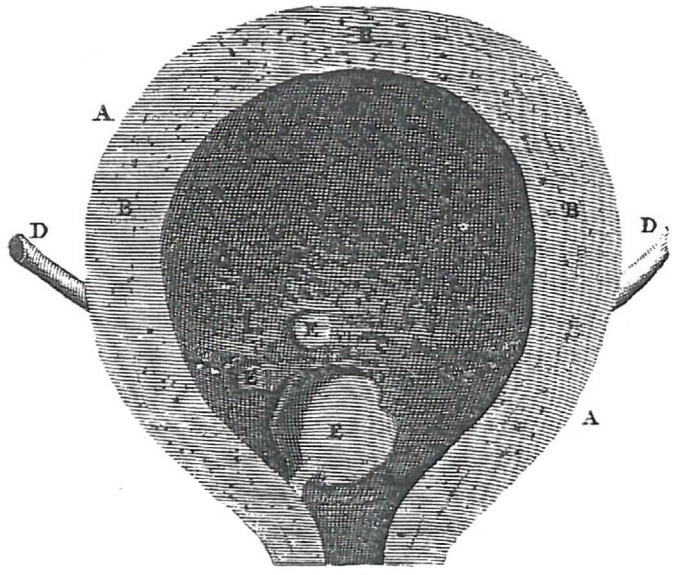

Figure 1.2 Drawing of Bladder Tumour by Sir Henry Thompson 1884

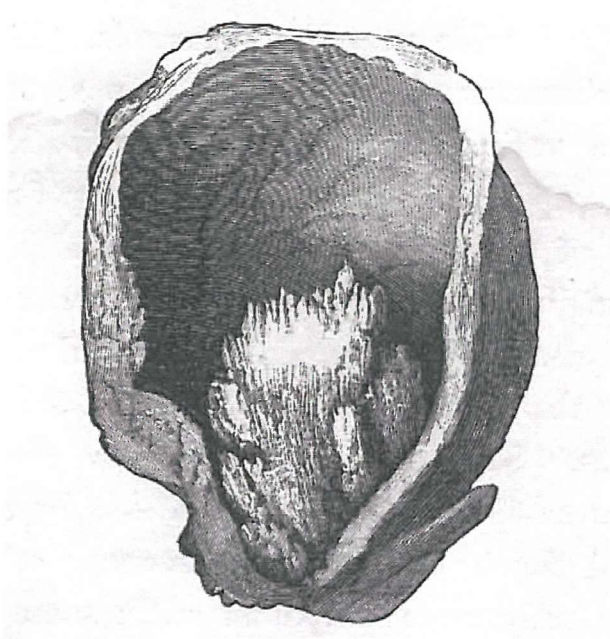

1.1.2 Epidemiology

Bladder cancer accounts for 3.2% of cancer cases worldwide, representing 8.1 million new cases diagnosed each year(35). However, in industrialised nations this percentage rises, due to environmental factors, such as smoking and industrial exposure, although this figure is now also increasing in the developing world. Recent figures reveal that bladder cancer (greater than 90% of which is TCCB) is now the third most common cancer among men and the tenth most common cancer among women within the Wessex region(172). Bladder cancer contributed 8.8% of new cancer registrations and 4.8% of deaths among men during 1990, as opposed to figures of 3% and 2.4% for women respectively in the same year.

In 1990 there were 801 new cases of bladder cancer in Wessex with crude regional incidence rates of 41.4 and 13.4 per 100,000 for men and women respectively. This compares with lower national incidence rates of 32.0 and 12.0 per 100,000 respectively for the same year, increasing to 34.0 and 13.0 for 1993. However, by 1997 national figures had increased to 42.6 for men and 15.6 for women. However, some of this apparent increase may be due to better reporting.

1.1.3 Aetiology.

The bladder acts as a storage organ and it is therefore the site where the majority of transitional cell carcinomas of the urothelial tract occur, because the bladder urothelium may be chronically exposed to carcinogenic chemicals. Over the last 100 years many of these substances have been identified, some of which are contained in tobacco smoke.

The first compounds to be identified were the aromatic amines, including Benzidine, α and β-Naphthylamine and 4-aminobiphenyl(17). These are mainly used in

the chemical dye, rubber and cable industries and also occur in the environments of those working with fuels, gas works and laboratories. Interestingly, aromatic amines may be absorbed via the skin as well as through the gastrointestinal tract and respiratory route. Patients who have worked in one of these industries and developed bladder cancer are entitled to special benefits and in certain cases compensation. The proportion of cases attributable to an occupational cause varies in studies from 8 to 30%, but in more recent series this figure appears to be falling.

The majority of cancers are probably attributable to a much more widespread and uncontrolled exposure to the range of carcinogens found in cigarette smoke. The association was first noted in 1956, with 30% and 50% of female and male cancers respectively attributed to smoking(98). As with other smoking-related cancers the relative risk increases with the more cigarettes smoked, and degree of inhalation(74). Compensation claims for smoking have been successful in the United States(91), and procedures for lawsuits in UK patients are in progress(38).

There are numerous other reports of other carcinogens including artificial sweeteners, analgesics, Tryptophan metabolites, Cyclophosphamide and Quercetin, found in bracken fern. Cyclamates and saccharin were shown to be mutagenic *in vitro* and in animal experiments, but only in quantities several hundred fold larger than would be found in normal human consumption. In 1974 a weak association was suggested between saccharin ingestion and bladder cancer(7), however the risk was minimal and other confounding factors such as smoking made the link difficult to validate. Similarly Hoover and Strasser in 1980 suggested that there might be some bladder cancer sub-group associations with artificial sweeteners, but no overall significant association(75).

1.1.4 Molecular Biology and Genetics.

The exact events leading to transformation of normal urothelium into transitional cell carcinoma (TCC) are unknown. They are, however, likely to involve the activation of oncogenes and the inactivation or loss of cancer suppressor genes.

Oncogenes contribute to the malignant phenotype in a dominant fashion, either by overexpression of a gene product or expression of a protein product with altered function. Overexpression of a normal product is the most common mechanism, achieved genetically by either gene amplification or chromosome translocation to an area downstream of a powerful promoter(93). Expression of a mutant protein product is a less common mechanism of action, exemplified in transitional cell carcinoma by the ras gene family member *H-ras*, which is mutated in 6 to 44% of TCC(93). Indeed the *H-ras* gene was the first human oncogene identified in the EJ cell line(120), other wise known as MGH-U1, as used in this work.

ErbB2, (chromosome 17q21) which encodes a transmembrane receptor similar to the epidermal growth factor receptor is over expressed in some TCC, especially those of high grade and stage. The mechanism of overexpression appears to be high level amplification(76;134). Additionally, the *myc* oncogene (chromosome 8q) has been associated with increased recurrence or progression of superficial bladder tumours(102).

The proto-oncogene *CCND1* (chromosome 11q13) is amplified and over expressed in some cases of TCC. The product of *CCND1* is cyclin D1, which is, in turn involved in cell cycle progression via the retinoblastoma (Rb) pathway. Overexpression of cyclin D1 may be associated with early tumour recurrence(142). Other studies have identified DNA over-representation in areas 1q, 3p, 3q, 5p, 6p, and 10p and gene amplification at 1q22-24, 3p24-25, 6p22, 8p12, 8q21-22, 10p12-14, 11q13, 12q15-21, 13q31-33, Xp11-

12 and Xq21-22(93). Further oncogenes associated with these areas are likely to be discovered as knowledge of the human genome expands.

Tumour suppressor genes are genes whose functional inactivation contributes to cancer development. It is generally thought that both alleles need to be deleted or mutated for the phenotypic effect to develop, normally achieved by loss of heterozygosity. Allelic loss of genes on 9p21 occurs in over 50% of bladder cancers, and appears to be an early event, occurring in all grades of bladder cancer(16). The gene losses at 9p21 focus on the *INK4 A/ARF* and *INK4B* loci. This region of the gene encodes three proteins (p16, p14ARF and p15), all negative cell cycle regulators(93). In contrast, deletion of material from the short arms of chromosomes 11 and 17 is more common in high-grade tumours, suggesting that loss of suppressor genes in these locations is associated with tumour progression. Alterations in the p53 and Rb proteins produced by the 17p13 *p53* and 13q14 *Rb* tumour suppressor genes, occur in approximately 50% and approximately 33% of bladder cancers respectively, and are associated with later stage, higher grade disease(59). *p53* and *Rb* alterations are also known to occur in early stage bladder carcinoma *in situ* where they are thought to represent a poor prognosis for tumour progression(134). Other areas of common genetic deletion in transitional cell carcinoma include chromosomes 3p, 4p, 4q, 8p, 11p, 11q, 14q and 18q(59). It is quite likely that further tumour suppressor genes will be discovered in these areas in the near future. Loss of tumour suppressor genes results in a more aggressive phenotype and hence leads to tumour progression.

Changes in the extracellular matrix have been implicated in TCC. High levels of matrix metallo-proteinases have been associated with cancer specific deaths in patients

with invasive TCC. These proteinases are capable of degrading the extracellular matrix and enhancing invasive disease(59). Similarly, microvessel density as a measure of tumour angiogenesis has been found to predict for both tumour recurrence and overall survival(32). It is thought that this is because microvessel density correlates with invasive potential, and therefore malignant potential.

1.1.5 Multi-Drug Resistance

Resistance of tumour cells to multiple chemotherapeutic agents is a major obstacle to the treatment of several types of human cancer, including bladder, and has been associated with treatment failure(53).

One mechanism of MDR is associated with the overexpression of the *MDR-1* product P-glycoprotein (PGP). This is a 170,000 MW membrane glycoprotein capable of the cellular efflux of a variety of anticancer agents, by an ATP-dependent pathway. Thus the mechanism of resistance in those cells that over express PGP is due to decreased cellular and in particular nuclear accumulation of drug resulting in reduced efficacy. There are certain recognised drugs, which fall into the group with so-called classical MDR due to the PGP mechanism. These are the Vinca alkaloids such as Vinblastine and Vincristine, the anthracyclines such as Doxorubicin and Epirubicin, Taxol, Colchicine, Actinomycin D, and Mitomycin C(40;55;56). The physiological role of PGP is probably in the cellular transport of endogenous substances, as it is found in liver, kidney, adrenal cortex and secretory epithelia. It may also protect normal tissues from cytotoxic chemicals. Other mechanisms of MDR include overexpression of glutathione S-transferases, mutation or loss of tumour suppressor p53 or mutation of topoisomerase II(14).

There are several other MDR mediating mechanisms. The Multidrug Resistance Protein (MRP) is a phosphoglycoprotein, which was first isolated from a small cell lung cancer cell line(21). The molecule has structural features associated with PGP and is associated with reduced intracellular drug accumulation. MRP mRNA has been identified in a large number of normal tissues and the protein has been found in bladder tumours with no prior exposure to cytotoxic agents(19).

The Lung Resistance-related Protein (LRP) is a major component of intra-cytoplasmic structures known as vaults and is also known as Major Vault Protein (MVP). It is widely found in MDR cell lines not expressing PGP and seems to be up regulated early in drug resistance(141). In a panel of 61 human cancer cell lines LRP and MRP were expressed in 78% and 87% respectively, as opposed to 24% expressing P-gp, suggesting that LRP might have a greater value as an MDR marker.

The DNA-repair enzyme *topoisomerase II* has also been implicated in MDR in the absence of other MDR mechanisms such as PGP. Its clinical significance though is uncertain. The Glutathione S transferases are cytosolic enzymes which are able to detoxify a wide range of foreign molecules by conjugation with glutathione and subsequent free radical production. These enzymes are also thought to be necessary for the export of drugs via the MRP(111).

There are several compounds that are able to inhibit these MDR mediated efflux of cytotoxic agents, thus enhancing the efficacy of their action. These include calcium channel blockers such as Verapamil(163), Calmodulin inhibitors such as the phenothiazines(163), indole alkaloids such as Reserpine(81), and Cyclosporins(165). The properties and efficacy of these drugs have been established *in vitro* but

unfortunately they have dose-limiting toxicity when used *in vivo*. For example, sensitive bladder cancer MGH-U1 cells take up Epirubicin into the nucleus where it can be detected by intrinsic fluorescence, whereas "resistant" cells localize the drug to the cytoplasm. This phenomenon may be reversed by the addition of Verapamil to the cultures(36).

1.1.6 Clinical Presentation.

The large majority of bladder cancers (75-90%) present with haematuria, either macroscopic or microscopic. Other presenting symptoms include loin or pelvic pain, or storage bladder symptoms such as frequency, nocturia, urgency of voiding, or dysuria. These irritable symptoms are sometimes associated with carcinoma-in-situ, but of course need to be differentiated from the symptoms of bladder outflow obstruction. A recent study indeed suggested there was a positive cost-benefit from performing urine cytology in patients with these symptoms (124). The pick-up rate for bladder tumours presenting in this way was 0.3%. Sometimes, transitional cell carcinoma may present with symptoms of local spread, renal failure or distant metastases in the form of bone pain, weight loss, malaise, and cachexia. Physical findings on examination are usually normal, although locally advanced tumours may present as a palpable mass. Urine dipstick testing will often reveal haematuria in the presence of transitional cell carcinoma with a sensitivity of 90%.

1.1.7 Investigation.

Haematuria, the commonest presentation of bladder cancer, has traditionally been investigated by intravenous contrast studies of the kidneys, ureters and bladder, intravenous urography (IVU) and cystoscopy. IVU is gradually being replaced by ultrasound scanning, although the precise role of each is still under discussion(169). Urinalysis using reactive sticks is almost considered a part of the examination, but nevertheless represents an important investigation. However, there is a high false positive rate, and so formal microscopy is still useful as an adjunct to this test. The role of cytology is also controversial, and is usually of most use in those cases where CIS or upper tract TCC is suspected. Computerised tomography (CT) scanning is generally reserved for further definition of renal or ureteric pathology or for staging of transitional cell carcinomas suspected to be locally advanced. Most patients with haematuria are found to have normal kidneys and ureters on radiological investigation and will then have their bladders examined at cystoscopy. Traditionally, rigid cystoscopy under general anaesthesia has been carried out. This has now been largely supplanted by flexible cystoscopy carried out with slim, fibre optic telescopes. These telescopes can be comfortably tolerated without the need for general anaesthesia. Cystoscopy is carried out in addition to radiological imaging, as IVU and ultrasound are not sufficiently sensitive at detecting small bladder carcinomas or CIS. Discovery of a transitional cell carcinoma necessitates careful resection of the tumour using a large, rigid cystoscope and resecting diathermy loop. The material removed can then be carefully examined histologically to determine the grade and stage (*qv*). The patient should have a bimanual examination at the time to determine if there is a residual mass post resection suggestive of locally advanced disease.

1.1.8 Staging and Grading.

A number of staging systems have been used historically in the treatment of bladder cancer. These have been replaced by a recently updated system jointly developed by the International Union Against cancer (UICC) and the American Joint Committee on Cancer Staging (AJC). The system is also known as the TNM system(65). The TNM system allocates the T stage depending upon the degree of local invasion, the N stage depending upon nodal invasion and the M stage depending upon metastatic spread. These stages are defined in appendix I.

Epithelium confined transitional cell carcinomas are classified as Ta and flat carcinoma in situ as Tis. Tumours invading subepithelial connective tissue are called T1 and muscle invasive tumours range from T2a to T4b.

Initial evaluation and staging is carried out by a combination of clinical examination and imaging. Tumours resected endoscopically or excised at open surgery will subsequently be submitted to pathological staging, and such tumour stages then receive the prefix pT. Muscle invasive tumours treated with radiotherapy or systemic chemotherapy do not receive a definitive pathological T stage performed on a whole bladder specimen. This has implications when comparing the above modalities.

There is no uniformly accepted grading system for bladder cancer, although most systems use three or four categories corresponding to well differentiated, moderately differentiated and poorly or undifferentiated(106). A strong correlation exists between tumour grade and tumour stage. Most well differentiated tumours are superficial, whilst most poorly differentiated tumours are muscle invasive. Stage for stage, grade can be shown to correlate with prognosis(106). Additionally, there is evidence to suggest that low grade tumours and high grade tumours have fundamentally different origins with the

former losing one or more tumour suppressor genes on chromosome 9 and the latter having p53 abnormalities as early initiating events(154).

1.1.9 Natural History.

The development of rational treatments for bladder cancer depends on an understanding of the natural history of the untreated disease. Population studies have shown that 55% to 60% of all newly diagnosed transitional cell carcinomas are well or moderately differentiated (G1 or G2) and non-invasive or "superficially" invasive Ta or T1(107). Many authors have demonstrated that the majority of such patients will go on to develop recurrences, the quoted figures varying from 60 to 90% depending on the study and its design. Usually, recurrences of such well differentiated and superficial TCC continue to reflect the characteristics of the original tumour throughout the patient's subsequent life(126). However, 16%-25% will recur with higher grade tumours. Approximately 10% of patients with superficial papillary tumours will subsequently develop muscle invasive or metastatic tumour(100), although this is a rare event in patients with well differentiated, Ta tumours(126). A characteristic of transitional cell carcinoma is that late recurrence and invasion may occur after many years of recurrence-free follow up, sometimes as many as 15 years later(159).

1.1.10 Carcinoma *in situ.*

Histologically, carcinoma in situ (CIS) is composed of poorly differentiated transitional cell carcinoma confined to the urothelium. CIS may be asymptomatic or may produce severe irritative bladder symptoms. It is rarely seen in the presence of low grade TCC but is present in up to 25% of patients with high-grade superficial tumours and in up to 75% of patients with high-grade muscle invasive TCC(127). Cytogenetic, molecular and immunological studies have shown high rates of p53 deletion or mutation in

CIS(106). These findings suggest that CIS is an important precursor lesion in the development of muscle invasive disease and suggest that CIS has little or no role as a precursor of low-grade tumours, as p53 abnormalities are seldom found in such lesions(154).

1.1.11 Theories of Recurrence.

Bladder cancer shows a tendency towards late recurrence and also recurrence at different sites within the urothelium. This pattern of disease suggests a polyclonal aetiology for bladder cancer(126). Late recurrence is at odds with the theory that recurrences represent clonal seeding of the original tumour, especially as even low grade TCC appears to be relatively fast growing. Additionally, immunohistochemical and immunocytochemical studies have confirmed that normal appearing bladder mucosa, biopsied at sites distant from tumour, also exhibits altered expression of tumour markers such as G-actin and the EGF receptor(105;130).

Evidence favouring the theory of tumour seeding includes studies using gene sequencing analysis(77;143). One paper demonstrated that multiple tumours from female patients all have the same X chromosome inactivated. Also, the same chromosome 9 allele was lost in each case. However, the status of 18q and 17p differed in different tumours in the same individual, suggesting a clonal aetiology for at least some simultaneous or sequential bladder cancers. A recent study of synchronous and metanchronous tumours suggested that most multifocal tumours are derived from the same progenitor cell. Chromosome 9 alterations showed the least discordance, with some differences in 11p, 17p, 4p, 4q and 8p suggesting independent evolution of different cells from the initial chromosome 9-altered population(157).

1.1.12 Treatment.

The histological grade and stage of the initial bladder tumour resection dictates future management. Patients with superficial (pTa, pT1) disease have regular cystoscopic follow up with additional intravesical chemotherapy or immunotherapy given for more aggressive superficial tumours. Staging investigations such as CT scanning and isotope bone scans are not indicated, as it is rare for metastases to be associated with superficial disease(85). Radiotherapy is not appropriate for superficial bladder cancers. It has considerable morbidity, does not prevent the occurrence of new tumours(52) and has been found to be relatively ineffective(106). Radical cystectomy in superficial TCC is rarely required. It is reserved either for patients with extensive multifocal tumours which are not controlled by trans-urethral resection alone, or progressive high-grade (G3) tumours unresponsive to intravesical treatments, which have a high rate of progression to invasive disease (>40%).

Muscle invasive tumours are generally unsuitable for endoscopic or intravesical treatment. One difficulty in managing muscle invasive tumours is in differentiating between patients with tumours suitable for radical, local and potentially curative treatment (pT2-pT4a) and those locally advanced or metastatic tumours unsuitable for radical treatment (pT4b, N+, or M1). CT scanning is used to try and determine the extent of local spread and curative potential under such circumstances. Unfortunately, CT is only capable of detecting gross extravesical tumour extension, considerably enlarged lymph nodes and liver metastases of 2 cms or more(106) with an estimated overall accuracy of between 40% and 85%(16). Post resection artefact results in further inaccuracies in staging. Magnetic resonance imaging (MRI) has few advantages over CT scanning and is not routinely used. Chest X ray is used to screen for metastatic lung

deposits although metastases less than 1 cm are not detectable by plain X ray(106). Bone scans are seldom diagnostic of skeletal metastases in the presence of a normal serum alkaline phosphatase but are sometimes performed as a "baseline" investigation for future comparison(106). Not surprisingly, there are considerable errors in the clinical staging of muscle invasive disease. These errors appear to be greatest in high and intermediate grade tumours with 33% of such carcinomas overstaged and 10% understaged(178).

Muscle invasive tumours with curative potential (pT2-pT4a, N0 M0) are suitable for either radical radiotherapy or radical cystectomy. Results of radical radiotherapy suggest 5 year survival rates of about 40% for stage T2, 35% for stage T3a, and 20% for stage T3b and T4(11;52;54;58;83). Additionally, 50-70% 5-year bladder recurrence rates were described by these studies. Approximately 70% of patients develop self-limiting complications during radiation therapy including urinary urgency, frequency and diarrhoea. Severe, persistent complications develop in 10%(106).

Radical cystectomy remains the most effective treatment for invasive TCC of the bladder. 5-year survival rates of 65-80% have been reported for pT2-pT3a disease(48;108;119;180). Stage pT3b has 5-year survival rates of 37-61%(108;144). These figures compared with radical radiotherapy may in part reflect the fact that current imaging techniques understage tumours. Hence, many of the tumours treated with radiotherapy may be of a rather higher stage than indicated by their investigations. However, even where T stages are used for patients treated by radical cystectomy, the results of cystectomy remain superior to those of radiotherapy(108).

Local pelvic recurrence rates are surprisingly low following radical cystectomy. Even T3b and T4 tumours have local recurrence rates of only 12%. This implies that

many patients dying following cystectomy do so from occult metastatic disease and has stimulated interest in both adjuvant and neo-adjuvant chemotherapy in this situation. Despite numerous trials, a recent overview and meta-analysis concluded that there was insufficient information to determine whether neoadjuvant chemotherapy improves survival in such patients(51). A recent case-control study of neoadjuvant PMV chemotherapy using Carboplatin, Methotrexate and Vinblastine in addition to cystectomy in T2 or greater bladder cancer has shown a statistically significant improvement in the treated arm after median follow up of 32.2 months. The authors acknowledge the need for longer follow up to determine if such promising results can be sustained(1).

Patients with nodal or metastatic disease (N+ or M1) are considered unsuitable for radical local treatment, although palliative surgery or radiotherapy may be considered for troublesome or life threatening local complications such as severe pain or haemorrhage. Distant spread of TCC has an extremely poor prognosis with negligible five-year survival rates. Single agent chemotherapy induces subjective tumour regression in 20%-30% of patients but most responses are only partial regressions with a duration of about 6 months(151) MVAC (methotrexate, vinblastine, doxorubicin and *cis*-platin) chemotherapy has objective response rates of 57%-70% and complete responses in 30%-50% of patients. However, survival at two years is only about 20% and long-term survival remains uncommon(106).

1.2 Intravesical Treatment.

1.2.1 General and pharmacokinetic considerations.

The guiding principle in this form of drug delivery as in other methods of regional chemotherapy is to optimise drug delivery to the tumour and its surroundings, whilst minimising systemic exposure. In patients with superficial tumours benefits include a high concentration of drug at the tumour site, the ability to manipulate the exposure time, reduced systemic availability leading to minimal toxicity, reduction in the chances of tumour implantation following TURBT, and a cytotoxic effect on any residual carcinoma or carcinoma *in situ*. Theoretically the need for cystectomy might be reduced.

Drug absorption into the mucosa is clearly important for cytotoxic effect, but the systemic absorption of any drug from the bladder is also unwanted. Absorption is determined by the lipophilicity of the drug and the integrity of the bladder wall. Therefore, drugs with high lipophilicity will penetrate the urothelium, but be readily absorbed, and drugs that do not penetrate will have low bladder wall concentrations. The major factors that influence rate of absorption are molecular weight, alterations in the urothelial surface, the pH of the solution, drug concentration and duration of exposure(71). It has been suggested that the optimum criteria are negligible ionisation at pH 6-7, a molecular weight (MW) greater than 200 and a partition coefficient of either –0.4 to –0.2 or –7.5 to –8.0. MW is important because, it is thought significant absorption through the bladder mucosa occurs at less than 200. For example, intravesical Thiotepa with a MW of 189 carries a greater risk of systemic absorption and myelosuppressive toxicity, than the other intravesical agents with higher MWs(71). Computer models predict that drug absorption into the systemic circulation increases the area under the plasma concentration-time curve (AUC), mean residence time (MRT) and elimination

half-life. Conversely, absorption decreases renal clearance and total body clearance. Absorption also decreases the amount of drug excreted in the urine and the fraction of unchanged drug excreted(28).

Transfer of drug through the bladder wall occurs in two stages, first it must cross the 200μm unperfused urothelium and then into the capillary perfused tissue layer, 200 to 4000μm thick. The first stage is governed by Fick's first law of diffusion, whereas the second stage is described by a more complex distribution equation which considers the diffusion of drug through the tissue that is dependent on the concentration gradient; and capillary removal of drug, dependent on the difference between tissue and perfusing blood. The following equations describe these two stages:

1) $C_{depth} = C_u - [(C_u - C_{200})/200] \times depth$

2) $C_{depth} = (C_{200} - C_b) \times [e^{-(0.693/W½) \times (depth-200)}] + C_b$

Where C_{depth} is concentration at tissue depth, C_u is concentration of un-ionised drug in urine, C_{200} is concentration at the interface between the urothelium and deep tissues, C_b is the averaged free blood concentration and W½ is the thickness of tissue over which the drug concentration declines by 50%.

In the urothelium the decline in C_{depth} is a linear relationship and depends on drug partition and diffusion, concentration gradient across the urothelium and C_u. In the perfused tissues C_{depth} declines exponentially from C_{200} to C_b. A proportion of the drug is removed by the capillary blood flow equivalent to $(C_{depth} - C_b)$. At increasing depths beyond W½, C_{depth} approaches C_b. Tissue concentration-depth profiles for individual drugs can be generated from W½, C_u/C_{200} and C_u/C_b, but C_u is different for each patient and changes with time(175).

Animal models have been used to investigate absorption from the bladder starting with the experiment by d'Etchepare in 1824 who instilled a dilute alcoholic extract of Strychnine into a dog's bladder, which then died 20 minutes later. Further 19th century and early 20th century studies showed that certain substances could be absorbed from the bladder of various mammals, although it was not until later that the significance of molecular weight was realised. More recently studies have suggested that substances absorbed from the bladder and then renally excreted may subsequently be reabsorbed. This suggests that the bladder is not always a simple non-return storage compartment(71).

1.2.2 Intravesical Chemotherapy.

The early attempts by Thompson, Jones, and Herring in the late 19th Century demonstrated that this was a route of therapy worth further investigation. However, after the introduction of electrocautery via the cystoscope by Beer, this simple method was laid aside for many years. The modern era began in 1961 when Jones and Swinney published their landmark paper on the use of intravesical Thiotepa(89). Thiotepa is an alkylating agent related to the nitrogen mustards, and has a molecular weight of 189. This is an important consideration when choosing an agent for intravesical therapy. It has long been established that the threshold for absorption of intravesical drugs is 200. Thus Thiotepa is absorbed and leads to dose-limiting side effects the most important of which is agranulocytosis. It is for this reason that Thiotepa has now been abandoned in favour of those drugs that have a higher molecular weight and hence minimal absorption.

Epodyl.

The alkylating agent, triethylene glycodiglycerol ether, otherwise known as Ethoglucid or Epodyl has a molecular weight of 250 was developed during the 1970's because of its lower systemic absorption and myelosuppression risk. 66% of patients responded completely or partially in one therapeutic trial(116); in another 30% patients demonstrated a complete response while 32% were failures from the outset(136). Late recurrence was found predominantly in patients whose tumours showed only a partial response during earlier treatment(116). Its association with severe chemical cystitis has limited the widespread use of this agent, and it has now fallen out of favour.

Anthracyclines.

In the 1950s, Farmitalia Research Laboratories of Milan initiated a program to study anticancer compounds derived from soil microbes(171). In 1957, a colony of *Streptomyces* was isolated from a soil sample collected at the Castel del Monte, near to the city of Andria in south eastern Italy. This organism produced an antibiotic that was named daunomycin, after a pre-Roman tribe in southeastern Italy called the Daunii. At the same time, Dubost and colleagues at the French company Rhóne Poulenc isolated an antitumour compound called Rubidomycin. Clinical testing was initiated in both countries with antitumour responses seen in a variety of tumours(171). Subsequent tests showed that Rubidomycin and daunomycin were the same compound and the name was subsequently changed to Daunorubicin.

The Farmitalia group began inducing mutation in the *Streptomyces* species. One variant produced a blue green-colour in its aerial mycelium and was named *caesius* after this colour. A new compound, 14-hydroxydaunomycin, was produced by this subspecies

and named Doxorubicin after the Adriatic sea, close to where the original soil sample was collected.

Doxorubicin was quickly introduced into clinical practice in the 1960s and rapidly proved itself as a potent antitumour agent, rapidly becoming popular in the treatment of haematological and solid tumours(12). It was the efficacy of doxorubicin in the treatment of solid tumours that differentiated this agent from Daunorubicin and stimulated a programme of development, leading ultimately to the development of the doxorubicin analogues epirubicin and idarubicin. Epirubicin was synthesised early in this programme and was soon found to have many of the properties of doxorubicin. Doxorubicin consists of an amino sugar, daunosamine, linked through a glycosidic bond to the C7 of a tetracyclic aglycone, doxorubicinone. In doxorubicin the OH group is in the axial configuration whilst in epirubicin the OH group is in the equatorial configuration. Idarubicin, like doxorubicin, incorporates daunosamine as the amino sugar, but in this case it is linked to a different aglycone, 4-demethoxy- doxorubicinone. Epirubicin differs from doxorubicin only in the configuration at the 4'-C atom, the amino sugar in this case being called acosamine (Fig.1.3).

The cytotoxic effects of Epirubicin appear to result from its ability to from a complex with DNA by interstrand intercalation, thus inhibiting replication and transcription. This action may be attributable, at least in part, to its interference with topoisomerase-DNA 'cleavable complex' and helicase activity. Reduction of anthracyclines to semiquinone free radicals may cause damage to DNA, cell membrane lipids and mitochondria(122). Its first use in intravesical chemotherapy was reported by Matsumura in 1986.

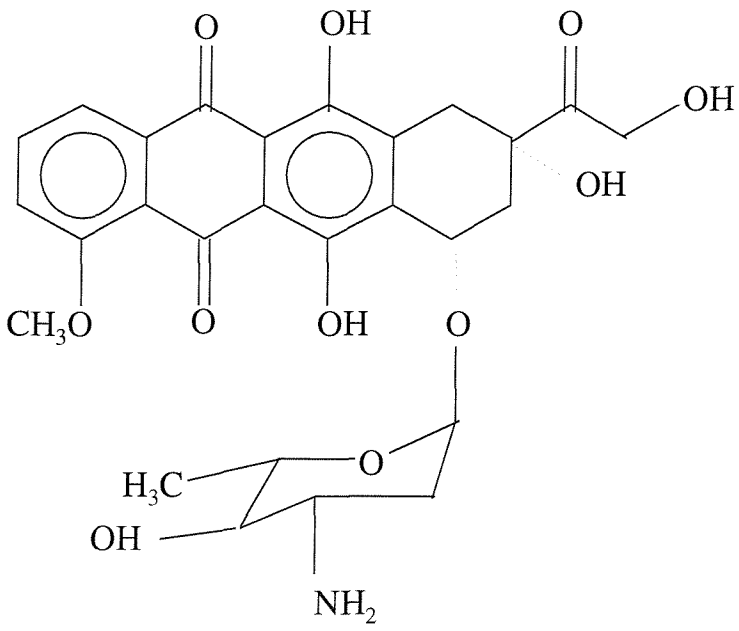

Fig.1.3 Epirubicin, molecular structure. (8S, 10S)-10-(3-Amino-2,3,6-trideoxy-α-L-arabino-hexopyranosyloxy)-8-glycolyl-7,8,9,10-tetrahydro-6,8,11-trihydroxy-1-methoxynaphthacene-5,12-dione hydrochloride. Molecular weight 580.

Mitomycin C

Mitomycin C is a highly water-soluble antitumour antibiotic with a molecular weight of 334 produced by the actinomycete *Streptomyces caespitosus,* and first described in Japan in 1960. It consists of a quinone ring linked to an indole group, with two side groups, a methoxy formamide side chain and an arizidine ring.

It acts via a metabolite produced following an NADPH-dependent intracellular bio-reductive alkylation reaction. During the course of this reaction the molecule loses the methoxy group and reduction of the quinone group occurs, followed by activation of the resulting metabolites(82).

The active moiety inhibits DNA synthesis, cross-links DNA in a manner proportional to the guanine/cytosine content, and exhibits highly reactive carbamate and

aziridine groups. Superoxide and hydroxyl radicals are also generated with resulting cytotoxic enhancement(99). Evidence also exists that single strand DNA breaks are induced by alkylation at the O-6 residue of guanine. These actions are more marked in the late G1 and early S phases of the cell cycle, but its effects are, overall, cell cycle non-specific(99). It is interesting to note that these same actions are also characteristics of carcinogens, yet there is no evidence that use of intravesical MMC enhances or accelerates bladder tumour recurrence or progression.

It was first used in the intravesical chemotherapy of bladder cancer in 1980 (31). Wajsman studied 18 patients receiving 40mg of Mitomycin C intravesically, and found only minimal plasma concentrations after serial measurements over the 2.5 hours following the initiation of treatment. No myelosuppression was noted(168). Other studies have addressed the issue of myelosuppression resulting from Mitomycin C, but few have found any significant instances(161).

Although intravesical Mitomycin C appears to cause little or no bone marrow toxicity, it has been implicated in the development of a rash on the palms of the hands, and sometimes on the face and feet, occasionally causing desquamation. Opinions vary as to the pathogenesis of this phenomenon. In one study a palmar rash and desquamation was noted in 4 out of 29 patients treated with 40mg of Mitomycin C for eight weeks and, after skin tests, attributed these signs to contact dermatitis following inadvertent contact with the drug(117). However, it is possible that this response is a delayed hypersensitivity response. In four patients studied, these problems only occurred after the second administration of the drug, and the authors also demonstrated that patients who

had received intravesical Mitomycin C had strongly positive cutaneous patch tests when compared with controls, compatible with the diagnosis of delayed hypersensitivity(22).

Mitomycin C can also cause local complications. Chemical cystitis has been widely recorded in association with intravesical Mitomycin C. The rates quoted in the literature vary from 6% to 41%, and the symptoms can be severe enough to necessitate discontinuation of the treatment(161).

Mitomycin C has also been implicated in the development of a reduced bladder capacity. A study in 1990 reported that 17 out of 75 patients developed bladder capacities of less than 200ml, with five having a capacity of less than 100ml. However, these patients underwent frequent treatments over periods of up to two years(39).

1.2.3 Intravesical Immunotherapy.

Although interest in immunotherapy for superficial bladder cancer has only attracted mainstream interest over the last ten to twenty years, non specific immunotherapy was being employed as long ago as 1893, when Coley attempted the inoculation of erysipelas into malignant tumours. Bacillus Calmette & Guerin (BCG) is an attenuated strain of *Mycobacterium* first described by its discoverers in the early 20th Century and first used as a vaccine in 1921. However, despite the antineoplastic effect of tuberculous infection reported by Pearl in 1929, it was not until 1969 that Mathe reported the use of BCG as an adjuvant treatment in acute lymphoblastic leukaemia(103). These reports stimulated interest in the use of BCG in bladder tumours, and in 1976, Morales published a landmark paper on intravesical BCG in superficial bladder tumours, showing a 67% complete response rate to intravesical BCG, although on a relatively small number of patients(109).

BCG is available in various different preparations including Pasteur, Tice, Connaught, Glaxo, Evans, Dutch, Tokyo, Moreau and Armand-Frappier. There is controversy over the relative efficacy of these strains, especially the Glaxo and Dutch strains(106).

Many studies have been carried out to determine the efficacy of intravesical BCG in the treatment of superficial transitional cell carcinoma. Most seem to report recurrence rates of 0-40%, with patients not receiving BCG having recurrence rates of 40-80%(106). BCG appears particularly effective relative to intravesical chemotherapy in the treatment of CIS. Short term response rates of up to 70% have been reported, although with longer follow up, up to 50% of patients may ultimately relapse (97).

A study by Herr *et al*(66) demonstrated a significant reduction in progression rates in patients with Ta and T1 tumours following treatment with BCG. Unfortunately, several much larger studies have failed to confirm this finding (106). Additionally, a study by Pycha(128) demonstrated that neither Mitomycin C nor BCG affected the chromosomal instability associated with chromosomes 7,9 and 17 in bladder biopsies taken from patients with bladder TCC, implying that genetic instability and hence the longer term risk of recurrent high grade disease remains after these intravesical treatments.

1.3 Novel chemotherapeutic Agents

1.3.1 Meglumine Gamma Linolenic Acid (MeGLA)

Gamma Linolenic Acid (GLA) is one of the essential fatty acids (EFAs) which consist of a hydrophobic lipid soluble hydrocarbon chain and a hydrophilic carboxyl group. There are usually 12 to 22 Carbon atoms, which when joined by double bonds, give rise to the term unsaturated for the fatty acid. Polyunsaturated refers to those with several double bonds. GLA is an 18 carbon fatty acid and is a member of the n-6 series of essential fatty acids derived from plant sources, of which the most abundant sources are from the oil of the Evening Primrose plant (10%), as well as blackcurrant seed oil (15%), and borage (20%). However, Linolenic Acid is more common in the diet and is converted to GLA by the enzyme delta-6-desaturase. Further desaturation produces Arachidonic acid, the precursor of series 1 prostaglandins, and then by further desaturations produces the other prostaglandins and leukotrienes.

The EFAs are also important in the construction of the cell membrane and dictate the fluidity and gating mechanisms of the cell. The fatty acids also form an energy source by combining three fatty acid chains to a glycerol molecule to produce triglycerides.

$CH_3(CH_2)_4CH=CHCH_2CH=CHCH_2CH=CH(CH_2)_4COOH$

Fig. 1.5 Chemical formula of the essential fatty acid γ-Linolenic acid (GLA)

The EFAs have been shown to be cytotoxic to a variety of human and animal cancer cell lines with differential cytotoxicity seen when their effects were compared to normal cells, such as fibroblasts or animal cell lines(8). Although the rate of growth was

slowed down, the normal cells survived(9). The cell lines studied have included breast, prostate, oesophagus and most recently urothelial cell lines in our laboratories(146-150). The most effective results have been with fatty acids with 3, 4 or 5 double bonds compared to those with 2 or 6 double bonds, from either n-3 or n-6 families. Indeed when human fibroblasts and cancer cells were co-cultured with GLA the fibroblasts outgrew the malignant cells, reversing the pattern that would normally be seen(8).

The mechanism of action of GLA is still not fully understood. It may be due to a variety of mechanisms. Free radical generation and lipid peroxidation are thought to be important mechanisms, originating from the Arachidonic Acid pathway. Tumour cells incorporate major portions of the fatty acids in the lipid and phospholipid fractions, but normal cells incorporate fatty acids primarily in the phospholipid fraction(30). In another study tumour cells supplemented with GLA produced more superoxide radicals than unsupplemented cells and cells containing EFA with lower cytotoxic potential(10). These studies suggest that the addition of GLA stimulates the initiation of its own peroxidation by increasing the amount of superoxide radicals and by increasing the substrate available for lipid peroxidation. This theory is supported by studies which show that antioxidants such as Vitamin E are able to block the cytotoxic effects of GLA(10). However, there are problems with these theories. It is not clear whether lipid peroxidation is the final common pathway of cellular toxicity or if other metabolites are involved. The studies on GLA were also conducted using relatively low doses. It is known that at higher doses there is a rapid onset of action, which probably simply represents direct cell membrane toxicity leading to cellular disintegration. This last concept has important consequences if GLA is to be used as an intravesical agent. The

duration of treatment is usually a maximum of 2 hours, limited by the washout effect of urine. Thus it is desirable if an intravesical drug has a rapid onset of action (*qv* section 1.2.1), and does not need continuing exposure to the drug.

However, GLA itself is unstable and therefore various conjugates have been developed to maintain its stability. Methyl glutamine (Meglumine) combined with GLA produces the stable conjugate Meglumine GLA (MeGLA), which has been shown in these laboratories to be cytotoxic to urothelial carcinoma cell lines in both parental and resistant forms, at concentrations as low as 12.5μg/ml(149). This cytotoxicity is limited to serum free applications because of the quenching effects of albumin on MeGLA due to its fatty acid binding sites. This is probably one of the reasons why trials of systemic GLA in pancreatic cancer have not shown significant efficacy(46;87). However, intravesical therapy is effectively a topical application on the bladder mucosa, and therefore represents an ideal setting for the use of cytotoxic drugs in superficial bladder cancer at high concentrations, not achievable systemically. Indeed a phase I trial of MeGLA in patients undergoing cystectomy, showed good tolerability at doses of 1mg/ml(25), and a phase IIa efficacy trial in superficial bladder cancer using pre and post instillation mapping techniques has shown response rates similar to conventional agents(62). A phase IIb efficacy randomised placebo controlled trial is currently recruiting.

Another potentially important property of GLA is its ability to increase the cytotoxic efficacy of conventional chemotherapeutic drugs by increasing cellular uptake(140) and also possibly by modulating the MDR status of the cell(170). Indeed in our laboratory, studies have shown that the combination of MeGLA with Epirubicin or MMC has synergistic effects on cellular cytotoxicity on both parental and resistant cells(147).

1.3.2 Indole-3-Carbinol.

The phytochemical I-3-C is a derivative of Glucobrassicin, a naturally occurring compound found in members of the Cruciferae plant family, such as Broccoli, Cabbage, and Brussels sprouts. Glucobrassicin undergoes autolysis during maceration to I-3-C, subsequently broken down by stomach acid to various metabolites, including Diindolylmethane (DIM) and Indolylcarbazole (ICZ).

Fig.1.5 Chemical structure of Indole-3-Carbinol.

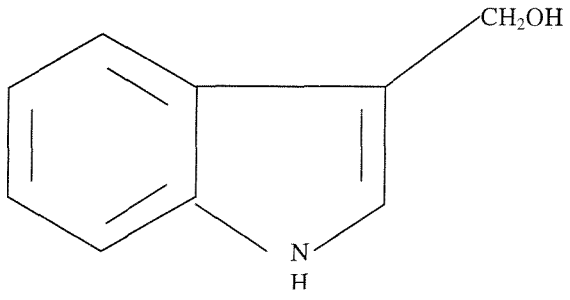

I-3-C has been shown to have chemopreventive properties by inhibiting the processes of tumour initiation and promotion. Some work has also suggested that it also has carcinogenic properties itself. More recently, studies have concentrated on its ability to modulate oestrogen metabolism, and so there is much work on the effects on breast cancer cell lines and in animal models of breast cancer. In animal models I-3-C is not active when given parenterally, but only when given orally. This has suggested that I-3-C is in fact a pro-drug, and it is the acid breakdown products DIM and ICZ that are the active drugs. However, I-3-C is active in cell cultures even in the absence of acid, and it has been shown that this is due to slow conversion over 24 hours in culture medium. Interestingly, work by Christensen and LeBlanc has shown that the acid-condensation

derivatives of I-3-C, but not I-3-C itself, are able to sensitise MDR tumours to chemotherapeutic drugs without any direct toxicity to the host.

There has been no work published on the effects of this compound on urothelial tumour cell lines. Therefore, studies have commenced in these laboratories on the cytotoxic effects of I-3-C. However, in this thesis I-3-C has been used to demonstrate the utility of the model under development, and so the work that follows is not a full investigation of the compound itself, but rather shows how a potential intravesical agent can be taken from monolayer cell culture experiments and then compared in the explant system. Whether, I-3-C will have any future clinical use in bladder cancer remains to be seen.

1.4 Estramustine

Estramustine is a stable conjugate of oestradiol and nornitrogen mustard. The original intention was to deliver the alkylating mustard moiety to oestrogen receptor positive tumour cells. However, subsequent studies showed very limited dissociation of the molecule at the carbamate linkage, and its toxicity profile was atypical for an alkylating agent. In fact the drug exerts its mechanism of action by binding to microtubule-associated proteins, tubulin and proteins of the nuclear matrix. In the field of urological oncology it has found use as Estramustine phosphate in androgen independent prostate cancer, most recently in combination with Vinblastine, Paclitaxel, or Etoposide.

The Estramustine mustard is insoluble in water and soluble in Dimethyl Sulphoxide. In order to make it soluble in water a phosphate group is added to facilitate administration of the drug. Estramustine Phosphate (EMP) is rapidly dephosphorylated in the body releasing Estramustine which is then partially oxidised to Estromustine. This is broken into oestrone and oestradiol which are responsible for its potential hormonal effects With daily oral EMP therapy the steady state concentrations of Estramustine and Estromustine account for about 80% of the administered dose, and which has cytotoxic

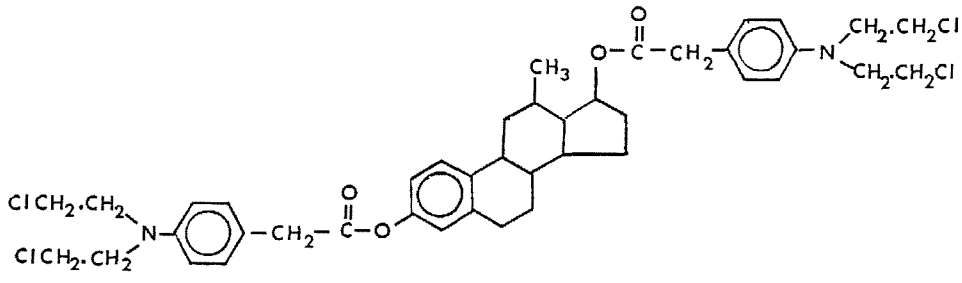

Fig 1.6 Chemical Structure of Estramustine

effects. The remaining 20% of EMP which is hydrolysed at the ester bond releases oestradiol from Estramustine and oestrone from Estromustine. This release of oestrogens

is sufficient to account for the castrate levels of serum testosterone seen after one month of daily dosing with EMP(78). The intact Estramustine molecule has neither alkylating nor steroidal properties *in-vitro*, but works by producing a build-up of cells in G2/M of the cell cycle, suggesting that it has anti-mitotic properties. Cells exposed to Estromustine are arrested in anaphase and have shortened mitotic spindle microtubules.

Binding of Estramustine and EMP to microtubule associated proteins (MAPS) has been demonstrated. MAPS are proteins which promote and stabilise tubulin polymerisation which is needed for microtubule growth. The normal function of microtubules requires cell cycle-dependent periods of assembly and disassembly, and it is thought that MAPS regulate this process. Estramustine has also been shown to bind to tubulin, although exactly which affinity is most important for its cytotoxic effects is not known. The carbamate group provides the structural basis for the binding as in other tubulin-binding drugs. This has been the basis for combining Estramustine with Vinblastine, and indeed pre-clinical studies have shown synergism(78).

Estramustine also binds proteins of the nuclear matrix which provides structure and organisation for the nucleus. The enzyme topoisomerase II which is involved in DNA repair and replication, and newly synthesised DNA are both found in association with the nuclear matrix. The topoisomerase II inhibitor Etoposide is also therefore a potential candidate for synergism with Estramustine, and this has been demonstrated in studies on prostate cancer cell lines.

It is also of interest that Estramustine binds to the multi-drug resistance protein p-glycoprotein, an efflux protein which mediates resistance to a wide variety of chemotherapeutic drugs including Taxol and the anthracyclines. However, Estramustine

itself is not a substrate and is not expelled from cells expressing the PGP phenotype. The potential for Estramustine to be a reverser of multi-drug resistance is tempered by the presence of physiological serum protein(145).

Clinical trials of Estramustine in breast cancer have been disappointing because of dose-limiting side effects, and unsatisfactory response rates(153). However, the drug has found some success in the treatment of hormone refractory prostate cancer both as a single agent and more recently in combination therapy. It has been combined with, Vinblastine, Etoposide and more recently Paclitaxel, and results have shown greater than 50% reductions in PSA levels.

1.5 *In Vitro* Models of Bladder Cancer.

1.5.1 Immortalised tumour cell lines.

There are 3 major methods for culturing tissue *in vitro*. Organ culture uses tissue extracted *in vivo* and attempts to preserve its architecture and viability as a 3 dimensional entity. The next step on from this concept is primary explant culture, in which fragments of tissue, either normal or from a tumour are placed on glass or plastic with the aim of promoting proliferation and migration. The third type of tissue culture involves disaggregating the parent tissue into a cell suspension, which is then cultured as such or as a monolayer. When this monolayer or suspension has significant growth it may be dispersed by enzymatic treatment and then reseeded. This is known as a passage and is the first stage in the development of a cell line. However, to produce an immortalised cell line a phenotypic change is needed which will allow continuous passaging without loss of the line(50).

The ability of a cell line to grow continuously reflects its capacity for genetic variation allowing subsequent selection of a cell type that will continue to proliferate. The ability to produce a spontaneous continuous cell line is dependent on the cell type and species of origin. For example, human fibroblasts do not give rise to continuous cell lines, whereas those from mice often do become immortalised. The transformation in the cell that gives rise to a continuous cell line may be spontaneous or may be chemically or virally induced.

There are often chromosomal changes seen in continuous cell lines, which usually result in aneuploidy. There may also be some variation in chromosome number between individual cells within the line population. The cells that give rise to a continuous line are either present at initial explantation, and are selected for because of their ability to

proliferate, or they arise from transformation through genetic mutation which gives rise to the immortalized phenotype. The process of transformation of a cell line involves morphological and kinetic alterations that lead to an increase in tumorigenicity.

The cell line used in this study was the urothelial tumour cell line MGH-U1 originally derived from an invasive, poorly differentiated transitional cell carcinoma of a 65 year old male patient at Massachusetts General Hospital in 1972(45). It was phenotypically characterised by Masters at University College, London(101). Unfortunately no information is available on the patient's prior therapy, although this is common for many tumour cell lines. Isozyme analysis shows that the cell line is very similar to the TCC cell lines T24, J82, MGH-U2, HU456, and HU961T. This suggests that at some stage these cell lines have been cross contaminated. MGH-U1 cells have a cytological appearance of differentiated TCC, which is curious as they are derived from a high-grade invasive tumour. When the cells are inoculated into nude mice they produce a tumour, which has the appearance of a G3 TCC with spindle cell areas and a high mitotic rate. The time taken for a palpable tumour to grow is typically in the order of 4 weeks or 1 month. MGH-U1 cells have a population doubling time of 20 hours and a colony forming efficiency of 76%(101).

1.5.2 Methods for assessing monolayer cultures.

Monolayer cultures form the mainstay of the assessment of potential cytotoxic drugs. They have advantages in facilitating highly reductionist experiments with many replicate data points, amenable to quantitative analysis. However, both structurally and functionally they are simplistic and results so obtained often require confirmation in more realistic models, specifically in the area of drug sensitivity. However, there is no doubt that as a baseline for further investigation, any new agent must first be tested in this type of model.

Before any assessment can take place the cell line must be chosen accordingly. This is governed by what is available and practical to use for the particular tissue in question. Continuous cell lines are generally the most convenient to use although they may not be as accurate a reflection of the tissue in question compared to finite cell lines. The growth characteristics of the cell line including population-doubling time, saturation density, cloning efficiency, growth fraction and its ability to grow in suspension need to be considered.

The growth of a cell culture may be assessed in several ways. The fundamental question that needs to be answered is the viability of the cells in culture, and in response to experimental manipulation. One of the common reasons for using cells in culture is to assess the effects of toxic agents, and it is therefore necessary to have systems in place to measure viability. This takes the form of quantitative assays that measure the growth or survival of the population. Growth is defined as regenerative potential measured by clonal growth, change in population, cell mass or change in a fundamental metabolic activity such as mitochondrial activity or DNA synthesis.

There are limitations to any system that aims to mimic the *in vivo* situation. Simple monolayer cultures can only measure cellular cytotoxicity, rather than simulate the complex pharmacokinetics that occur *in vivo*. The choice of assay depends on the agent under consideration, the nature of the response, and the target cell. There are 2 major types of assay, the immediate or short-term response, and long-term survival.

Short-term Assays

These take the form of dye exclusion, dye uptake or radioisotope release experiments. Dye exclusion relies on the ability of viable cells to exclude Naphthalene black and Trypan blue, and of dead cells to take up the dye(92). After exposure it is a case of counting the ratio of stained to unstained cells, using a haemocytometer. This method has the disadvantage of overestimating viability, as the percentage viable often does not translate into subsequent plating ability.

Dye uptake uses the ability of cells to take up Fluorescein diacetate and hydrolyse it to fluorescein, to which the cell membrane is impermeable(138). Analysis may be undertaken using a haemocytometer and fluorescence microscope and counting the green fluorescing cells, or using a FACS machine to do the counting. In order to show dead cells, Propidium iodide may be used, which fluoresces red. This allows a viability percentage to be given.

Viable cells take up reduced $^{51}Cr^{3+}$ in the form of $Na_2{}^{51}CrO_4$ and oxidize it to $^{51}Cr^{2+}$, which cannot leave the cell(73;182). Dead cells release the $^{51}Cr^{2+}$ into the surrounding medium. The cells and medium can be separately measured using a γ counter to give a ratio of viable to dead cells. However, the test can only be used for a few hours,

because of spontaneous release of ^{51}Cr. This is most commonly used to measure T-cell activity.

The above tests form the mainstay of short-term viability assays. There are certain metabolic tests available, but these are specific to the pathway being measured. Examples are glycolysis, respiration, enzymatic activity and incorporation of labelled precursors(49).

Long-term assays

In cases where an assay is required several hours or days after a toxic insult, a different type of test is needed. This is the case when a cytotoxic agent has its effects delayed as in the case for example of the anthracyclines. The dead cells will have disintegrated and so the assay must measure the residual viable cell population. In bacterial assays plating efficiency is used as a measure. However, many mammalian cells have poor plating ability, and so it is not possible to use this measure in all cases. Other parameters must be used, which include cell number, increase in total protein or DNA, or the ability of the cell to synthesise protein or DNA.

If the cell line allows, plating efficiency may be used, and is a relatively simple technique. The cells are treated with the experimental drug for a set time period at various concentrations, after which the cells are trypsinized and seeded at low density. After a period of incubation of a few days to weeks, the resulting colonies are stained with crystal violet and counted. The plating efficiency is calculated as a percentage of control, and plotted against drug concentration on a log scale, known as a survival curve. The inhibitory concentration of 50% or 90% of the cells may then be calculated (IC>50 or IC>90). This method of analysis is common to all techniques.

The problem with this technique is that the density of cells during exposure may alter the response. If the effects of the drug are subtle, then there may well be a reduction in colony size, but this will not be measured because of the technique of counting colonies. In these cases the size of colonies may be determined by densitometry(104), or image analysis, or even by counting individual cells within colonies. The choice of solvent for dissolving the drug in question may also have influence on the results as it may have toxic effects itself. For example, ethanol, propylene glycol, and dimethyl sulfoxide all have toxic effects themselves. Thus the minimum concentration of these solvents should be used, and ideally their own cytotoxicity profiles should be known. The controls should have a plating efficiency of 100%, but this is often difficult to achieve. Furthermore, plating is a time-consuming process where a large number of samples are involved over a period of several weeks. Nevertheless, plating efficiency is a good method for testing cell survival, but not the gold standard as was once thought. Microtitration plates have become the accepted method for assessing residual viable biomass. They have advantages in being able to produce a large series of results with standardisation and replication economically and efficiently. The most commonly used is the 96 well plate, with each well 28 to 32 mm^2 and able to accept 200µl of medium. There are several ways in which the residual biomass can be measured. One method uses the incorporation of [^{35}S]-Methionine. Living cells will take this up and incorporate it. The plate is read by attaching an X-ray film, which becomes exposed by those cells which have taken up the isotope, and quantified by reading on a densitometer. Alternatives to Methionine include simple cellular stains such as Methylene blue which can be read in a spectrophotometer, cell counting, fluorometric DNA, dehydrogenase

activity, or labelling with [^{3}H]-thymidine for DNA synthesis. Analysis can also be undertaken using a specialised scintillation counter.

The most commonly used microtitre plate assay uses the water-soluble Tetrazolium dye MTT(6;20;110). Viable cells will take up MTT and convert it to purple formazan crystals, which are water insoluble, but dissolvable in DMSO. The plate is read with a specialized spectrophotometer set at 570nm. The amount of absorbance corresponds to the residual viable biomass and can be plotted as described above.

1.5.3 Spheroids.

Monolayer tissue culture was developed in order to standardise the cell density to which the cultures were plated. Whilst this gives reproducible results representative of individual cellular toxicity during cytotoxicity experiments, it does not provide an accurate reflection of events *in vivo* where complex interactions between cells and overall tissue properties influence the effects of drugs. Spheroids are clumps of reassociated cells derived from cell suspension, the aim being to impart a 3-dimensional structure more akin to tissue. This allows the study of drug penetration and properties of resistance to agents, dependent on cellular interaction.

Spheroids may be derived from a heterogeneous population, and this is exemplified by the re-aggregation of embryonal tissue. The cells in these experiments are able to sort themselves into groups and even form tissue like structures. Unfortunately, adult cells do not exhibit these properties although some attempts have been made(34). Spheroids are in fact more easily formed from cell lines than primary cultures, although the formation of spheroids from primary bladder tumour explants has been described(174).

Reaggregation occurs when cell suspensions are placed in a gyratory shaker, or by growth on special types of agarose gel. The resulting spheroids then continue to grow and may be used for chemotherapy experiments(42) or for the characterization of invasion. Spheroids have been produced from the MGH-U1 cell line, and were compared to monolayers and xenografts(42;43). Co-culture experiments using MGH-U1 spheroids and endothelial monolayers, have been used as a model of tumour metastasis and invasion(95). Indeed the ability of MGH-U1 cells to form spheroids is so good that they can be used to study the basic mechanisms of tumour growth. For example one study showed that by creating a sub-line lacking the Na^+/H^+ exchanger, the cells were no longer able to form spheroids(137).

The 3-dimensional nature of spheroids allows the study of drug penetration into the multilayered structure. It therefore represents a better imitation of the *in vivo* situation, especially as applied to intravesical therapy. Spheroids are produced by placing a cell suspension into an agar-coated flask. Over 2 to 3 days cell aggregates form, and these are then transferred to a magnetic stirrer vessel or multiwell plate. Continuing growth over a period of 2 weeks produces spheroids that may be up to 1000μm in diameter(181). The size is limited by the ability of nutrients to diffuse to those cells at the centre of the spheroid. A steady state may be achieved in which proliferation at the outer layers is balanced by necrosis at the centre.

Any of the endpoints used in monolayer or plating experiments may be applied to spheroids. Thus, treatment-induced growth delay, proportion of spheroids destroyed by a cytotoxic agent, and colony forming ability after disaggregation may all be used to

quantify the effects of cytotoxic agents(156). The penetration of drugs into the centre of the spheroid also forms a specialist use of the method(15).

In order to assess the effect of *in vitro* models on the expression of key genes known to be implicated in the development or progression of cancer, real-time quantitative PCR was used to study the expression of 28 key genes in three bladder cancer tissue specimens and in their derived cell lines, studied either as one-dimensional single cell suspensions, two-dimensional monolayers or three-dimensional spheroids. Analysis of gene expression profiles showed that *in vitro* models had a dramatic impact upon gene expression. Quantitative differences in gene expression of 2 to 63-fold were observed in 24 out of 28 genes among the cell models. It was also observed that the *in vitro* model which most closely resembled an *in vivo* mRNA phenotype varied with both the gene and the patient. These results have suggested that mRNA expression databases based on cancer cell lines must be carefully interpreted(29).

1.5.4 Organ Culture.

This is a specialized form of tissue culture, which entails using the original tissue intact and maintaining its integrity by ensuring that all parts have sufficient metabolic support. The essential ethos of organ culture is the study of cell interaction and the effects of external stimuli or toxins on the subsequent development of the culture(50).

The first problem that has to be overcome in organ culture is the lack of a vascular system to disseminate nutrients and gas exchange to all parts. This limits the size of the culture. Thus, aggregates of cells start to become limited by diffusion at 250μm diameter, and central necrosis occurs at greater than 800μm. There are various methods for overcoming these problems. The simplest involves placing the explanted tissue in a position that allows maximum gas exchange, whilst also allowing access to medium. This may be achieved by placing the explant on a grid, placing it on a raft or gel exposed to the air, or by having a rocking mechanism that exposes it alternately to air or medium.

The availability of oxygen for the culture can be increased by simply increasing the FiO_2 or by using hyperbaric oxygen. However, this method has its limitations because of the toxicity of high oxygen tensions. Furthermore, this does nothing to facilitate extraction of the resulting CO_2. The technique has been recorded though for tissues such as prostate, trachea and skin.

If the explant is placed on a solid base then there is potential for outgrowth of the various cell types found therein. This property has been extensively exploited in the case of bladder explants, which will grow out skirts of urothelial cells, which can be grown in their own right as cell lines(155). Bladder explants have also been used to study the effects of initiating and promoting carcinogenic agents on the urothelium, and have been maintained in culture for over 200 days(94). The main methods for examining these

explants are by conventional H&E histology, or by electron microscopic techniques. The fundamental characteristic of these cultures is that their structure remains intact, and can be altered in a pathophysiologically realistic fashion. There is only growth in the epithelial component, and not in all parts of the explant. Thus these cultures form a good model for examining cell differentiation and its regulation.

However, organ cultures suffer from the problem of consistency, in that every explant has some inherent individual variation in size and growth characteristics; and also difficulty in quantification. This is because analysis is by microscopic description. They are also more time-consuming than cell lines, and may not yield large data sets. Each explant is an "end experiment" and cannot be propagated, meaning that each new experiment requires recourse to the original tissue of origin.

Tumour biopsy specimens grown in culture have become an established technique for the study of bladder cancer properties and response to therapeutic agents (27). Their morphology and growth characteristics may then be assessed, such as the expression of p53 in normal and tumour cells(61). This method, as well as the tumour response to cytotoxic agents may assess the drug resistance status of the tumour cells as judged by nuclear uptake of Epirubicin(23). However, sophisticated methods are required to maintain these explants in culture, and by their nature they represent a heterogeneous population of cells.

Attempts have been made before to combine tumour cell lines and normal tissue. As a model of invasion, various grades of chemically induced rat bladder tumours were inoculated adjacent to rat femurs and destruction of bone monitored radiographically and histologically(121). The interaction between tumour explants and an artificial

extracellular matrix suggested that firm attachment of cells occurs within one hour (123). In a further development towards a full model, the interaction between normal and superficial tumour with normal bladder stromal cells showed that there was no stimulatory effect on growth. However, cells derived from an invasive cell line were strongly stimulated(125). The rat bladder carcinoma cell line NBT-II were grown as spheroids and then their effect on bladder explants measured in terms of invasiveness in the presence of growth factors(164). An *in vitro* model has also been designed in which mouse tumour cell lines of various grades were inoculated adjacent to mature urothelial explants(132). The system described here is the first attempt to simulate a superficial bladder tumour, and record the effects over time of cytotoxic agents at clinically relevant concentrations.

1.6 Animal Models.

Animal experiments have formed the basis of medical investigation for centuries. However, it is only in the last 100 years that cancer models have been developed in various mammalian species. Historically, inbred species were chosen from which high rates of spontaneous tumours were produced. This was a haphazard method, without any consistency of tumour type, although the most "natural" method. Thus, two major methods have been developed to provide a model of bladder cancer, either by induction or inoculation of tumours.

1.6.1 Induction of Bladder Tumours

This may be accomplished by either a chemical carcinogen or a virus. Research into carcinogens produced as a by-product bladder tumours, and this in turn lead to the development of this approach as a model of bladder cancer. The first chemical shown to produce tumours in hamsters, monkeys and dogs was 2-naphthylamine(79). 2-acetyl-aminofluorence (2-AAF) with the concomitant administration of DL-Tryptophan or deficiency of Vit B6 may also induce tumours. However, in this model hepatic tumours were also produced, causing early death and difficulty in interpreting results(37). More recently dibutylnitrosamine (DBN) and its derivative N-butyl-N-(4-hydroxybutyl)nitrosamine (BBN) have been shown to be specific carcinogens for urothelium in rodents, producing TCC resembling those found clinically. Similar tumours may be induced in dogs, and the dose used corresponds to the degree of invasion seen in the resulting tumours(129). The tumours induced in rats are multiple papillary lesions with low-grade cellular atypia, whereas BBN induces non-papillary invasive high-grade tumours in mice(129). It has therefore been suggested that the rat model be used for the study of superficial bladder cancer and the murine model for invasive TCC.

Interestingly in dogs the dose of BBN determines the nature of the cancer. At low doses BBN yields low grade, low stage papillary TCC after long periods. In contrast at high doses, high grade, invasive tumours are produced in a relatively short time. However, the TCC produced can show quantitative and qualitative differences from human TCC. In rats, immunohistochemical studies have shown an increased incidence of squamous differentiation and the presence of cytokeratins characteristic of keratinising squamous epithelium in undifferentiated cells(64).

N-methyl-N-nitrosurea (MNU) may also be used to induce tumours in rodents. It is usually given intravesically either alone or in combination with oral BBN. In dogs, the combination approach produces dysplastic changes by 6 weeks, and cis by 64 weeks(139). Using MNU alone as repeated intravesical injections rats develop TCC and in some cases squamous carcinomas of the bladder(70). The tumours produced have a relatively low potential for metastasis with deposits being found in abdominal lymph nodes and within the abdominal cavity in only 13% of animals. MNU induced tumours can be used as a model of dysplasia and the study of cell surface markers induced by MNU(94). A model has also been used in which MNU was used at low non-carcinogenic dose in combination with potential carcinogens Saccharin, Cyclamate, and Cyclophosphamide(69).

The other major carcinogen in use is N- (4-(5-nitro-2-furyl)-2-thiazolyl formamide (FANFT). This has been used to induce invasive, malignant tumours in mice, rats, and dogs(44), which may also be transplanted into syngeneic animals. In most species the tumours are predominantly TCC with the full spectrum of disease from superficial tumours to cis to invasive tumours, although they are predominantly

malignant, invasive, metastatic tumours. However, work by Soloway showed that the tumours do not metastasise as commonly as their human counterparts(152).

Carcinogen-induced bladder tumours may also be transplanted into syngeneic hosts in order to study the effects of tumour promoters and subsequent development of the tumour. The transplantation may be into either bladder or into sub-dermal tissues, for easier access. Mention should also be made of the "Brown-Pearce" carcinoma. This was originally an anaplastic carcinoma that arose from a rabbit syphilitic scrotal ulcer, and can be transplanted into the bladder of syngeneic animals, where it has a rapid rate of growth. However, it does not really represent a true model of TCC, even though it has for example been used as a model in photodynamic therapy(86).

Tumours may also be induced by viral transformation. The HaSV ras transforming gene transfected into normal urothelium provides an example. Stripped adult bladder mucosa incubated with HaSV, in the presence or absence of helper virus, was transplanted beneath the renal capsule of syngeneic animals and maintained for periods up to three months. Control implants, exposed to helper virus alone, formed heterotopic bladders lined by urothelium displaying focal areas of full differentiation. Exposure of urothelium to HaSV resulted in increased proliferative potential of mucosal and submucosal elements with the appearance of a normal differentiated heterotopic bladder 10 days post-implantation. Implants left for 28 days developed mild to severe hyperplastic lesions. Experiments conducted with HaSV and helper virus resulted in the generation of mesenchymal lesions at 28 days with little surviving urothelium. This study therefore suggested that the H-ras oncogenic protein could induce hyperplastic lesions in

normal urothelium, characteristic of preneoplastic changes seen in bladder carcinogenesis(167).

1.6.2 Inoculated Bladder Tumours.

General considerations.

These have been more commonly used in recent years because of their greater convenience and reliability in producing tumours. In simple terms the technique involves either seeding a tumour cell line or a chemically induced tumour, into the bladder or subdermal tissue of an immune-compromised or nude animal.

The nude mouse was found as a spontaneous mutation and is an autosomally recessive trait, which results in a hairless mouse that has no thymus. The total number of circulating lymphocytes is greatly reduced. Compared to neonatally thymectomized mice they have no pre-natal contribution of the thymus and no risk of incomplete thymectomy. A variety of human tumours including primary and metastatic tumours and derived cell lines have been xenografted into nude mice, but with variable results. They are only useful for studying the growth characteristics of tumour cells, and also the study of chemotherapeutic agents. However, the animals are labour intensive, expensive and difficult to maintain and breed(96).

Another type of mouse used as a site for tumour models is the scid (severe combined immunodeficiency) mouse. These have an autosomal recessive mutation on chromosome 16, which results in a lack of any functional T or B lymphocytes. For this reason they are highly susceptible to infectious agents unless raised in aseptic barrier-maintained conditions. Certain tumour types such as bone and retinoblastoma will only grow in scids, and yolk sac tumours and seminomas grow better in scids. Tumours metastasise more commonly and certain normal or benign tumours can be grown in scids.

Scids are also good models for the use of immunotherapeutic approaches because of their lack of Immunoglobulin-producing B cells. Scids also allow tumour-infiltrating leukocytes in the human xenograft to remain alive and active for up to 5 months. However, this persistence may elicit a graft vs. host response. The T and B cell deficit is not always absolute with up to 25% of young and nearly all older mice developing a few lymphocytes(96). As with nudes the animals are highly susceptible to infection and their maintenance is labour intensive and expensive, but they are easier to breed (personal communication Dr J Chowaniec).

Inoculated bladder tumours.

Chemically induced tumours such as the FANFT tumours in various species can be successfully transplanted into inbred animals' bladders to mimic a spontaneously arising tumour(152). Chemically induced tumours may also be inoculated to ectopic sites that are more accessible for tissue monitoring and analysis. This is most commonly achieved by implanting tumour cells sub-dermally. This technique has also been used to implant human fresh tumour specimen into nude mice, although this has the disadvantage of variability in the tumour characteristics and lack of a consistent supply(47).

In another study FANFT induced tumours were transplanted in syngeneic rats by intravesical, s.c., i.v., and orthotopic routes. No success was achieved in transplantation by either the s.c., i.v., or intravesical routes when primary tumour cells were transplanted as cell suspensions. However, orthotopic implantation into the bladder submucosa was successful. Fragments obtained from either the primary tumour or its lung metastases resulted in 10.6 and 36% tumour takes, respectively, when implanted s.c. However, after one orthotopic passage in the bladder submucosa, the tumour cells injected as cell

suspension grew s.c. in 14% and orthotopically in 79% of the animals. Tumour fragments obtained from orthotopic tumours and implanted s.c. resulted in 15% tumour takes. This study suggested that implanting in the bladder resulted in better tumour take in the bladder than elsewhere(80). A similar procedure was used to assess intravesical Mitomycin C and Levamisole (a form of immunotherapy) by cautery of the bladder mucosa and subsequent implantation of tumour cells(3).

Murphy *et al* developed a murine bladder tumour model; again using FANFT induced tumours, which were then transplanted subcutaneously. This model produced invasive, metastatic tumours of an anaplastic type. It was therefore used to assess systemic chemotherapeutic agents such as Cis-dichloro-trans-dihydroxy-bis-iso propylamine platinum IV (CHIP), Cis-diaminedichloroplatinum II (DDP), Cyclophosphamide (CTX) and Methotrexate (MTX)(112). This model was adapted by implanting the mouse bladder tumour MBT-2 directly into the bladder to examine the effects of BCG administration on tumour growth and natural killer cell activity(131).

Animal models have also been used to study human TCC implanted at various sites. The long term cell lines RT4, EJ (=MGH-U1) and LD-71 were injected sub-cutaneously, intravenously and intraurethrally into athymic mice. Interestingly the RT4 cells, which are originally derived from a superficial TCC, produced histologically non-invasive tumours in the bladder; whereas the EJ cells, from a more aggressive tumour, produced invasive tumours, which metastasised spontaneously(2). Rats were used in a model using human RT4 bladder cancer cell lines, which is of low malignant potential, in an attempt to produce a more superficial tumour. The cells were inoculated into the bladder at cystotomy after bladder injury by cautery or acid treatment in order to facilitate

tumour take. The animals were sacrificed at varying intervals, and histologically examined. The authors claimed a high rate up to 93% of tumour implantation and growth, and suggested the model was highly reproducible(118). However, others have found this model difficult to reproduce and not consistent in its production of tumours.

Assessment of tumour growth with the above types of tumours is achieved by measuring the weight of the excised tumour and by recording the depth of invasion seen on histology achieved in a certain time period, usually after sacrifice of the animal. Other novel methods have included the use of trans-rectal ultrasound in a murine model using MB49 cells inoculated into the bladders of syngeneic mice. The 6.2 Fr 20MHz probe was inserted after 3 weeks of growth and compared to histological analysis, giving good correlation(4). Magnetic resonance imaging (MRI) has been used to follow the progress of MBT2 murine orthotopic bladder cancers. It enabled early detection of the tumours and allowed a study to be performed looking at intravesical immunotherapy with TNF alpha. The MRI findings correlated well with visual inspection and histological cuts(18). Despite the promising nature of this model, there has been no significant use of the technique, probably because of the limited availability of MRI scanning for use in the research setting. Recently two different groups have used transfected GFP cell lines to produce tumours in syngeneic or athymic animals. In one study the human bladder cancer cell line KU-7 was used(183). Results were encouraging showing good correlation between image analysis using FACS and whole bladder imaging. This study has been followed up by a comparison of whole bladder imaging and cytological examination of urine for GFP-expressing cells(158). In the other study the MBT2 murine cell line was transfected with GFP and analysis was by enzyme-linked immunosorbent assay

(ELISA)(162).

The human bladder cancer cell line 253J was implanted into the muscular wall of the bladder of athymic nude mice, and by a process of *in vivo* recycling two new cell lines were produced which had greater malignant potential. These 2 cell lines showed enhanced tumorigenicity, measured by a decreased latent period, and rapid growth compared with the parental cell line. Orthotopic implantation of these cell lines resulted in lung metastases. The cell lines exhibited unique karyotypic alterations, increased anchorage-independent growth, overexpression of basic fibroblast growth factor, altered expression of adhesion molecules and the ability to migrate through Matrigel. This represents yet another method for producing alternative models of bladder cancer from an already existing and established model(33).

However, all these animal models suffer the same basic difficulties. The animals are labour-intensive and expensive and need specialist secure facilities. The techniques are idiosyncratic, time consuming and the tumours produced not always consistent. Thus it would be desirable to have a more readily available and consistent model with the utility of monolayers combined with the realism of animal models.

Aims and Objectives.

The overall aim of this work is to develop and test an *in vitro* model of superficial bladder cancer that is amenable to rationalised experiments with cytotoxic agents, at clinically relevant concentrations, and which can be followed over time, without terminating the experiment.

The specific aims for this to be achieved are as follows:

1. To achieve transfection of the readily available and reliable urothelial tumour cell line MGH-U1 with Green Fluorescent Protein (GFP), with appropriate methods for selection of transfectants, such as antibiotic or FACS selection
2. To demonstrate the stability of GFP transfection in the new cell line, with no adverse effects on cell line characteristics
3. To establish the technique of rat bladder explant culture *in vitro* and demonstrate the behaviour of the explants and their urothelial skirts
4. To develop techniques to enable transfected cells to grow on the explants, and establish the optimum method for recording that growth over time
5. To use the tumour explant colonies to perform experiments with genotoxic and non-genotoxic cytotoxic drugs, in order to simulate the clinical setting of intra-vesical instillation
6. To enable the use of drug concentrations in clinical use, or for novel drugs, at doses in excess of the maximum tolerated concentration on monolayers

Thus, the objective is to produce an *in vitro* model of superficial bladder cancer, which combines the convenience and reproducibility of monolayer cultures and the greater clinical realism of *in vivo* animal tumour models.

2. Materials and Methods.

2.1 GFP Transfection of MGH-U1

2.1.1 Tumour Cell Lines

The urothelial cell lines MGH-U1 were used in their parental and resistant forms. This cell line was originally produced in 1972 from a grade II Stage 3 transitional cell carcinoma and was characterised by Masters *et al* at University College, London. The cells were a gift from that institution, and have been maintained in these laboratories for 7 years. The resistant type was produced in-house by chronic exposure to Mitomycin C, and was therefore known as MMC-MGH-U1(63). It was also cross resistant to the Anthracyclines, such as Epirubicin(63).

The cell lines were maintained in Dulbecco's Modified Eagle's Medium (DMEM) containing 10% foetal bovine serum (FBS), and 1% v/v of an L-glutamine penicillin-streptomycin cocktail (Sigma cat # G1146), in an incubator at 37°C. in 5% CO_2, 100% humidity and 1 atmosphere pressure. The cell lines were maintained in culture, and subcultured using 1% trypsin-EDTA (Sigma Chemical Co.) and centrifugation at 1500g for 3 minutes. Passaging in this manner was performed at intervals of 2 to 5 days with a split rate of 1:5, which was maintained at this rate after at least 100 passages.

Fig. 2.1 25cm^2 flasks, laminar flow hood and incubator

2.1.2 Production of Green Fluorescent Protein transfected cell lines.

GFPs are secondary fluorescent proteins used in an energy transfer reaction to

produce green light by several bioluminescent coelenterates. The most exploited species is the jellyfish *Aequorea victoria.* GFP from this species can be expressed by many prokaryotic and eukaryotic cell types including mammalian cells and hence is used as a marker of gene expression and protein localisation in fixed or living cells and tissues. The GFP cDNA encodes a 283 amino-acid polypeptide with a molecular weight of M_r 27,000. Variants with more intense fluorescence or alterations in the excitation and emission spectra have been produced.

Green Fluorescent Protein (GFP) cellular transfection was achieved using the GFP vector pEGFP-N1 (Clontech Laboratories Ltd., Basingstoke, UK). The MGH-U1, MGH-U1R and MMC-MGH-U1 cell lines were used. Instructions with the kit were followed precisely. After incubation with the plasmid vector for 4 hours, the cells were passaged into flasks. The success of the initial transfection was checked with a fluorescent microscope and an estimate made of the percentage of cells expressing GFP. This was done by taking 3 high-powered fields and counting the fluorescent and non-fluorescent cells, and calculating the percentage of transfected cells. If this was greater than 20% then the selection process was initiated.

The GFP vector also contains a gene for resistance to the antibiotic G418 (as recommended by ClonTech) at a dose of 200μg/ml, thus allowing selection by application of this cytotoxic antibiotic. G418 is used to select and maintain stable eukaryotic cell lines that have been transfected with vectors containing the gene for neomycin resistance. Kanamycin was also used because of difficulties with G418.

However, neither antibiotic was adequate, and therefore, all selection was performed by Fluorescence Activated Cell Sorting (FACS), on a Beckton-Dickinson

machine (Fig.2.2). The instrument is equipped with a single 15mW air-cooled argon laser emitting light at 488nm. The green emitted fluorescence of the GFP was detected using the FL1 channel (510 ± 15nm). Acknowledgement goes to Dr Ruth French who operated the machine and sorted the cells for these experiments, and to Dr Claire Davies who performed initial transfection on the MGH-U1 and MMC-MGH-U1 cells.

The cells were split into two regions, the untransfected cells with low fluorescence and the transfected high fluorescence population. Intermediate populations were sorted in early experiments, but had no distinctive value for experimental purposes. For both cell lines post FACS sorting the two cell populations, transfected (high fluorescence) and non-transfected (low fluorescence) were expanded for further experiments.

The production and sub-cellular localisation of the GFP in the cell populations were detected using the confocal microscope.

Fig. 2.2 The Beckton-Dickinson FAC Sorting machine.

2.2 Explant Characteristics.

2.2.1 Explantation.

Bladders were obtained from female Wistar rats between 6 and 12 weeks old terminated by carbon dioxide in a Home Office approved technique. 70% alcohol spray was used as an antiseptic and the bladders removed by sharp dissection with operating scissors. They were transported in phosphate buffered saline (PBS), and then cut into 4-5mm squares, using the surface of a 35mm petri dish as a sterile cutting surface. The serosal surface was glued to the bottom of a 35mm petri dish using a minimal volume of proprietary cyanoacrylate glue ("Locktite" or "Superglue"). Control experiments were performed to assess the toxic effects of the glue on cell lines. A 96 well plate was used. The first column of 8 wells was used as a null control, the second seeded with MGH-U1 cells and nothing else. In the other two columns 1μl and 5 μl of cyanoacrylate were placed, and immediately washed with medium, before being seeded with MGH-U1 cells. The residual viable biomass was assessed at 5 days of culture by the MTT assay (see section 2.3.1 for details of this technique).

Waymouth's medium (Sigma Chemical Co.) supplemented with 10% foetal bovine serum, L-Glutamine and streptomycin-penicillin antibiotic mixture was used to incubate the cultures with early changes of medium at 4 hours, then daily for the first 4 days and every 2 to 3 days thereafter. The minimum volume of medium was used in order to just cover the surface of the explant. The explants were regularly inspected by conventional inverted light microscopy within the laboratory, for the development of monolayer "skirts" of urothelial cells. Human ureter was obtained at operation, and similarly treated to produce larger explants of about 7-8mm square. However, the supply

of this material was not guaranteed and therefore no further development of the model used human explants.

Experiments were performed in which explants and the tumour cell lines were separated from each other by attaching the explant with cyanoacrylate glue in the well of a six-well plate and the tumour cells in a plastic insert with permeable membrane, or attaching the explant with cyanoacrylate glue to the membrane of the insert, and placing it into the well of a six-well plate containing a confluent monolayer of MGH-U1 cells. Controls consisted of cyanoacrylate glue, in the well or insert, and controls with MGH-U1 cells in the well or insert. Null controls were used with medium only for calibration of the plate reader. After 5 days of culture the MTT assay (section 2.3.1) was used to assess the residual viable biomass of MGH-U1 cells in either the well or insert. This was not possible for the explant itself. The tables below show the combinations used in these two experiments:

Experiment 1:

Insert	Medium	Medium	Cyanoacrylate	Explant
Well	Medium	MGH-U1	MGH-U1	MGH-U1
=	"Null"	"Cell Control"	"SG Control"	"Experiment"

Experiment 2:

Insert	Medium	MGH-U1	MGH-U1	MGH-U1
Well	Medium	Medium	Cyanoacrylate	Explant
=	"Null"	"Cell Control"	"SG Control"	"Experiment"

2 wells were used per combination, and four replicates were performed for each experiment. Only the MGH-U1 wells were amenable to analysis with the MTT assay.

2.2.2 Staining and cytotoxic agents on the skirts and urothelium.

The explant surface and urothelial skirt if present were supravitally stained using either Acridine Orange (AO) or Fluorescein Diacetate (FDA) that stain the nucleus or cytoplasm respectively. Evans Blue dye was also used to show the underlying explant surface. This was performed at various time intervals after establishment of the explant to demonstrate the viability of the urothelial surface, and surrounding skirt if present.

A limited number of experiments were also conducted to investigate the effects of water and the intravesical cytotoxic drug Epirubicin on the explant surface. The aim of these experiments was to assess the effects on the intact urothelium, and compare with the IC>50 and IC>90 doses on MGH-U1 monolayers. Epirubicin at 10 or 100μg/ml was applied for one hour in a similar manner to that described in section 2.4.1, as well as water in a separate experiment. Subsequent imaging was at 3 hours and 3 days. However, theses experiments were not pursued any further because of the difficulty of quantifying the results, and the limited supply of explants, which were needed for development of the tumour model.

2.2.3 Bromodeoxyuridine (BrDU) Staining.

A BrDU staining kit (Boehringer Mannheim/Roche, Lewes, UK) was used to stain those cells in S phase. The technique was first established on monolayer cultures, followed by the urothelial surface of the explant and skirt and finally used to verify cell turnover on the GFP MGH-U1 colonies. The explant tumours were incubated with 10μM BrDU for 30 to 480 min., and then fixed in 70% ethanol in glycine buffer pH 2, for 20 minutes. Mouse anti-BrDU primary antibody incubation for 30 min. was followed by TRITC-conjugated anti-mouse secondary antibody for 30 min. The resulting specimen was then viewed using the confocal microscope with a TRITC filter (see confocal microscopy).

2.2.4 Confocal Microscopy.

Imaging was by confocal microscopy using the Leica TCS 4D system with an Argon-Krypton laser emitting at 490nm.A x5 lens was used to provide wide field images of the explant surface and GFP tumour cells. Higher powers were not possible without removing the petri dish lid, and thus increasing the chances of infection. The FITC filter (Excitation Wavelength: 465-495 nanometres, dichroic mirror Wavelength: 505 nanometres) was used to image GFP cells, Acridine Orange, and FDA stained cells. The TRITC filter (Excitation Wavelength: 530-560 nanometres, dichroic mirror Wavelength: 570 nanometres) was used for Evans Blue fluorescence and Epirubicin fluorescence.

An explant was brought to the distantly located confocal microscope with the petri dish lid intact, to help avoid contamination. The microscope was then set up with the FITC filter and X5 objective lens. In order to obtain an image, the laser scans the field as a confocal slice, and produces a digitised picture amenable to analysis. Up to 15 slices through the field up to a total depth of 166μm are possible (see Fig.2.3).

Fig.2.3 Schematic diagram showing method of obtaining confocal slices through the tumour colony, in transverse section.

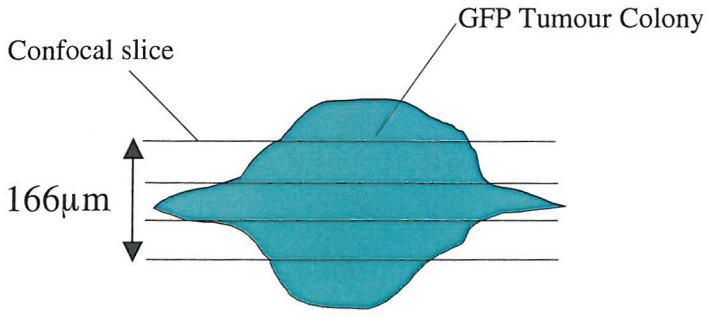

However, to obtain this number of images was time-consuming, and therefore, four images were taken at appropriate depths from the top to the base of the colony, and recombined to produce a single image for analysis, in the cytotoxicity experiments. This reduced the time the explants were out of the incubator, and was not thought to significantly affect the quality of the images obtained. A mark was made with an indelible pen on the petri dish base and lid so that the explant colony could be similarly orientated for subsequent serial imaging. The previous image of the explant colony could also be retrieved to ensure that orientation and depth were similarly set. Fortunately, the tumour colony was always small enough to fit into the one low power field used, allowing further growth to fill the field over a period of several days.

The computer software allowed light intensity measurements of a chosen field, thus enabling analysis of fluorescence before and after application of cytotoxic agents. The software records the intensity measurements in two different ways. Integral intensity refers to the total intensity measured at the given wavelength. Mean intensity is a measure of the mean intensity of the pixels on the digitally processed image, which are assigned numerical values according to their individual intensity. These two types of

intensity measurements were readily available, and were therefore recorded for all explant colonies and presented in the results.

However, fluorescence intensities, of either type, were found to be highly variable over the lifetime of the colony. Therefore, the area of the colony was also recorded. As drawing a line round the colony was a subjective exercise, 3 colony areas were drawn and the mean taken. The mean initial colony area was assigned 100%, and subsequent areas were calculated in percentage terms relative to that initial recording, and therefore known as "relative area". Interpretation of the effects of experiments with drugs or controls used this measurement as an indicator of the size of the colony.

Image processing allowed rotation of the series of combined confocal slices to give a transverse representation of the tumour colony. The image could also be reconstructed to give a 3D SEM type appearance or for viewing with red-green 3D glasses. These techniques were employed for comparison with SEM images of the same tumour colonies.

Serial imaging of the explants was undertaken after GFP cell seeding to verify the survival of the colony over several days.

2.2.5 Scanning Electron Microscopy (SEM).

Attempts had been made to fix the explant tumours with Formaldehyde, and then process them as standard Haematoxylin & Eosin (H&E) blocks for standard light microscopy. However, this technique proved too destructive for meaningful interpretation. Therefore, scanning electron microscopy was used as an alternative to corroborate the presence of tumour colonies on the explant surface.

Osmium tetroxide was used in a standard ethanol critical point drying fixation technique. The specimen was treated with a series of graded alcohols, and then critically point dried. The specimen was then mounted on a stub and fixed in 3% Glutaraldehyde plus 4% formaldehyde in 0.1M PIPES buffer pH 7.2, followed by rinsing with 0.1M PIPES buffer at pH 7.2. The specimen was then fixed in 1% Osmium tetroxide in 0.1M PIPES buffer at pH 7.2. The final step was a spatter-coat with gold-palladium, in order to earth the specimen, so that electrons do not build up a charge on its surface during imaging. The resulting gold-palladium treated specimen was viewed using a Hitachi S-800 scanning electron microscope.

2.2.6 Production of MGH-U1 Tumour Explants.

The transfected parental MGH-U1 and MMC-MGH-U1 cell lines were used for experiments with explants. The transfected MGH-U1R cell line was also used for a limited number of experiments, but for pragmatic reasons, the main work with explant colonies was carried out using the transfected MGH-U1 and MMC-MGH-U1 cell lines. Tumour cell seeding took place between 1 to 10 days after establishment (harvesting and attachment to the petri dish), before a standard protocol was decided on for cytotoxicity experiments (See section 2.4.1 for further details of timing protocols).

The GFP labelled cells from a confluent $25cm^3$ flask were passaged by Trypsin-EDTA separation followed by centrifugation in a universal tube for 3 minutes at 1500rpm. The supernatant was poured off to leave an almost dry pellet of cells. The culture medium was carefully removed from the edge of the explant petri dish using a polypropylene pipette. A hollow was created in the explant surface by sticking the tip of an air displacement pipette into the centre of the explant surface until it almost reached the bottom of the petri dish. This produced a break in the urothelial surface into which

was seeded 5µl of cell pellet. The number of cells in the cell pellet is dependent on the cell density of the pellet. This was assumed to be constant, as a standardised centrifugation technique was used. The cell density is not dependent on the size of flask used to harvest the cells, although the overall yield is dependent on the flask size used. One $25cm^3$ flask was enough to seed up to 10 explants, with enough cell pellet left over to continue maintaining the cell line. The explant with new tumour cell implant was then left to incubate for 1 hour at 37'C. in 5% CO_2 without medium (although a tiny film of medium remains along with the high humidity of the incubator), in order to allow adherence of the cells to the surface. Waymouth's medium was then carefully reapplied to the edge of the petri dish, taking care not to disturb the pellet of cells within the explant. The minimal volume needed to just cover the surface of the explant was employed. Subsequent imaging was as detailed in section 2.2.4.

2.3 MTT assays using 96-well plates.

2.3.1 General principles

The aim of these experiments was to provide data for comparison with the subsequent drug experiments on tumour explant colonies. As a secondary aim these cytotoxicity experiments were also used to verify that the transfected MGH-U1 still behaved in a similar manner to their non-transfected counterparts.

The cell lines were passaged and resuspended in DMEM. The suspension was then adjusted to produce a cell concentration of $1x10^4$ cells/ml using a haemocytometer. Using an 8-chamber air displacement pipette, 100µl was placed in each of the wells of a 96-well plate (Nunc). The first column of 8 wells was left blank to act as a null control for later plate reader calibration. The cells were then allowed to become confluent over a 24-hour period. Experiments were then performed in which the culture medium was

removed with an 8-chamber air displacement pipette, and replaced by the study drug in question dissolved in PBS. Eight wells were used for each log concentration of drug, as well as a control using PBS for one hour. The experiments were performed in triplicate.

2.3.2 Cytotoxic Drugs

The MTT assay was applied to experiments with Epirubicin (Pharmorubicin™ Pharmacia), Mitomycin C (Kyowa Hakko, Japan), Estramustine (Sigma Chemical Co.), MeGLA (Scotia Pharmaceutical, Stirling, Scotland) and Indole-3-Carbinol (Sigma Chemical Co.). The transfected MGH-U1, MGH-U1R and MMC-MGH-U1 cell lines were employed. The cells were exposed for 1 hour, representative of intravesical therapy. In the case of I-3-C a further study was made with exposure for 5 days in culture medium. After the 1 hour exposure the study drug was removed and the wells washed with PBS. DMEM was then replaced 100µl into each well, and incubation continued for 3 to 5 days.

At the required time, the medium was tipped off and 50µl of MTT at 2.5mg/ml dissolved in PBS was added to each well. This was incubated for 4 hours at 37°C. and 5% CO_2. At the end of this incubation the excess solution was tipped off and the resulting purple formazan crystals dissolved in 100µl of DMSO to each well. The plate was then read in a "Biokinetics" plate reader at 570nm to give absorbance readings for each well. The null control wells' absorbance readings were subtracted from the cell-seeded wells readings, and then the drug-exposed wells were expressed as a percentage of control wells not exposed. This gives the optical density percentage, which is directly proportional to the residual viable biomass.

2.4 Explant Drug Experiments.

2.4.1 General Principles

The aim of these experiments was to show that the tumour colonies could have an investigational agent applied and subsequently image it over several days. The second aim was to show that the tumour colonies could survive higher concentrations of drug than monolayers, and potentially up to those doses in clinical use, where applicable.

The general principles of experimental design described apply to controls and also to the investigational agents. A tumour explant was established as described in section 2.2.6, and initial confocal imaging performed to verify the existence of a tumour colony and to make measurements of intensity, and area. These measurements were taken as the 100% baseline. The explants' petri dishes were labelled with an indelible marker for identification and a mark made on one edge of the base and lid of the dish, so that the explant colony could be viewed in the same orientation on subsequent occasions. This was also aided by retrieval of the previous image for comparison.

The tumour explants were removed from the incubator and placed in a laminar flow extraction hood. Culture medium was removed carefully from the petri dish using an air-displacement pipette, and discarded. Sterile technique was observed at all times. 2.5ml of PBS or cytotoxic agent was then applied carefully to the petri dish. This volume ensured that the explant was always fully immersed in fluid. The petri dish lid was replaced and the explant replaced in the incubator for one hour at 37'C. in 5% CO2. At the end of this period the explant was removed from the incubator and once again placed in the laminar flow hood. Again, observing sterile precautions the study fluid was removed with a pipette and discarded. Waymouth's medium was added to the explant, and then immediately taken off again, in order to wash out any residual drug. A further

application of medium restored the culture medium to its previous minimal volume. The explant was replaced in the incubator, until the next day's imaging.

Timing Protocols:

It was also necessary to establish the optimum timing protocol for these experiments, and so initial "range-finding" experiments are named "early". Later experiments are those in which a standard protocol had been established, and adhered to for all subsequent drug investigations.

Early experiments with Epirubicin, Mitomycin C and MeGLA in PBS were performed after the colonies had been established for 5 days on the explants. The rational for this was that the colonies would have had time to produce a multilayered growth similar to that seen *in vivo*, and thus be a more realistic model of the clinical situation, in terms of drug penetration into the colony, and therefore its sensitivity to drug exposure.

However, two problems arose from this approach, the first being the increased chance of loss from fungal infection. Secondly, imaging with both confocal and SEM suggested that the tumour colonies were growing out as a monolayer on the explant surface, and not providing the multilayered colony being sought.

Therefore, a new "rapid sequence" protocol was developed as follows. Colony seeding took place 5 to 7 days after explantation. After colony seeding and initial confocal imaging the drug application experiment was performed within 12 to 24 hours. The colonies had enough time to become established on the explant, but were still in a multilayered structure, and there was less chance of fungal infection, allowing the colonies to then be followed for several days. This approach will be referred to as the "standard protocol".

2.4.2 Controls

Phosphate buffered saline (PBS) was used as a control to investigation agents. Initial experiments were performed on a series of 5 explants synchronously, to show the behaviour of the tumour colonies over time. Subsequent experiments with investigational agents on a series of 5 explants included one control with PBS. These results were pooled to provide the data presented for MGH-U1 and MMC-MGH-U1 colonies.

2.4.3 Classical MDR Drugs

The genotoxic agents Epirubicin and Mitomycin-C were both investigated in the model. "Resistant" cell lines exposed to these drugs elicit classical multi-drug resistance (MDR). It was therefore the aim of these experiments to show that these characteristics were maintained in the tumour colonies. Mitomycin C is used at a dose of 1mg/ml and Epirubicin at 500μg/ml to 1mg/ml in intravesical therapy, and so the experiments were also designed to test the model up to these doses. Concentrations of 1, 10, 100μg/ml and 1mg/ml were used for both drugs.

The early and standard protocols were used for Epirubicin and Mitomycin C. Both sensitive MGH-U1 and resistant MMC-MGH-U1 colonies were tested in the system.

2.4.4 Estramustine

The non-MDR agent Estramustine was used to show that the colonies behave in a similar fashion to monolayers, with regard to their MDR status. The basic aims of the model were also in question, that is the demonstration of colonies over several days after drug exposure. Estramustine is not used in intravesical therapy, and so it is not possible to give a comparative clinical dose.

A stock solution of Estramustine was made up with 100mg/ml of DMSO, and subsequent dilutions were in PBS. The standard protocol was used, as described previously, with concentrations of 1, 10, 100, and 500μg/ml for both parental and resistant colonies. Estramustine is not used for intravesical therapy at present, and so the doses were chosen as those close to the IC>50s for monolayers, and higher doses for comparison.

2.4.5 MeGLA

In order to test the model for novel agents, Meglumine Gamma Linolenic Acid (MeGLA, Scotia Pharmaceutical, Stirling) was tested in the system. The aim was to demonstrate that the model could be used for a novel agent already under clinical investigation and compare with monolayers assessed by the MTT assay. The core aims of sequential imaging over time, and high drug concentration compared to monolayers, were also sought. MeGLA has been used clinically up to a dose of 2.5mg/ml(62).

The early and standard protocols were employed for MeGLA dissolved in PBS. The standard protocol was used for MeGLA in culture medium with 10% FCS. The experiments dissolved in FCS were to produce conditions like those immediately after TURBT when there is a high serum content and therefore high protein concentration in the bladder effluent(150).

2.4.6 Indole-3-Carbinol

The aim of these experiments was to demonstrate the model with an entirely novel agent. This compound has not been tested before on urothelial cancer cell lines. The objective was therefore to show how the model could be used to compare the results

from monolayer experiments with this model. I-3-C has not had any *in vivo* use and therefore there are no clinical comparisons to be made.

A stock solution of I-3-C was made up by dissolving in DMSO at 100mg/ml. Subsequent dilutions were made in PBS. The standard protocol was used for I-3-C explant experiments with the parental MGH-U1 and resistant MMC-MGH-U1 colonies. Doses of 1, 10, and 100μg/ml and 1mg/ml were used for the parental MGH-U1 colonies. Doses of 10, 25, 50, and 100μg/ml and 1mg/ml were used for the MMC-MGH-U1 colonies. A second series using concentrations of 100, 250, 500 and 1000μg/ml for the MMC-MGH-U1 colonies became infected and therefore no results are shown. The rational had been to produce a more complete range of experimental concentrations for the resistant cells.

3. Results.

Fig.3.1 Schematic diagram showing the different elements of the explant system.

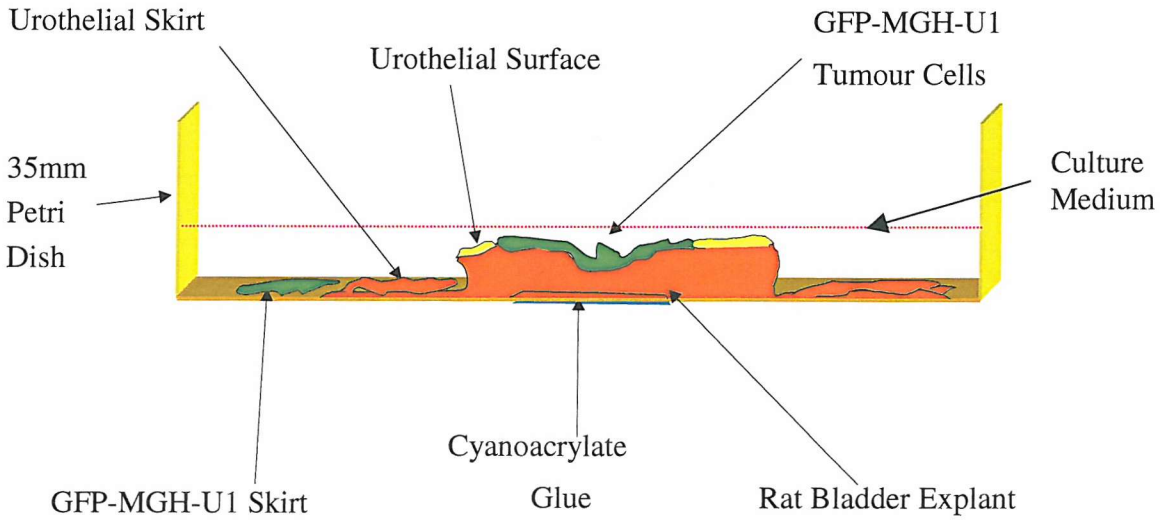

3.1 GFP Transfection.

This was successfully accomplished for MGH-U1, MGH-U1R and MMC-MGH-U1 cell lines with FACS being the method of choice for selection of transfectants. Imaging at high power showed high fluorescence in both nucleus and cytoplasm. The GFP expressing cell lines were stable over 12 months and over 100 passages. They also maintained their respective MDR characteristics in Epirubicin imaging studies. Furthermore, co-culture experiments showed that there was no lateral transfer of GFP from transfectants to non-transfected cells. See results below for further details.

3.1.1 Antibiotic Selection

Within the GFP viral genome is a code for antibiotic resistance, inserted to facilitate purification of transfectants by allowing untransfected cells to be killed by an appropriate antibiotic in the growth medium. The antibiotic used was G418 (as recommended by ClonTech) at a dose of 200μg/ml. However, difficulties were encountered in the use of this selection antibiotic. Both transfected fluorescent cells and non-transfected non-fluorescing cells continued to grow, as observed by conventional fluorescence microscopy, after six passages in the selection medium. The concentration of G418 was raised to 1mg/ml. After six passages at this concentration the cells were viewed again but there was still no change in the percentage of cells expressing GFP. Another antibiotic Kanamycin sulphate was also tested but had no selective power on either cell line at any dose over the same time periods.

Therefore, attempts to select transfected cells with G418 were abandoned in favour of FACSorting.

3.1.2 Fluorescence activated cell sorting

The successful alternative to antibiotic selection was found to be fluorescence activated cell sorting. The MMC-MGH-U1 resistant cells produced two distinct peaks of fluorescence on flow cytometry, Fig. 3.1.1a. Approximately 25% of cells displayed high fluorescence with 70% showing no or little fluorescence. The transfected MGH-U1 cells' FACS histograms showed a similar pattern of GFP expression. Approximately 40% of cells emitted detectable green fluorescence with the majority (60%) of cells apparently untransfected. Imaging both transfected cell lines showed varying levels of green fluorescence intensity and distribution. Cells displayed high fluorescence in both nucleus and cytoplasm, the apparent differential between the two being influenced strongly by the level of the confocal slice. Fig. 3.1.2a and b illustrate transfected MMC-MGH-U1 and parental MGH-U1 cells prior to FACSort, and Fig. 3.1.2c and d show high fluorescence populations after FACSort.

Fig.3.1.1 FACSort histogram fluorescence analysis of the initial transfection of GFP within MMC – resistant (cell passage number 0) and the stability of the FACSorted transfections over time 24 cell passages (three months growth).

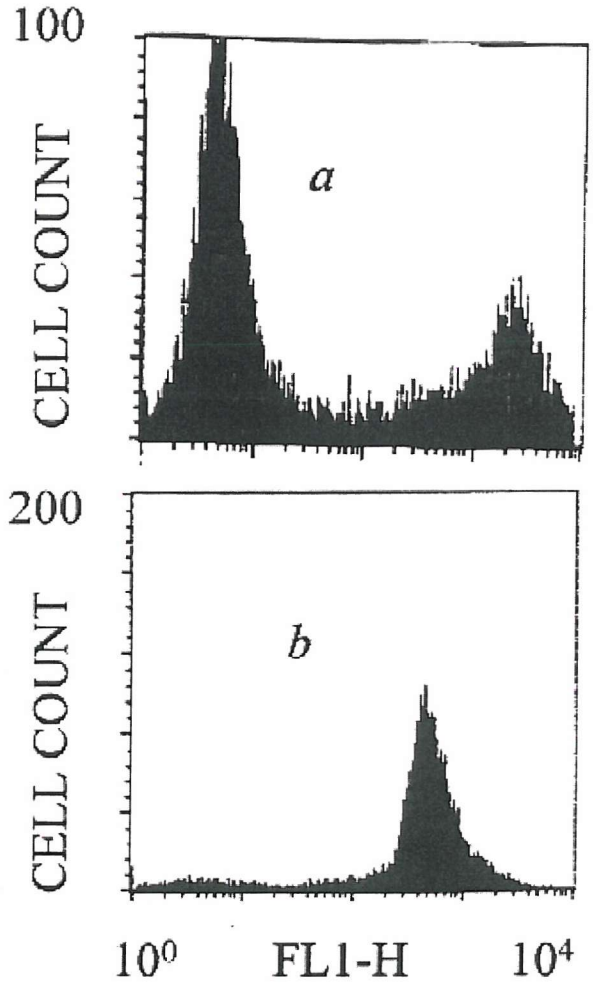

a) MMC-MGH-U1 cells, after initial transfection.

b) MMC-MGH-U1 cells, three months after initial FACSort

In both cell lines the cells sorted for high fluorescence (transfected cells) still displayed a range of cellular fluorescence distribution and intensity by confocal microscopy, e.g. Fig. 3.1.2c and d. Over 80% of positive sorted cells showed fluorescence with the majority displaying fluorescence over both nuclei and cytoplasm

although some expressed mainly nuclear localisation. Plating the cells at a low seeding density yielded colonies of consistent but varied intensity, suggesting that the variation is primarily clonal rather than due to cell cycle or other microenvironmental causes of fluctuation. The non-transfected cells selected using the FACSort contained a small population (less than 5% of the total) of cells that fluoresced.

Fig.3.1.2 Sub-cellular distribution of GFP within MMC-resistant and drug sensitive cells pre- and post- FACSort detected using the confocal microscope.

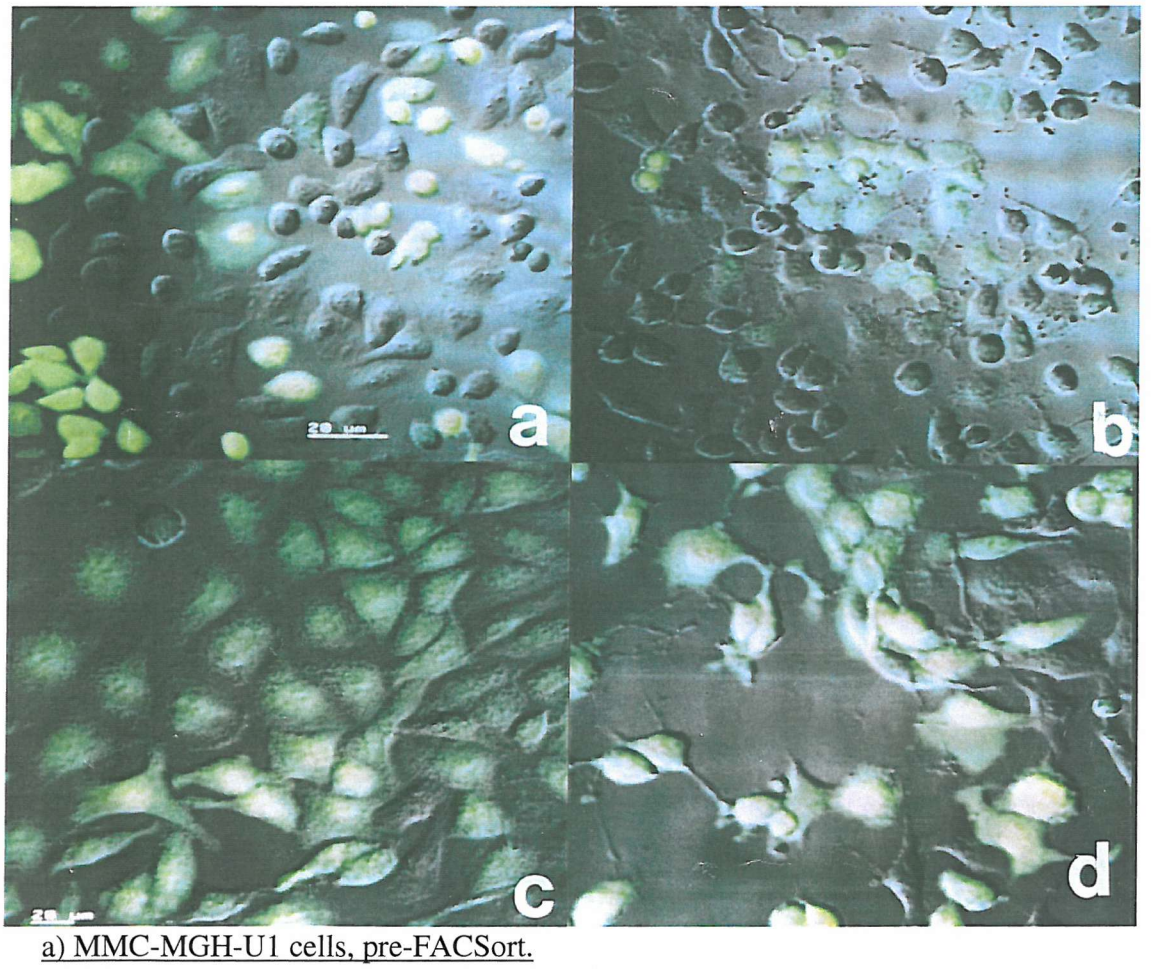

a) MMC-MGH-U1 cells, pre-FACSort.

b) MGH-U1 cells, pre-FACSort.

c) MMC-MGH-U1 cells, post-FACSort.

d) MGH-U1 cells, post-FACSort.

3.1.3 Lateral transfer of GFP

To ensure there was no passive transfer of GFP from transfected cells to non-transfected cells these two types of cell were grown in co-culture experiments. Non-transfected cells were seeded in a six well plate and separated from transfected cells growing on 0.4μm pore size membrane inserts (Falcon). After 72h the non-transfected cells and medium were viewed under the confocal microscope and observed not to fluoresce. As GFP is small enough to be able to diffuse across the membrane if free in the medium, this indicates that there was no passive diffusion of the GFP molecule from transfected cells into non-transfected cells.

3.1.4 Stability of transfection

The high fluorescence sorted populations of both cell lines were allowed to continue growing and were regularly subjected to FACS analysis. After 3 months (24 passages) no loss in fluorescence intensity was observed in the MMC-MGH-U1 cells, fig.3.1b. This indicates that the expression of GFP in this cell line was effectively stable over this period. GFP transfection did not alter cell growth rates, passageability or viability, and the cells were liquid nitrogen freezed in 10% DMSO, and subsequently thawed without any deteriorative effects.

The parental MGH-U1 cells were shown to give unchanged flow cytometry histograms after 12 passages, and high fluorescence cell populations were observed with fluorescence microscopy for over 12 months and over 100 passages. This time scale is more than adequate for the experiments for which the model is designed.

3.1.5 Fixation

Green fluorescence in transfected cells was lost in formaldehyde and organic solvent based fixatives. Acceptable, though reduced GFP detection was retained in paraformaldehyde fixed material.

3.1.6 Epirubicin handling by parental and MDR transfectants.

In this *in vitro* model, responses to cytotoxics by parental or resistant colonies can be assessed, as transfectants of both cell lines were available. Transfected parental cells displayed the typical pattern of mainly nuclear (sensitive) drug accumulation with Epirubicin Fig.3.1.3a. MMC resistant cells took up much less Epirubicin and had a mainly cytoplasmic drug distribution, with apparent nuclear exclusion, Fig. 3.1.3b.

Experiments using Epirubicin, however, required the cells to be studied live as fixation led to a loss of Epirubicin fluorescence and a disruption of the intracellular distribution pattern, especially within resistant cells. In resistant cells the green fluorescence of the GFP tended to obscure the (relatively weak) red fluorescence of Epirubicin when the two files were superimposed. Using low detection settings for the green channel and employing co-localisation image analysis software reduced this problem. The images obtained Fig.3.1.4 indicated where the two fluorescent labels overlapped within the cells. In the majority of MMC-MGH-U1 cells the area of highest co-localisation was peri-nuclear with a decrease in intensity away from and within the nucleus. A few of the cells show highest intensity of co-localisation within the nucleus.

Fig. 3.1.3 Patterns of intracellular Epirubicin (10μg/ml) in GFP transfected cells (fully selected at 3 months), detected using the confocal microscope.

a) Parental MGH-U1 cells

b) MMC-MGH-U1 cells

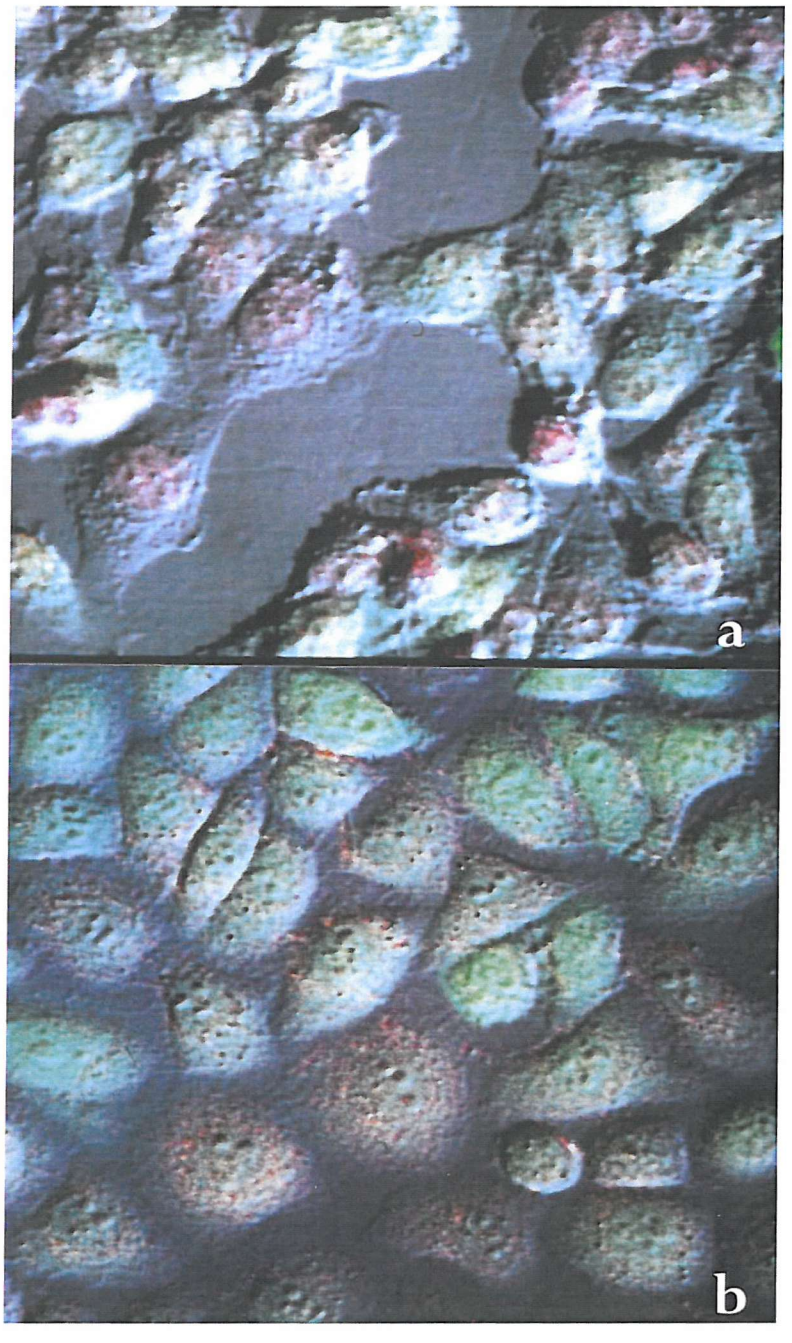

Fig. 3.1.4 Co-localisation of the intracellular distribution of epirubicin and GFP within (a) MGH-U1 parental and (b) MMC-MGH-U1 cells detected using the confocal microscope, where white / pink indicates the areas of highest overlap between the two fluorescent markers. Note nuclear uptake in parental and perinuclear uptake in resistant cells.

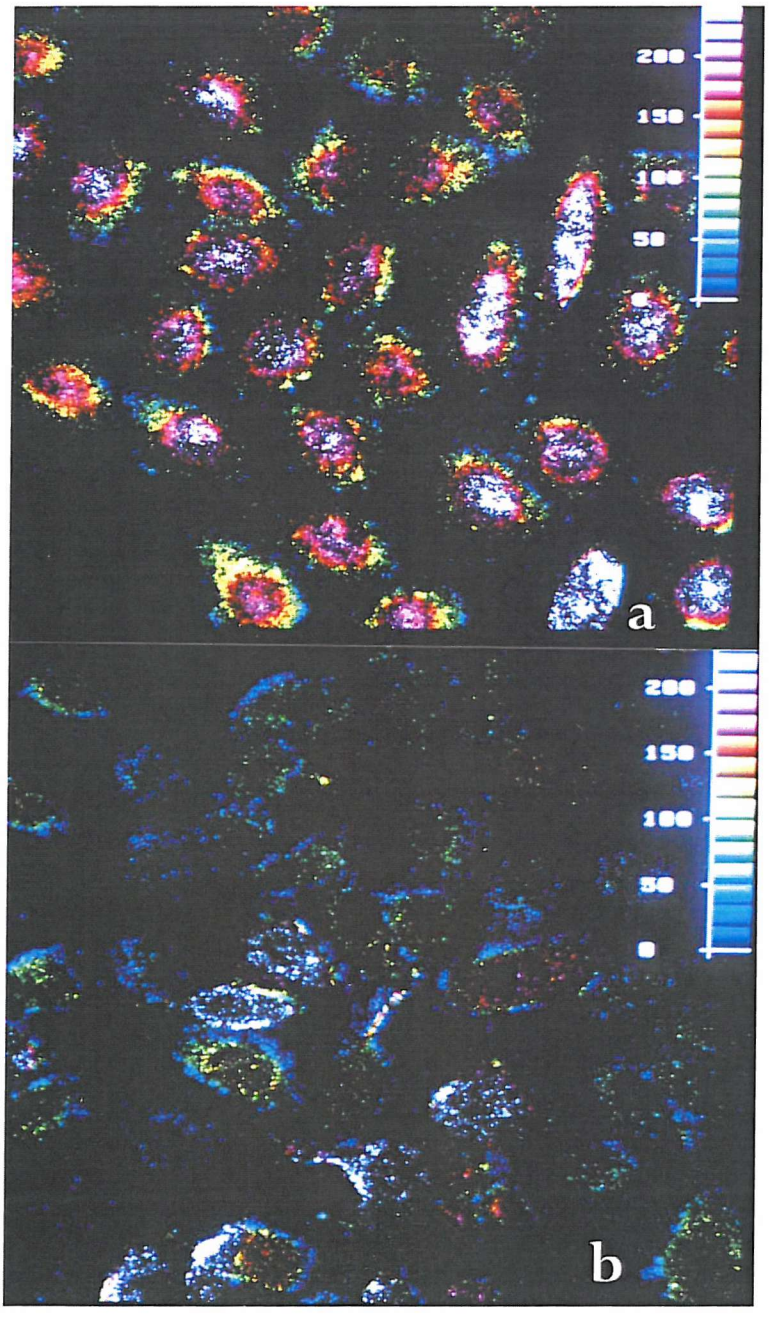

3.2 Explant Characteristics.

A schematic diagram is shown in figure 3.2.1 (above) showing the various elements of the explant system, which are discussed below. The explant itself was successfully stuck to the surface of the petri dish in all cases and the glue did not appear to penetrate into the explant or interfere with its growth. In a few of the cultures, the explant became detached after performing an experiment. Fungal infection of the explants was a constant problem, with many experiments infected before completion. However, GFP cell seeding was achieved in a majority of cases enabling the results that follow to be collected. The different elements of the model system are illustrated schematically in figure 3.1 at the start of this section.

3.2.1 Skirts

A skirt of urothelial cells usually started growing between 3 to 7 days after establishing the explant. The appearance and size of a skirt was variable and could not be predicted accurately, although it was observed that excessive use of cyanoacrylate glue did inhibit its development. Occasionally the skirt was made up of fibroblasts, and this was accepted as unwanted development. Once established the skirt could be kept growing for up to another 3 to 4 weeks. In some cases an almost confluent monolayer of urothelial cells was achieved. No skirts were observed growing out of the human ureteric explants, probably because these were too thick to allow migration of urothelial cells from the explant surface to the plastic surface of the dish.

Acridine Orange and FDA staining demonstrated the viability of the skirt (Figs 3.2.2 and 3.2.3). After staining, the skirt cells shrunk and became disaggregated and took several days to recover to their former confluence. Further experiments were, therefore, not carried out on these cultures. This is because of the toxic effects of these agents.

Water also showed similar effects, and therefore experiments with other cytotoxic agents were performed in PBS. BrDU labelling of the skirt showed a small number of positive cells after long incubations of up to 6 hours (Fig. 3.2.4), showing that the urothelium is undergoing slow turnover.

Experiments were also performed in which the interaction between urothelial skirt and applied MGH-U1 cells was followed over a period of several days. A typical series is shown in Fig. 3.2.5. Note that the explant urothelial skirt gradually deteriorates in the presence of the tumour cells.

Fig. 3.2.2. Combined transmission and FITC filter images of an FDA stained explant urothelial skirt.

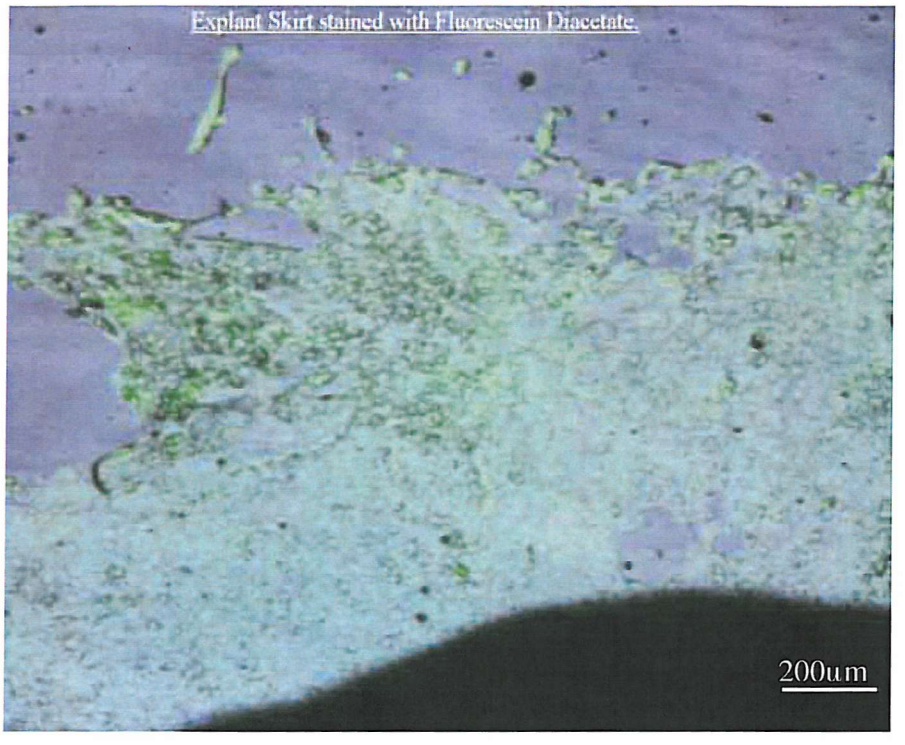

Fig. 3.2.3 FITC filter image of FDA stained explant urothelial skirt.

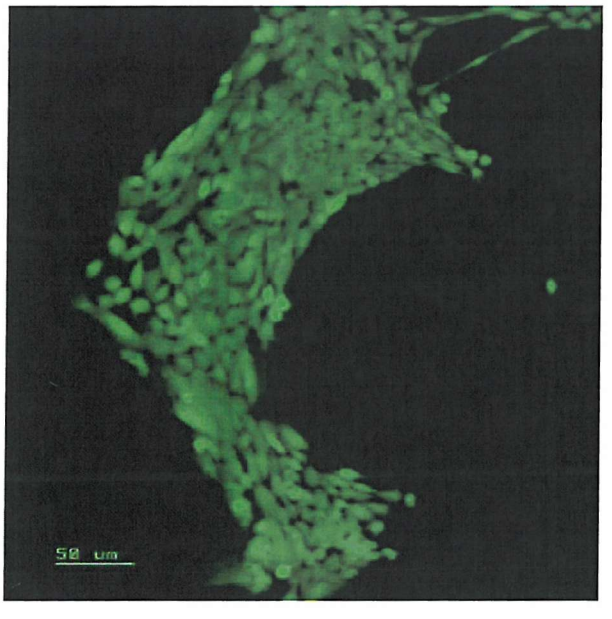

Fig. 3.2.4 Combined transmission and FITC filter image of explant skirt after 6 hour incubation with BrDU. The green BrDU labelled cells are those in S-phase.

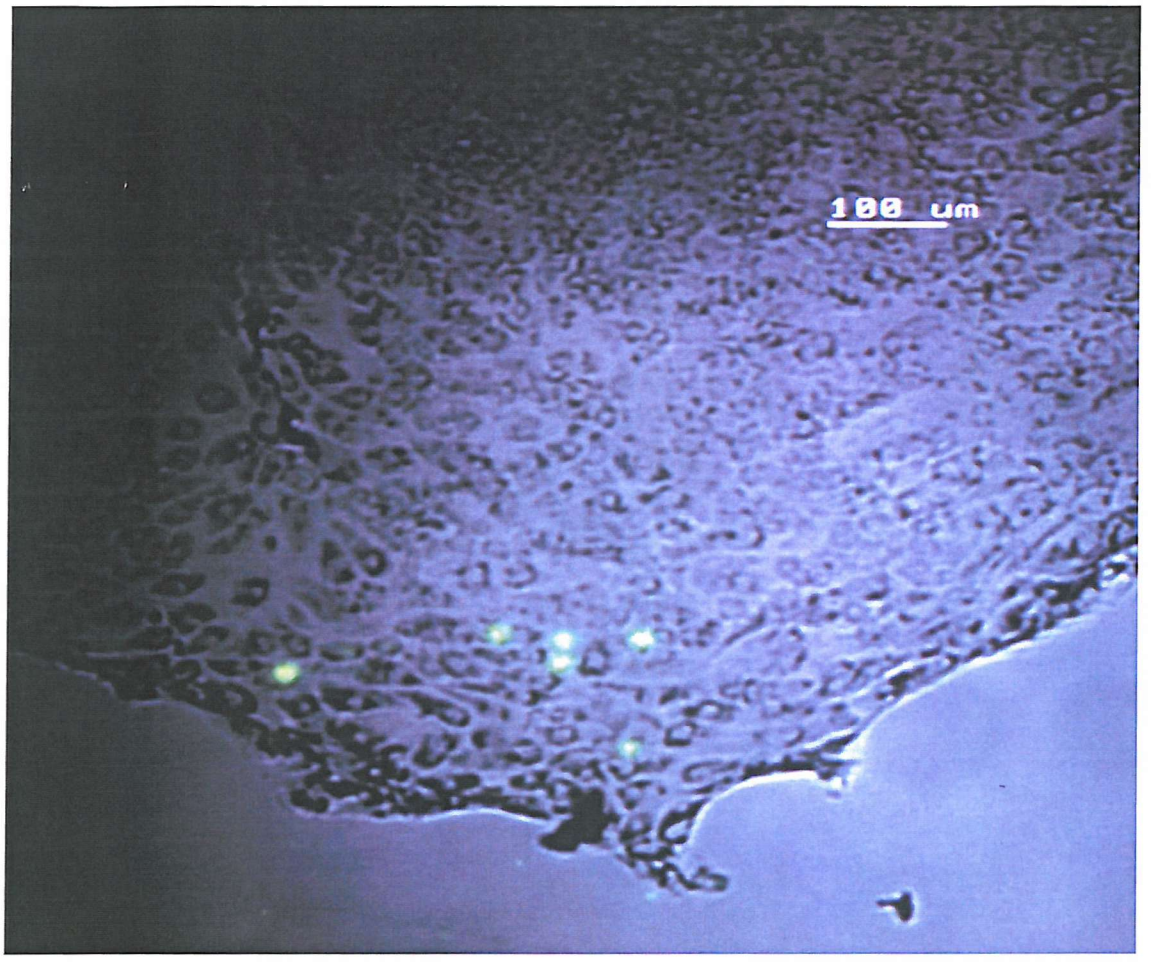

Fig.3.2.5 Sequence of images showing the interaction between explant urothelial skirt and tumour cells over several days.

a) GFP labelled MGH-U1 cells

b) Explant urothelial skirt

c) Explant

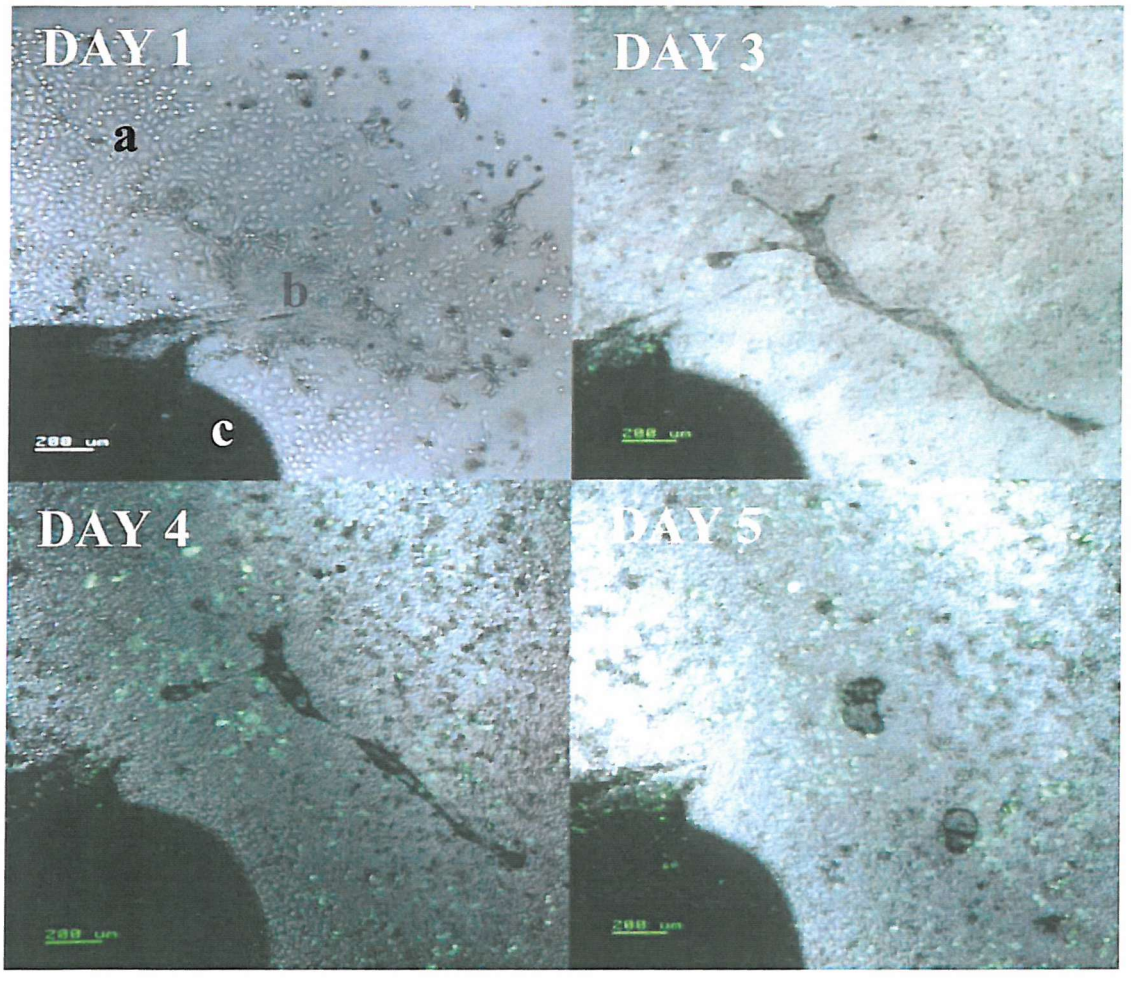

3.2.2 Urothelial surface

The urothelial surface of the explant was intact and viable at 1, 3, 7, 14 and 28 days after establishment. Acridine Orange staining showed the urothelial surface under fluorescence microscopy to best effect (Fig. 3.2.6 and 7). It was observed that as the explants aged the urothelial surface became flattened. This usually occurred after 2 weeks of culture. The macroscopic appearance changed from a raised furry, to a smooth flat surface. Figure 3.2.8 shows the SEM appearance, demonstrating a smooth flat surface, with minimal space between cells.

The experiments performed to demonstrate the effects on the urothelial surface after application of cytotoxic agents showed that after application of Epirubicin for 1 hour at 100μg/ml or at 10μg/ml, and subsequent imaging, there was still a viable covering of urothelial cell nuclei on the surface of the explant, at 3 hours and 3 days. Similarly water showed no appreciable effect on the urothelial surface. This compares with the cytotoxic effects of these agents on urothelial monolayer cell lines (see section 3.3.1). This avenue of work was not pursued further (as mentioned in methods section 2.2.2).

Fig. 3.2.6 Urothelial surface stained with AO at day 3. Note prominent mucosal folds and viable urothelium.

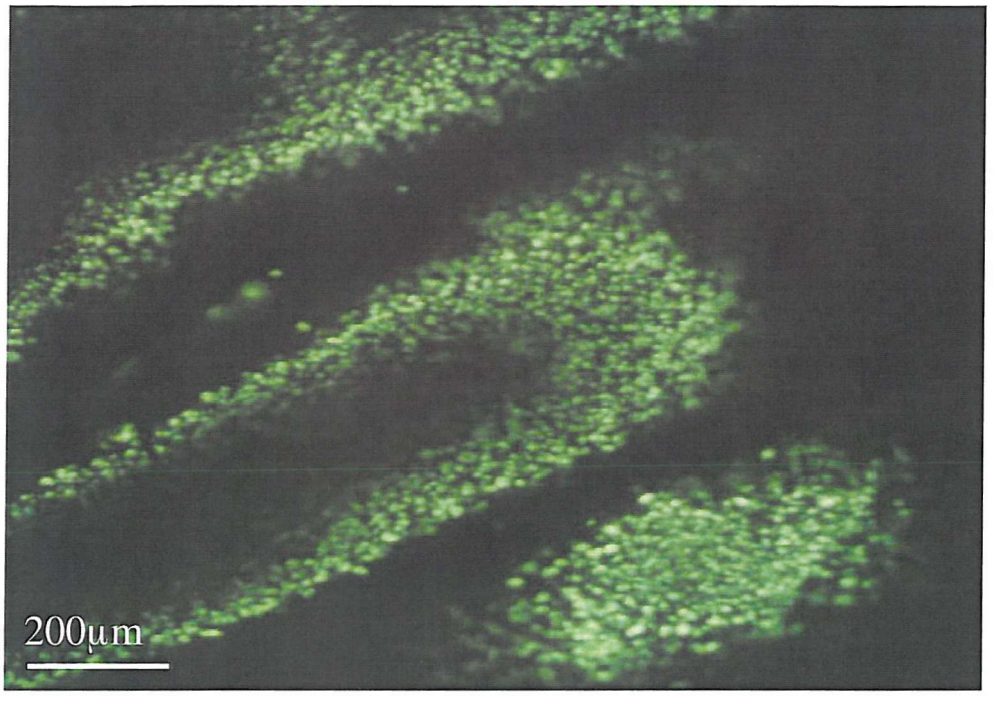

Fig.3.2.7 Urothelial surface stained with acridine orange at day 14. Note less prominent mucosal folds and viable urothelium.

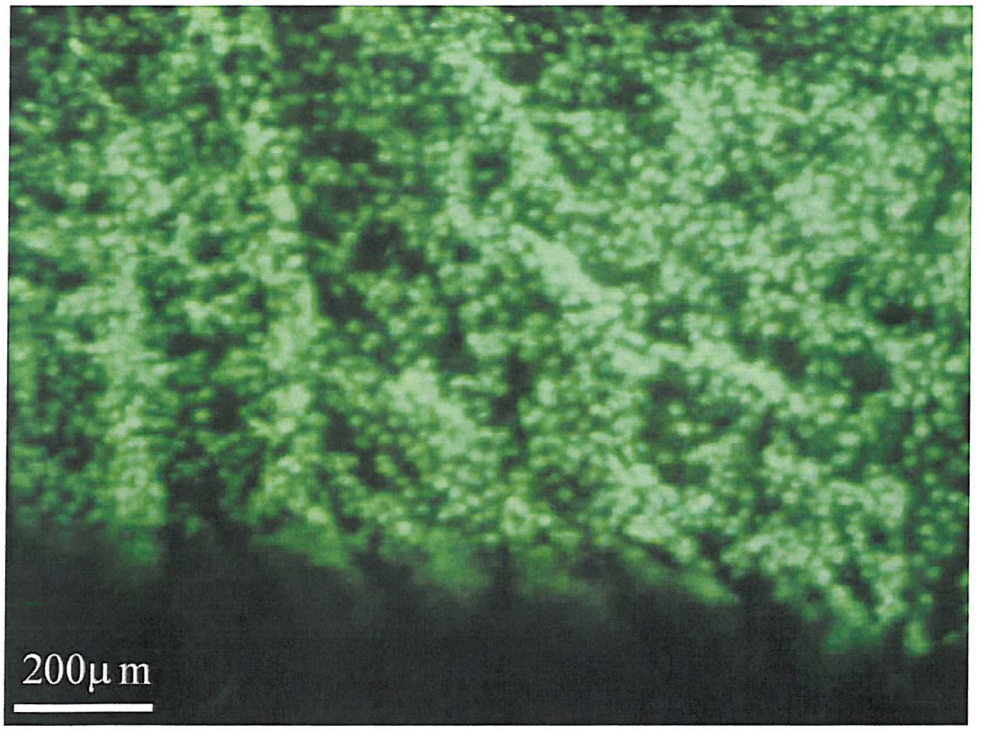

Fig.3.2.8 Low power SEM view of urothelial surface at 14 days, X1000. Note the smooth surface and tight bonds between cells.

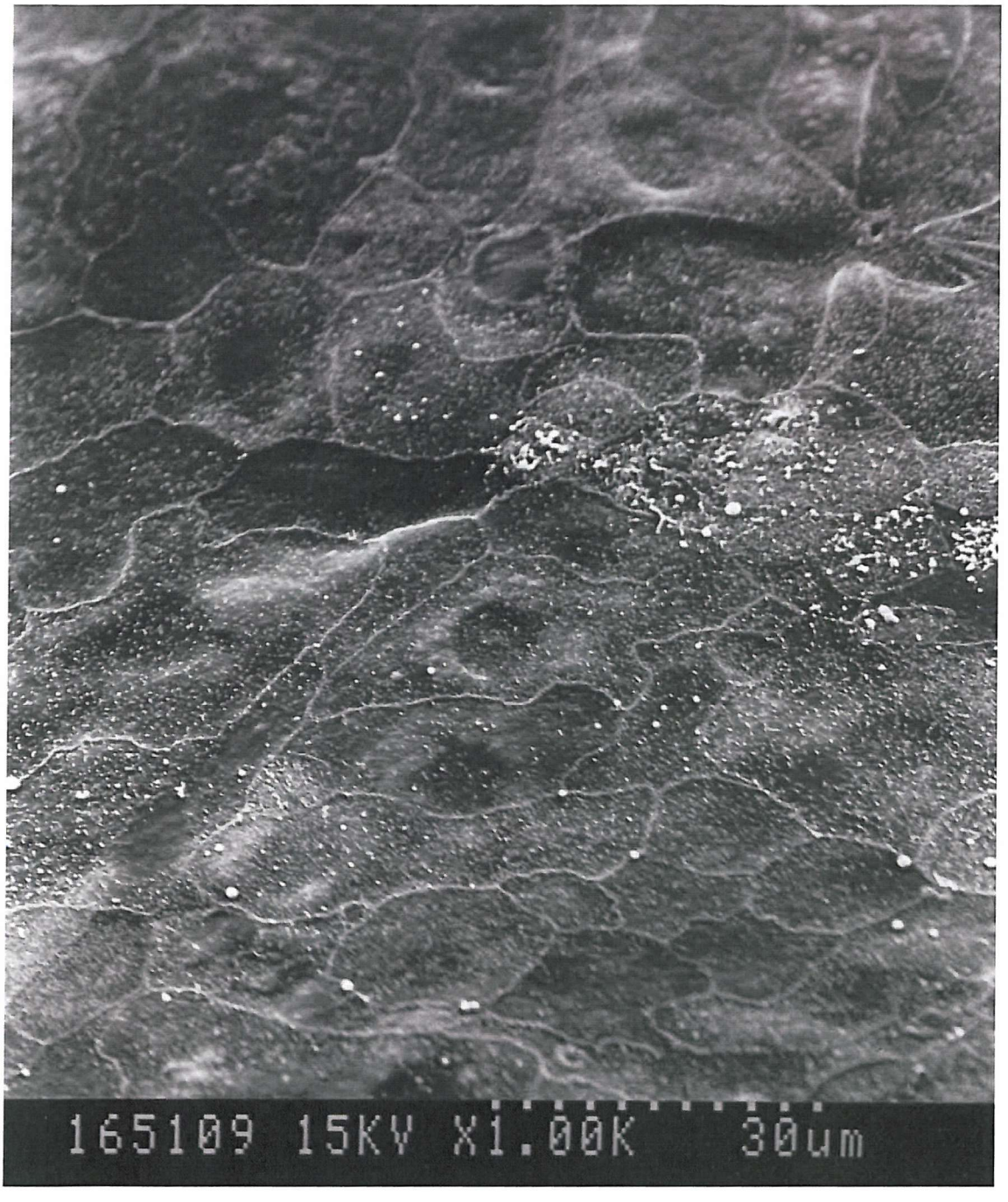

3.2.3 Tumour Explants

GFP cell seeding early in the life of the explant, between 0 to 5 days tended to produce smaller colonies compared with the larger colonies produced by seeding between 5 and 10 days. The cells were usually found in the centre of the explant and at the edges. It was also observed that the parental cell line produced smaller, less fluorescent colonies, compared to the resistant cells, which produced larger three-dimensional colonies. A typical combined confocal image of an explant colony at several levels is shown in figure 3.2.9. Scanning electron microscopy showed the tumour cells in the central pipette hole with others spreading out in an epithelial pattern adherent to the explant surface. The explant urothelial surface appeared flattened with the cell outlines visible as a honeycomb pattern. The confocal and SEM images showed good correlation (Fig. 3.2.10 and 11).

Serial imaging of explants after GFP seeding showed that initially the cells remained in a well-defined clump, but after 2 to 3 days started to spread on the surface of the explant (Fig 3.2.12, 13, 14, and 15). This was the case for the resistant cells even after application of a high dose of Epirubicin. The colonies would then continue growing for up to 14 days after seeding. A confluent monolayer also arose on the petri dish surface surrounding the explant, which allowed a direct comparison between the surface colony and skirt. In some of the MMC-MGH-U1 seeded dishes these monolayers became superconfluent with cells heaped up or even found in large discrete multilayered colonies. Similarly some of the explant surface colonies occasionally produced papillary structures, reminiscent of those found *in vivo*.

Fig.3.2.9 A gallery of confocal images showing a typical explant colony at different levels.

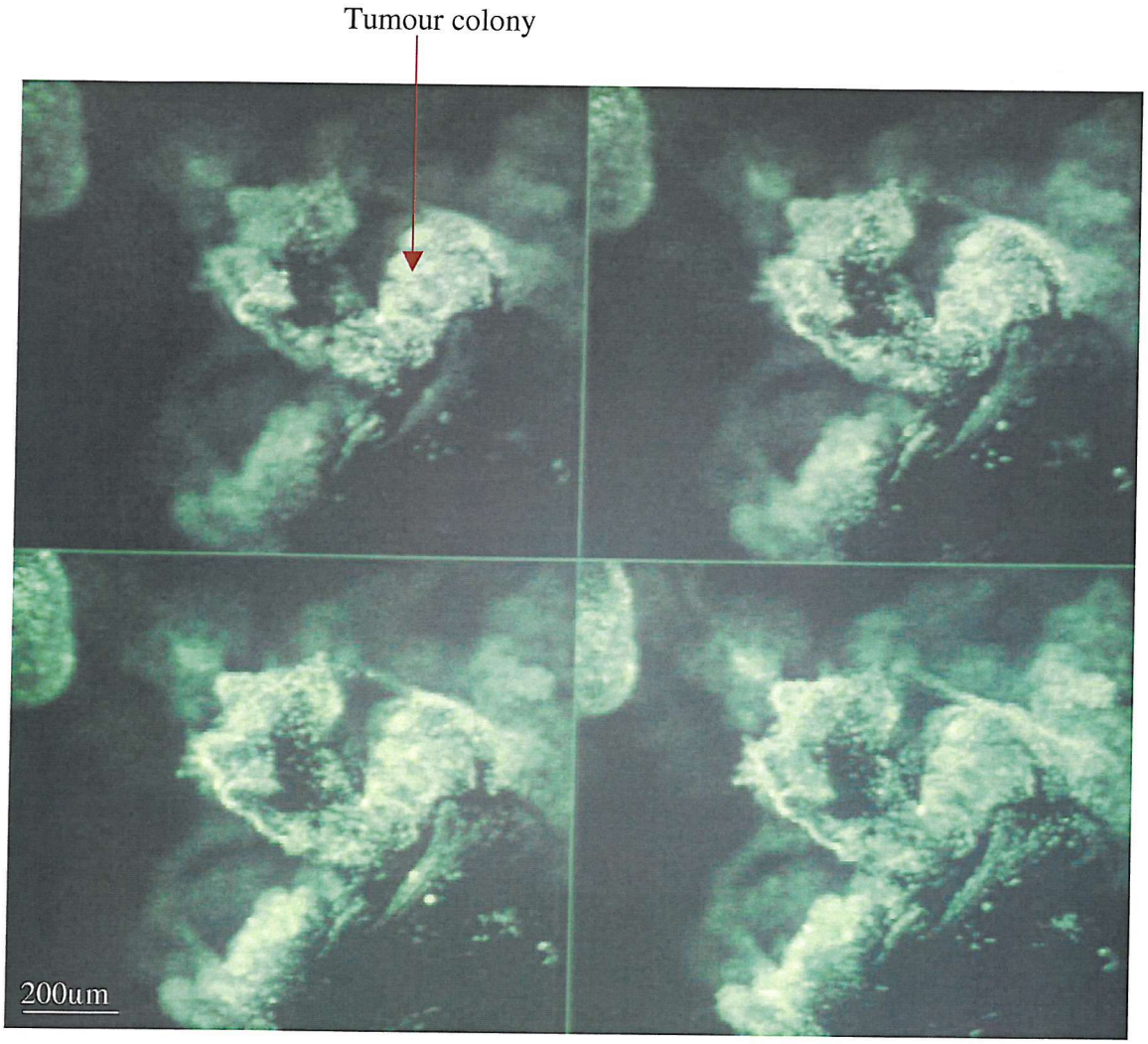

Fig. 3.2.10 A typical explant colony viewed with the confocal microscope using software to give the combined images of fig 3.2.9 an SEM type appearance. The red lined areas are shown for comparison with the SEM image of Fig. 3.2.11.

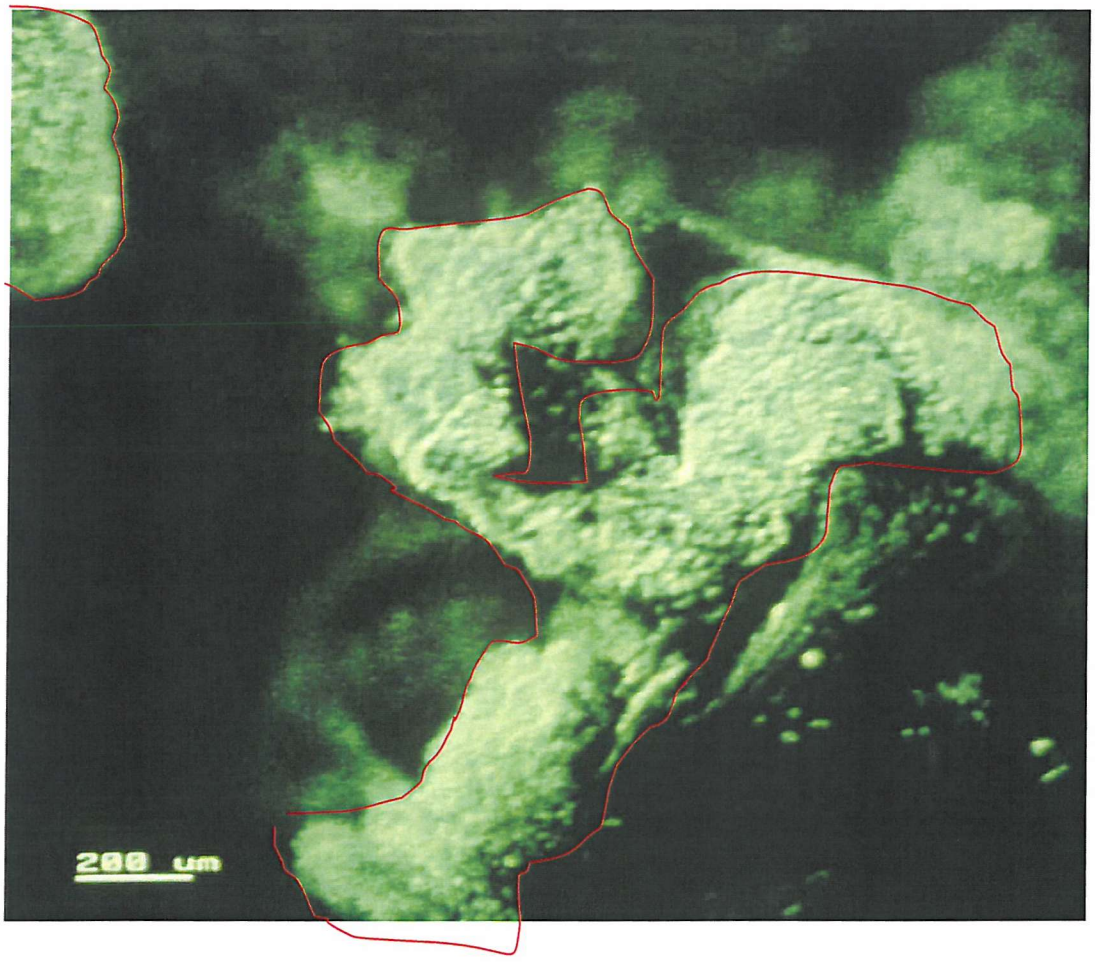

Fig. 3.2.11 Low power SEM image of the same explant colony shown in fig 3.2.10. The red lined areas are shown again for comparison.

a) Normal urothelium

b) Tumour colony

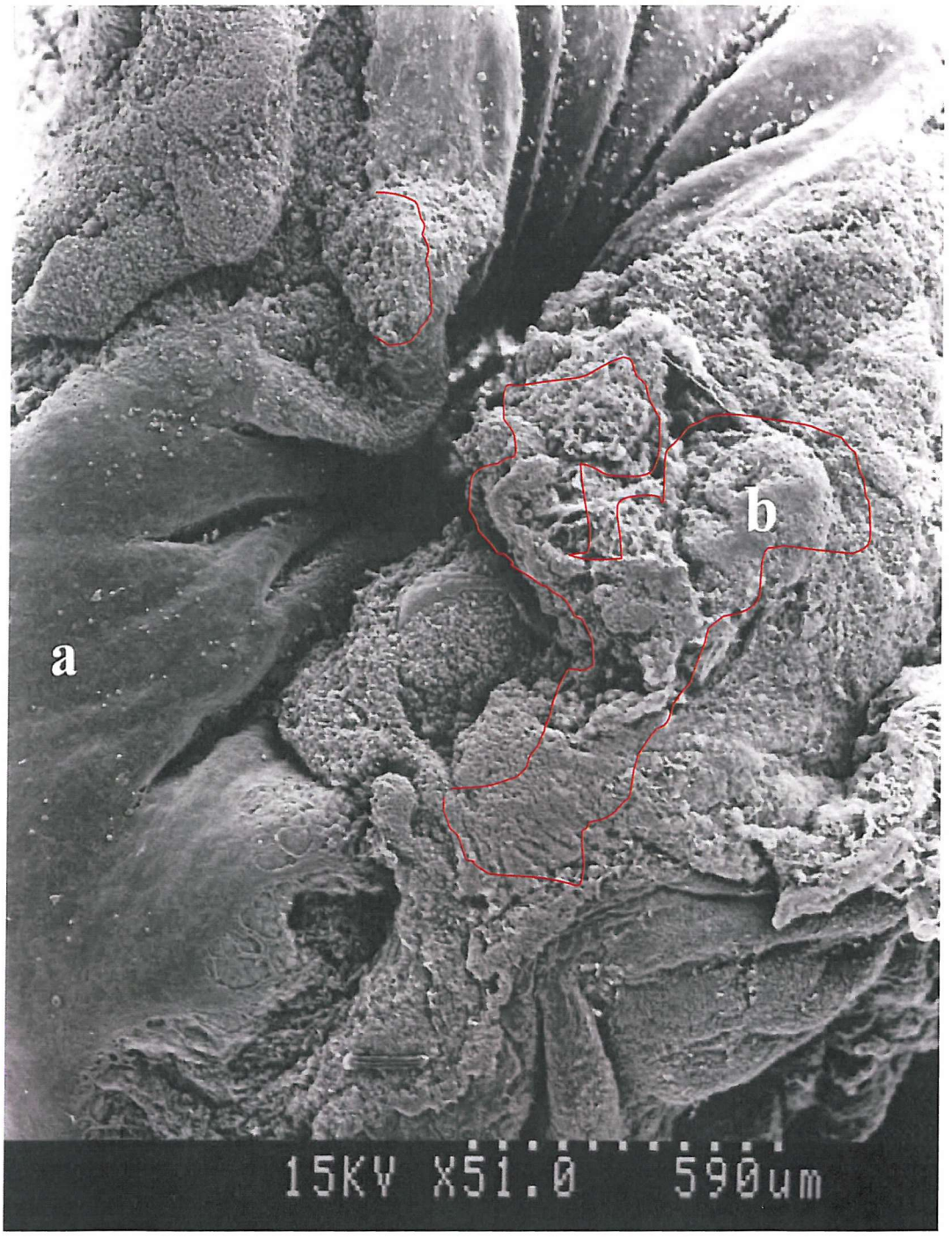

Fig. 3.2.12 Low power SEM image of another explant colony day 7 after explant establishment, and day 3 after tumour cell seeding. Note the smooth surrounding urothelium (a), central heaped tumour cells (b), and spreading MMC-MGH-U1 cells on the explant surface (c).

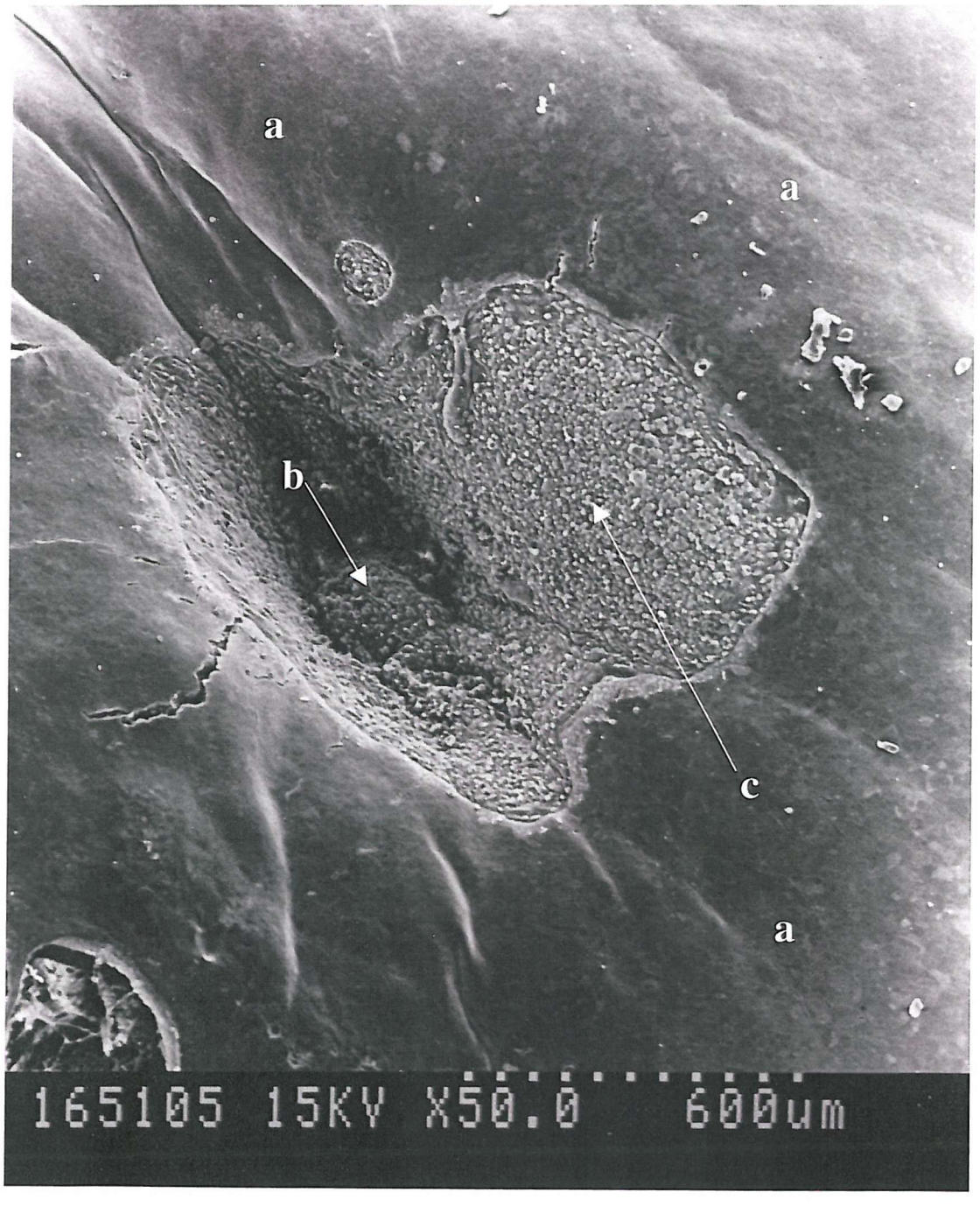

Fig.3.4.13 SEM Close-up view of MGH-U1 cells on urothelial surface. X1500. Note junctional bonds (a), and irregular surface of tumour cell (b).

Fig.3.2.14 Reconstructed transverse view of an explant colony, from 15 confocal slices.

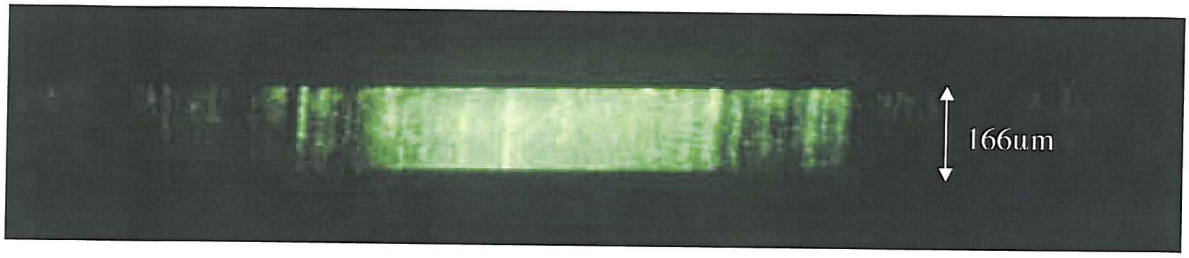

Fig.3.2.15 Schematic transverse section derived from the above image

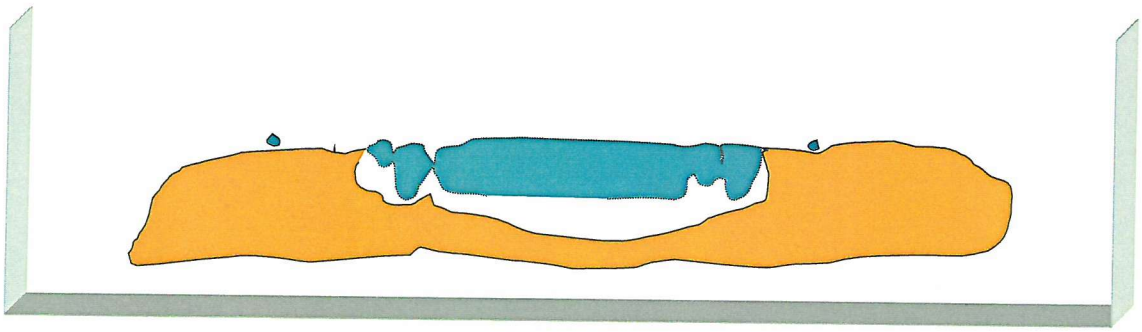

3.2.4 Control Experiments with superglue.

What is the effect of using this adhesive with bladder explants? Experiments were performed to assess the potential effects on the model of cyanoacrylate glue.

The results shown below (Fig.3.2.16) demonstrate that at the smaller volume of glue, similar to that used with the explants there was a small (c.20%) effect on the growth of the cells. At a higher dose there was an appreciable inhibitory effect. Thus all experiments with explants used the minimal volume of glue necessary i.e.1µl, and also incorporated immediate and early regular medium changes. In addition cell seeding on the explants was delayed for 4 to 5 days so that the toxic products of the superglue had been washed out with the medium changes.

Fig. 3.2.16 The effects of cyanoacrylate glue on MGHU1 cells at 5 days. Error bars are standard deviations.

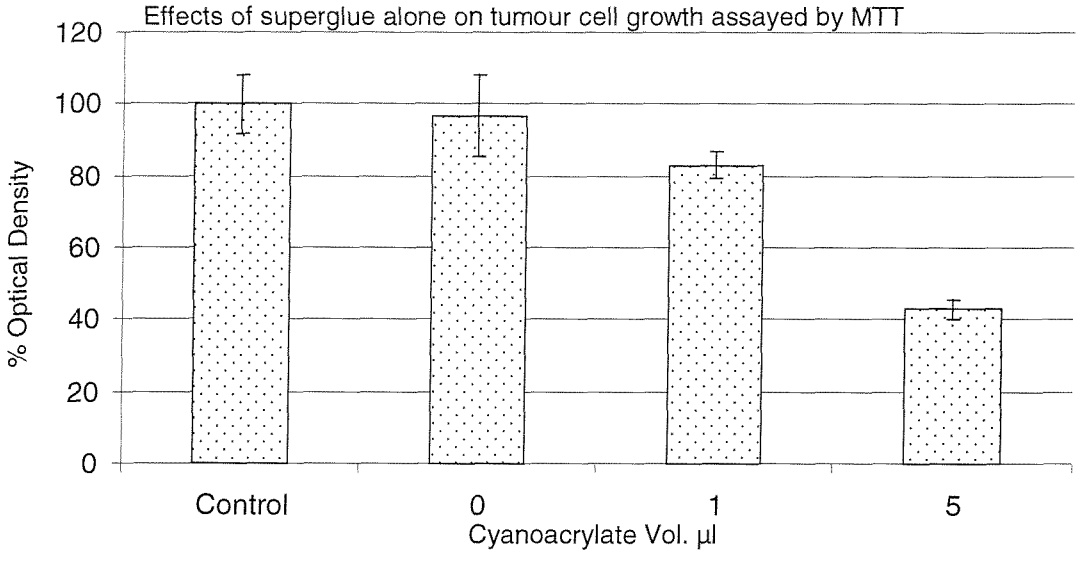

3.2.5 Lateral Transfer Insert Experiments with Explants and Tumour Cells.

The results are shown in Fig. 3.2.17a and b. The bar charts correspond with the tables shown in methods section 2.2.1. The results have been recalculated from the optical density reading taking the null control as 100%. Thus the other results are relative figures. They indicate that whether the explants were placed on top or below, there was no significant effect on MGH-U1 cell growth, when compared with the SG control and the cells only control. A paired student's t test was used to test the statistical significance of this finding, and p levels were below 0.05 for all comparisons. It can also be seen that once again (see Fig 3.2.16) there was no significant effect of the SG *per se* on the growth of the tumour cells in either experiment.

The results are presented in tabular form below:

Table 3.2.1 Results of insert experiments with explants, SG and MGH-U1 cells.

	Null (SD)	**Cell Control (SD)**	**SG Control (SD)**	**Explant Exp (SD)**
Exp 1: Explants on wells	100% (0.9)	189% (8.0)	194% (12.9)	221% (7.5)
Exp 2: Cells on wells	100% (1.0)	173% (6.3)	171% (6.2)	179% (6.8)

Fig.3.2.17 The results of insert experiments. Error bars are standard deviations.

a) Experiment 1

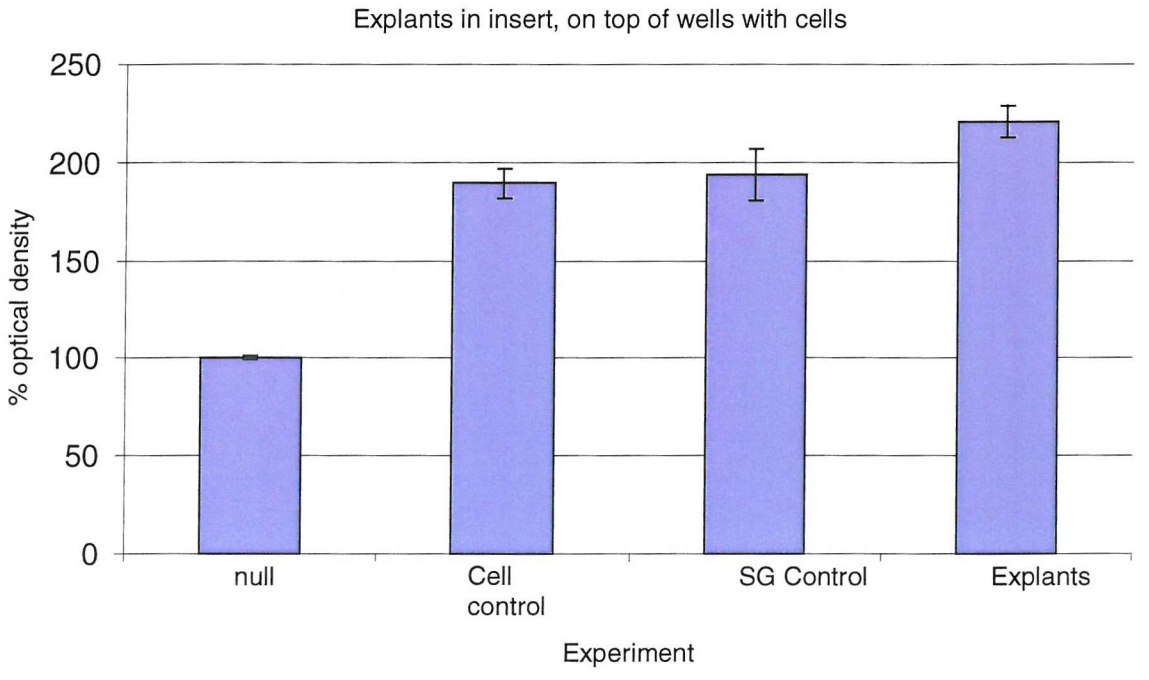

b) Experiment 2

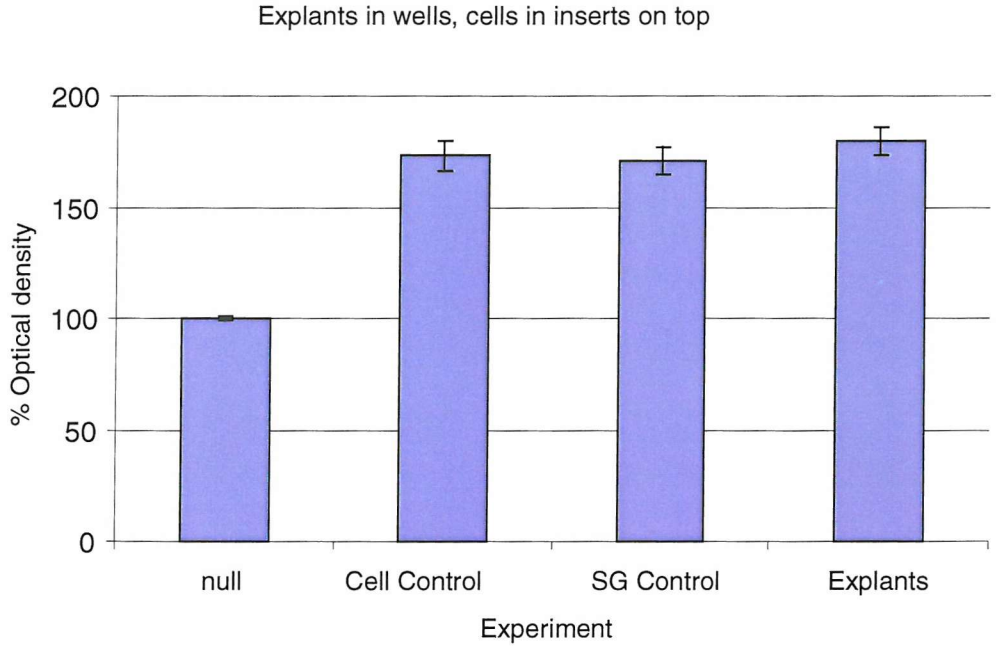

3.2.6 BrDU Staining.

When MGH-U1 cells were stained the GFP fluorescence was quenched by the ethanol fixative, and alternative fixatives did not solve this problem. Thus when the GFP colonies were stained the pre-stained colony was imaged and mapped before BrDU staining of the colony. This demonstrated that a proportion of cells stained positive to BrDU (Fig.3.2.18), although the technique did not allow for accurate quantification.

Fig. 3.2.18 BrDU Stained MGH-U1 colony cells in S phase demonstrating active proliferation.

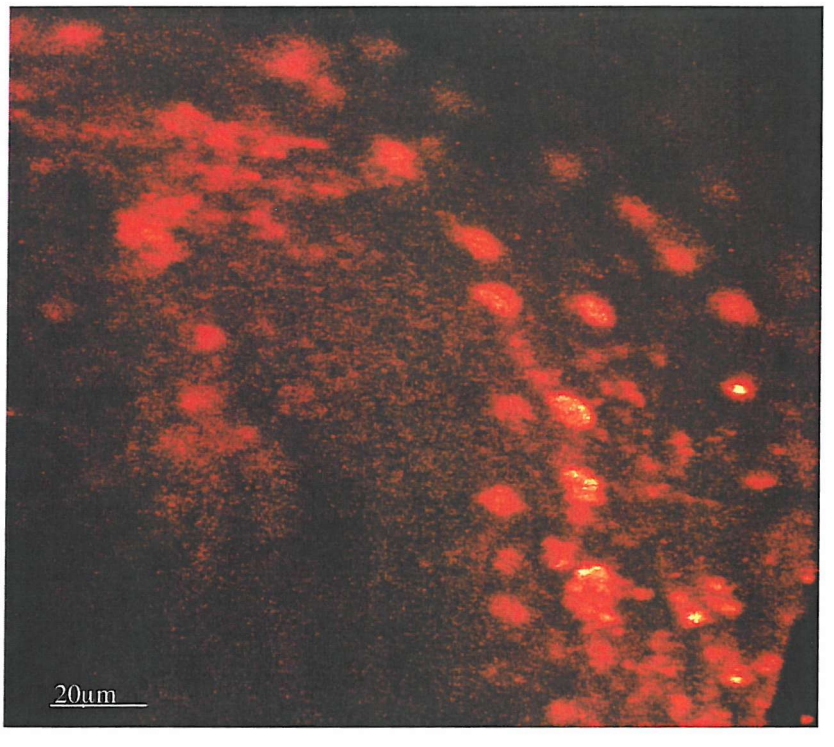

3.3 MTT Assays

3.3.1 Conventional Cytotoxic Agents

The aim of these experiments was to demonstrate the cytotoxicity profile of Epirubicin and Mitomycin C on monolayer cultures of parental and resistant GFP labelled MGH-U1 cells. These experiments were also performed in order to confirm the continuing multi-drug resistance status of the cell lines. The concentrations employed were chosen to allow comparison with those used in the explant colony cytotoxicity experiments. Figure 3.3.1. shows the effects of a one hour exposure on all three cell lines. Note that for Epirubicin the IC<50 for parental cells is well below 1μg/ml, compared to about 100μg/ml for the resistant cell lines. These results are similar to those obtained with non-transfected cell lines(84).

Mitomycin C shows a similar profile (Fig.3.3.2), with an IC>50 of 0.1μg/ml for parental cells and 1μg/ml for resistant cells. Note however, that MMC has a lesser differential effect between parental and resistant cells. For Epirubicin the differential is a factor of $x10^2$, but for MMC this is only $x10^1$. Again these results are similar to those for non-transfected cell lines(63).

The results presented here include those for the transfected MGH-U1-R cell line, but this was not subsequently used in any explant colony experiments.

Fig. 3.3.1 The effects of a 1 hour exposure to Epirubicin assessed at 5 days by MTT assay (below). Error bars are Standard deviations.

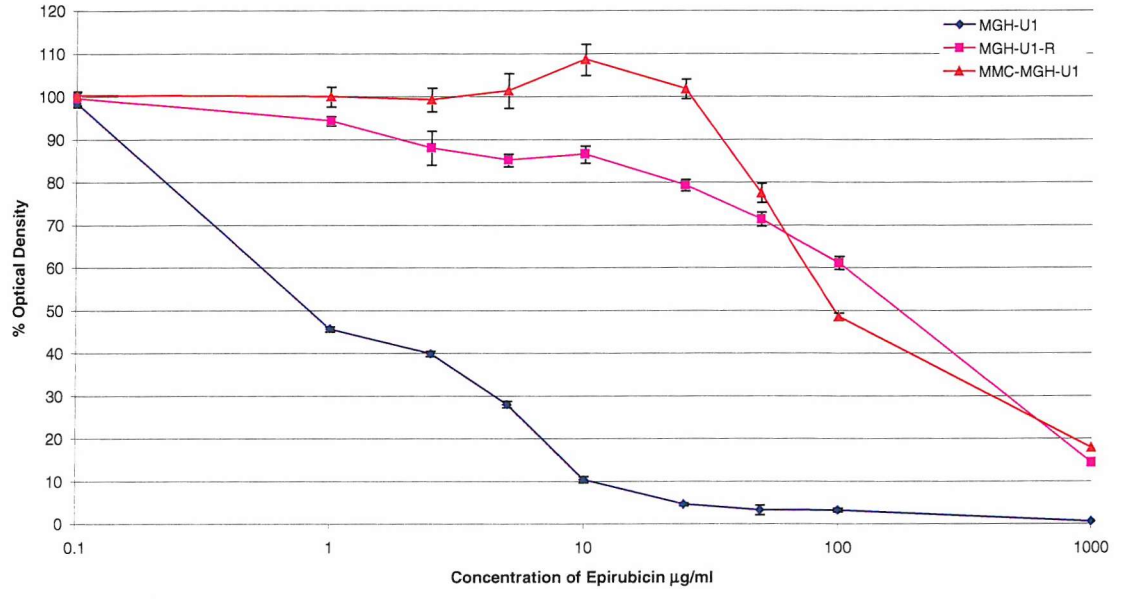

Fig. 3.3.2 The effects of a 1 hour exposure to MMC assessed at 5 days by MTT assay (below). Error bars are standard deviations.

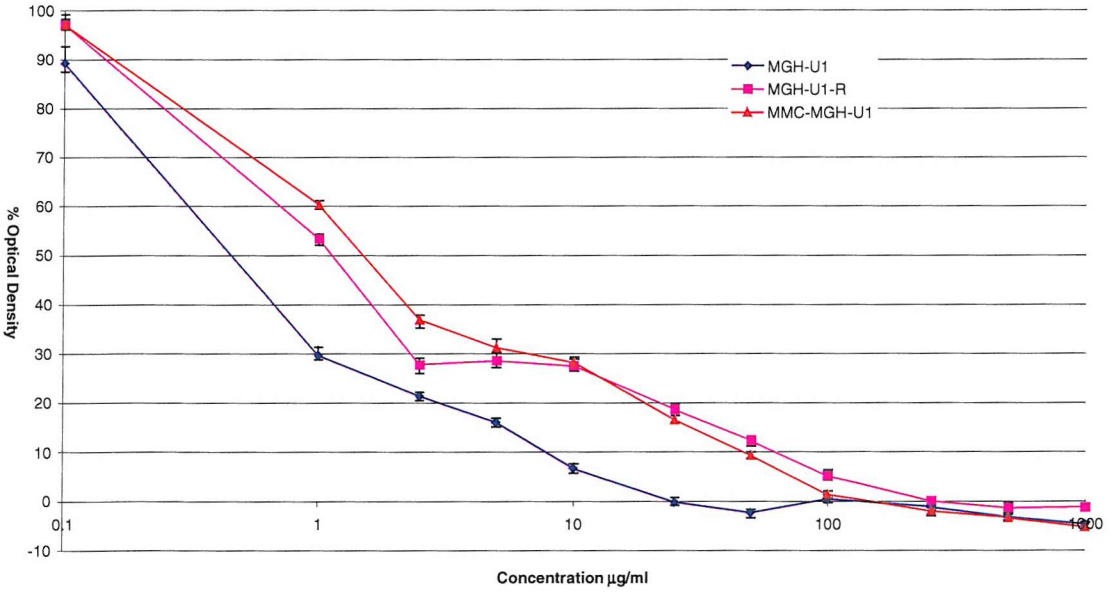

*3.3.2 Estramustine.

The aim of these experiments was to demonstrate the cytotoxicity profile of Estramustine on monolayer cultures of parental and resistant GFP labelled MGH-U1 cells, and also to show any differences in the resistant characteristics of the cells. The results also serve as a comparator for the later explant colony experiments. Figure 3.3.3 shows the effects of a one hour exposure on all three cell lines.

The IC<50 for each of the cell lines are broadly similar at 35μg/ml, 42μg/ml and 22μg/ml for MGH-U1, MGH-U1-R and MMC-MGH-U1 cell lines.

Fig. 3.3.3 The effects of a 1 hour exposure to Estramustine assessed at 5 days by MTT assay (below). Error bars are standard deviations.

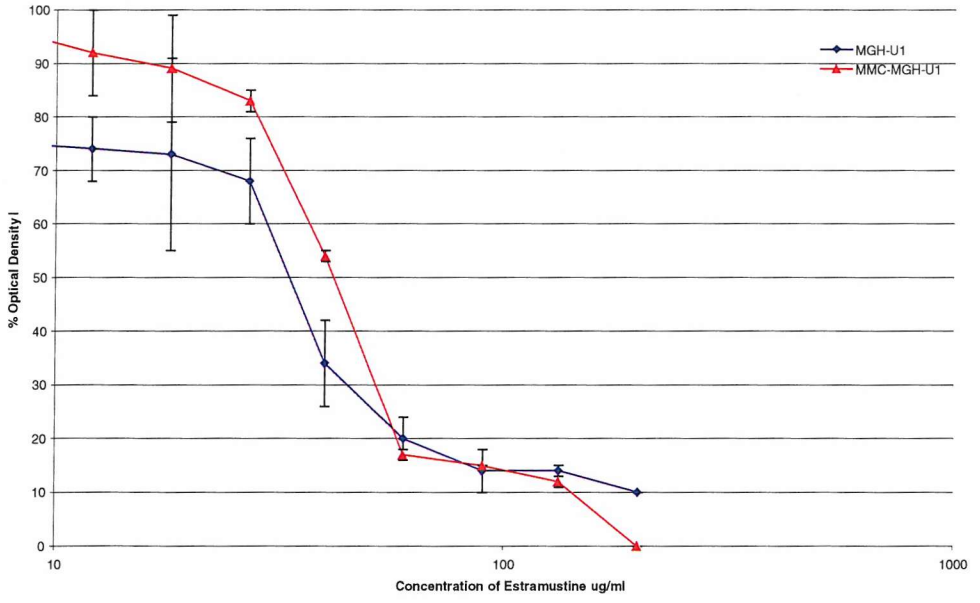

* The majority of the author's work in this section was lost to infection, and so these results are a combination of data supplied by Mr Andrew Jennings FRCS and the author. See Acknowledgements.

3.3.3 MeGLA

The aim of this experiment was to demonstrate the cytotoxicity profile of MeGLA on parental and MMC resistant MGH-U1 cells using the MTT assay. A one hour exposure, equivalent to that commonly used in intravesical therapy, was used and the results read at 5 days. MeGLA shows a steep threshold concentration typically at between 10μg/ml and 50μg/ml, with a calculated IC>50 of 20μg/ml for parental cells and 30μg/ml for resistant cells (Fig.3.3.4). These are in keeping with previous work on MeGLA cytotoxicity. Note that there is similarity in the response of the 2 cell lines. These results are useful for comparison to the results obtained with the explant colony cultures.

Fig.3.3.4 The effects of a 1 hour exposure to MeGLA on MGH-U1 and MMC-MGH-U1 cells assessed at 5 days by MTT assay. Error bars are standard deviations.

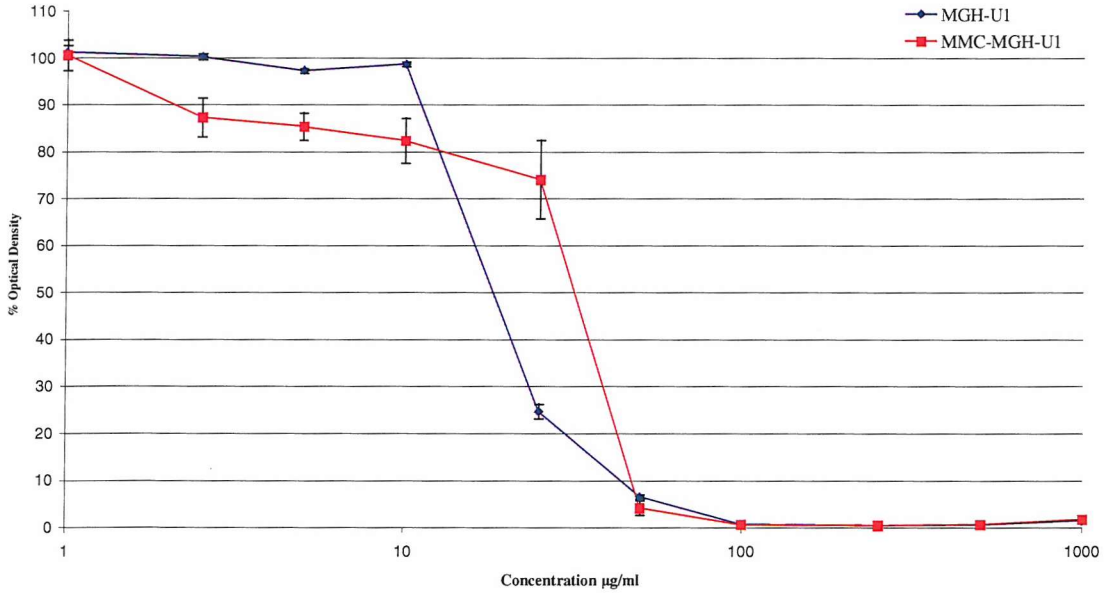

3.3.4 Indole-3-Carbinol

Continuous Exposure.

The aim of these experiments was to investigate the cytotoxic effects of I-3-C on the 3 cell lines for either continuous exposure or a 1 hour exposure, in order to provide comparison to its use in the explant colony experiments. This novel agent showed cytotoxic effects at concentrations greater than 25μg/ml when cells were exposed continuously for 5 days (Fig.3.3.5). Interestingly, there appears to be a differential response between the 3 cell lines at this concentration, with the parental cell lines right shifted compared to the resistant cells, suggesting that the parental cells are more resistant to the agent than the classically resistant cells. The negative values seen at higher concentrations are an artefact produced by subtraction of a null control from the absorption readings taken from these wells. The cause of this is not clear, but is only seen with experiments using I-3-C.

One Hour Exposure to I-3-C

These results show that at a shorter exposure, equivalent to that used in intravesical instillations there is right shift of all IC>50 concentrations, between 100 and 250μg/ml (Fig.3.3.6). Again the parental cell line graph is right shifted compared to that at of the resistant cells suggesting that the latter are more prone to apoptosis with this agent.

These experiments are not intended as a full investigation of this novel agent, but rather to provide a comparison for the cytotoxicity experiments with the explant cultures. Again all three cell lines were used and the results presented here, although the transfected MGH-U1-R cells were not subsequently used in explant experiments.

Fig.3.3.5 The effects of continuous exposure to I-3-C for 5 days on MGH-U1 cells (below). Error bars are standard deviations.

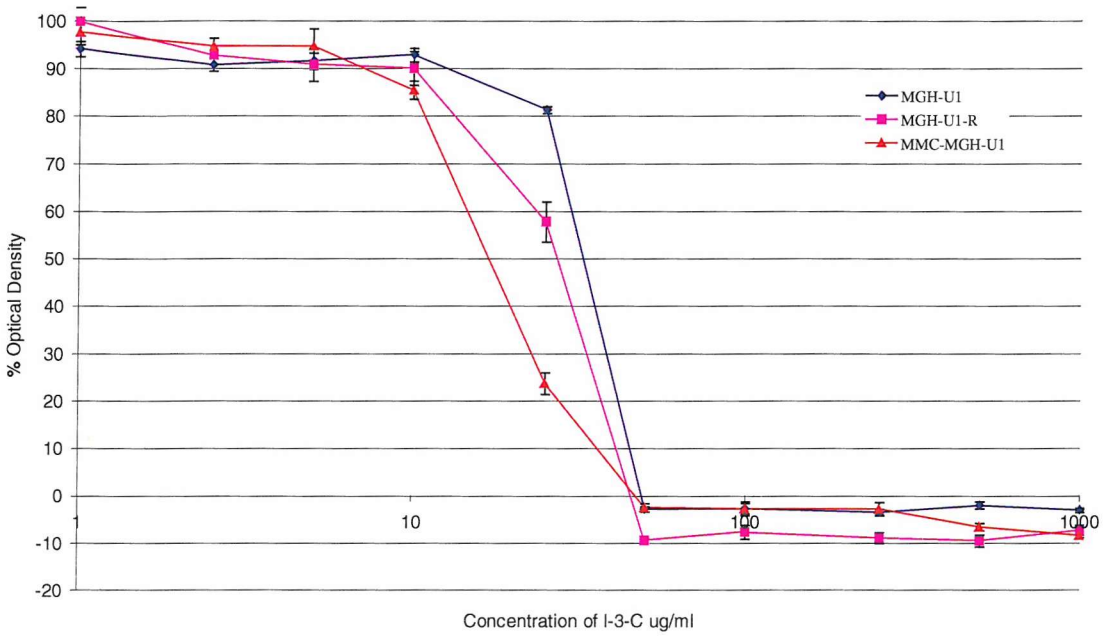

Fig.3.3.6 Graph showing the effects of a 1 hour exposure to I-3-C on MGH-U1 cells assessed at 5 days by MTT assay (below). Error bars are standard deviations.

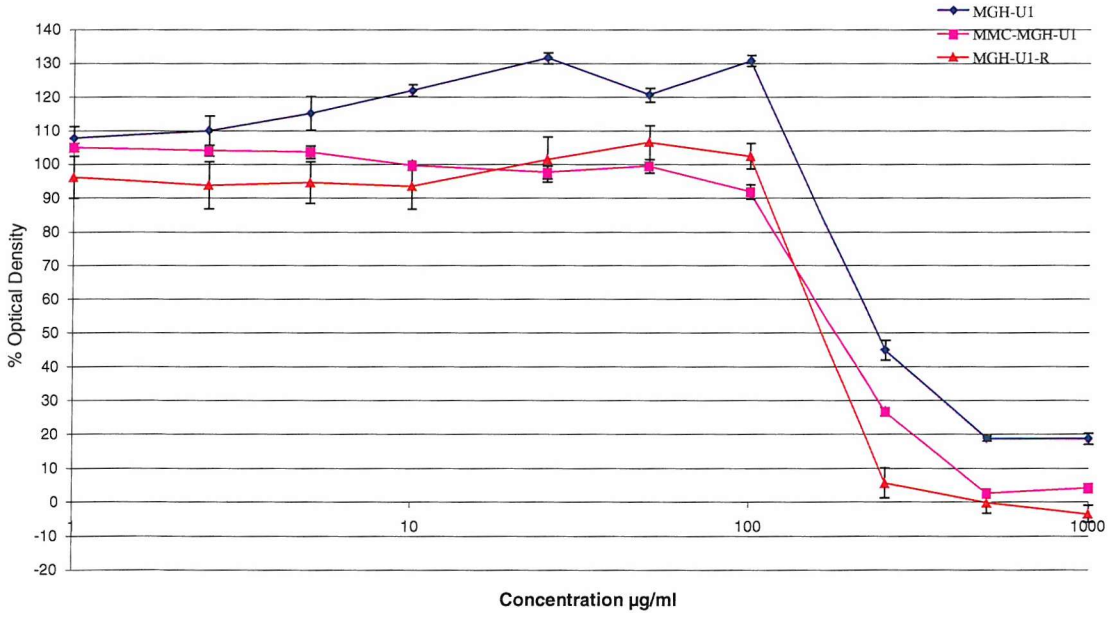

3.4 Explant Cytotoxicity Experiments.

Throughout these results "early" experiments means those experiments carried out in the initial stages of development of the model, and which contribute to the knowledge of model behaviour. "Later" experiments are those carried out using a standard protocol decided after experience with earlier experiments.

3.4.1 Control Experiments.

The aim of these experiments was to establish the characteristics of the explant colonies without exposure to any drug. The colonies were followed over several days and the relative area, mean intensity and integral intensity were recorded. The results of parental and resistant colonies are shown in figures 3.4.1 to 3.4.6. Figure 3.4.1. shows an example of a parental colony which did not show significant growth and slowly deteriorated after only 1 days establishment. However, figure 3.4.2. demonstrates a parental colony which showed steady increase in area, with a doubling time of 8 days. Again, the intensity measurements remain at a similar level. These two examples show that there was some variability in the behaviour of "control" colonies. Overall the average areas of several parental colonies are shown in Fig. 3.4.3. This is an amalgamation of several different experiments, hence the different numbers of colonies averaged for each time point. Also note that the number of colonies reduces as the days go by, because of loss through infection. The standard deviation error bars also illustrate that there was a wide range of growth and in some cases deterioration of control colonies. In general terms there was an increase in the size of the area, with a plateau phase after about 3 days. Intensity measurements as demonstrated in the individual colony graphs were too variable to be used as indicators of residual biomass.

A similar pair of graphs is shown for resistant colonies, along with an average graph (Figs. 3.4.4 to 3.4.6). These experiments showed that there was some variability in control colonies. Overall they show growth as measured by change in area. These experiments also showed that the intensity measurements were not useful as indicators of colony growth. Lastly the average graphs showed what was suspected from experience with the cultures. The MMC resistant MGH-U1 colonies grow better than parental colonies, and survive for longer. Taking a mean of all the values gives an average growth over 11 days of 146.2% for parental colonies and 170.4% for resistant colonies.

MGH-U1 Colonies.

Fig.3.4.1 Graph showing the progress of an explant colony exposed to PBS for 1 hour after 7 days of colony culture, and followed over 7 days.

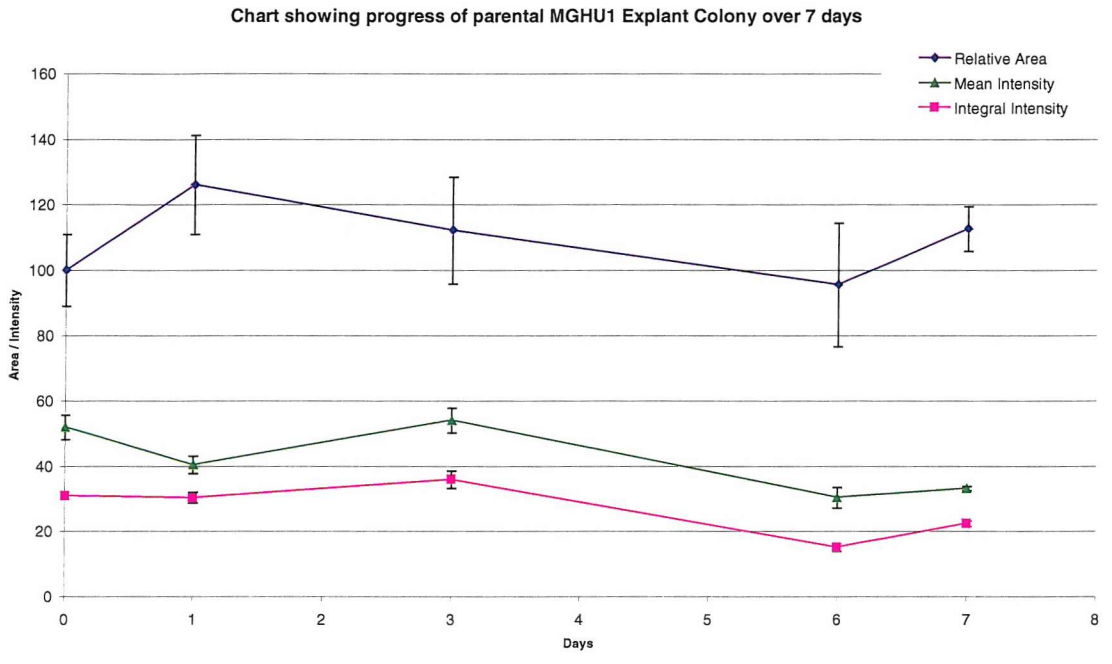

Fig.3.4.2 Graph showing the progress of an explant colony exposed to PBS for 1 hour after 2 days of colony culture, and followed over 8 days.

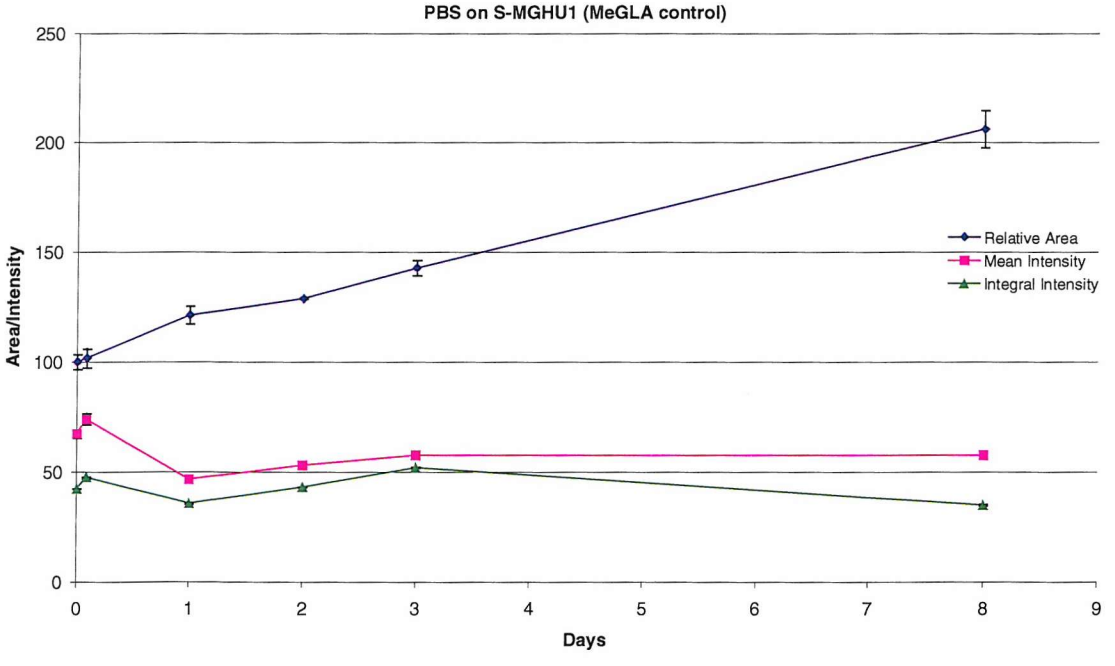

Fig. 3.4.3 Graph showing the average change in relative area of all parental explant colonies (n=20).

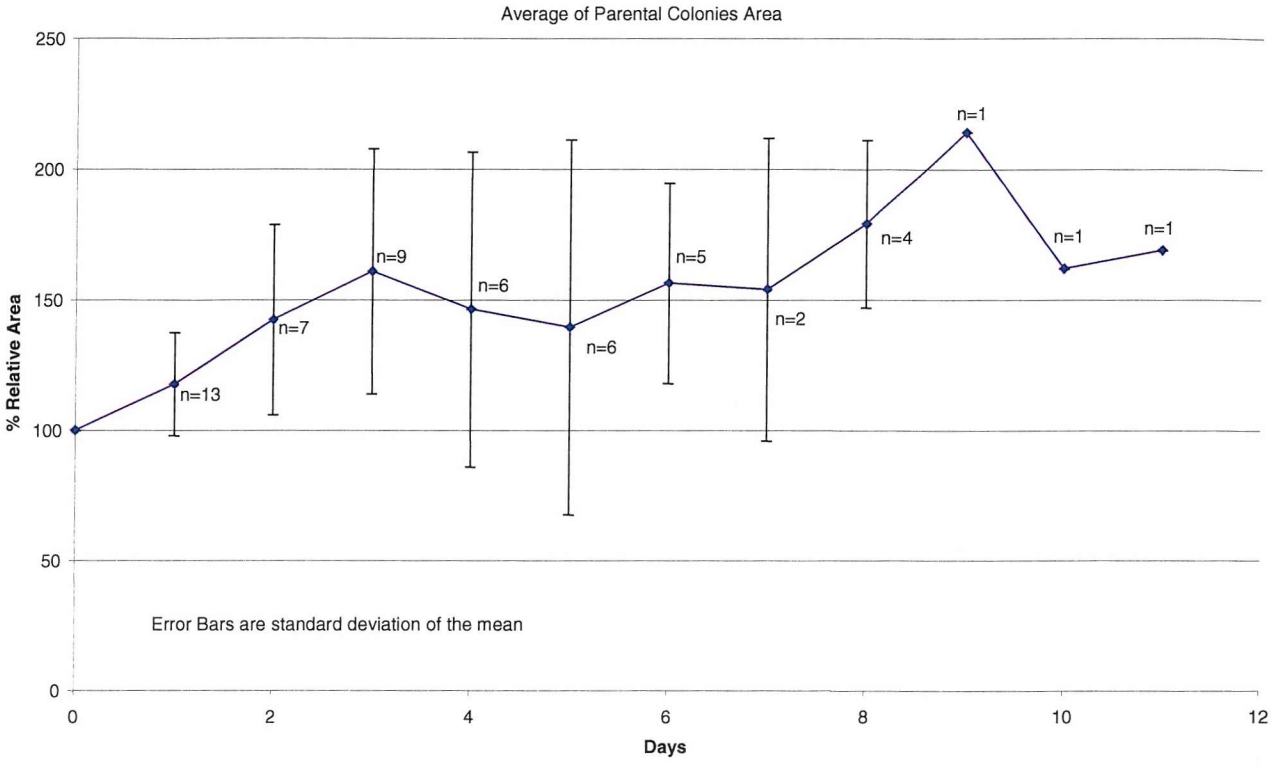

MMC-MGH-U1 Colonies.

Fig.3.4.4 Graph showing the progress of a resistant explant colony exposed to PBS for 1 hour after 7 days of colony culture, and followed over 6 days.

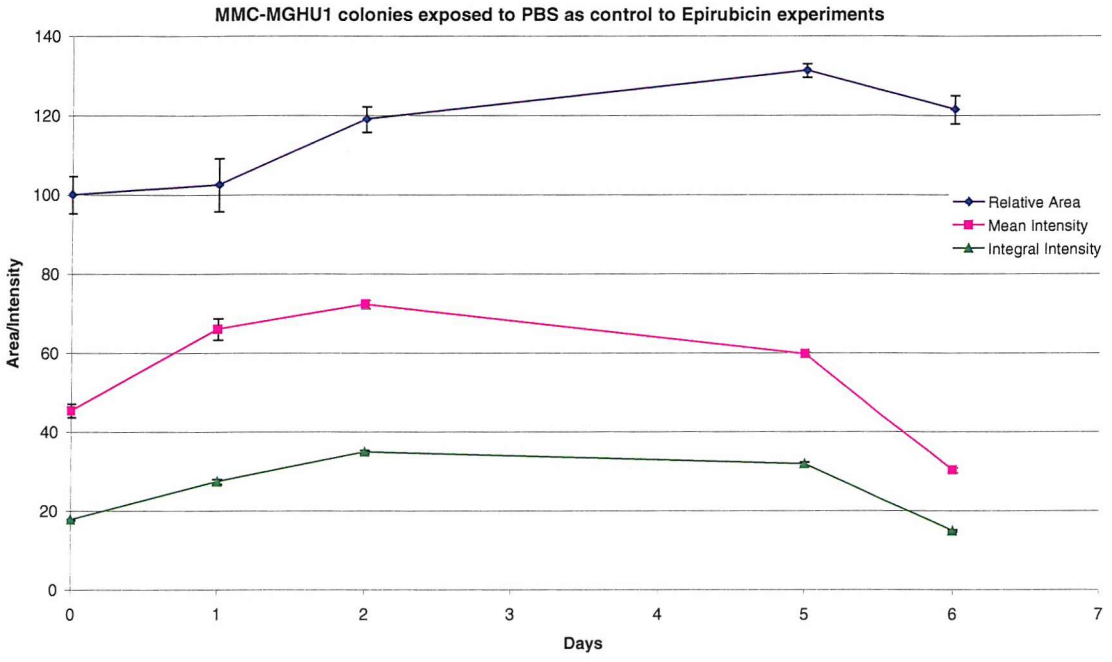

Fig.3.4.5 Graph showing the progress of a resistant explant colony exposed to PBS for 1 hour after 2 days of colony culture, and followed over 7 days.

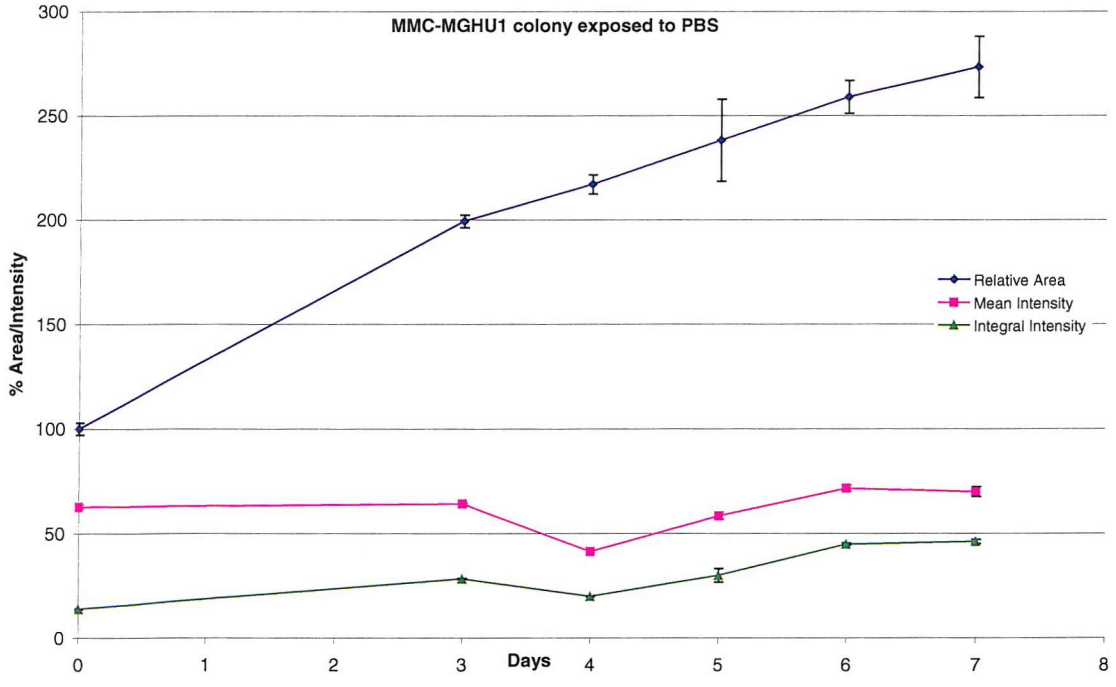

Fig. 3.4.6 Graph showing the average change in relative area of all resistant explant colonies (n=20).

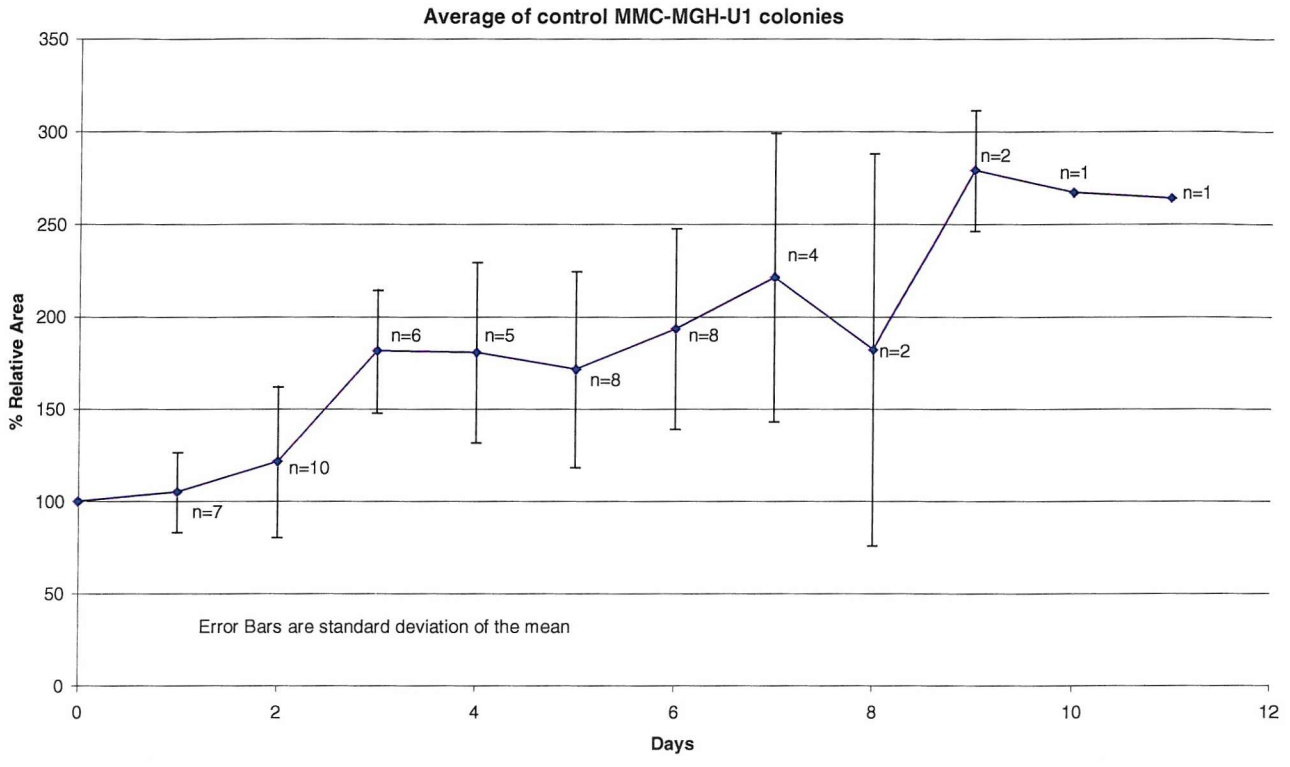

3.4.2 Classical MDR Drugs.

Epirubicin

Early Experiments.

The aim of these experiments was to show that it was feasible to apply a cytotoxic agent (in this case Epirubicin) to the tumour colony and subsequently image it over several days and also show that the cell lines retained their differential MDR properties. As explained in the methods section this protocol was part of initial experiments aimed at producing tumour colonies by growth on the explant surface, thereby creating a multilayered 3 dimensional tumour. Thus cytotoxicity experiments were performed 5 days after seeding to give the colony time to mature. Exposure was for 1 hour with Epirubicin in PBS, with washing and reapplication of DMEM after this period. Both parental and resistant cell lines were used in order to seek the differential response to Epirubicin.

Figures 3.4.7 and 3.4.8 show that after 10μg/ml of Epirubicin there was little change after 1 day, but at 5 days the parental colony was reduced in size by 40%, with a small reduction in size of the resistant colony. At the higher dose of 100μg/ml there was a more immediate effect at 1 day with a 60% and 40% reduction in area of the parental and resistant colonies respectively. By 5 days this had translated to complete destruction of the parental colony, but, interestingly, growth of the resistant colony.

These experiments showed that it was possible to apply a cytotoxic drug to the colonies, which could be subsequently imaged. They retained their expected MDR properties, and also demonstrated the ability to recover from the toxic insult. However, imaging of the colonies showed that the majority were not forming 3 dimensional structures, but rather appeared to be spreading out as a monolayer on the explant surface.

Fig.3.4.7 Chart showing the change in area of parental and resistant MGH-U1 colonies at 1 day and 5 days after exposure to 10μg/ml Epirubicin.

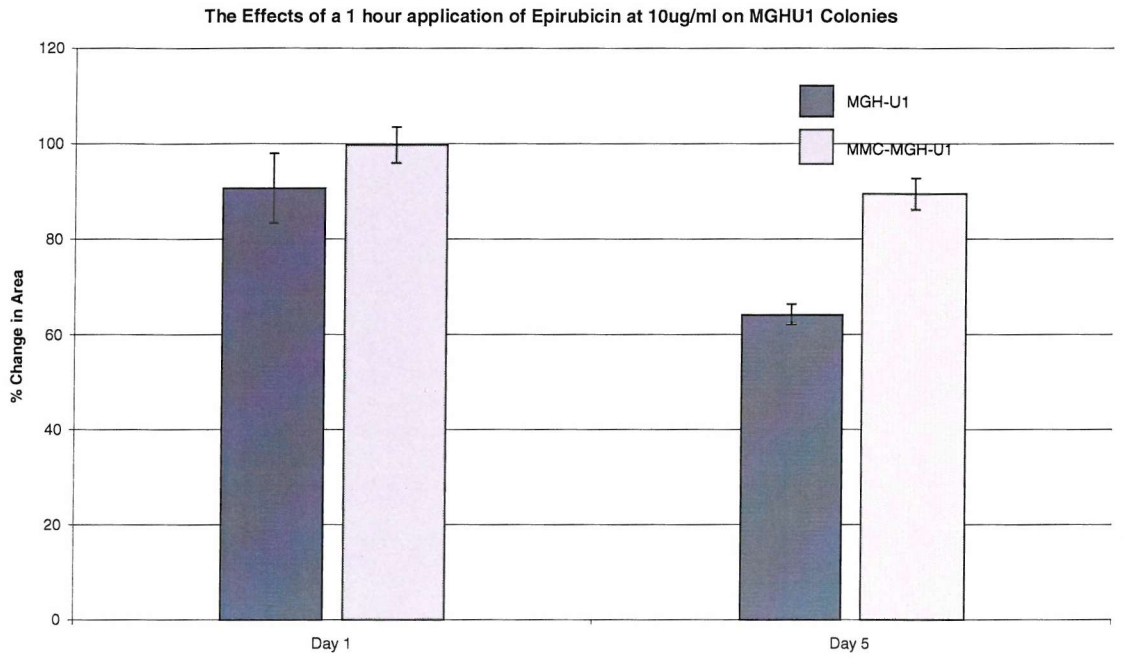

Fig.3.4.8 Chart showing the change in area of parental and resistant MGH-U1 colonies at 1 day and 5 days after exposure to 100μg/ml Epirubicin.

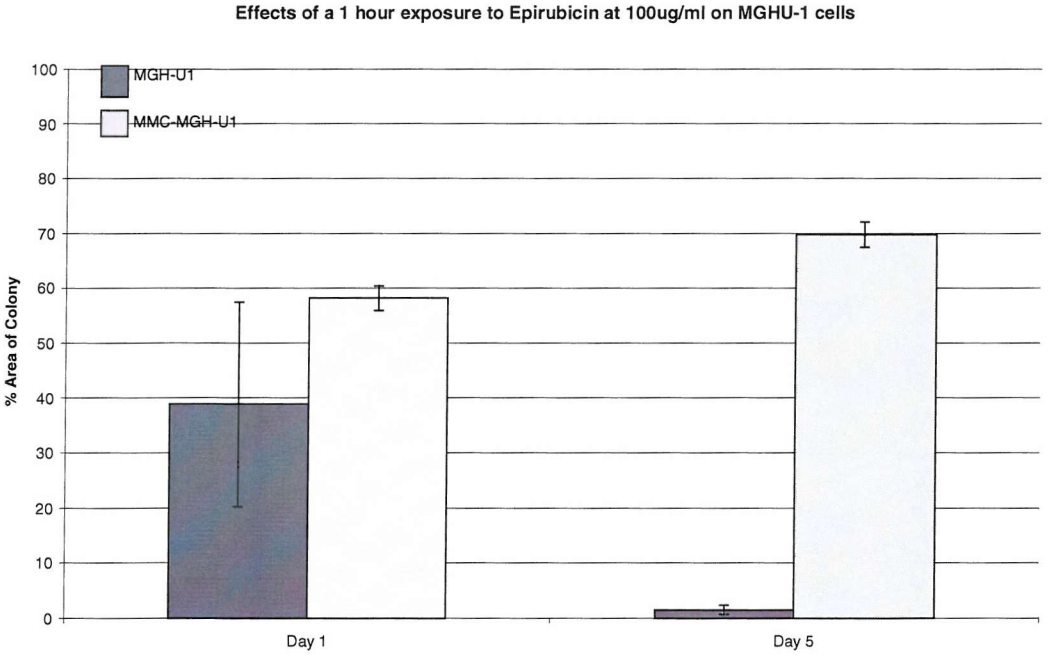

A further series of experiments are shown in figures 3.4.9 to 3.4.12 at doses of 1, 10, and 100μg/ml. They demonstrate growth of the MGH-U1 colonies exposed to 1μg/ml and little change in the colony exposed to 10μg/ml. The MMC-MGH-U1 colony exposed to 100μg/ml initially reduced in relative area, but then recovered to be followed to 8 days, showing a relative increase in area. The intensity measurements show considerable variability and interpretation is difficult. As these are single colony experiments no statistical interpretation can be applied, but they do serve to demonstrate that the model is amenable to quantitative assessment over several days.

Fig. 3.4.9 Graph showing the progress of an MGH-U1 colony over 5 days after exposure to Epirubicin at 1μg/ml. Error bars are standard deviations.

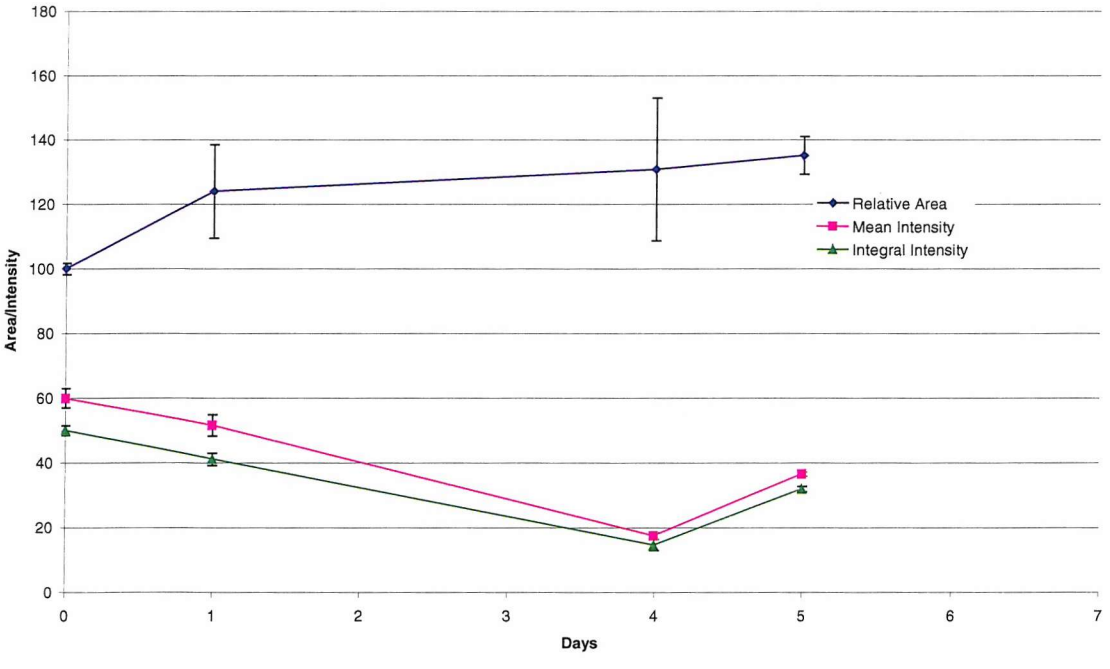

Fig.3.4.10 Graph showing the progress of a parental MGH-U1 colony over 5 days after exposure to Epirubicin at 10µg/ml. Error bars are standard deviations.

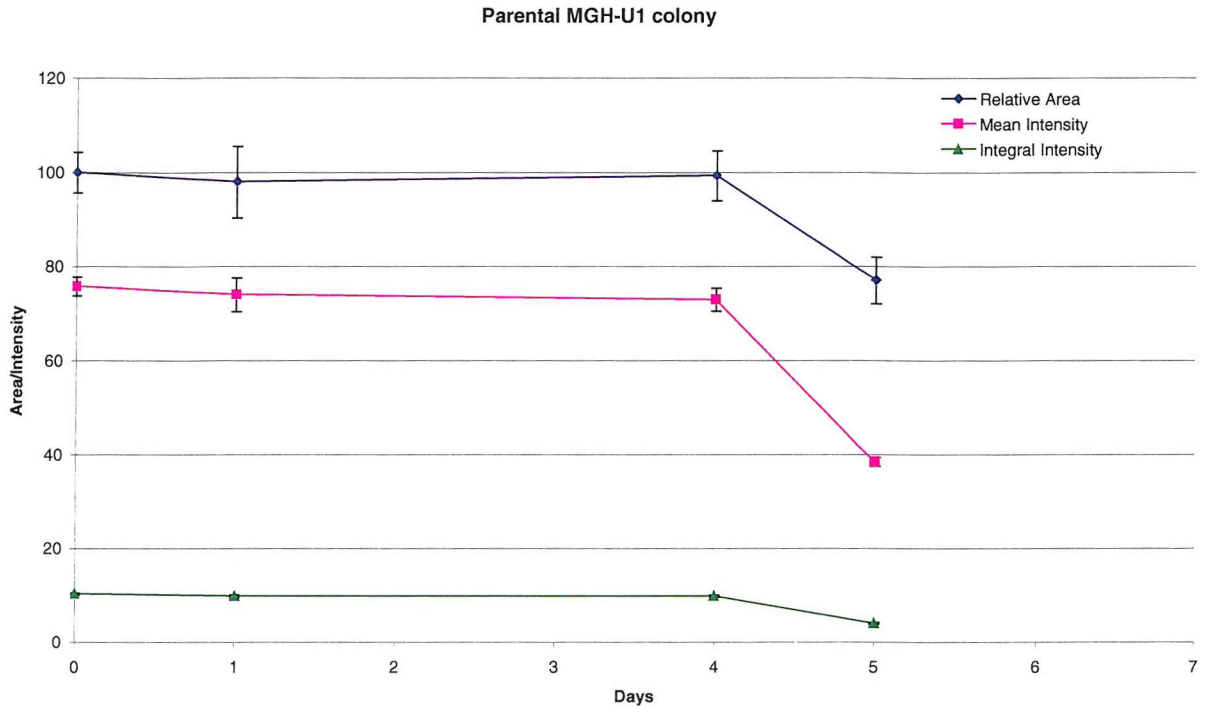

Fig.3.4.11 Graph showing the progress of an MMC-MGH-U1 colony over 8 days after exposure to Epirubicin 10µg/ml Error bars are standard deviations

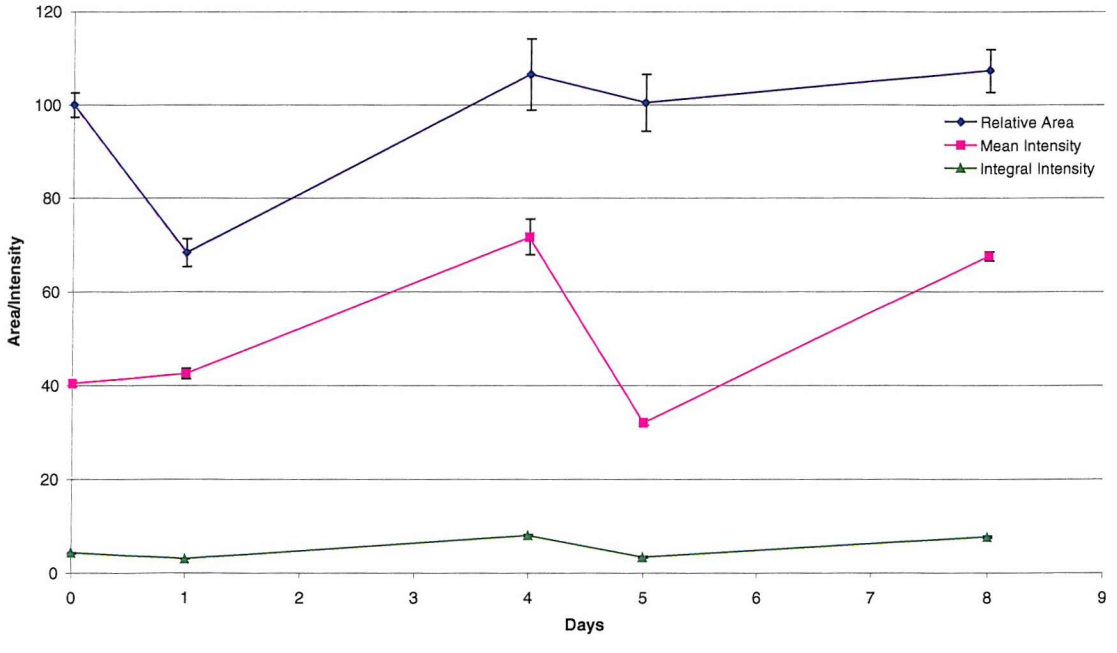

Unfortunately the MMC-MGH-U1 colony exposed to 1ug/ml in this series became infected with fungus, and therefore no results are shown.

Fig.3.4.12a Graph showing the areas of the above colonies exposed to for comparison. Error bars are standard deviations.

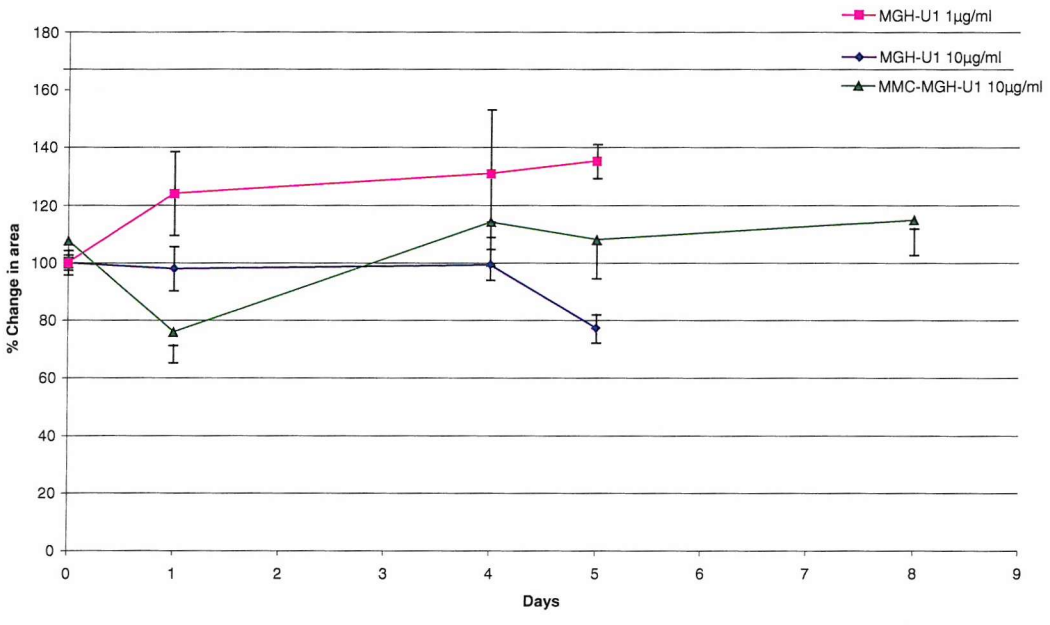

Later experiments.

The colonies were exposed to drug between 12 and 24 hours after seeding of the cell pellet. The aim of this approach was to use the 3-dimensional nature of the cell pellet to mimic a multilayered tumour, and increase the survival of colonies to very high doses of drug, and in doing so mimic more closely the *in vivo* situation. A similar protocol to that described above was followed for drug exposure.

Figures 3.4.13 to 3.4.16 show a series of explant parental colonies each of which was exposed to a $\log_{10}$ concentration of Epirubicin, i.e. from 1μg/ml to 1000μg/ml, and then imaged at 1,3 and 6 days after exposure. The graphs show the relative area, mean intensity and integral intensity for each colony. Error bars shown in the graphs are all standard deviations of the mean. The colonies' areas are then compared on a single graph (Fig.3.4.17) giving a "splay" result. This graph suggests that the best time to assess the cytotoxic effect of drug exposure would be at 5 to 6 days. To enable comparison of the cytotoxic effects at each concentration the area for each colony at each time point after exposure was averaged, and is displayed in figure 3.4.18

These graphs demonstrate the utility of the model. The individual parameters of the colonies once again show that the intensity measurements are not a useful measure of overall biomass, as they stay fairly constant. However, they do add useful information confirming that the colony is viable and also confirming the consistency of area measurement. The summary graphs showing area and average area are useful representations of the expected effects of the cytotoxic agent. A similar set of experiments are shown in figures 3.4.19 to 3.4.22 for resistant colonies, with equivalent splay and summary bar chart (figs. 3.4.23 & 3.4.24). The images obtained for one colony

exposed to a high 1mg/ml dose of Epirubicin are shown in Fig. 3.4.26. If the bar chart is examined it will be seen that the areas of the resistant colonies increases with increasing dose. This is emphasised in figure 3.4.25 showing overall growth of resistant colonies, similar to the overall growth of control colonies.

Fig.3.4.12b Combined FITC and TRITC filters confocal image at low power of an MMC-MGH-U1 GFP tumour colony (green) 1 day after exposure to Epirubicin at 1mg/ml (cf. *in vivo* dosing). Note the Epirubicin take-up in urothelial surface cells (red).

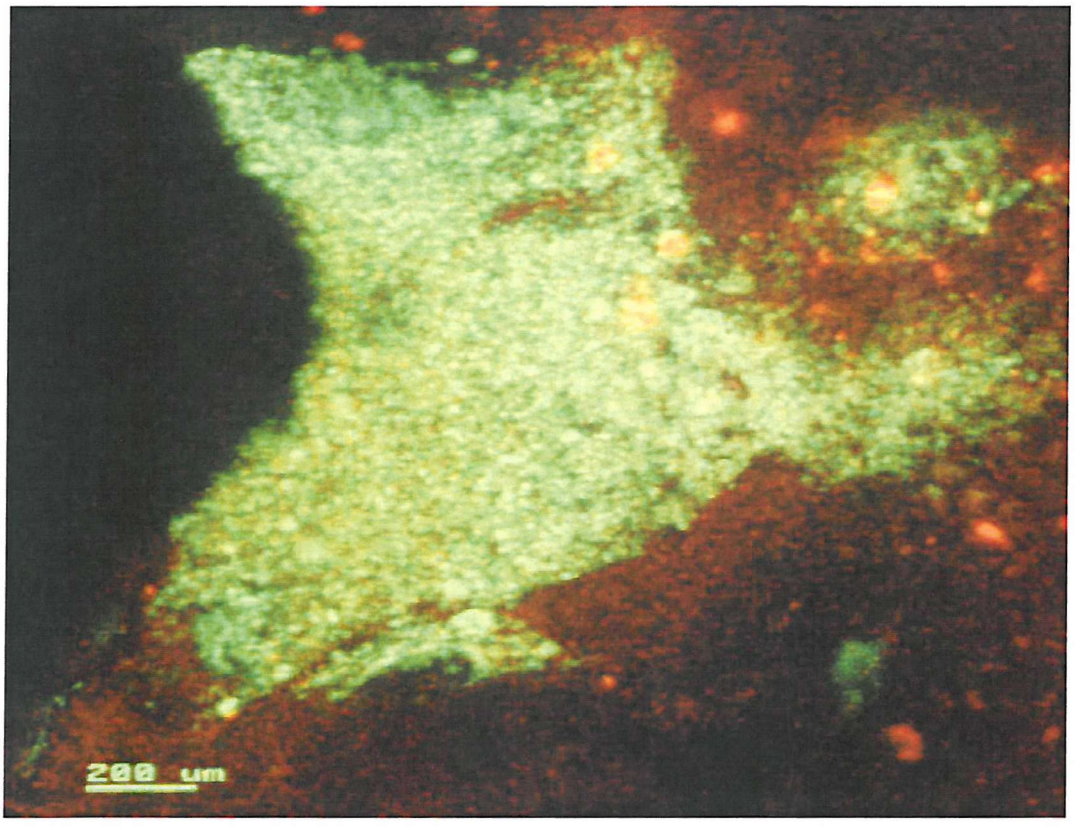

Fig.3.4.13 Graph showing an MGH-U1 colony exposed to 1µg/ml of Epirubicin for 1 hour, over a period of 6 days. Error bars are standard deviations

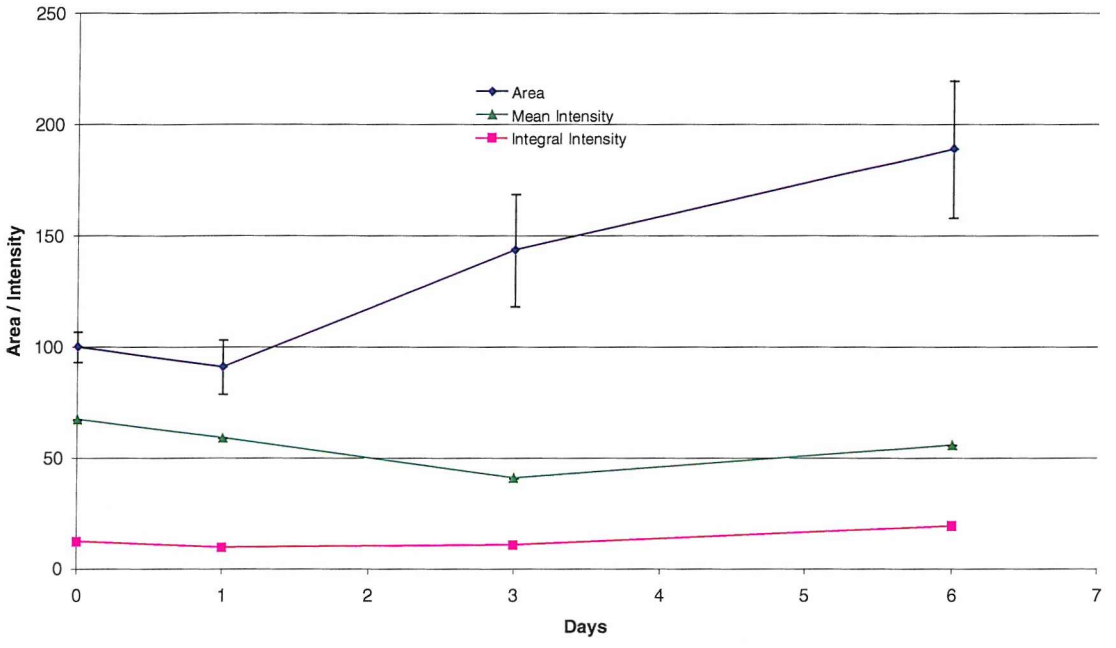

Fig.3.4.14 Graph showing a parental MGHU1 colony exposed to 10µg/ml of Epirubicin for 1 hour, over a period of 10 days.

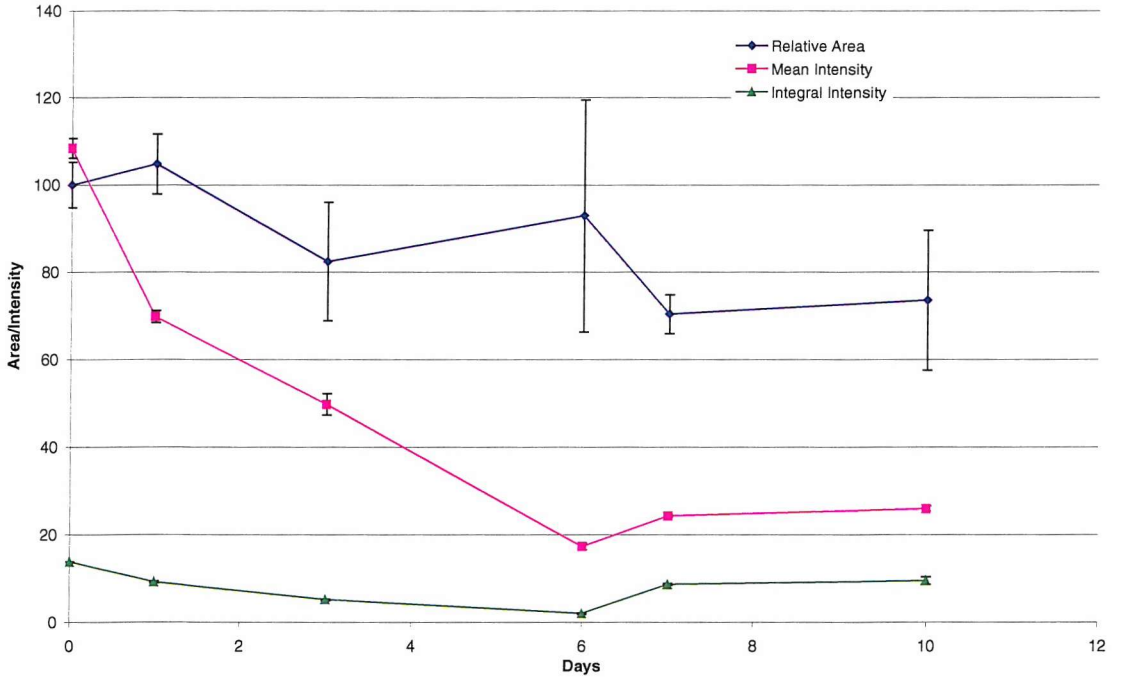

Fig.3.4.15 Graph showing a parental MGH-U1 colony exposed to 100µg/ml of Epirubicin for 1 hour, over a period of 7 days.

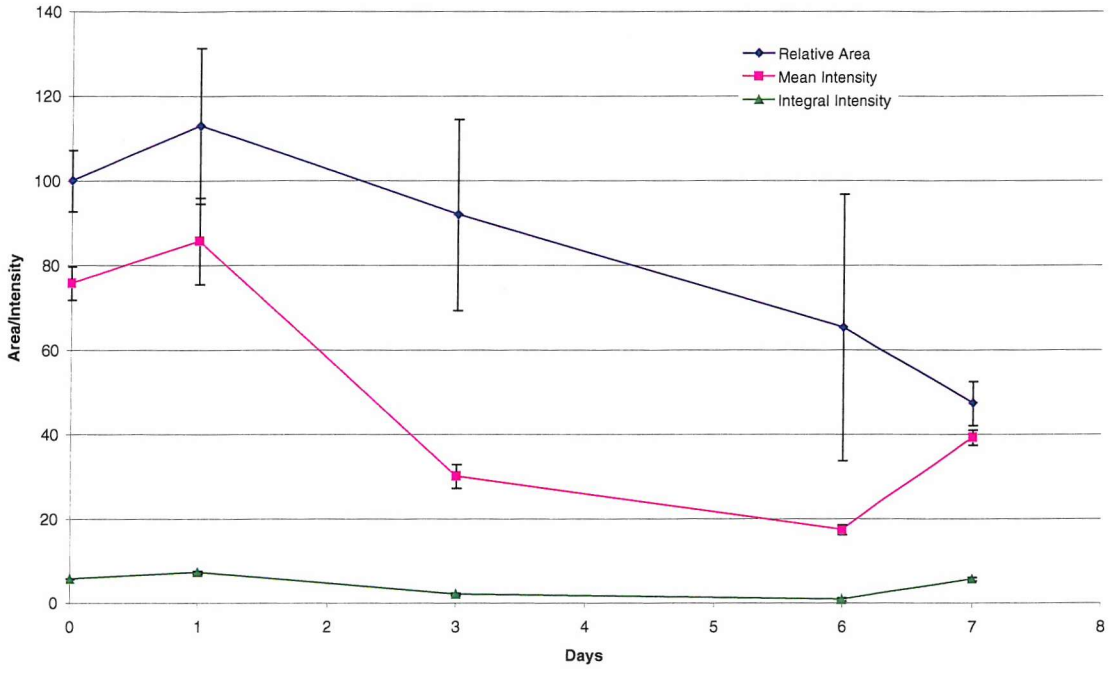

Fig.3.4.16 Graph showing a parental MGH-U1 colony exposed to 1mg/ml of Epirubicin for 1 hour, over a period of 7 days.

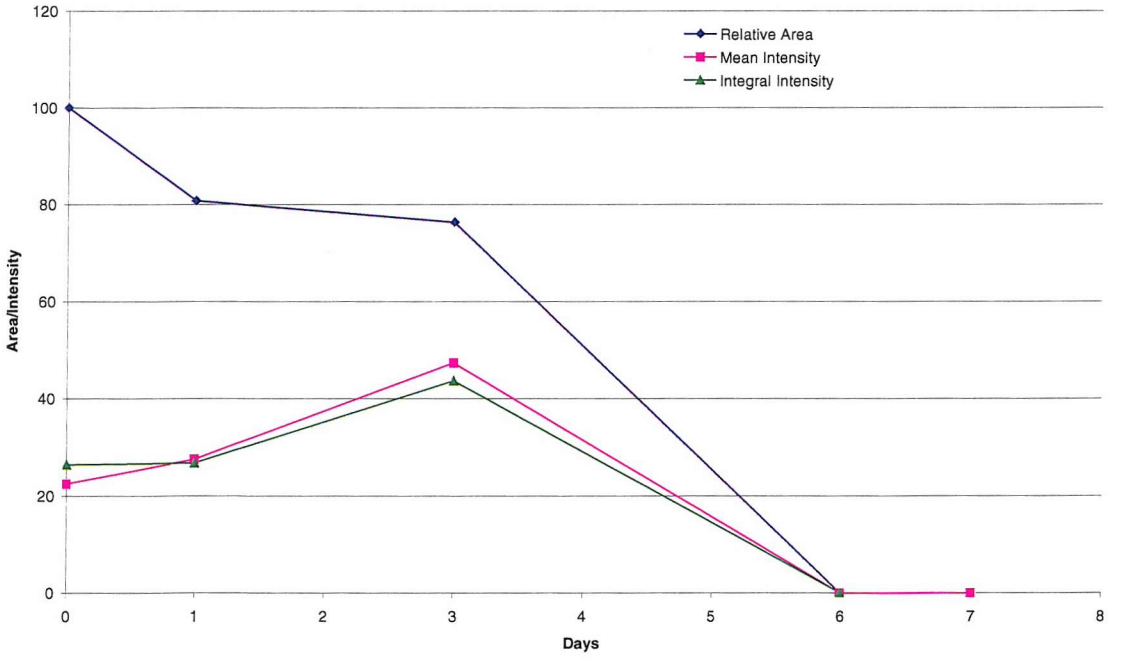

Fig.3.4.17 Graph showing the areas of MGH-U1 colonies exposed to the above concentrations of Epirubicin for 1 hour, measured up to 6 days.

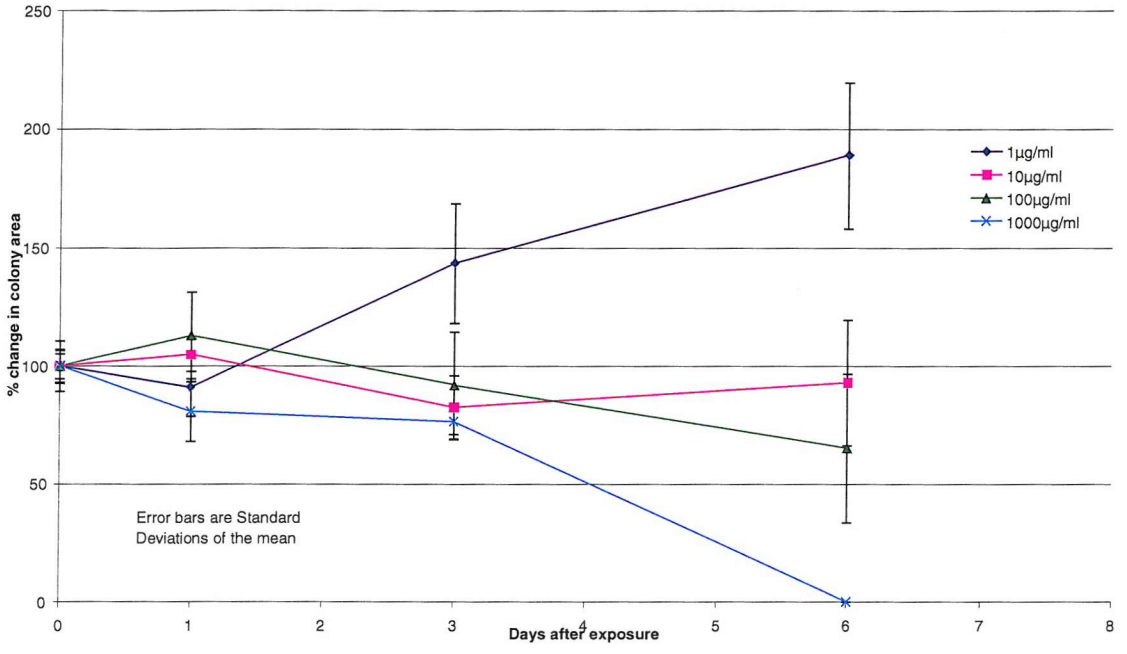

Fig.3.4.18 Graph showing the average area of the above colonies exposed to Epirubicin, and measured over 6 days.

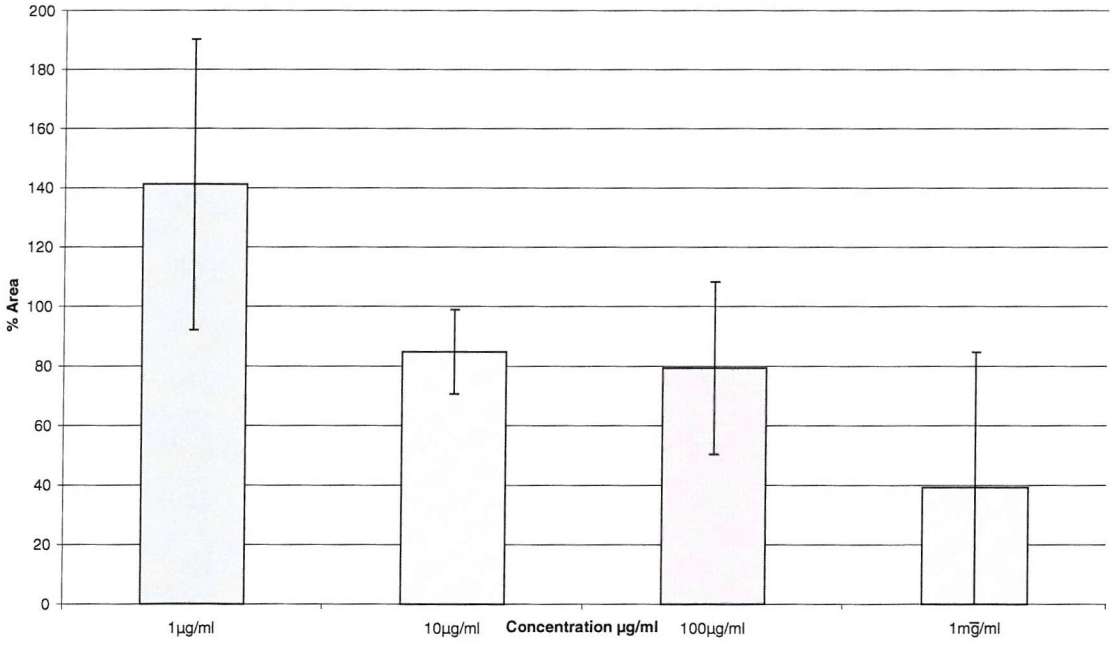

Fig.3.4.19 Graph showing an MMC resistant MGH-U1 colony exposed to 1µg/ml of Epirubicin for 1 hour, over a period of 7 days.

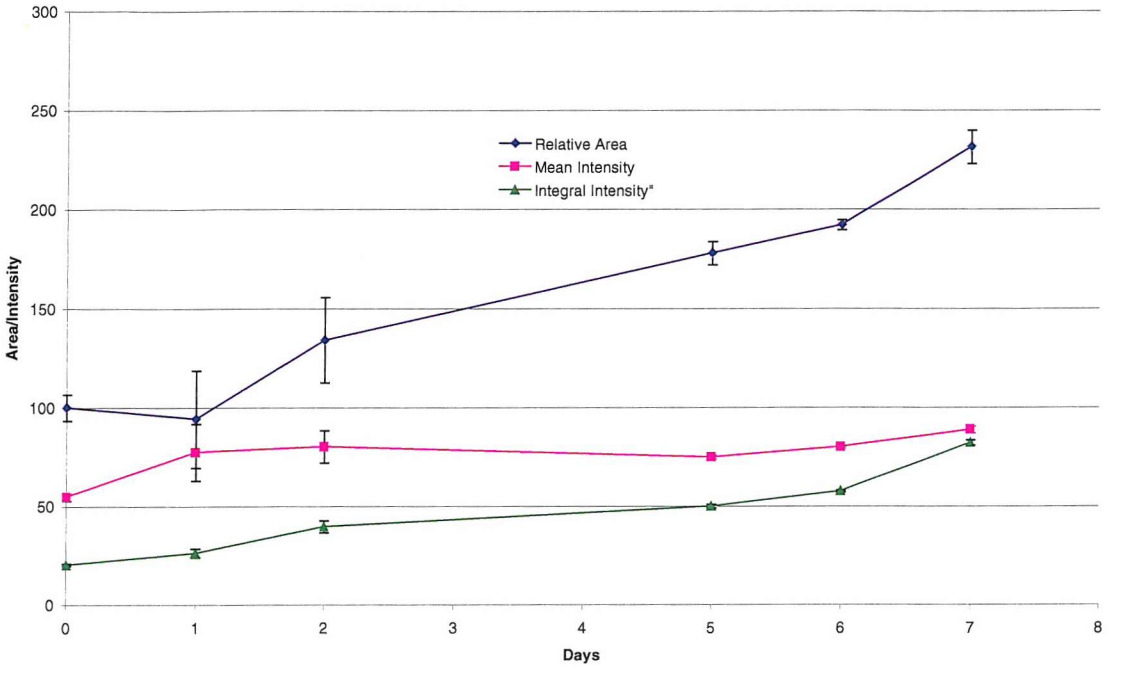

Fig.3.4.20 Graph showing an MMC resistant MGH-U1 colony exposed to 10µg/ml of Epirubicin for 1 hour, over a period of 7 days.

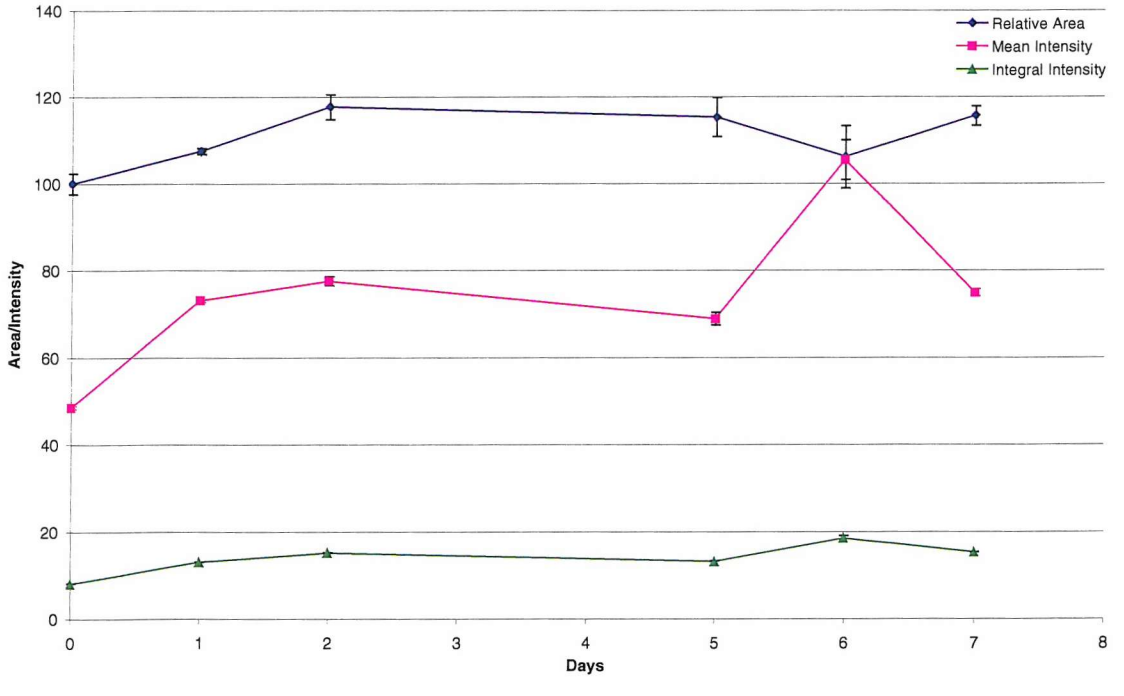

Fig.3.4.21 Graph showing an MMC resistant MGH-U1 colony exposed to 100µg/ml of Epirubicin for 1 hour, over a period of 7 days.

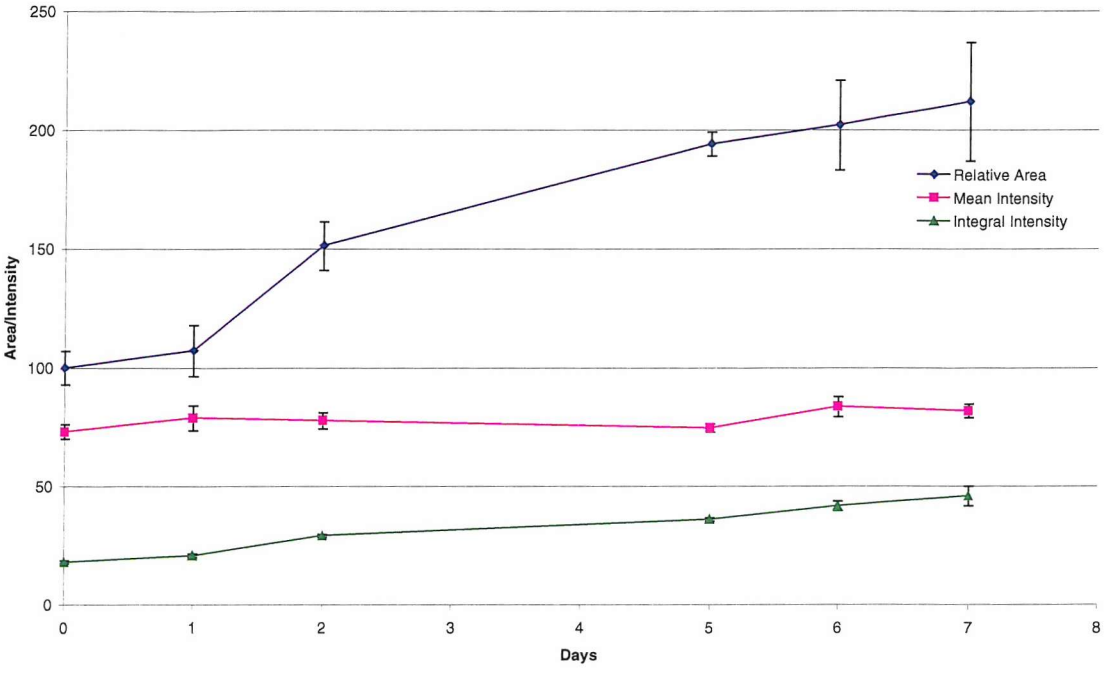

Fig.3.4.22 Graph showing an MMC-MGH-U1 colony exposed to 1mg/ml of Epirubicin for 1 hour, over a period of 9 days.

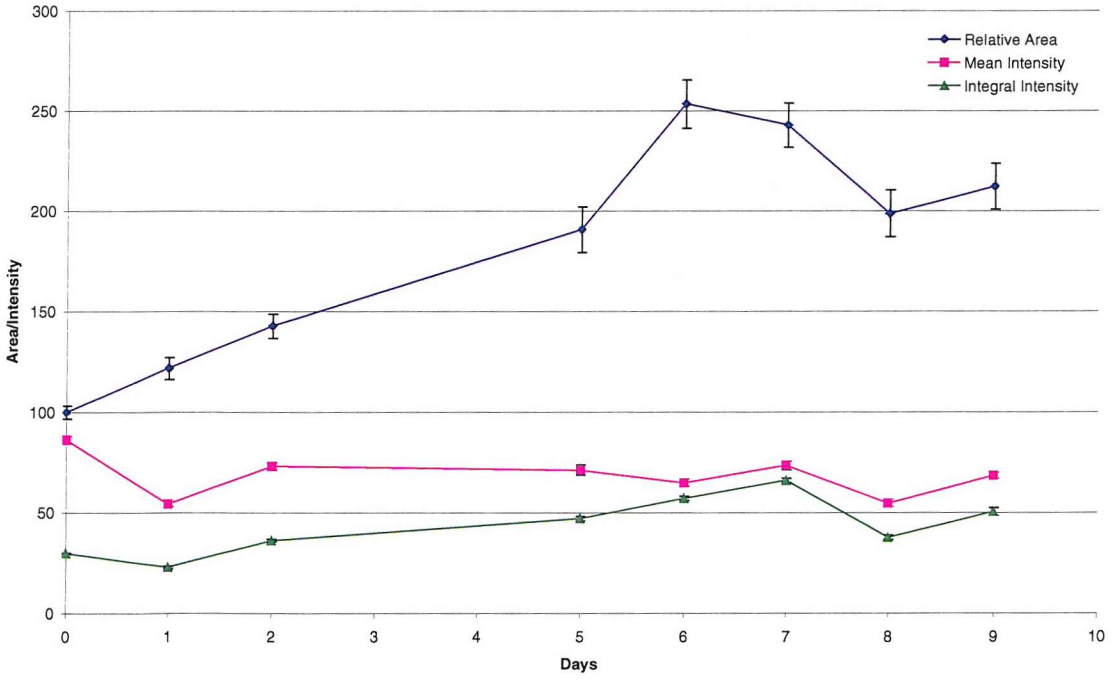

Fig.3.4.23 Graph showing the areas of each MMC resistant MGH-U1 colony exposed to the above concentrations of Epirubicin for 1 hour, over 7 and 9 days.

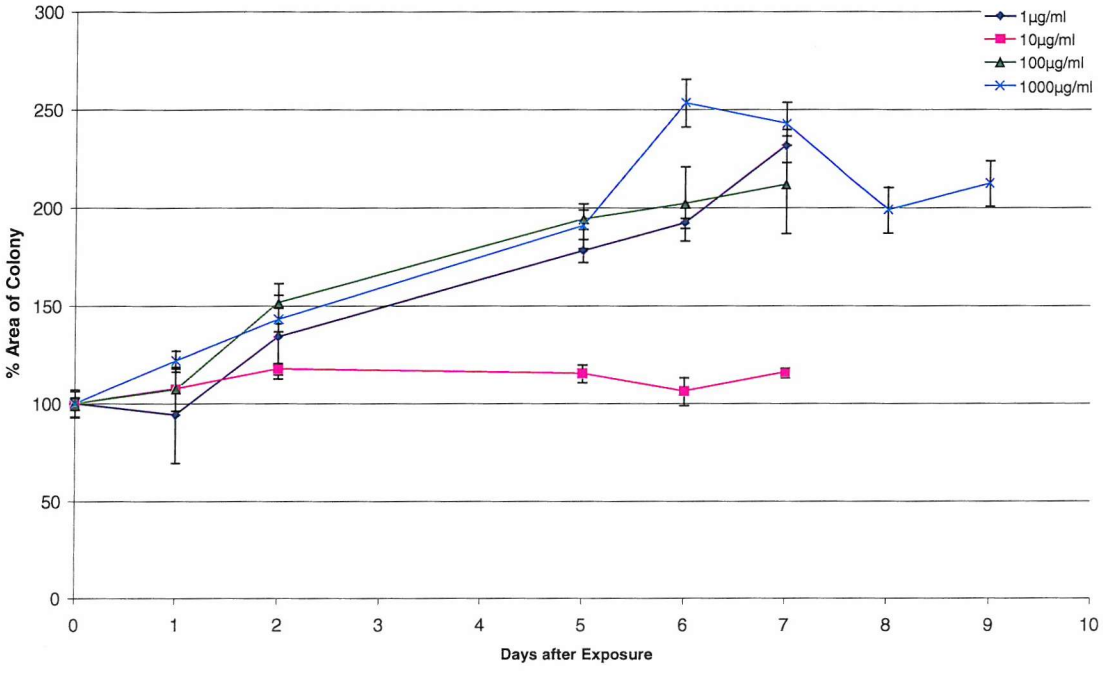

Fig.3.4.24 Graph showing the average area of MMC-MGH-U1 colonies exposed to Epirubicin for 1 hour, over 9 days.

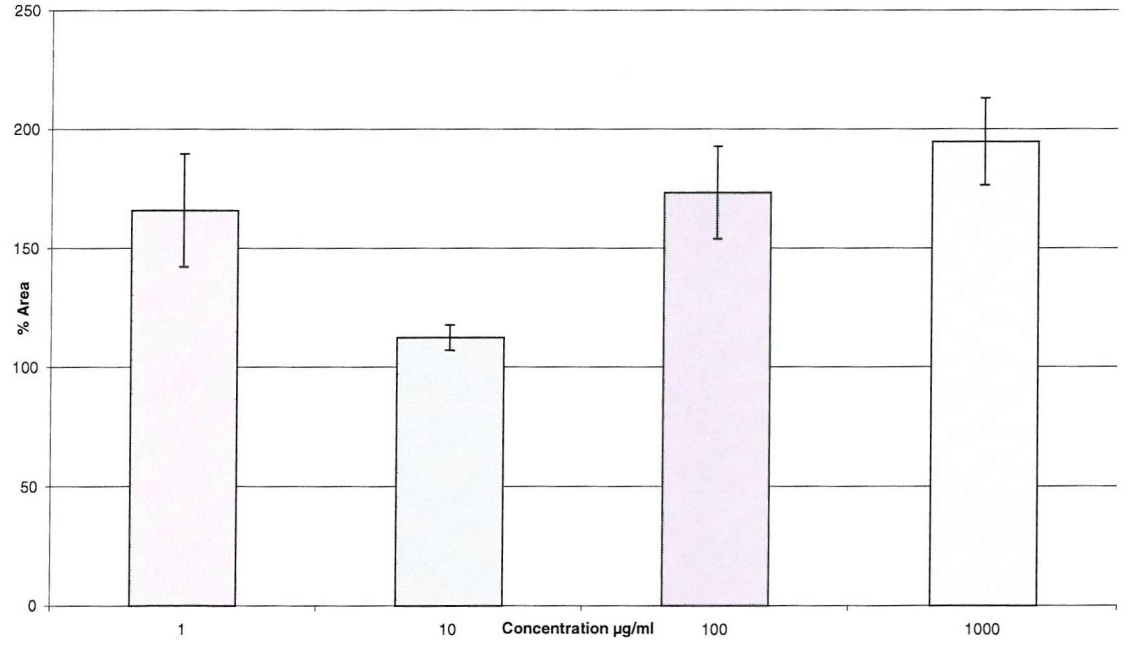

Fig.3.4.25 Graph showing the overall mean of all 4 resistant explant colonies exposed to Epirubicin at various concentrations

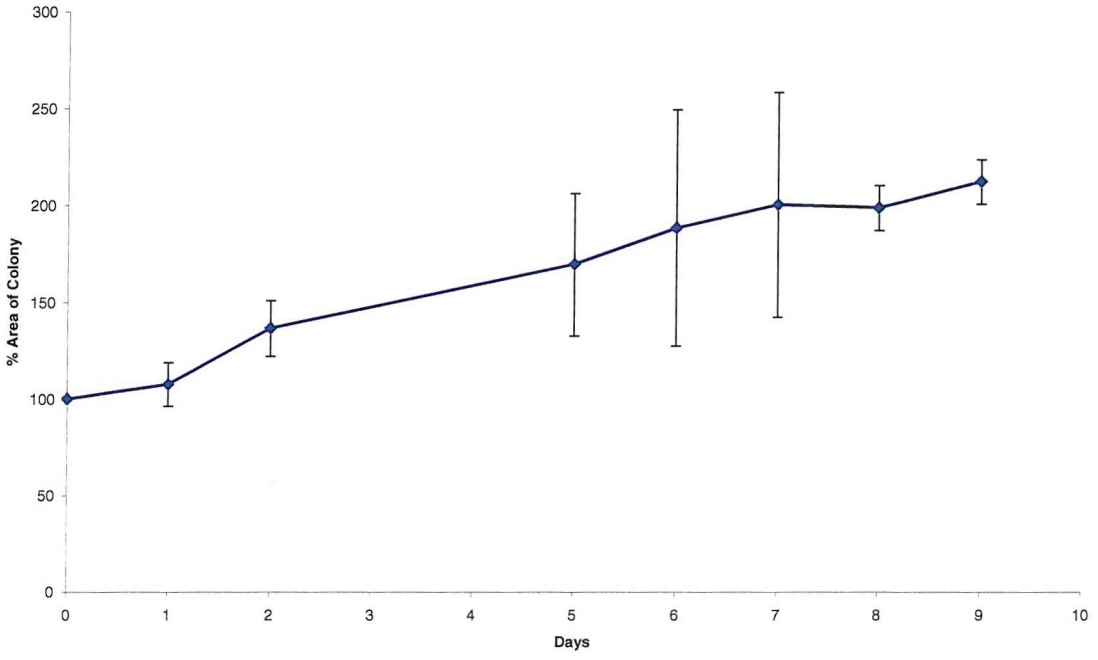

Fig.3.4.26 Confocal Images of the MMC-MGH-U1 colony exposed to Epirubicin for 1 hour at 1mg/ml. Numbers indicate days after exposure.

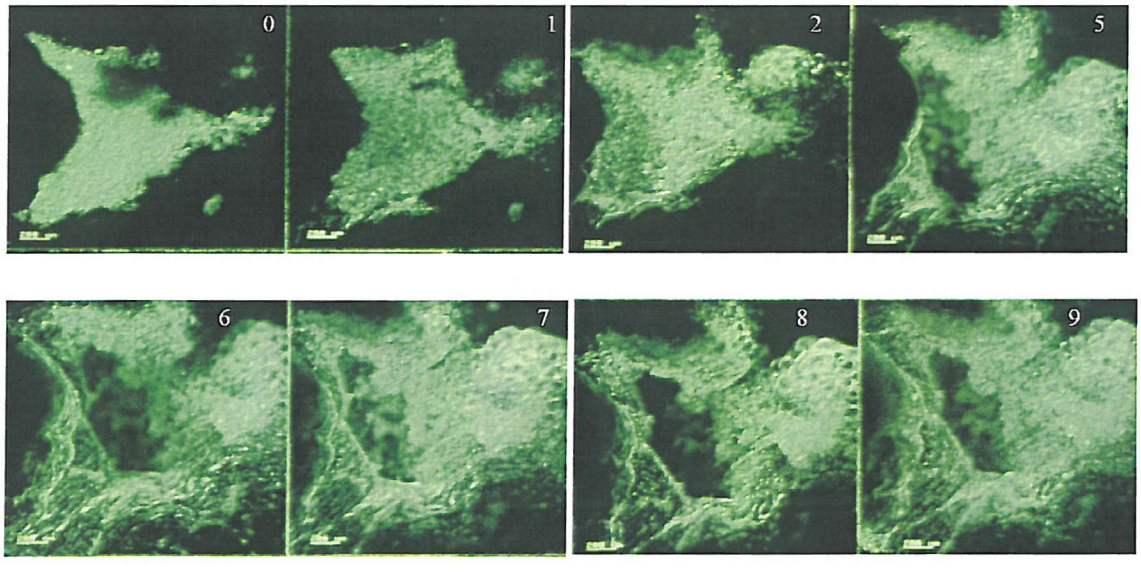

Mitomycin C

Early experiments.

The aim of these experiments was to show that it was feasible to apply a cytotoxic agent (in this case Mitomycin C) to the tumour colony and subsequently image it over several days and also show that the cell lines retained their differential MDR properties. Like the Epirubicin experiments, these early experiments form part of the learning curve of the development of the model. A similar protocol was used for the experiments, with drug exposure 5 days after seeding. The results shown in Figure 3.4.27 show that the parental colonies were destroyed by both doses of MMC, whereas the resistant colonies were either unaffected or showed some reduction in size at the higher concentration.

The second graph shows an early experiment in which the resistant colony was visualised on two separate occasions after exposure to 100μg/ml MMC (Fig.3.4.28), demonstrating that it was possible to follow the colony over several days, and for the colony to survive relatively unchanged at a dose of MMC 40 times the IC>50 for monolayer lines (2.5μg/ml). The parental counterparts for this experiment were lost to fungal infection and were not repeated in the same format as the development of the model had progressed. Later experiments effectively repeated these "lost" results, although at a more advanced stage of development of the model, as explained below.

Fig.3.4.27 The effects of a 1 hour exposure to MMC at 10 and 100µg/ml on MGH-U1 and MMC-MGH-U1 colonies, 2 days after exposure.

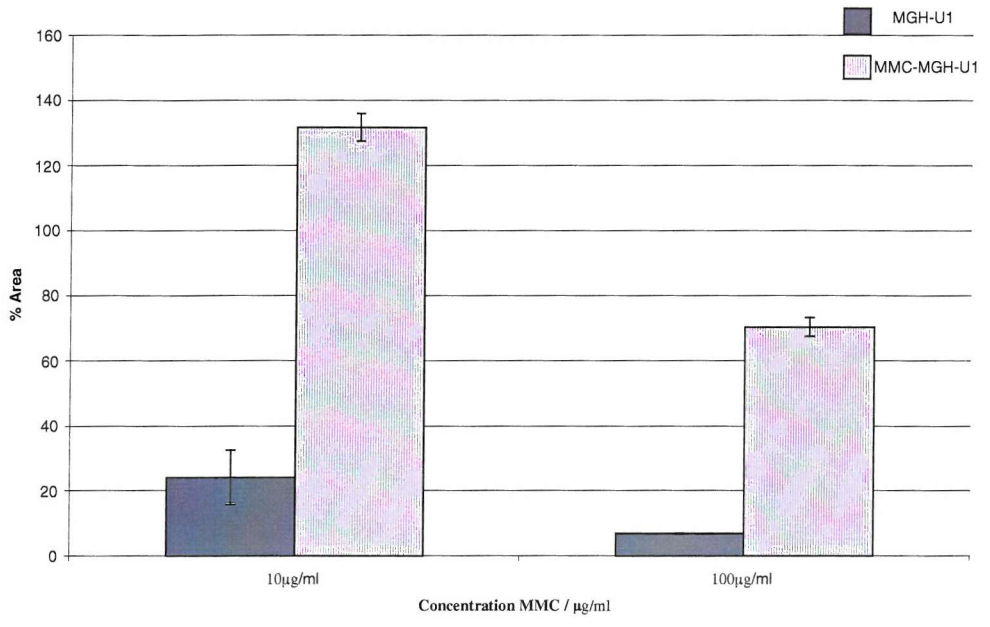

Fig.3.4.28 The effects of a 1 hour exposure to 100µg/ml MMC on an MMC-MGH-U1 colony at 1 and 3 days.

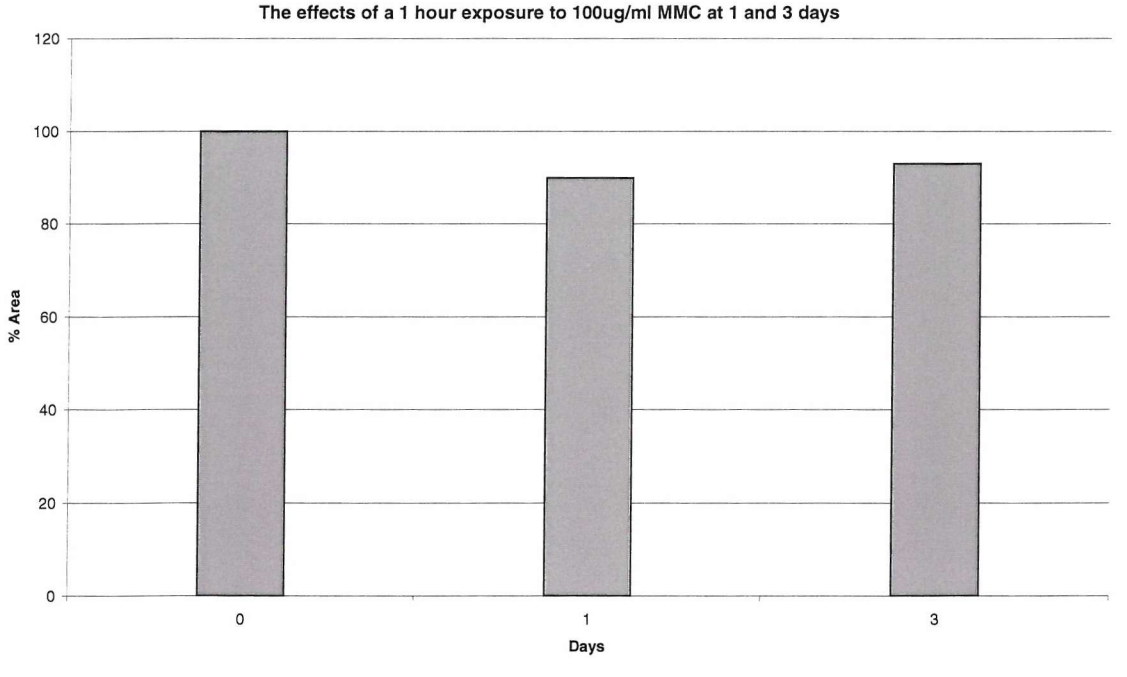

Later Experiments.

As with the Epirubicin experiments drug exposure was 12 to 24 hours after cell pellet seeding, for the same reasons outlined in that section, and as described in the methods as the standard protocol. The results are presented in a similar format, with 4 graphs showing the progress of parental and resistant explant colonies, followed by a summary area splay graph and average bar chart (figs.3.4.29 to 3.4.40).

The experiments performed with MMC had a long run over 11 days for both parental and resistant colonies. This allowed effects in the later stages to be observed, and showed that after 5 to 6 days there was deterioration in the colonies exposed to the higher concentrations of MMC, and which had shown initial growth. Unfortunately, it was impossible to know if this effect was due to the exposure to MMC or because of a more general property of the colonies. The control colonies rarely survived beyond 7 days, and so it is not possible to give a proper comparison to several controls.

Nevertheless, the splay graph and overall area average bar chart demonstrate again the unique feature of this model in being able to follow a tumour colony for several days. Comparing the parental and resistant colonies showed that the expected differential effects were maintained in the model. The parental colony was destroyed by the 1mg/ml dose, whereas the resistant colony still retained on average 50% of its area over the 11 day period. This compares to the IC>50 for resistant cells in monolayer of 2.5μg/ml. Thus, whereas early experiments enabled the colony to survive doses of 40x, these experiments showed survival of the colony at a dose 400x the IC>50 for monolayers.

Parental colonies.

Fig.3.4.29 Graph showing the progress of a parental MGH-U1 colony over 11 days after exposure to Mitomycin C at 1µg/ml

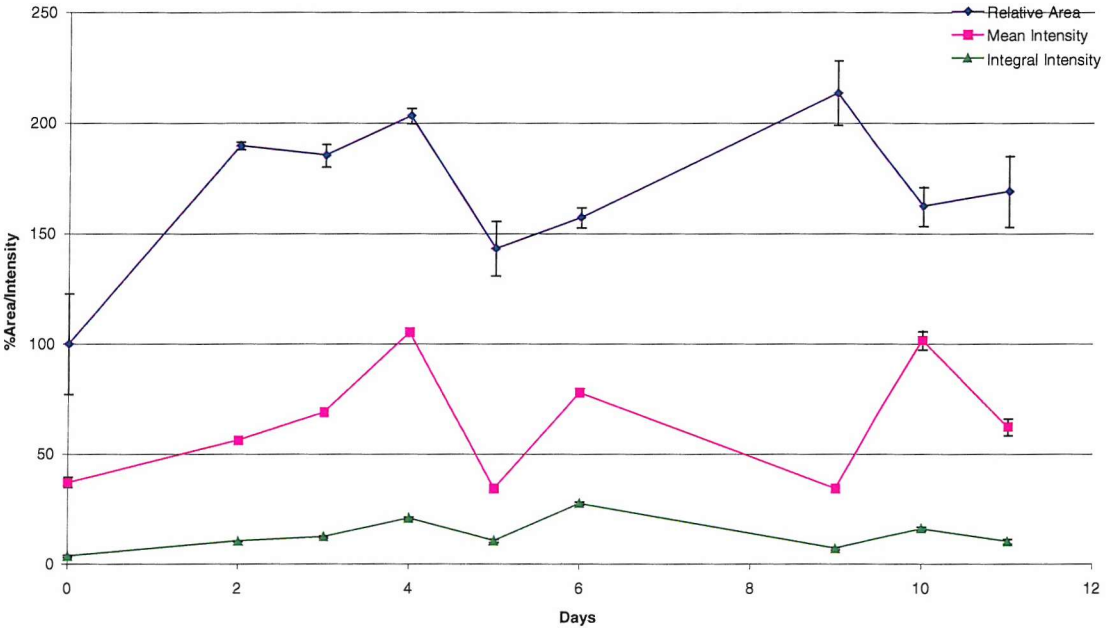

Fig.3.4.30 Graph showing the progress of a parental MGH-U1 colony over 11 days after exposure to Mitomycin C at 10µg/ml

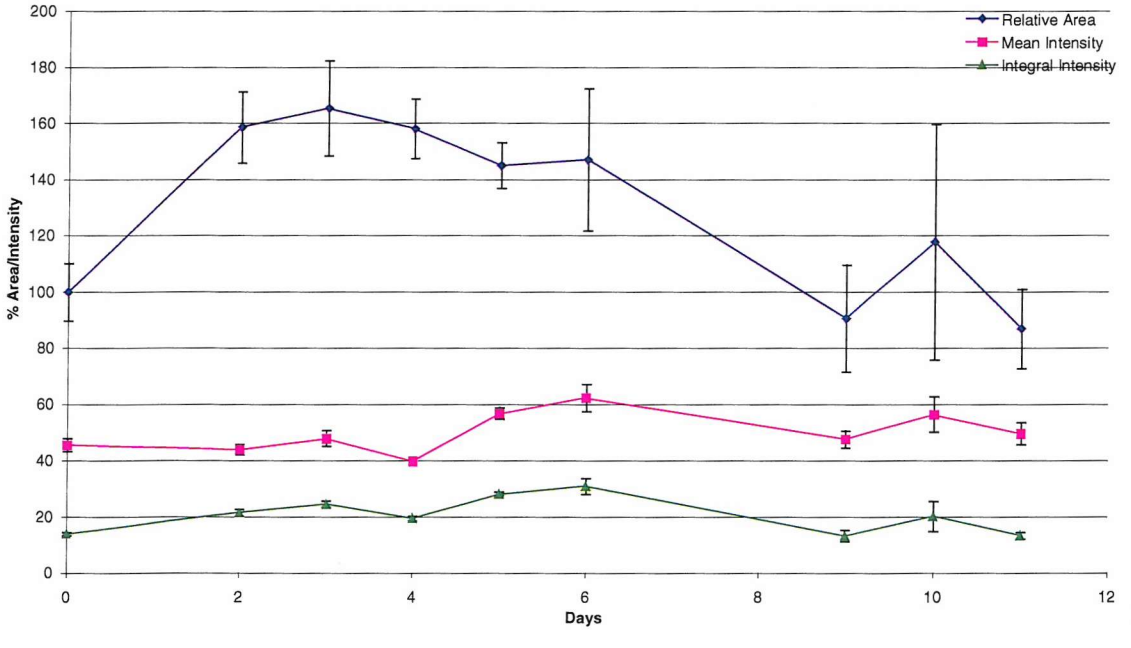

Fig.3.4.31 Graph showing the progress of a parental MGH-U1 colony over 11 days after exposure to Mitomycin C at 100µg/ml.

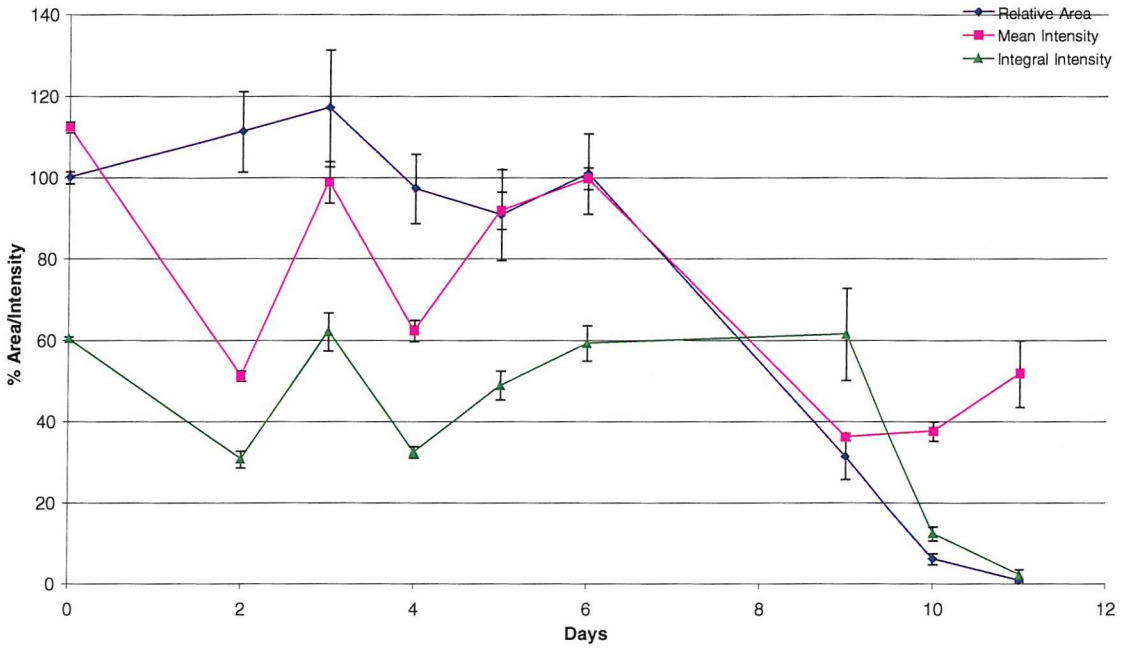

Fig.3.4.32 Graph showing the progress of a parental MGH-U1 colony over 11 days after exposure to Mitomycin C at 1 mg/ml.

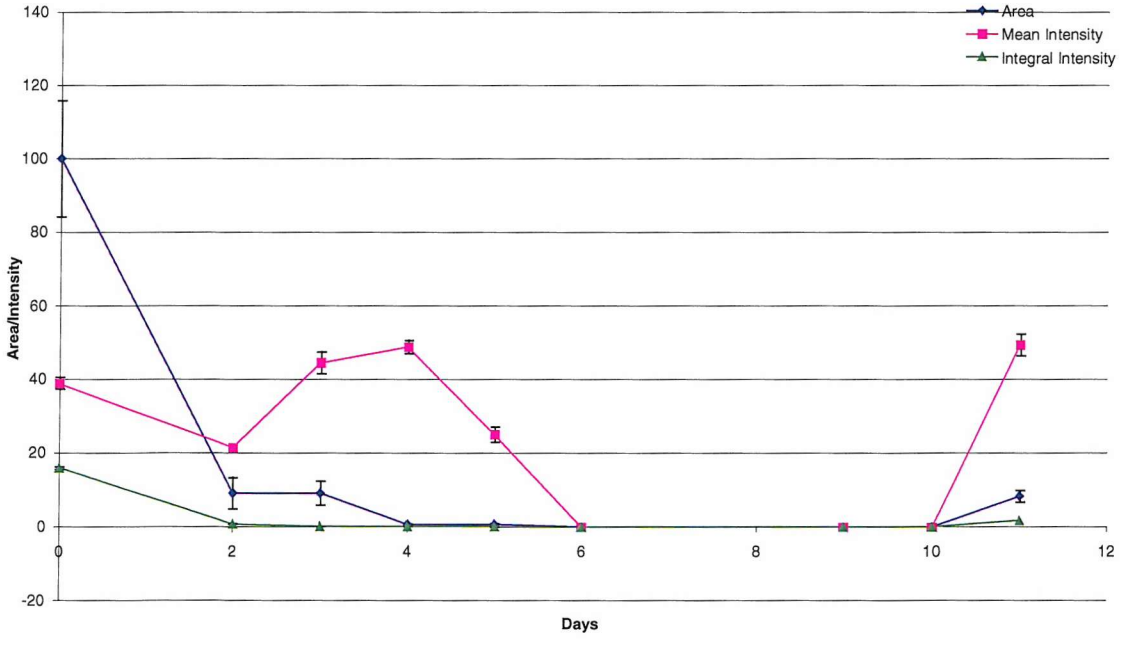

Fig3.4.33 Graph showing the areas of each parental MGH-U1 colony exposed to the above concentrations of Mitomycin C for 1 hour.

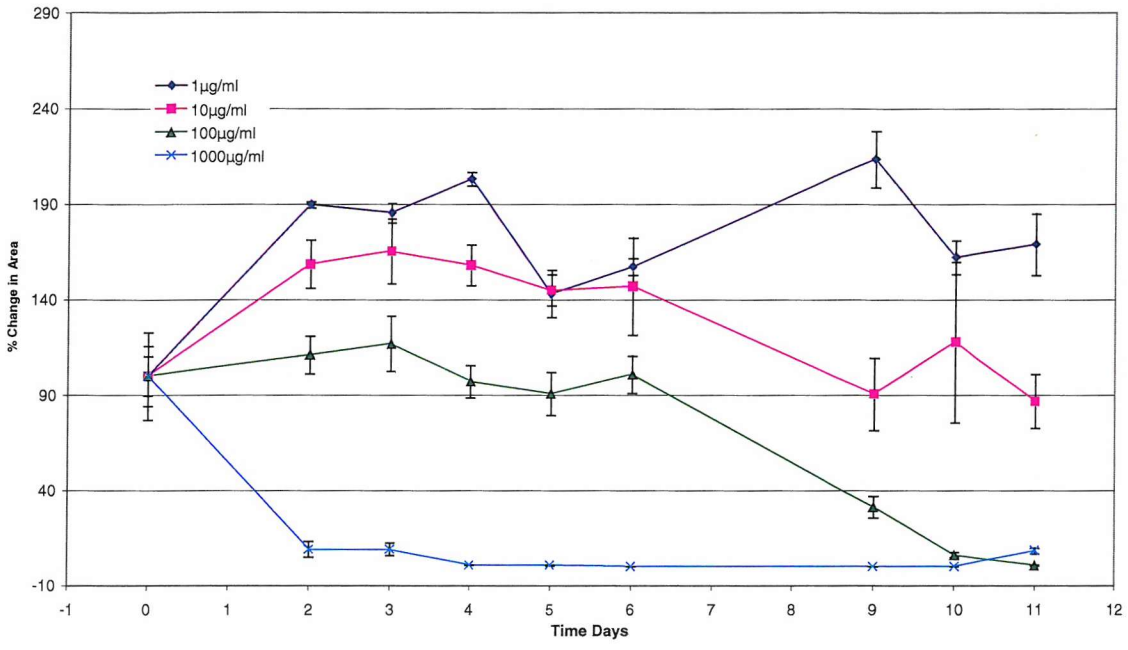

Fig.3.4.34 Graph showing the average area of the colonies exposed to the above concentrations of MMC

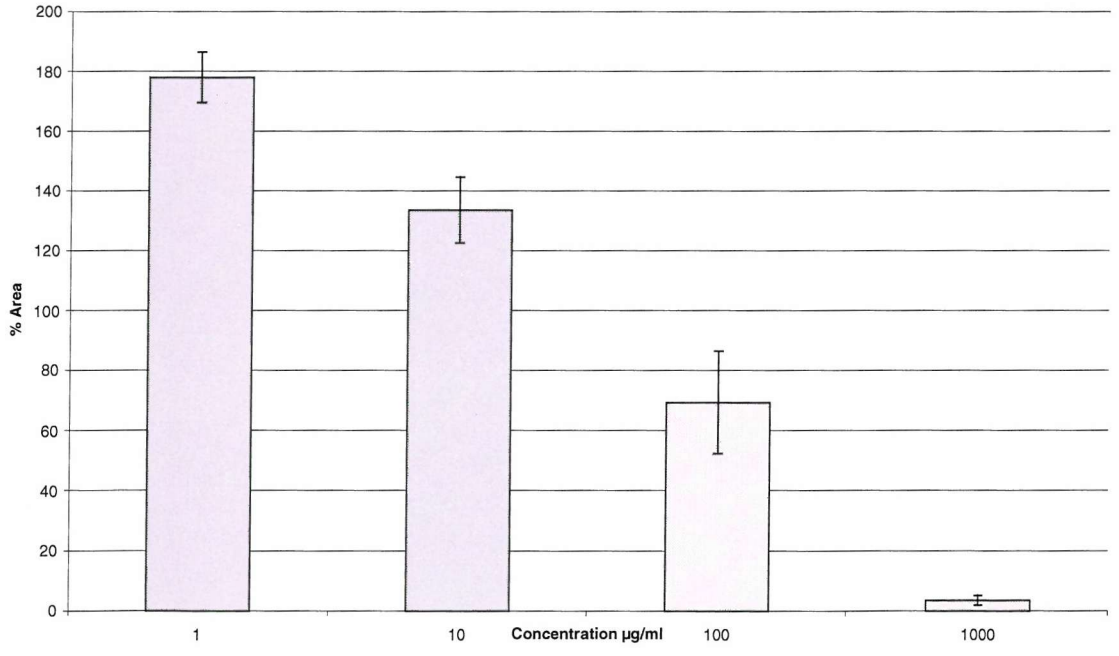

MMC-resistant colonies.

Fig.3.4.35 Graph showing the progress of an MMC resistant MGH-U1 colony over 11 days after exposure to Mitomycin C at 1 µg/ml.

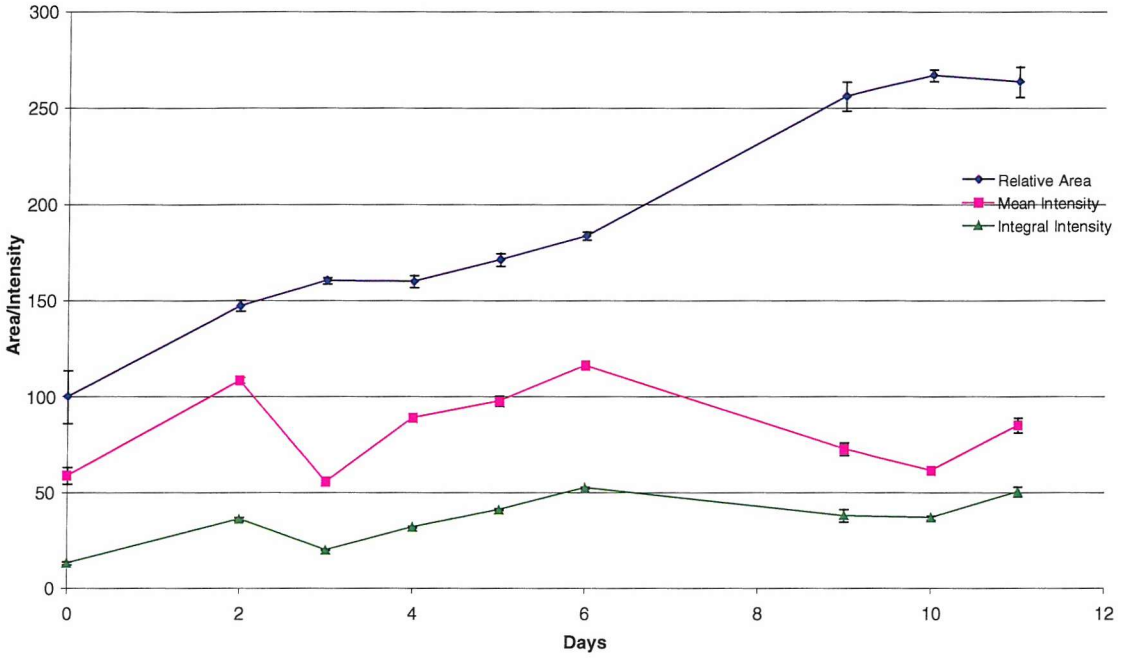

Fig.3.4.36 Graph showing the progress of an MMC resistant MGH-U1 colony over 11 days after exposure to Mitomycin C at 10 µg/ml.

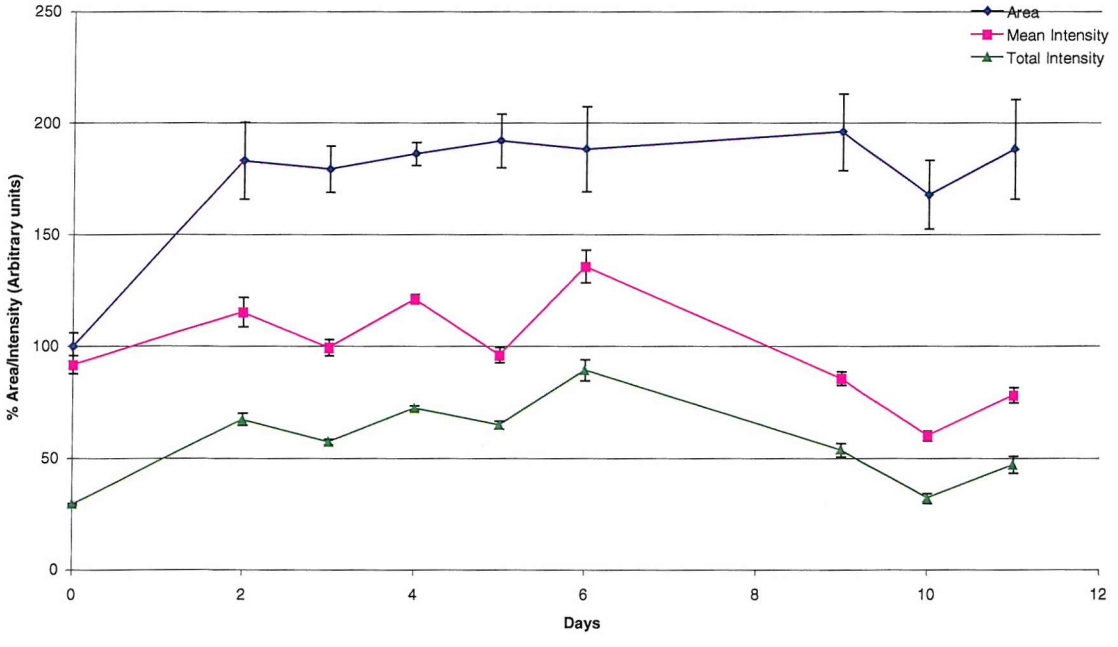

Fig.3.4.37 Graph showing the progress of an MMC resistant MGH-U1 colony over 11 days after exposure to Mitomycin C at 100 µg/ml.

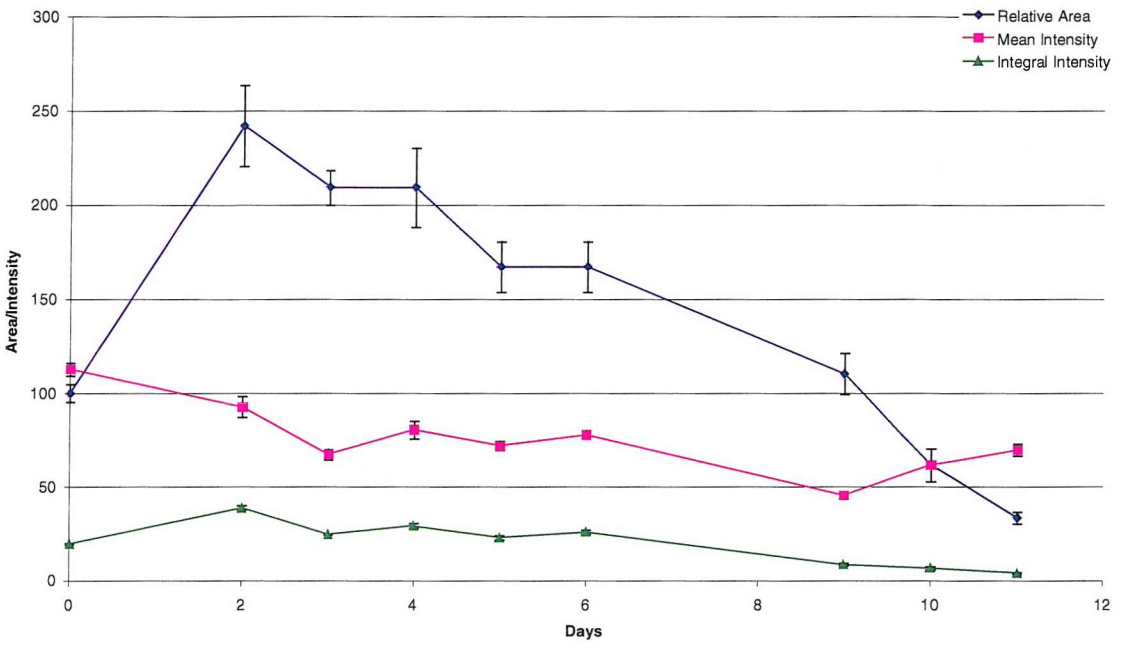

Fig.3.4.38 Graph showing the progress of an MMC resistant MGH-U1 colony over 11 days after exposure to Mitomycin C at 1 mg/ml.

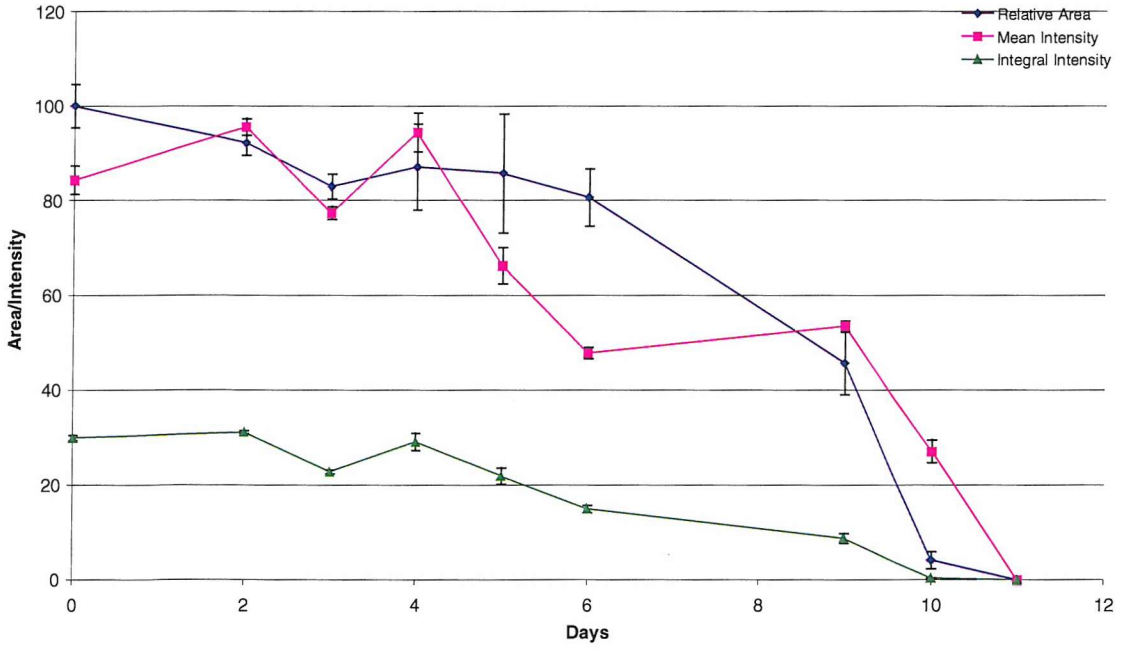

Fig.3.4.39 Graph showing the areas of each MMC-MGH-U1 colony exposed to the above concentrations of Mitomycin C for 1 hour.

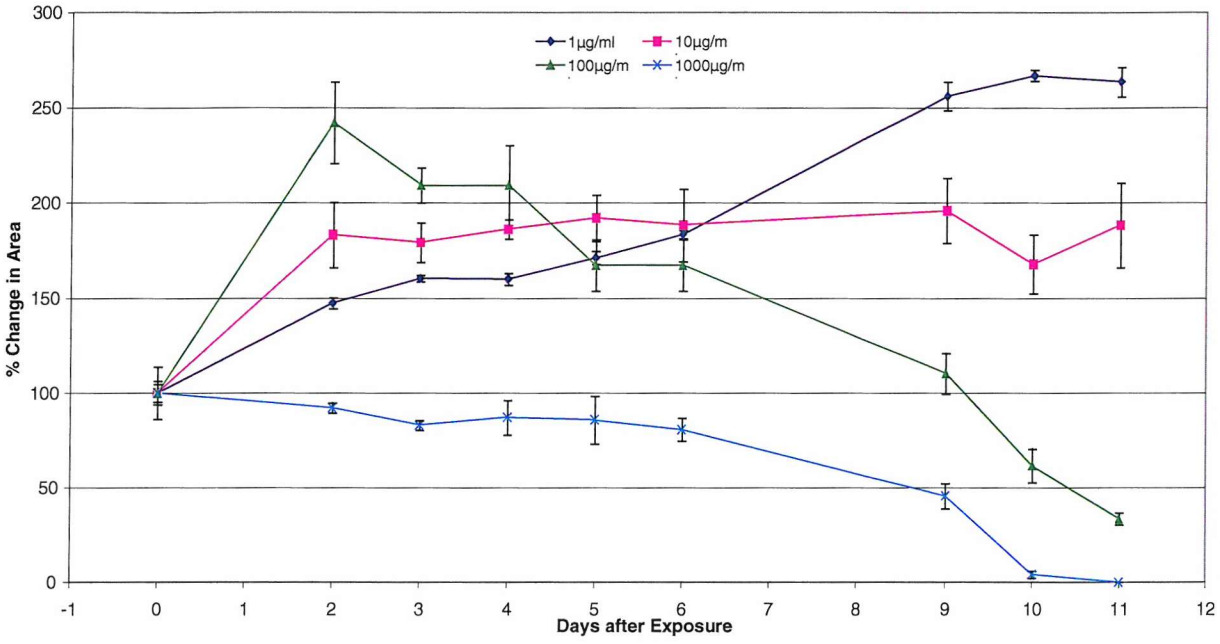

Fig.3.4.40a Graph showing the average area of the colonies exposed to the above concentrations of MMC

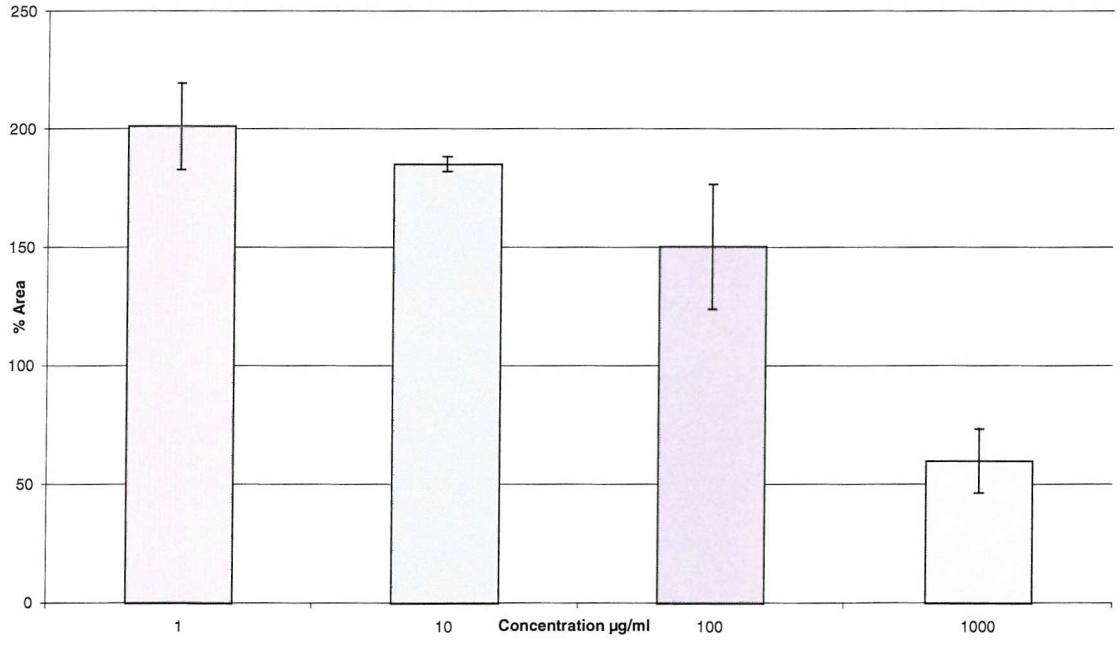

Fig. 3.4.40b Confocal images of the MMC-MGH-U1 colony exposed to 1mg/ml of Mitomycin C at days 5,6,9 and 10, showing gradual deterioration of the colony.

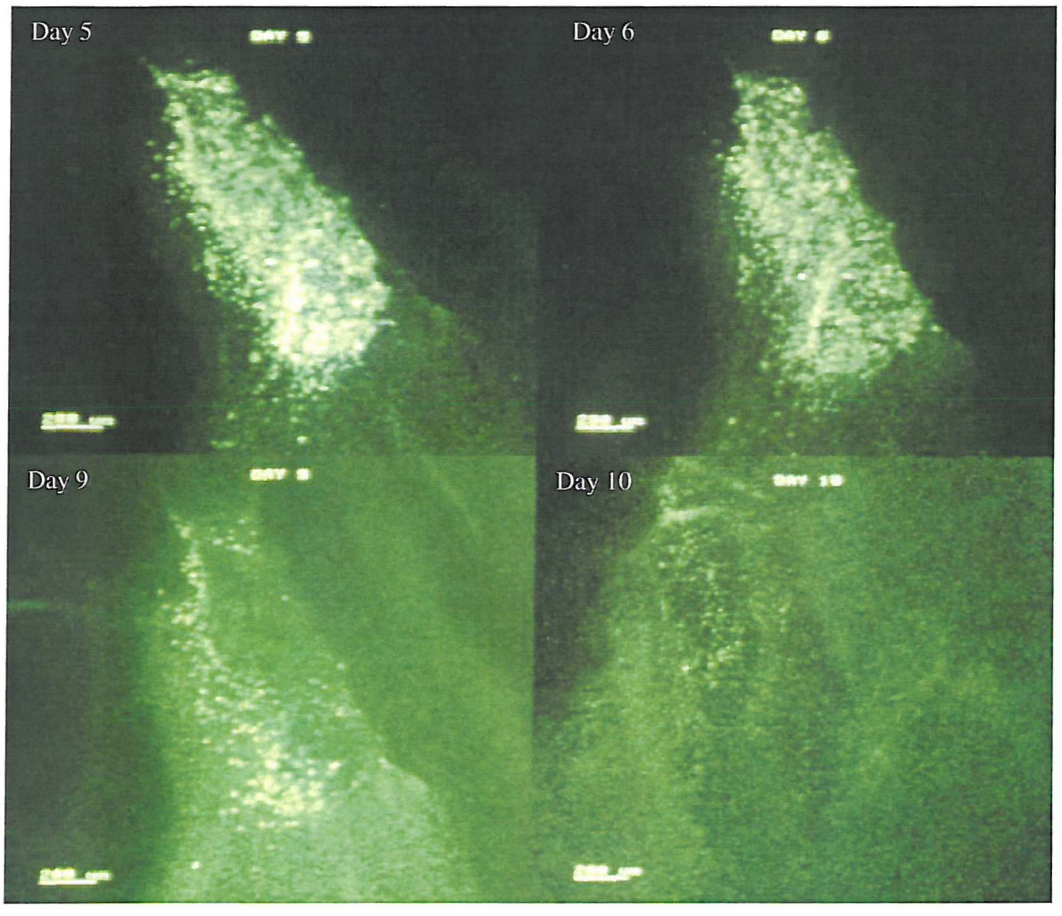

3.4.3 Non-MDR drug Experiments

Estramustine

Experiments with Estramustine, which does not show classical MDR, were performed in accordance with the protocol designed after the later experiments with Epirubicin and MMC. The aim of these experiments was to show that parental and resistant cells had a similar response to the drug, and also to demonstrate again the utility of the model. Thus the colonies were exposed within 24 hours after seeding onto the explant, and then subsequent imaging taken at various time periods after. The results are presented in a similar graphical format to the above experiments. The experiments are recorded over a 3 day period, as Estramustine has a rapid onset of action.

Figures 3.4.41 to 3.4.44 show 4 parental colonies exposed to various concentrations of Estramustine. They show little effect on the colony at a low dose of 1μg/ml, no growth at intermediate concentrations of 10 and 100μg/ml and colony destruction at 500μg/ml. This produces a satisfactory splay graph and dose response when all concentrations are compared on a single graph and bar chart respectively (Figs. 3.4.45 and 3.4.46). A similar picture is seen for the resistant colonies (Figs. 3.4.47 to 3.4.52). The IC>50 for Estramustine on monolayers was 22 to 42μg/ml, thus the colonies were able to survive a dose at least 5x that dose. There was no difference in the MDR response, as expected.

Parental Colonies.

Fig.3.4.41 Graph showing the progress of a parental MGH-U1 colony over 3 days after exposure to Estramustine at 1 µg/ml.

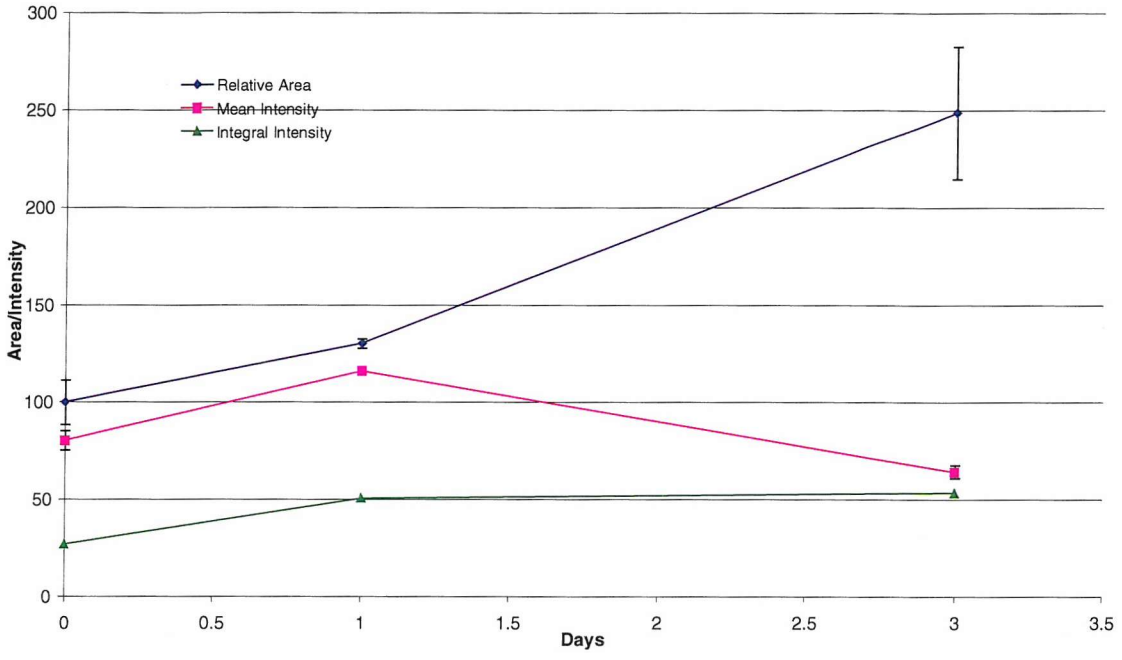

Fig.3.4.42 Graph showing the progress of a parental MGH-U1 colony over 3 days after exposure to Estramustine at 10 µg/ml.

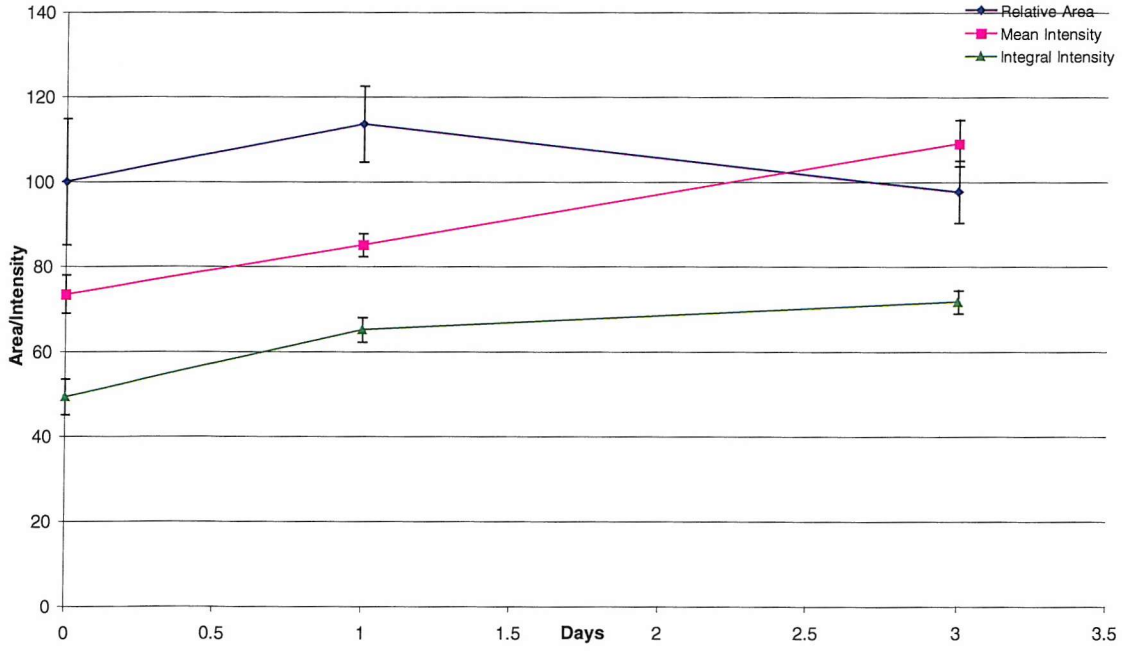

Fig.3.4.43 Graph showing the progress of a parental MGH-U1 colony over 3 days after exposure to Estramustine at 100 µg/ml.

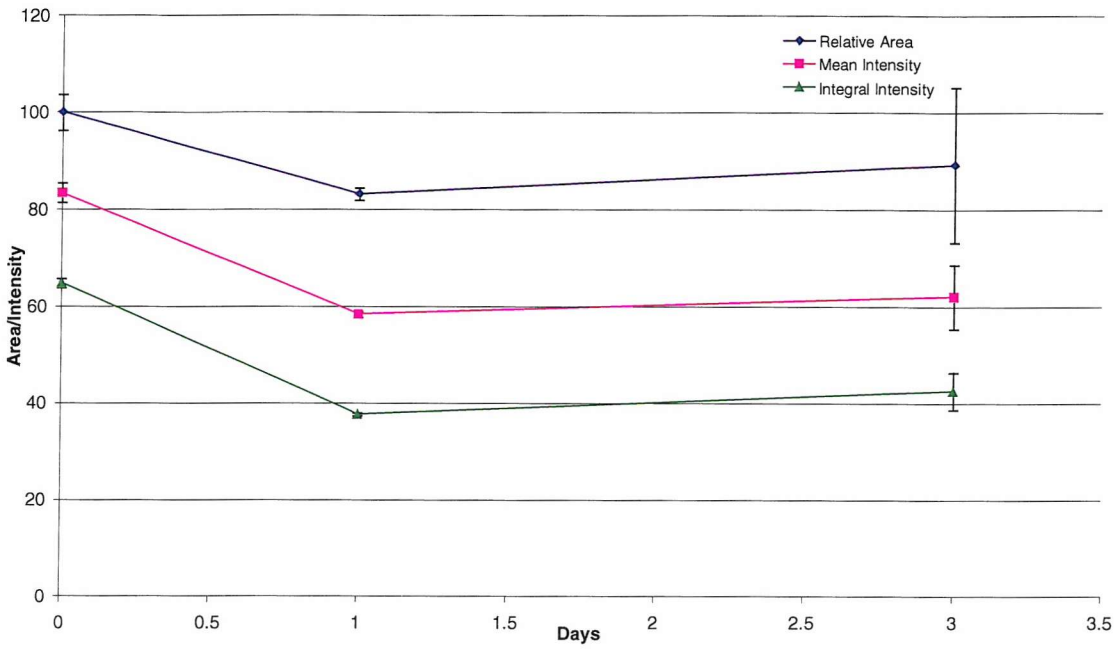

Fig.3.4.44Graph showing the progress of a parental MGH-U1 colony over 3 days after exposure to Estramustine at 500 µg/ml.

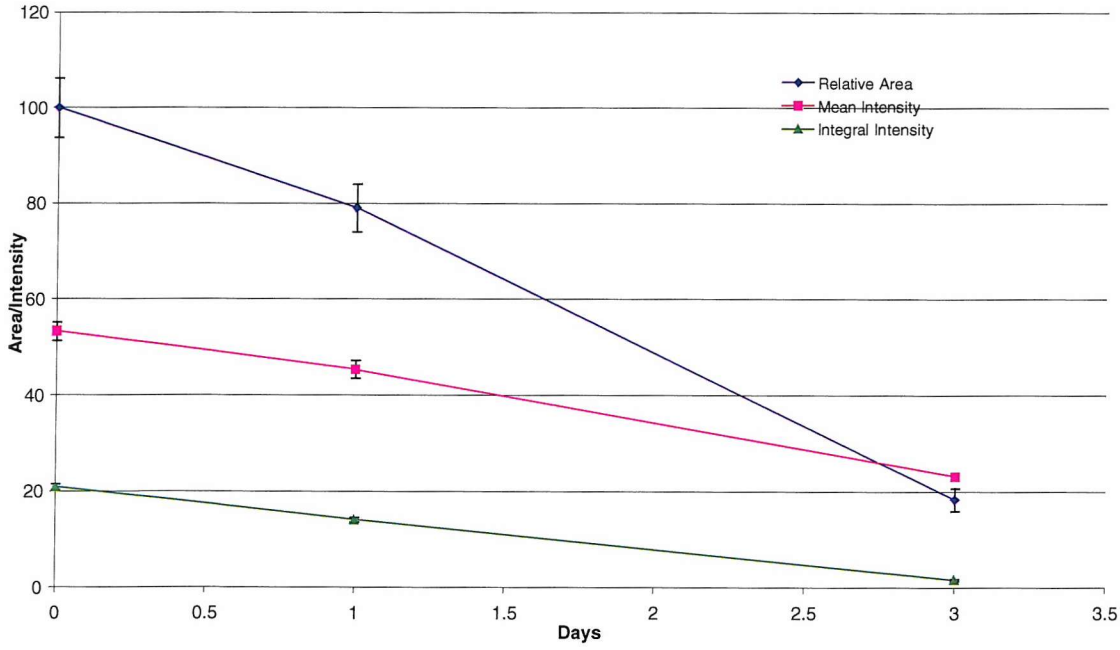

Fig.3.4.45 Graph showing the areas of each MGH-U1 colony exposed to the above concentrations of Estramustine for 1 hour.

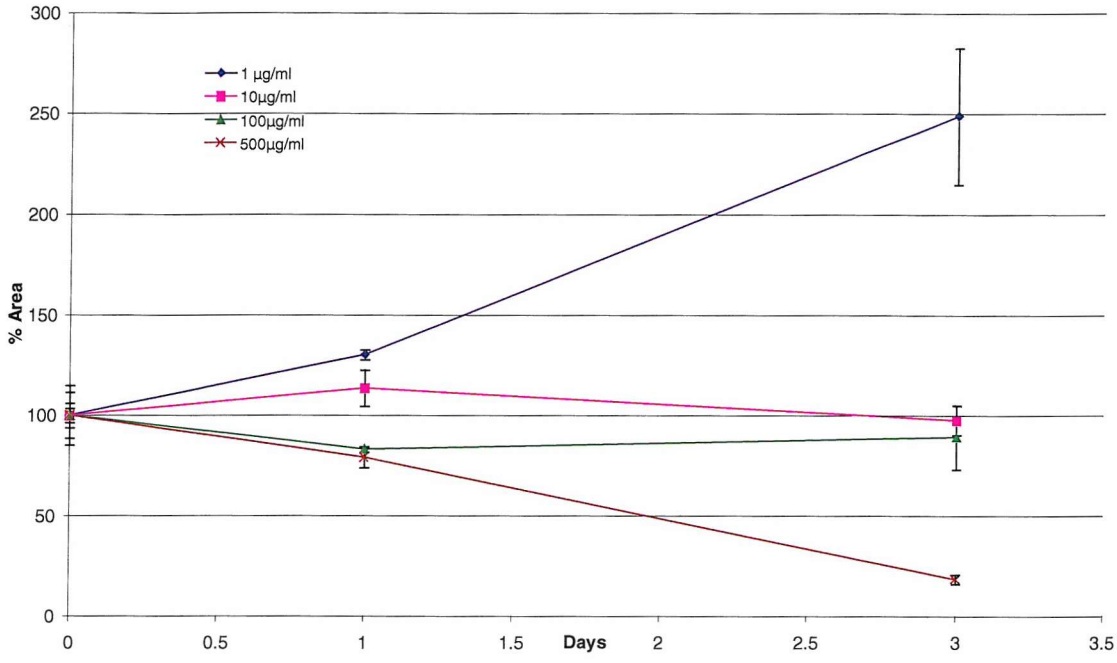

Fig.3.4.46 Graph showing the average area of each parental colony exposed to Estramustine over 3 days

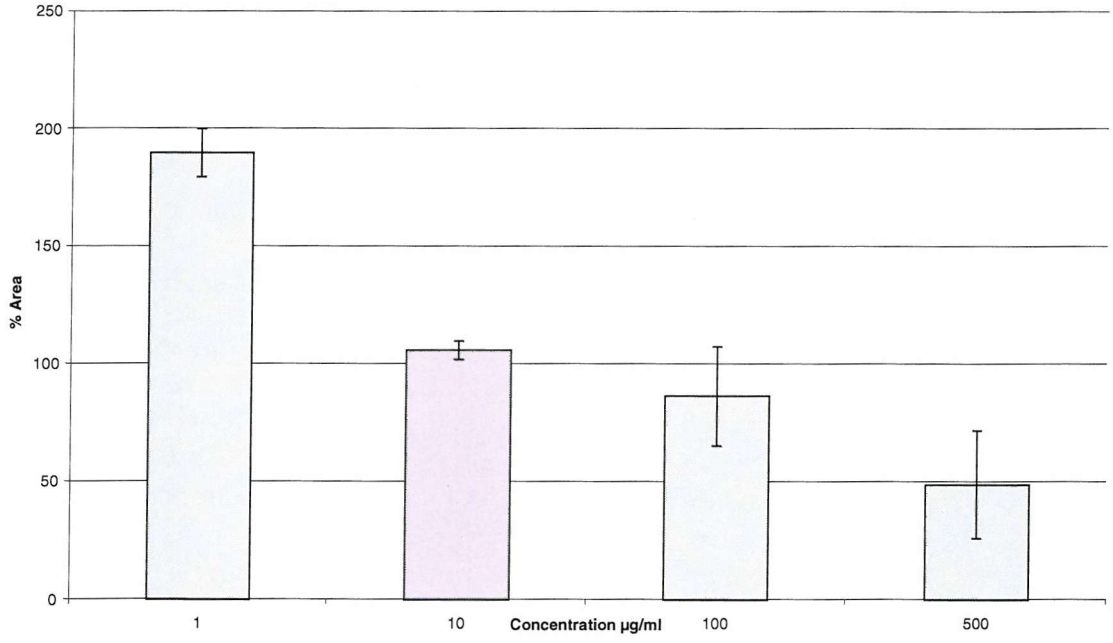

Resistant Colonies.

Fig.3.4.47 Graph showing the progress of a resistant MMC-MGH-U1 colony over 3 days after exposure to Estramustine at 1 µg/ml.

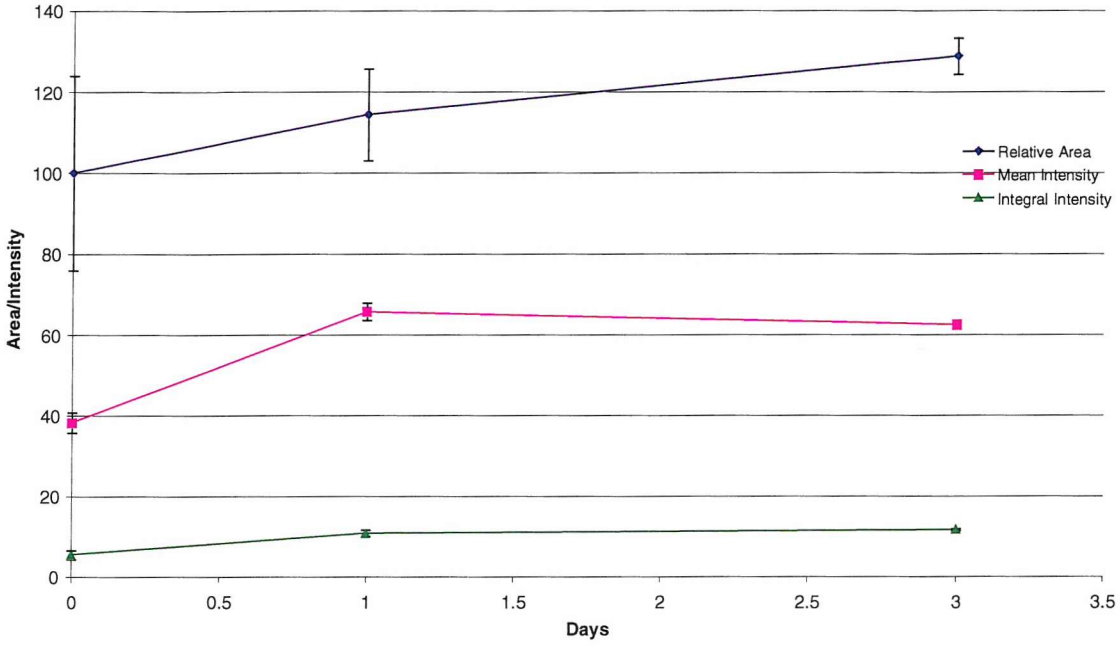

Fig.3.4.48 Graph showing the progress of a resistant MMC-MGH-U1 colony over 3 days after exposure to Estramustine at 10 µg/ml.

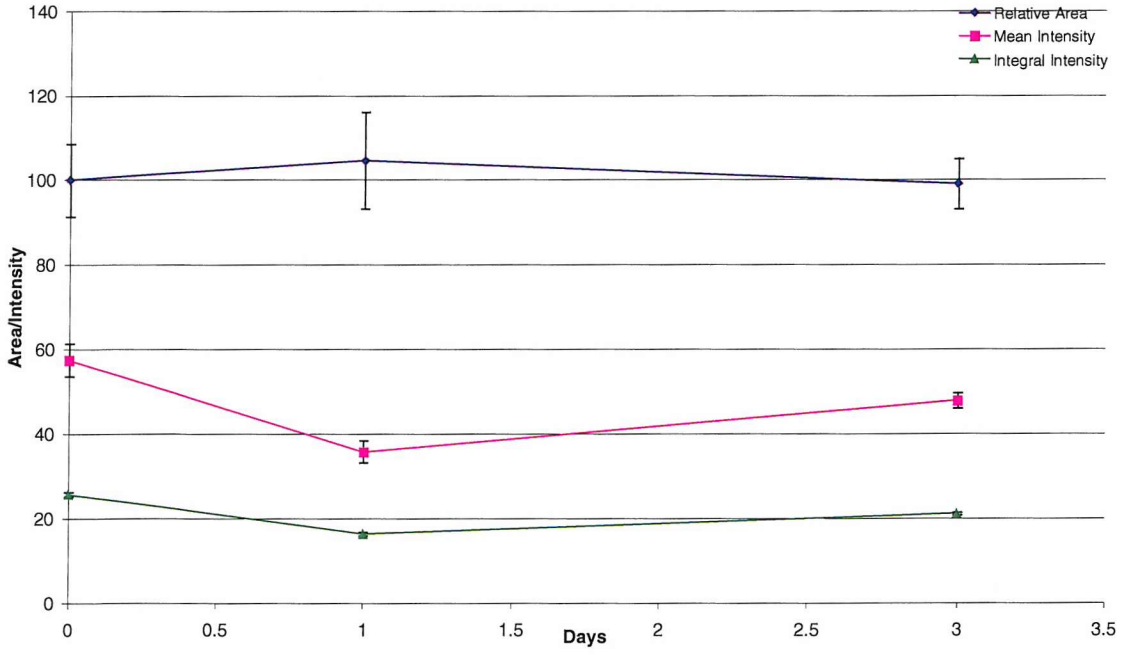

Fig.3.4.49 Graph showing the progress of a resistant MMC-MGH-U1 colony over 3 days after exposure to Estramustine at 100 µg/ml.

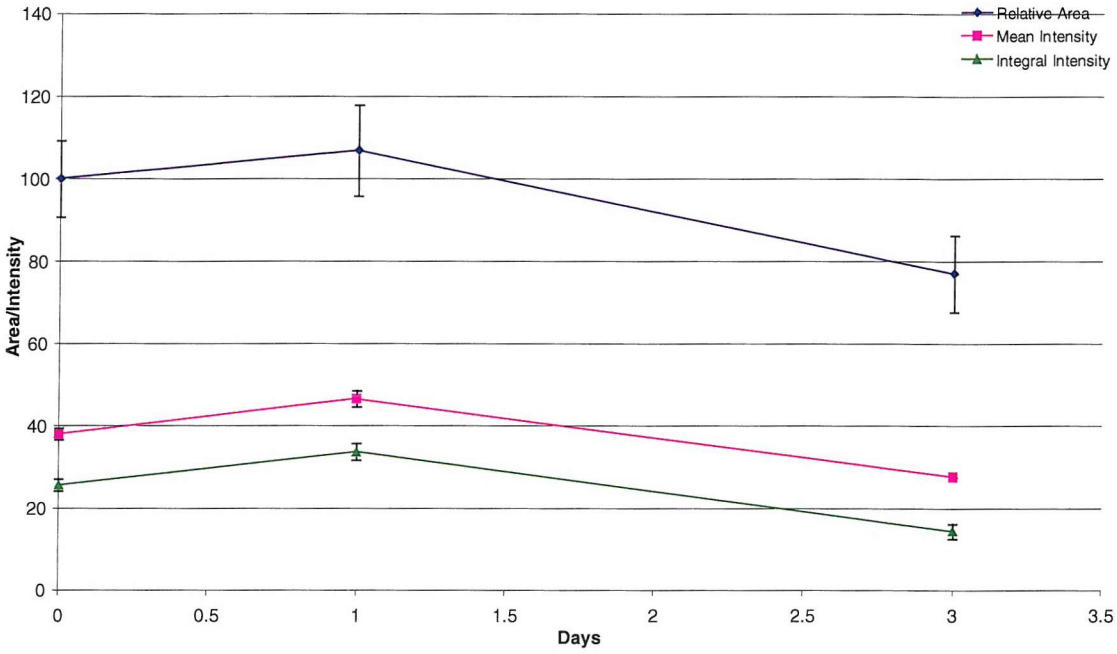

Fig.3.4.50 Graph showing the progress of a resistant MMC-MGH-U1 colony over 3 days after exposure to Estramustine at 500 µg/ml.

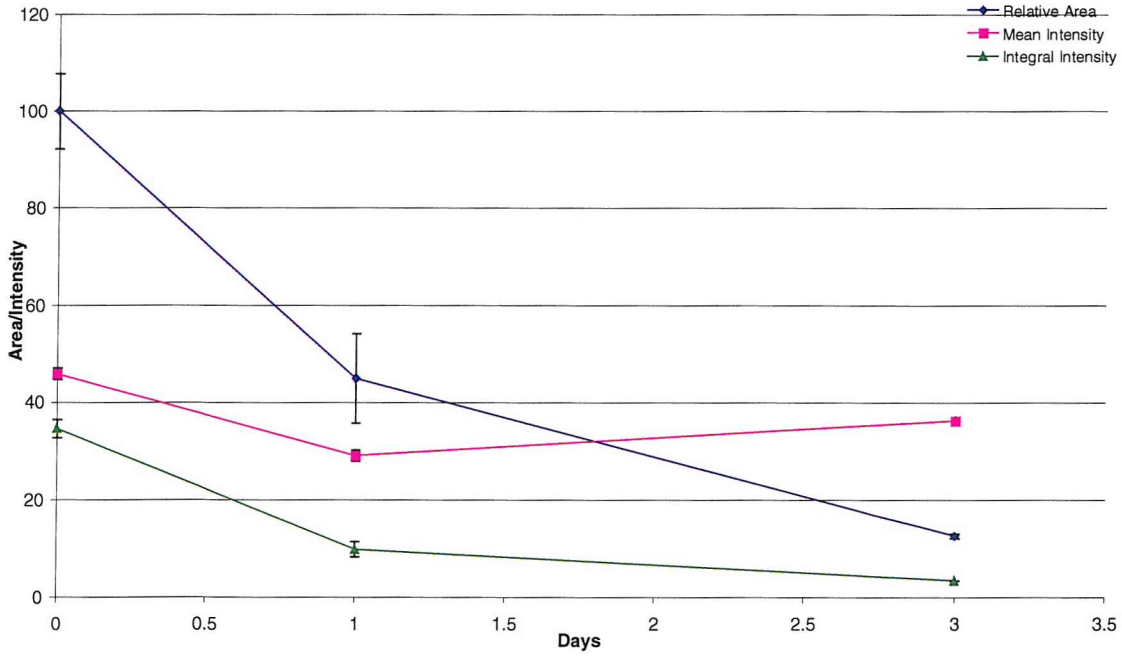

Fig.3.4.51 Graph showing the areas of each MMC-MGH-U1 colony exposed to the above concentrations of Estramustine for 1 hour.

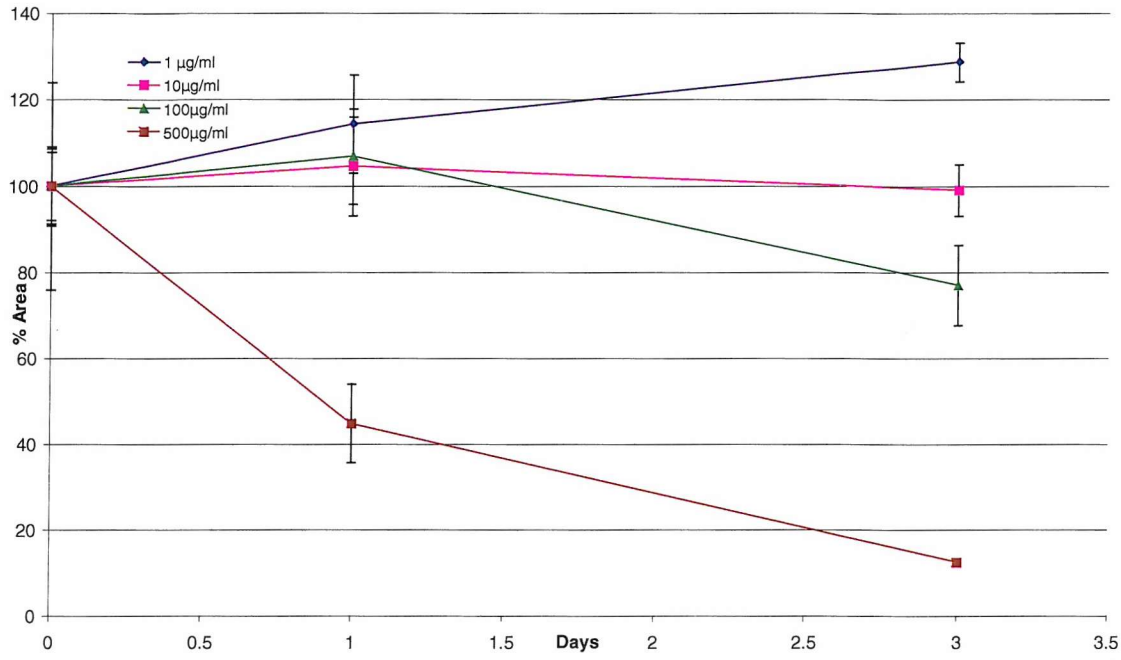

Fig.3.4.52 Graph showing the average area of each MMC-MGH-U1 colony exposed to Estramustine over 3 days

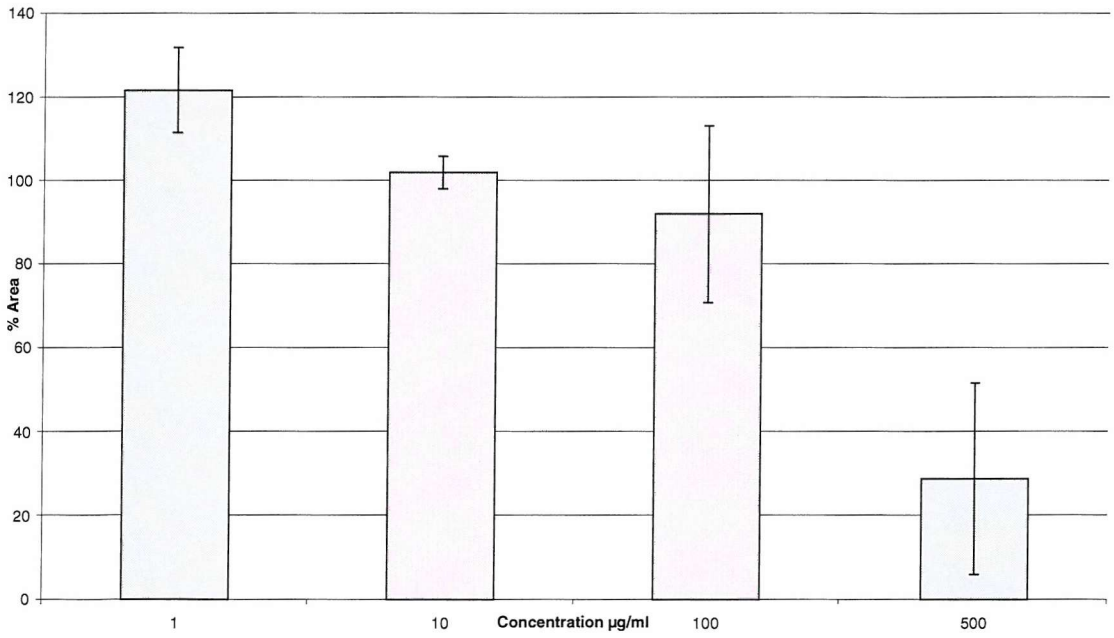

3.4.4 MeGLA

Early Experiments.

The aim of these experiments was to demonstrate the effects of the novel agent MeGLA on the explant colonies, and compare with its effects on monolayers. As with the early experiments on Epirubicin and MMC, these experiments were performed at 5 days after GFP cell seeding. The results are shown in figures 3.4.53 and 3.4.54, which show the areas of colonies exposed to various concentrations of MeGLA. Note that in these early experiments the colonies were destroyed by a high dose at 500μg/ml, and showed no growth at the lower concentrations. These results were little different than from those obtained on monolayer cultures, where the IC>50 was 25μg/ml. In fact at the dose of 10μg/ml growth would have been expected, but as with some control colonies after 5 days of seeding, there was no further increase in area.

Fig.3.4.53 Graph showing the areas of each parental MGH-U1 colony exposed to various concentrations of MeGLA for 1 hour, after 7 days of culture.

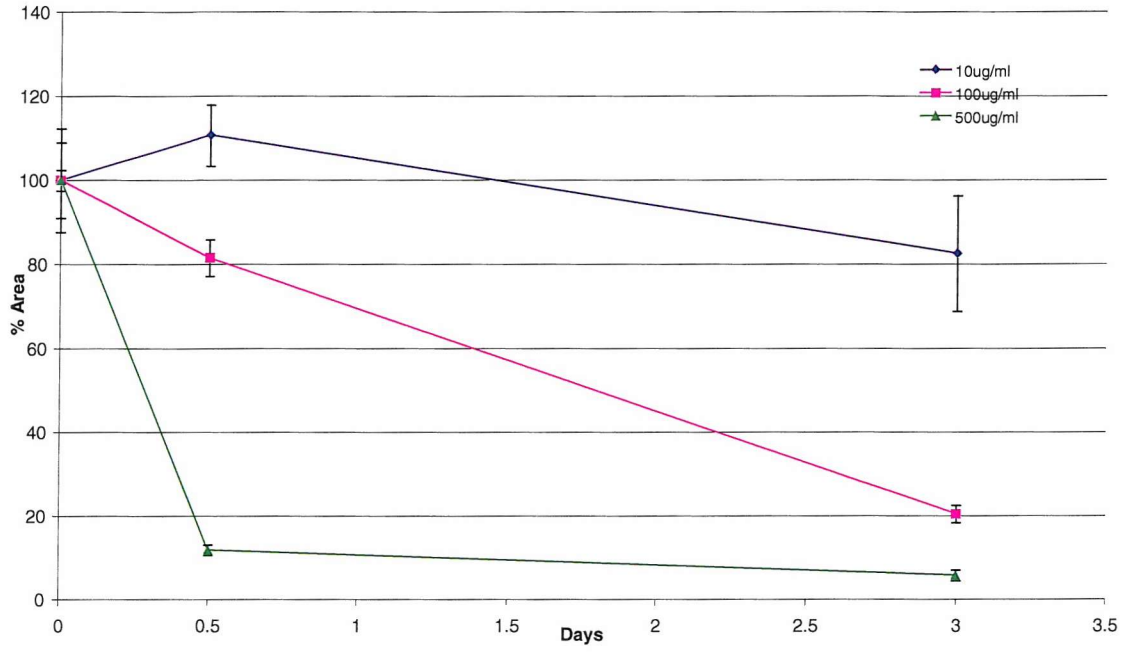

Fig.3.4.54 Graph showing the areas of each resistant MGH-U1 colony exposed to various concentrations of MeGLA for 1 hour, after 7 days of culture.

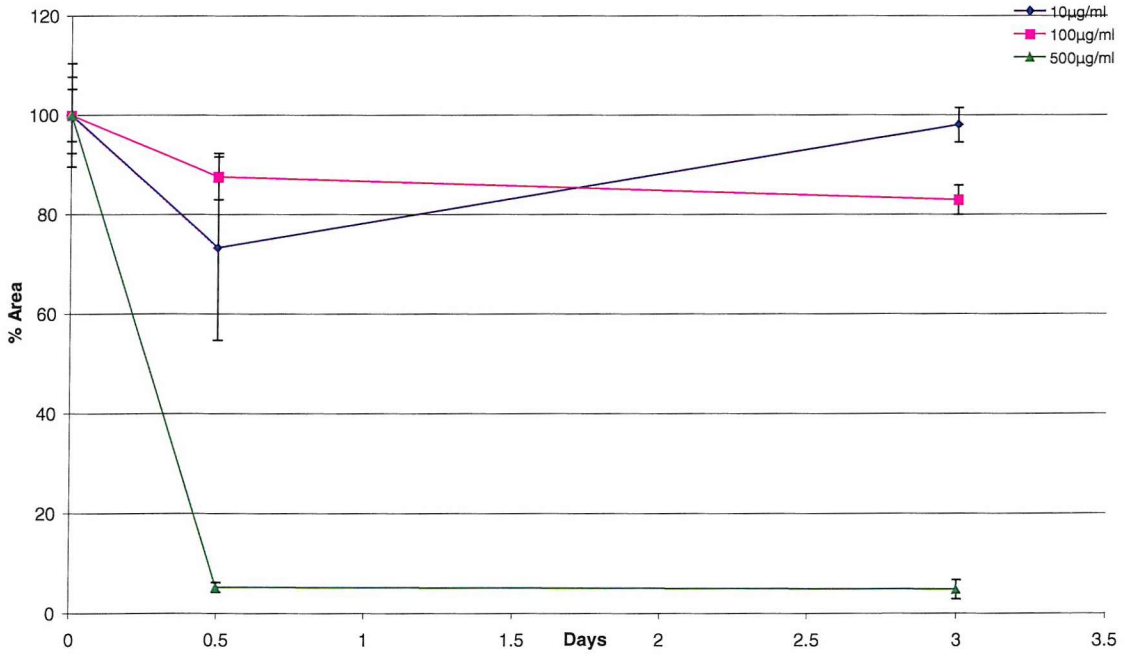

Later experiments.

These were performed with the standard protocol of cell seeding followed by imaging and drug exposure within 24 hours. The graphs follow the same format as for previous results. Figures 3.4.55 To 3.4.60 show the graphs for area and intensity for each parental colony exposed to a different dose of MeGLA, followed by a summary area splay graph and summary average area bar chart. This set of results is repeated for resistant colonies in figs. 3.4.61 to 3.4.65.

The colonies showed increase in area at the low doses of 1 and 10μg/ml for both parental and resistant colonies. At the IC>90 dose of 100μg/ml there is still growth for parental colonies, and no change in area for the resistant colonies. This difference is probably related to the variability inherent in the model. The most interesting comparison is seen at the highest dose of 1mg/ml. The initial measurement of area at 12 hours for the parental colony shows an initial reduction in colony size of over 50%, but the colony then recovers after that point to continue growing.

Parental Colonies.

Fig.3.4.55 Graph showing the progress of a parental MGH-U1 colony over 6 days after exposure to MeGLA at 1 µg/ml.

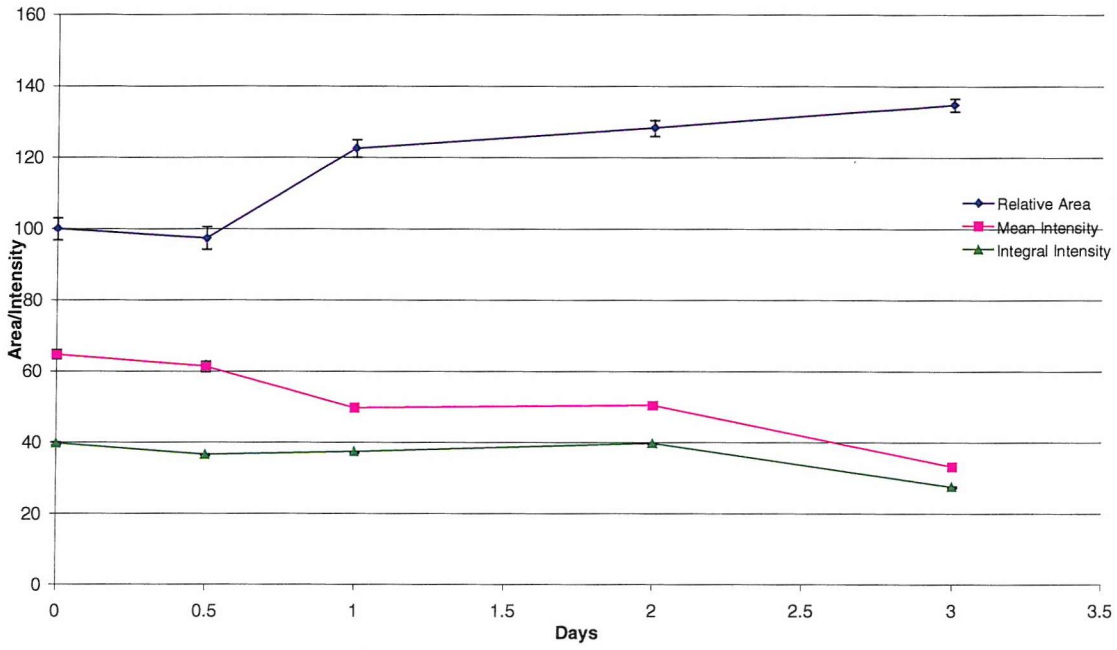

Fig.3.4.56 Graph showing the progress of a parental MGH-U1 colony over 3 days after exposure to MeGLA at 10 µg/ml.

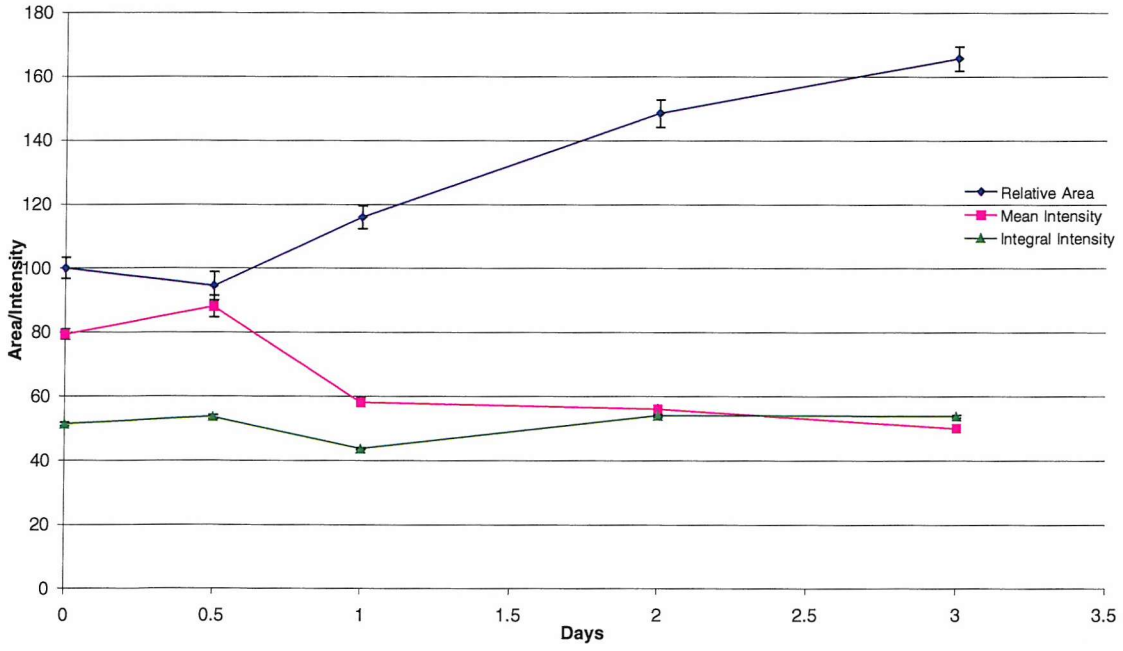

Fig.3.4.57 Graph showing the progress of a parental MGH-U1 colony over 3 days after exposure to MeGLA at 100 µg/ml.

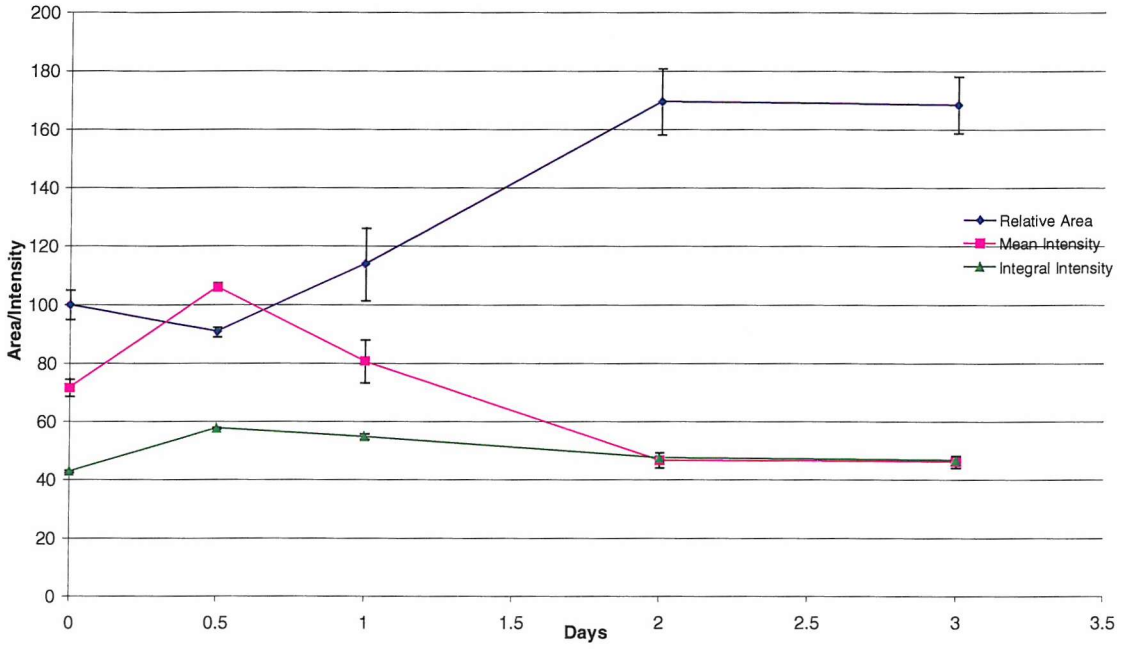

Fig.3.4.58 Graph showing the progress of a parental MGH-U1 colony over 3 days after exposure to MeGLA at 1 mg/ml.

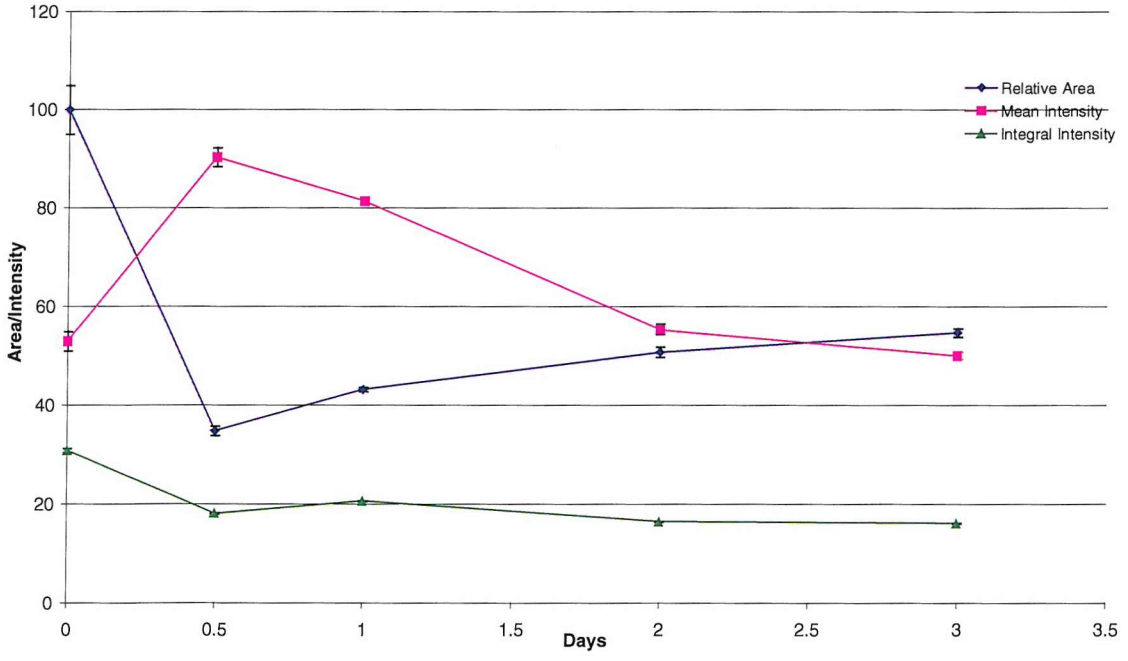

Fig.3.4.59 Graph showing the progress of the above parental MGH-U1 colonies over 3 days after exposure to 1 hour of MeGLA.

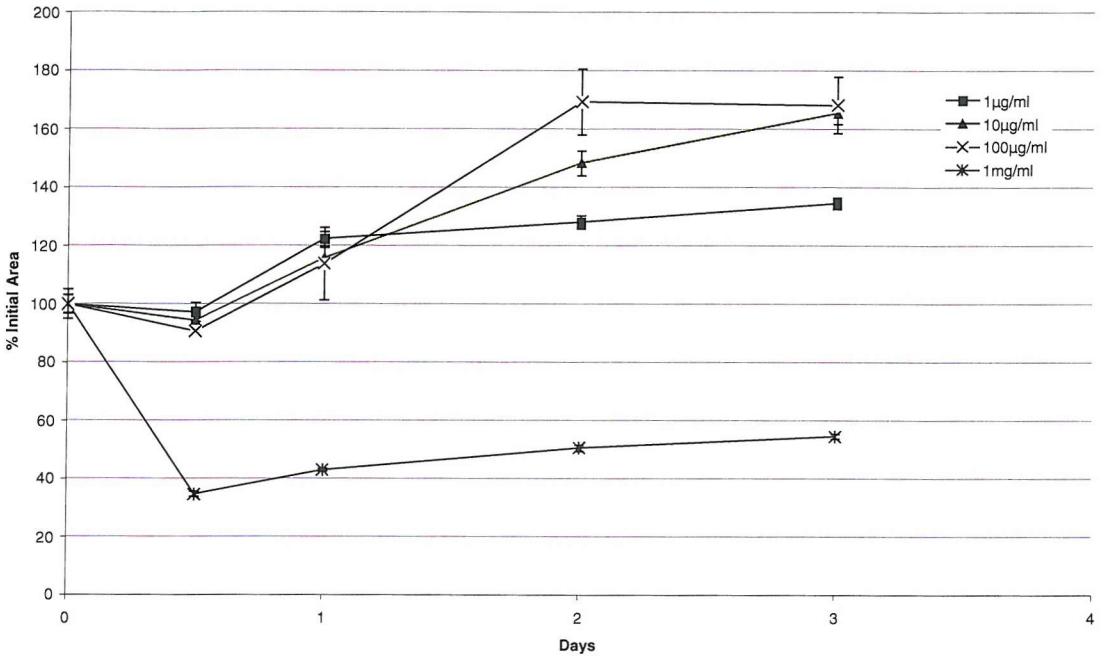

Fig.3.4.60 Graph showing the average areas of each parental colony exposed to MeGLA over 3 days

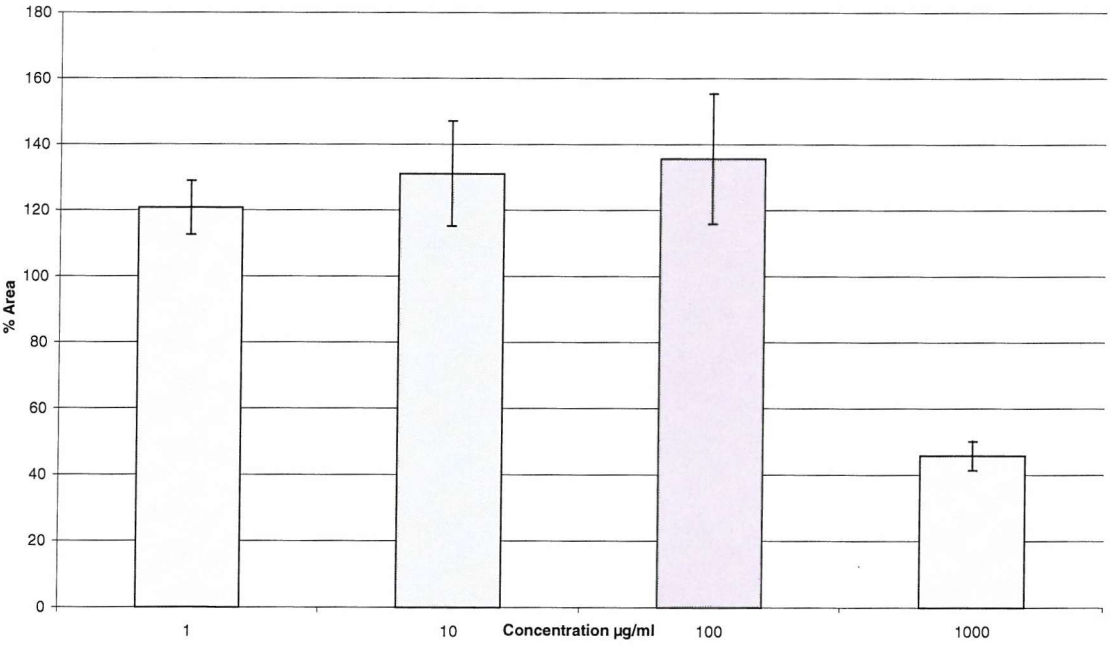

Resistant Colonies

Fig.3.4.61 Graph showing the progress of an MMC-MGH-U1 colony over 6 days after exposure to MeGLA for 1 hour at 1 µg/ml.

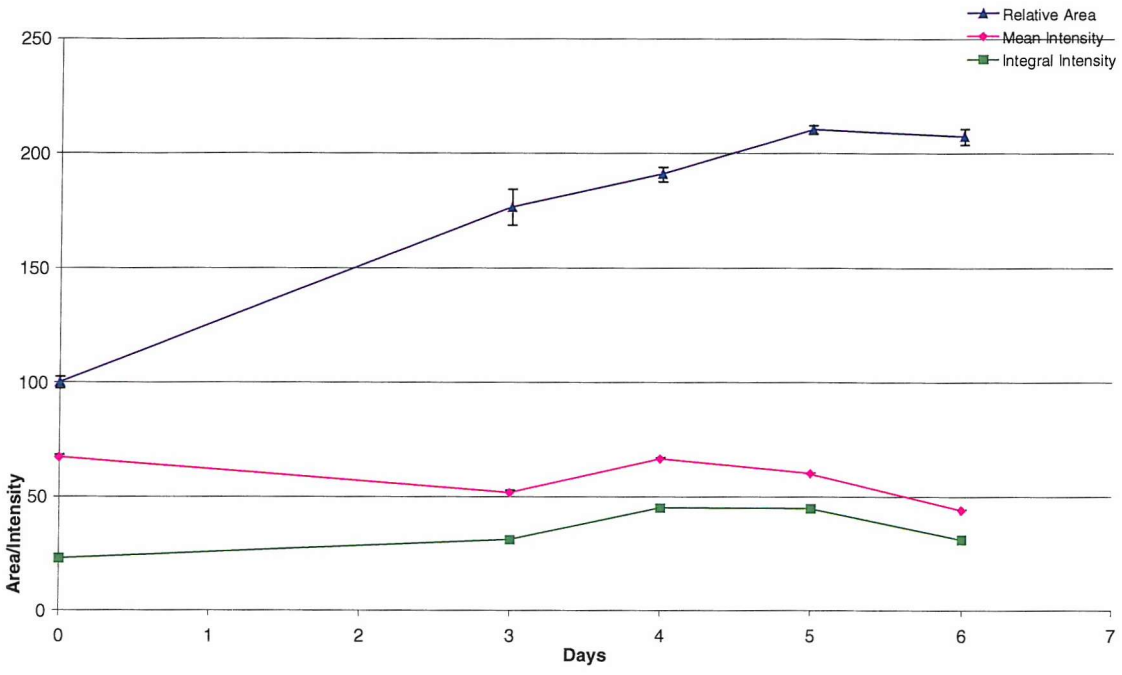

Fig.3.4.62 Graph showing the progress of an MMC-MGH-U1 colony over 6 days after exposure to MeGLA at 10 µg/ml.

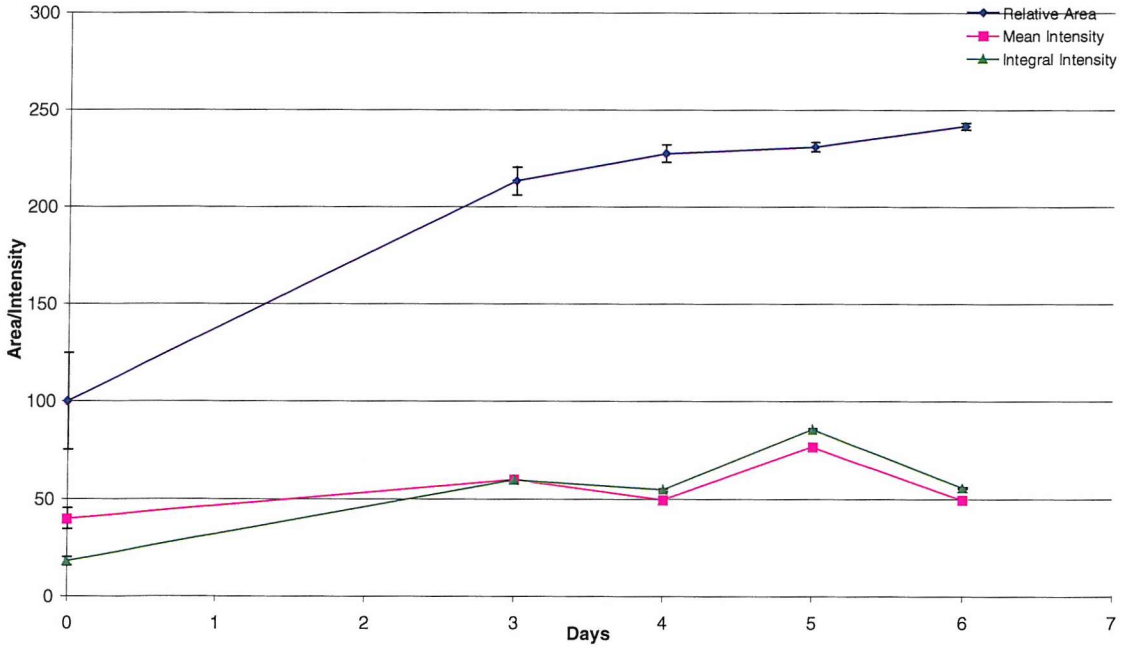

Fig.3.4.63 Graph showing the progress of an MMC-MGH-U1 colony over 6 days after exposure to MeGLA at 100 µg/ml.

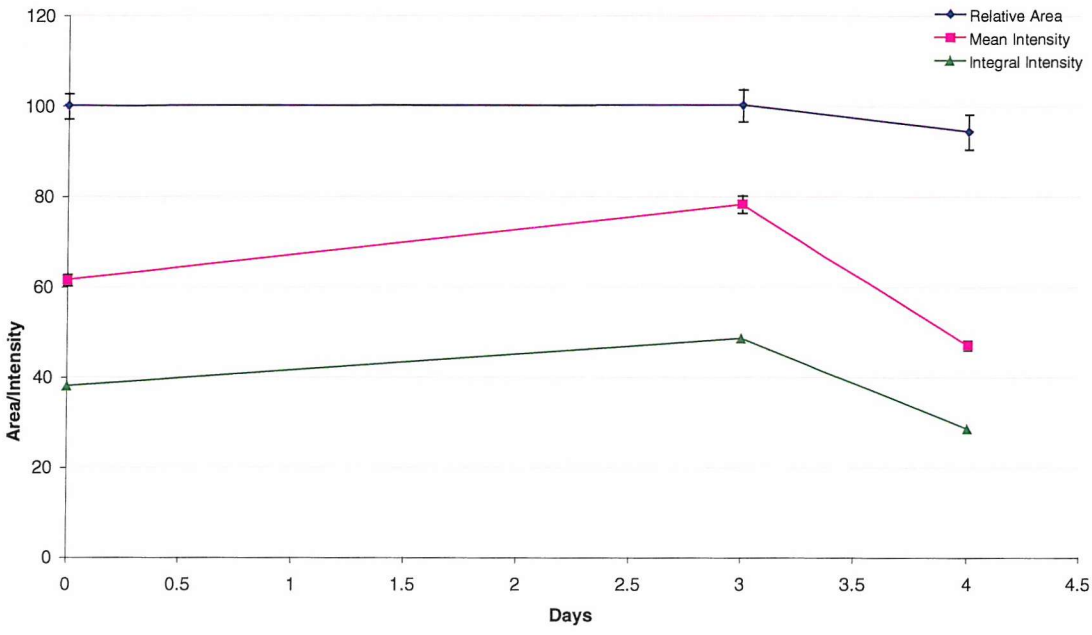

Fig.3.4.64 Graph showing the progress of the above MMC-MGH-U1 colonies over 6 days after exposure to MeGLA.

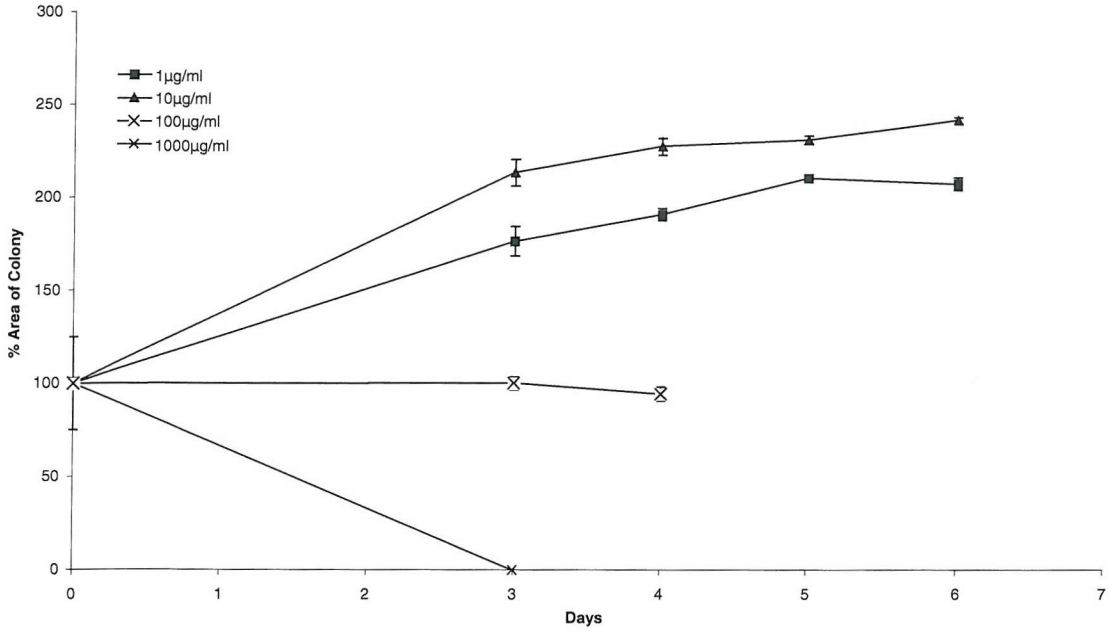

Fig.3.4.65 Graph showing the average areas of each resistant colony exposed to MeGLA over 3 days

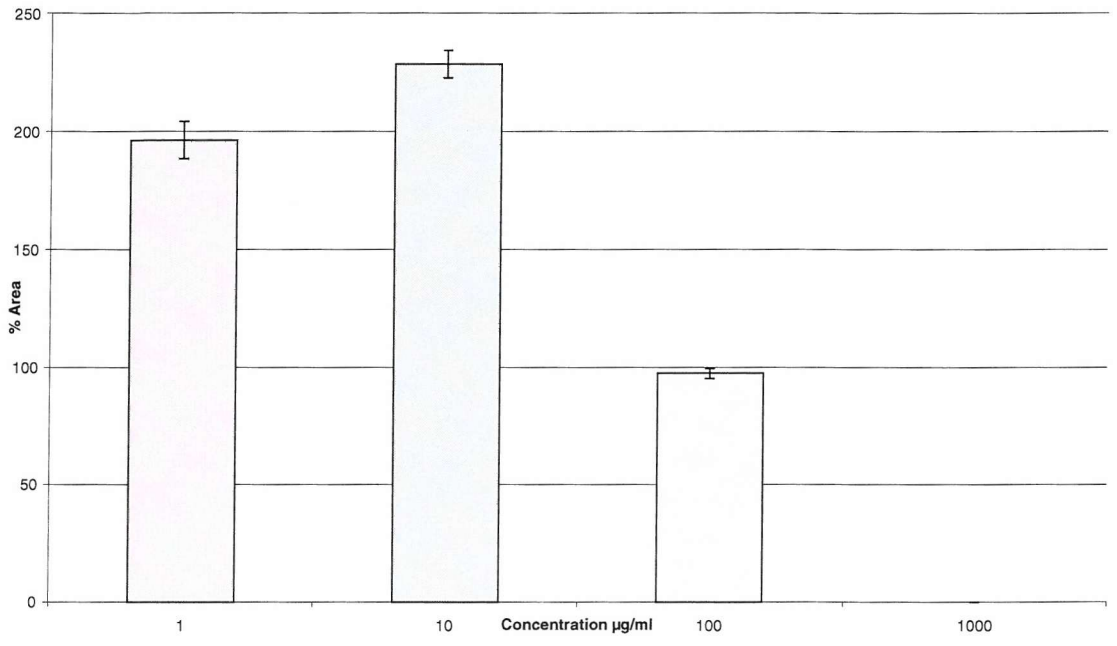

3.4.5 MeGLA in albumin.

Previous studies with MeGLA have shown that its cytotoxic properties are quenched in the presence of albumin. This has important implication if it were to be used in the immediate post-TURBT period when there are significant amounts of serum in the irrigant fluid. Thus a series of experiments were performed on resistant colonies with MeGLA dissolved in standard DMEM with 10% FCS. The standard protocol was followed of early drug exposure. These experiments were relatively long lasting, and the low doses of 1 and 10μg/ml, which would not be cytotoxic to monolayers, can be regarded as controls. The graphs in figs. 3.4.66 to 3.4.72 show the usual pattern of area increase and intensity variability. The summary splay graph shows similar growth for all concentrations except for the highest 1mg/ml, which shows the colony area remained at a similar size throughout the experiment.

Fig.3.4.66 Graph showing the progress of an MMC-MGH-U1 colony over 7 days after exposure to MeGLA in 10%FCS at 1 µg/ml.

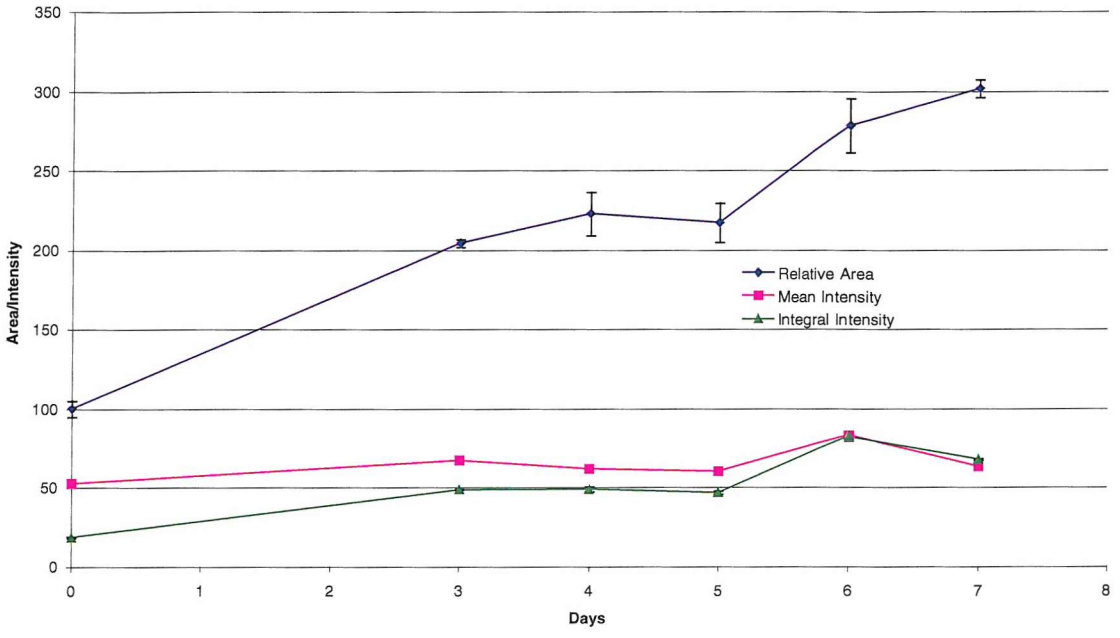

Fig.3.4.67 Graph showing the progress of an MMC-MGH-U1 colony over 6 days after exposure to MeGLA in 10%FCS at 10 µg/ml.

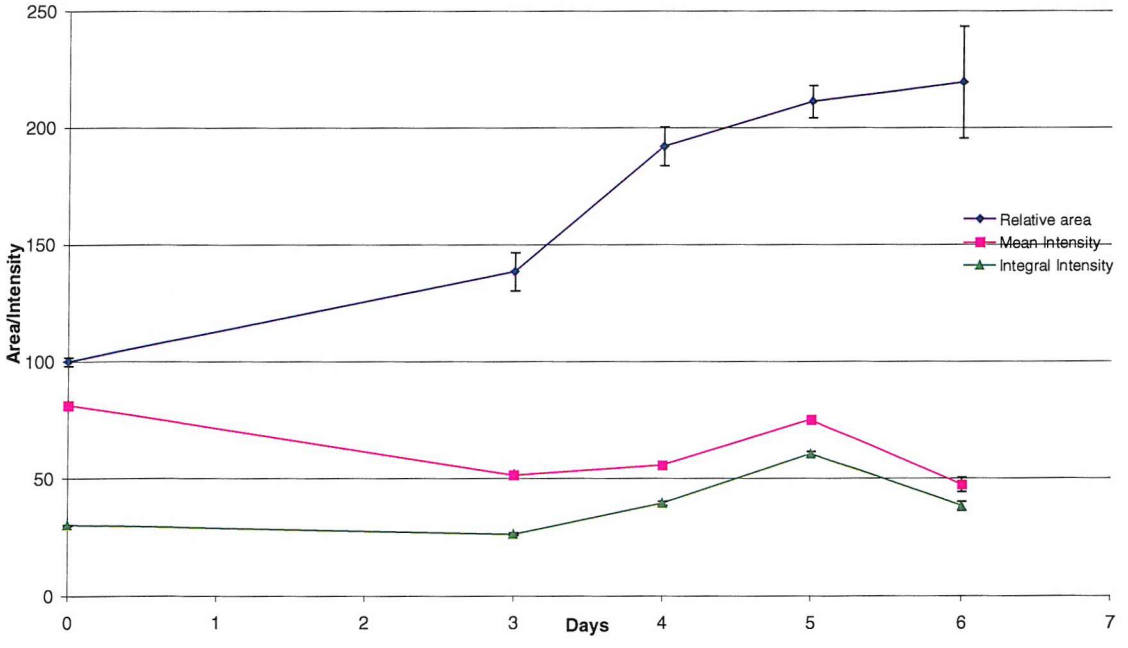

Fig.3.4.68 Graph showing the progress of an MMC-MGH-U1 colony over 7 days after exposure to MeGLA in 10%FCS at 100 µg/ml.

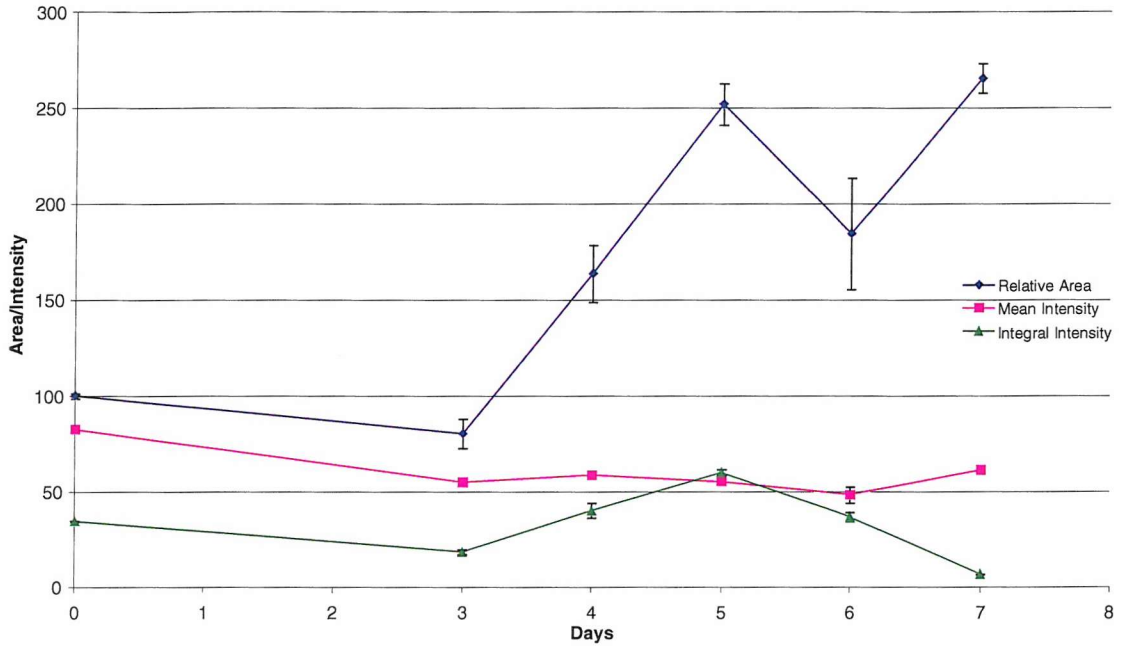

Fig.3.4.69 Graph showing the progress of an MMC-MGH-U1 colony over 7 days after exposure to MeGLA in 10%FCS at 500 µg/ml.

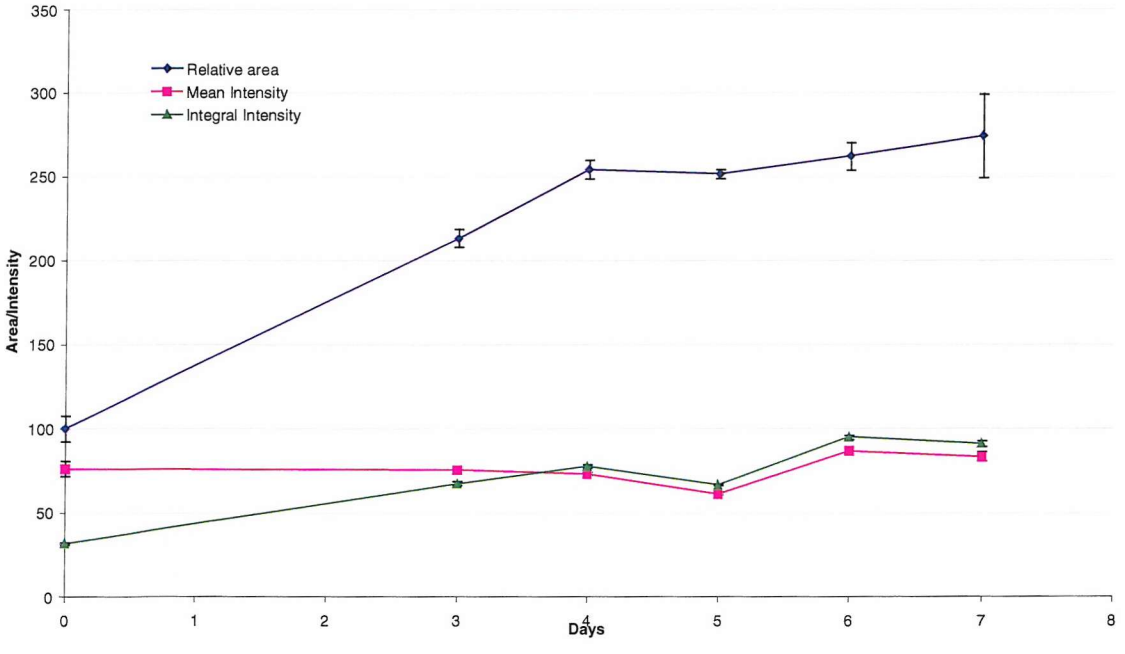

Fig.3.4.70 Graph showing the progress of an MMC-MGH-U1 colony over 12 days after exposure to MeGLA in 10%FCS at 1 mg/ml.

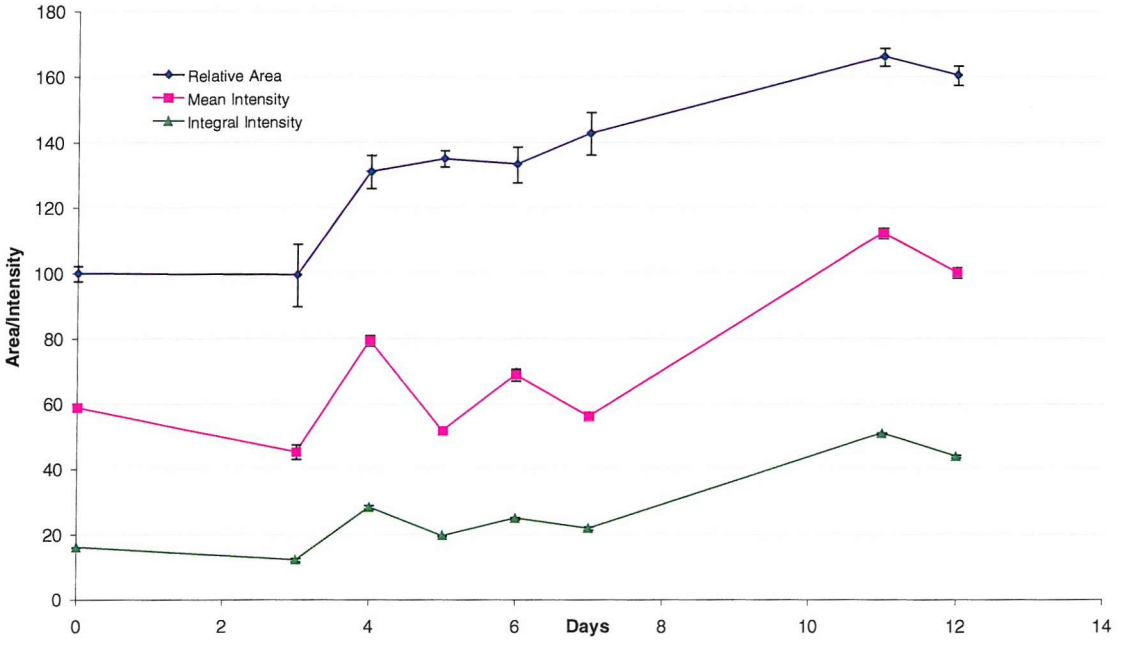

Fig.3.4.71 Graph showing the progress of the above MMC-MGH-U1 colonies over 7 days after exposure to MeGLA in 10% FCS.

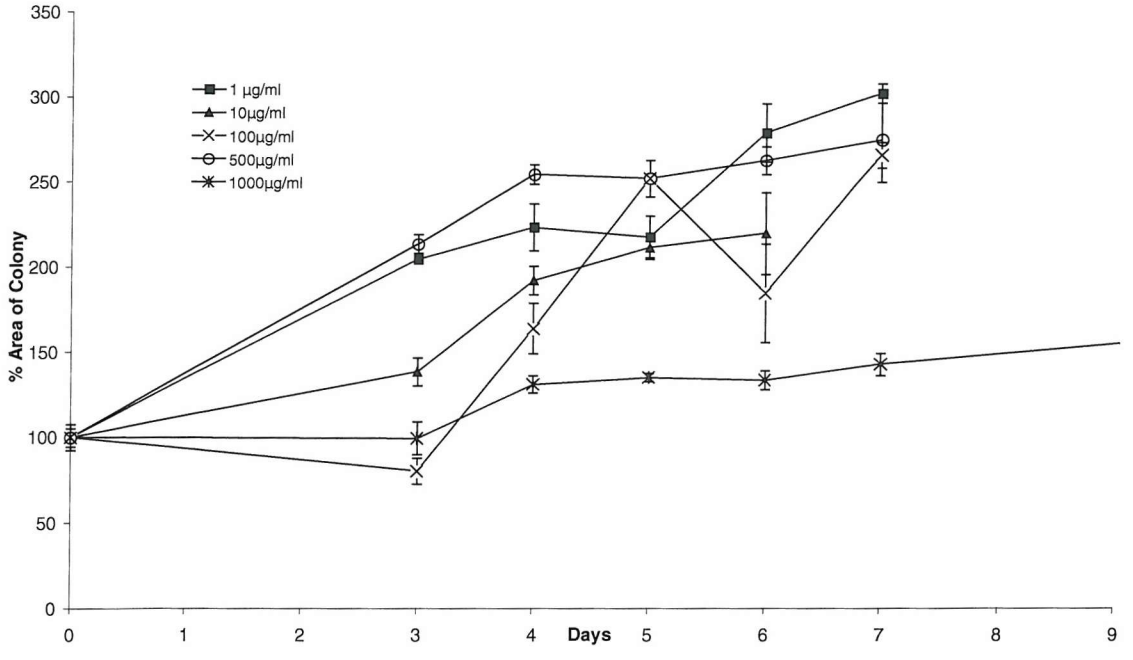

Fig.3.4.72 Graph showing the average areas of MMC-MGH-U1 colonies exposed to various concentrations of MeGLA in FCS.

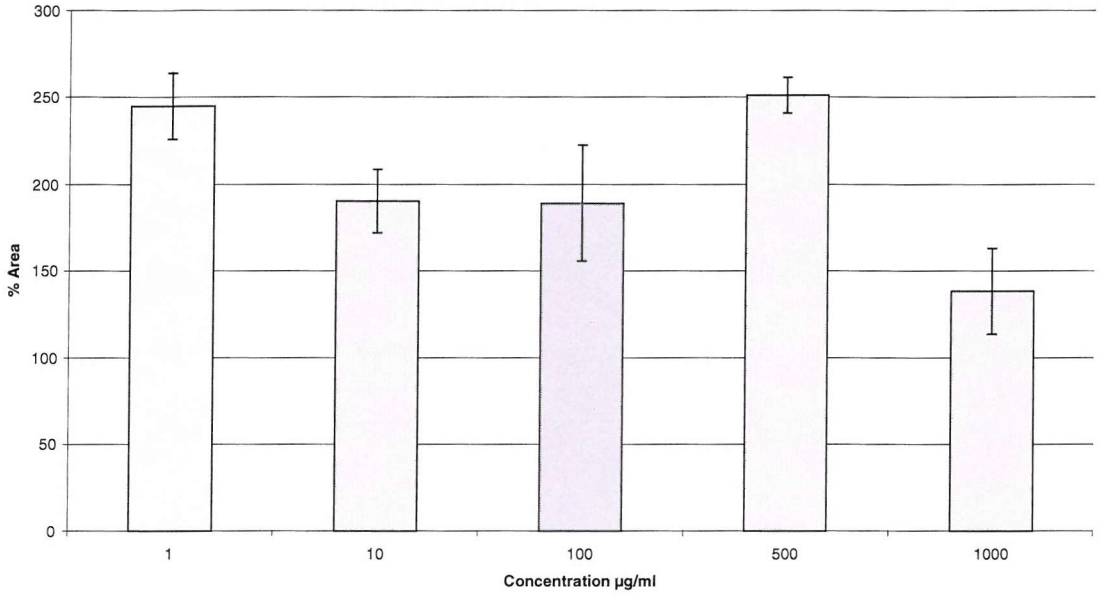

3.4.6 Indole-3-Carbinol

Parental and resistant colonies were used, and the results are shown in figs.3.4.73 to 3.4.81. As expected the lower concentrations showed no effect on the colonies, whereas at the higher concentrations there was a deterioration in the cultures by the 5th day after exposure. The lower doses of 1 and 10 μg/ml showed increase in area, whereas the 100 and 1000μg/ml doses showed decrease. The MTT assay of I-3-C suggested there was no effect for the MGH-U1 cells at a dose of 100μg/ml. Thus the colonies in this case were more sensitive to the drug effects.

The experiments with the MMC-resistant colonies showed increase in colony area with 1, 10 and 100μg/ml doses after exposure. At the high dose of 1mg/ml there was steady deterioration of the colony area. This is more in keeping with the results from MTT assays, but does not suggest the colonies were better able to survive the higher dose.

Parental Colonies.

Fig.3.4.73 Graph showing the progress of parental MGH-U1 colonies over 6 days, after exposure to I-3-C at various concentrations.

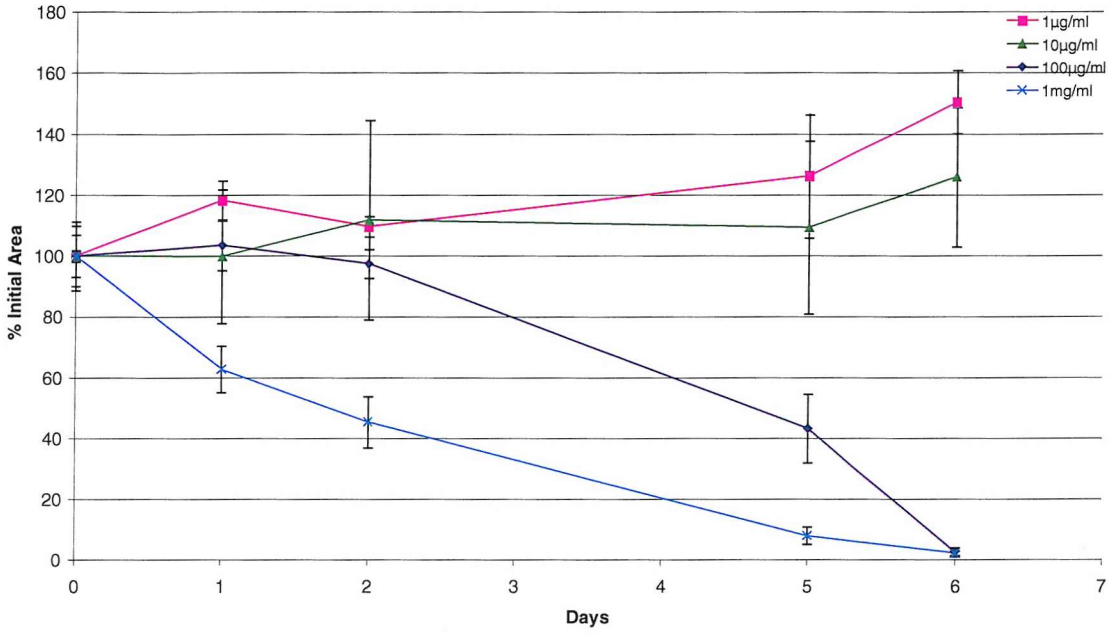

Fig.3.4.74 Graph showing the average areas of each parental colony exposed to a different concentration of I-3-C

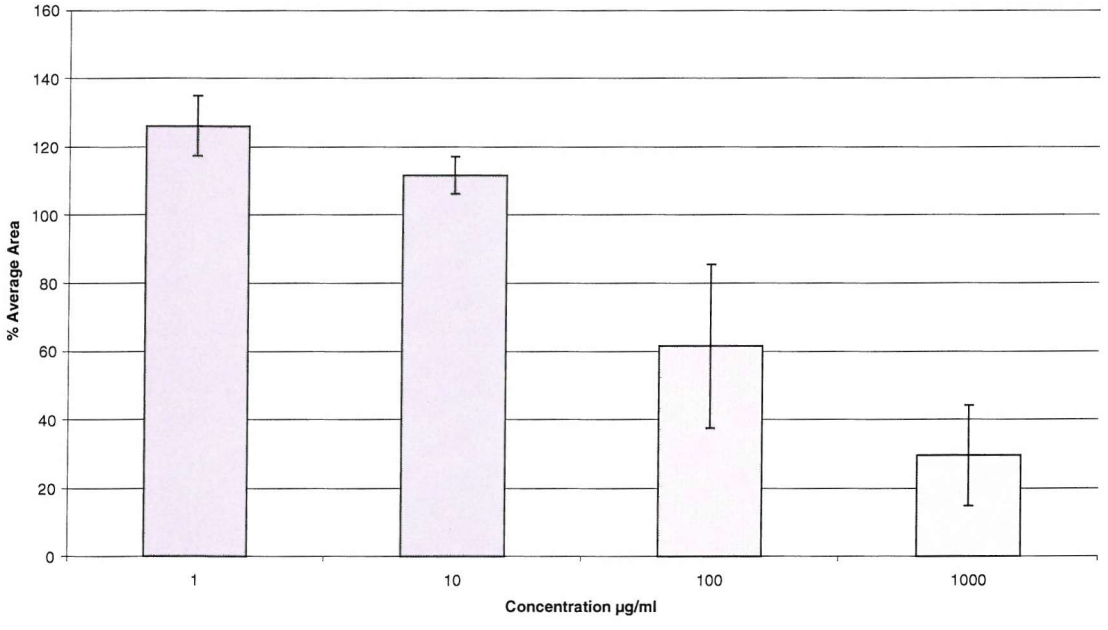

Fig.3.4.75 Graph showing the progress of an MMC-MGH-U1 colony over 9 days after exposure to I-3-C at 10 µg/ml.

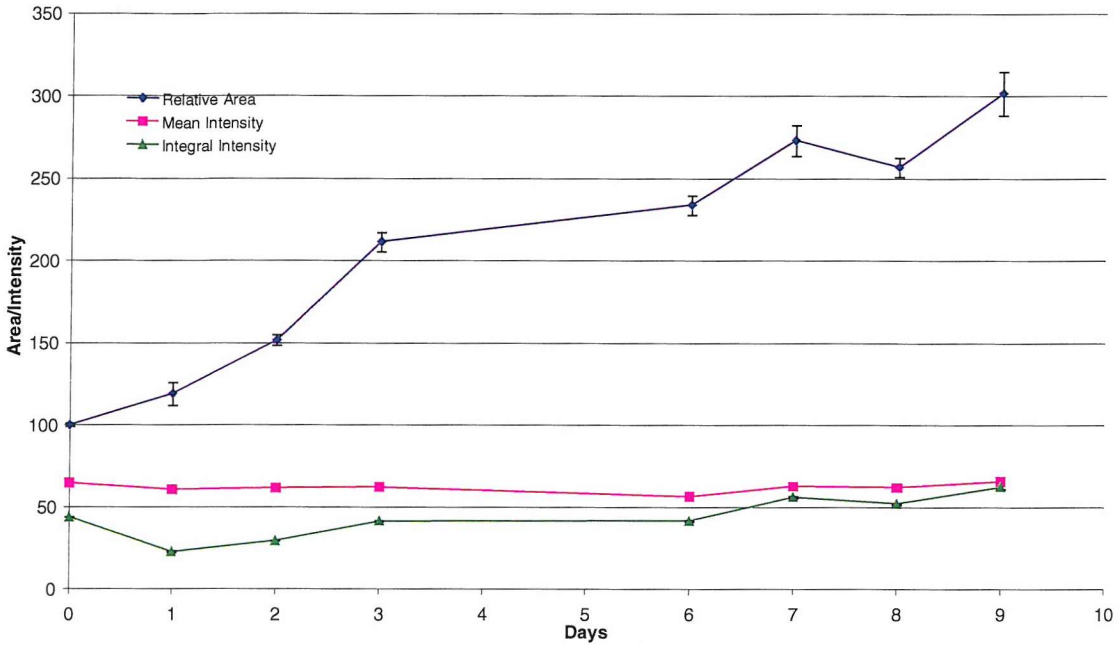

Fig.3.4.76 Graph showing the progress of an MMC-MGH-U1 colony over 9 days after exposure to I-3-C at 25 µg/ml.

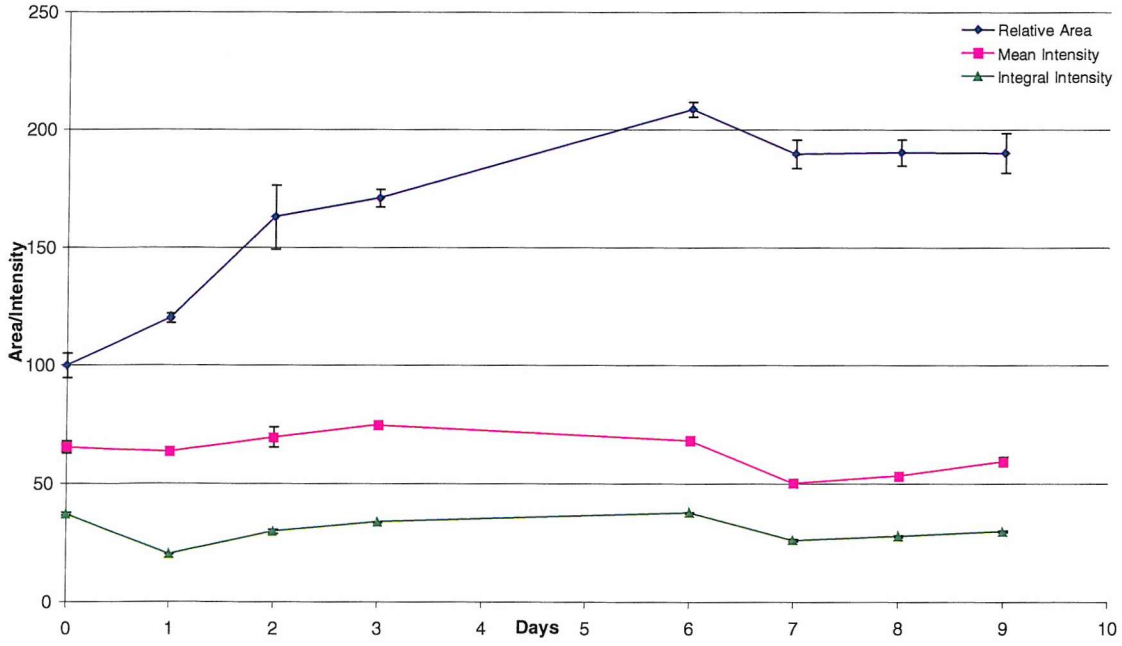

Fig.3.4.77 Graph showing the progress of an MMC-MGH-U1 colony over 9 days after exposure to I-3-C at 50 µg/ml.

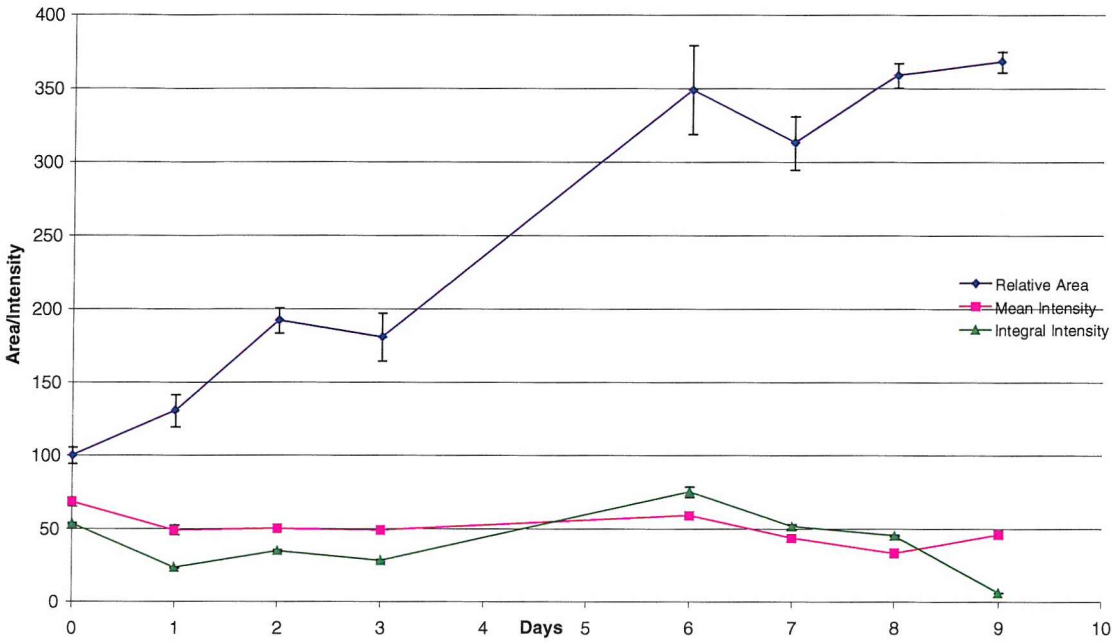

Fig.3.4.78 Graph showing the progress of an MMC-MGH-U1 colony over 9 days after exposure to I-3-C at 100 µg/ml.

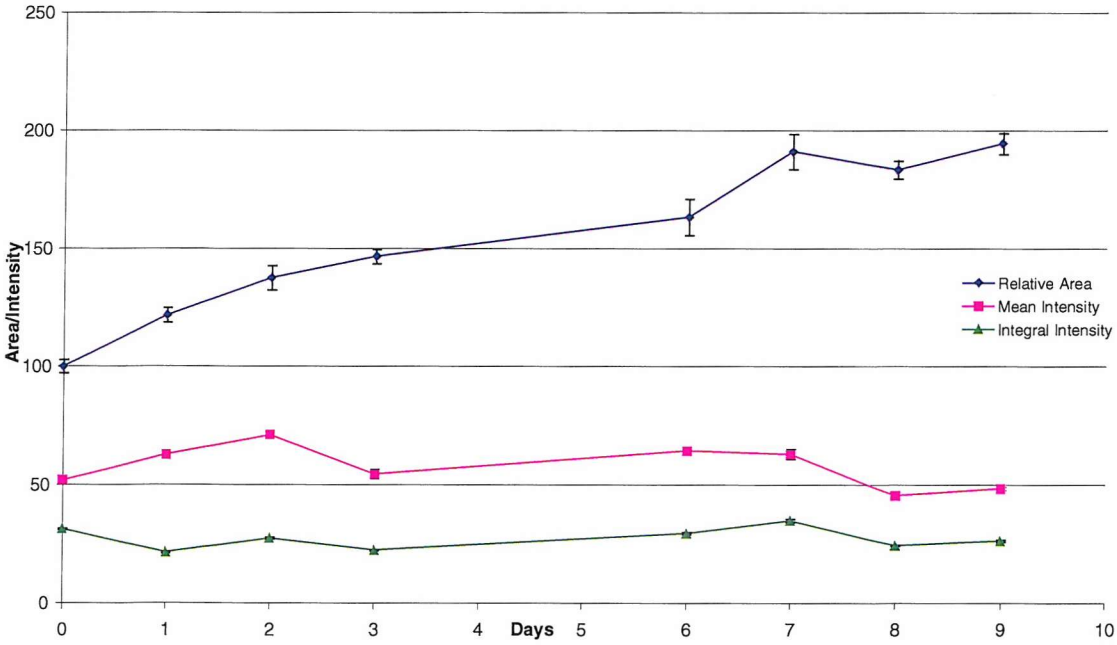

Fig.3.4.79 Graph showing the progress of an MMC-MGH-U1 colony over 9 days after exposure to I-3-C at 1 mg/ml.

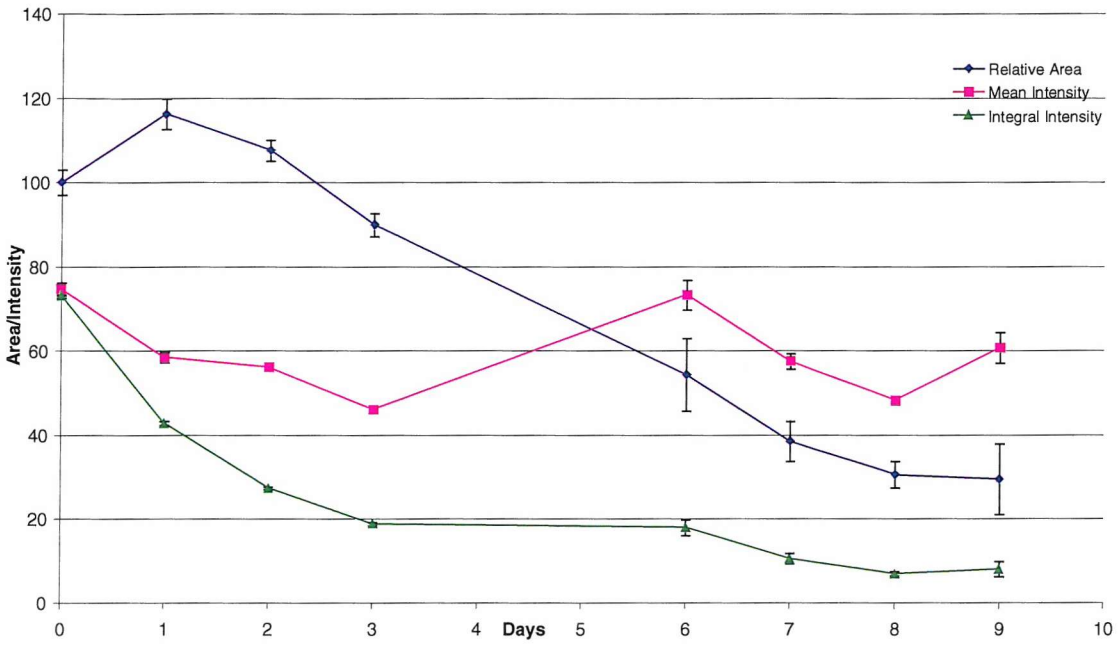

Fig.3.4.80 Graph showing the progress of MMC-MGH-U1 colonies over 9 days, after exposure to I-3-C at various concentrations.

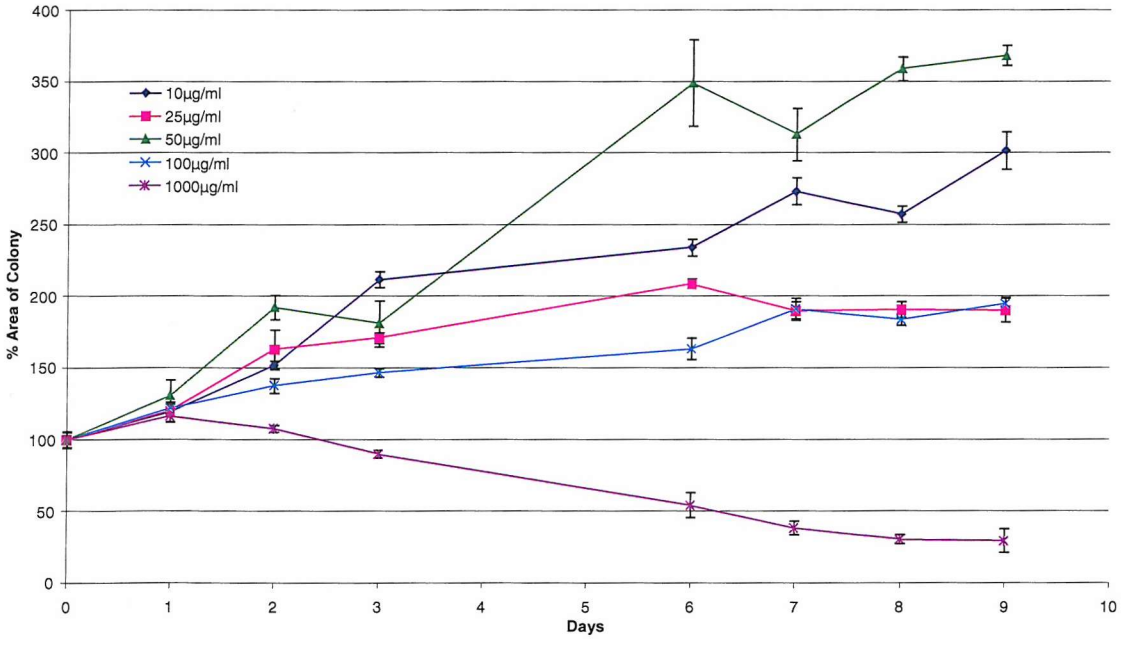

Fig.3.4.81 Graph showing the mean areas of MMC-MGH-U1 colonies exposed to various concentrations of I-3-C over 9 days.

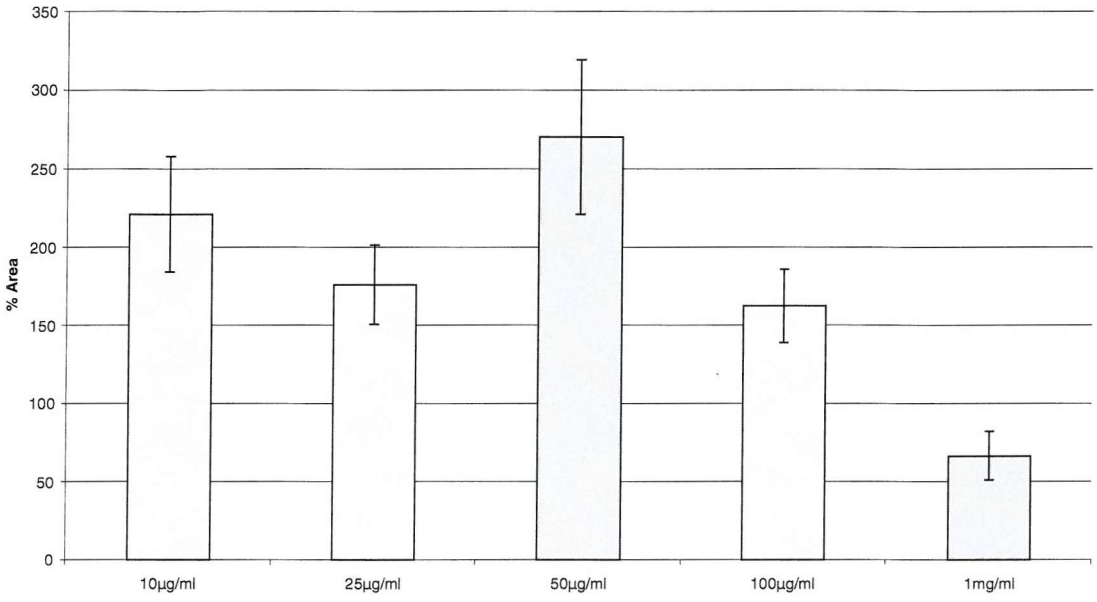

4. Discussion

These results demonstrate that the explant colonies can survive high concentrations of cytotoxic agents, and allow the same colony to be followed over time.

4.1 GFP Transfection.

Transfection of both the parental and MMC resistant MGH-U1 cell lines proved straightforward, although it is not known why only about 20% are initially transfected. Selection to enrich the transfectants was more problematic. Antibiotic selection was not successful in either cell line using reasonable, non-damaging concentrations of drug. For the MMC-MGH-U1 cells this could be explained by their MDR phenotype; cross-resistance to G418 is a possibility. The parental line was indeed more sensitive to G418, but not enough to give the basis for a selection protocol. Alternatively, the antibiotic may be cytostatic rather than cytotoxic and the cell cycle of resistant cells slower than that of the parental line.

The enrichment problem was circumvented by the use of fluorescence activated cell sorting, a more direct and accurate approach although more limiting in terms of the numbers of cells processed. Sorting relatively sticky epithelial cells is not as efficient as sorting haematogenous cells (the task for which FACS systems were originally designed). More cells are lost to sorting through interruptions due to clumping; an average sort session yielded around 10^4 high fluorescence cells. This and the discontinuous nature of the method compared to antibiotic selection, makes more demands on the stability of transfection.

In practice, the transfection proved remarkably stable. Ten passages, on average 72 hours apart, take approximately one month, which is well within the limits of time for which an explant culture might last. The time between passages can be lengthened by

simply reducing the plating density at each passage, allowing weekly passaging. To be useful as an intrinsic marker for cancer cells in organ culture, background fluorescence due to laterally transferred GFP should be minimal. This was the case in the co-culture experiments. Stability of GFP expression in mammalian cells has also been described in Chinese Hamster Ovary cells where no growth disadvantage was observed eighteen weeks after transfection(60).

Neither did transfection change the characteristics of the intracellular distribution of Epirubicin within the sensitive and resistant cells, indicating that the MDR status of the cells was not compromised by the vector, despite the antibiotic resistance cassette. The relationships between cytotoxic assessments of resistance and drug handling has been established for these cell lines(84)

These results show the transfected cells to express stably high levels of GFP without compromising the characteristics of the cell line.

4.2 Explant Characteristics.

4.2.1 Skirts.

The development of monolayer skirts from the explant cultures themselves shows that the urothelium is living and capable of migration and growth, and corresponds to the observations of previous work on explant culture(88). Supravital staining of both the explant surface and the surrounding skirt confirmed the viability of the urothelial cells of the explant. Perhaps more importantly for this model, these observations also suggest that the cyanoacrylate glue does not cause significant toxicity when used in small quantities.

Experiments applying MeGLA to the skirt showed that it might be possible to study the effects of drugs on the urothelium by imaging the skirt. However, this

approach was not pursued further, as culture of primary urothelial cells is a well-established and successful technique. Although in theory it could be used to study the differential effect on urothelial cells and tumour cells.

4.2.2 Explant surface.

The experiments with cytotoxic agents on the explant *per se* further showed that the urothelial surface is able to withstand a toxic insult without complete denudation of the epithelial surface. These were qualitative experiments. As with the urothelial skirts, this proved to be a difficult area of development, as it was difficult to quantify the numbers of urothelial cell nuclei on the explant surface.

The characteristics of these explants are similar to those described before (72;94;133;135) with a similar division of the explant into normal surface urothelium, and epithelial-like growth on the surrounding base (155). The behaviour, conditions for culture and morphology of these explant systems is, therefore, well established. The explants in this model behaved in a similar fashion. The primary method of examining these models has been by conventional histology or by SEM, whereas this system produces the advantage of being able to view the living tumour colonies, without terminating the experiment. However, frequent removal of the cultures from the incubator increases the chance of microorganism contamination and effectively limits the period for which the explants are maintained to about 20 days. This compares to other studies in which the urothelium has been maintained in culture for up to 200 days(115). However, this did not appear to be a disadvantage in these experiments, as tumour colonies survived up to 11 days.

4.2.3 Use of Cyanoacrylate Glue

Cyanoacrylate glue is known to have toxic properties, which is why its octyl derivatives are only licensed for topical application, and not for internal use. Formaldehydes are released when exposed to air, which are cytotoxic. Control experiments demonstrated that the use of this glue in the model was not a confounding factor, as long as sufficient rinsing took place after explant establishment.

4.2.4 Tumour Colonies.

The SEM images helped to confirm the presence of tumour cells in a defined colony, and showed the morphology of surrounding urothelium. The cancer cells could be readily identified by their roughened appearance and larger size. Stranded processes between the tumour cells and urothelium suggested that junctional bonding had occurred. Previous studies using SEM have shown similar images of the normal and hyperplastic surface(72;155). The SEM images also showed that the tumour cells were probably spreading out from the central pipette "hole" onto the surface of the explant urothelium. The question then arises whether any invasion of the urothelium is taking place, as MGH-U1 cells have this potential. The attempted H&E sections did not answer this question, as they were destroyed in the process of microtoming. However, another group have worked with this model and demonstrated invasion into the urothelium (personal communication Mr Henry Lazarowicz FRCS, Newcastle, UK). An alternative transfected cell line, such as RT112, which is more superficial in its behaviour, would provide an interesting comparison.

The advantage of using a fluorescent tumour cell line inoculated into normal urothelium is that it provides a patho-physiological imitation of the *in vivo* superficial bladder tumour, whose progress may be closely followed. Although as mentioned above,

the superficial nature of the tumour colonies in this model has not been proven. Potential therapeutic agents may, therefore, be investigated in a manner that will relate better to the clinical scenario, in terms of allowing clinically relevant concentrations of drugs to be tested. It is the fluorescent nature of the transfected tumour cells, which allows the visualisation of the tumours without recourse to histological examination, and also demonstrates their viability.

The serial examination of tumours is possible, allowing the progress of a drug to be followed in its action on both the urothelium and tumour over a period of several days. The application of various cytotoxic agents demonstrated that the explant tumours could be used to assess the efficacy of cytotoxic agents. Application of Mitomycin C at 100μg/ml, for example, showed that the effects of this drug were less pronounced than when applied to monolayer tumour cells. A similar effect was noted with Epirubicin. Interestingly, even parental "sensitive" tumour cells could be observed to survive after high concentrations of these cytotoxic agents, perhaps helping to explain the recurrence rates which are still seen after a single instillation following TURBT(5). It is not clear why this effect was observed. The tumour cells may be protected by their attachment to normal urothelium, or the multilayered colony may prevent full penetration of the drug(177). It was also possible to simultaneously assess the surrounding petri dish monolayer tumour cells for changes. The essence of the model is demonstrated by this comparison. Whereas an explant colony might survive a high concentration of drug, the surrounding tumour cell skirt was destroyed. Concurrent staining of the urothelial surface enabled demonstration of surviving normal urothelium.

4.2.5 BrDU Staining

BrDU staining is an established method to demonstrate DNA replication(57). BrDU staining of the explant colonies showed a proportion of cells staining positive suggesting these cells were in S phase. This suggests that the colony is capable of proliferation, although it was not possible to accurately quantify because of difficulties in synchronously staining both non-S phase and S phase cells.

4.3 Cytotoxic agents

The main priority in this work was the development of the model, but in using a variety of established and novel compounds in the system, some comments can be made on these agents in their own right.

4.3.1 MTT assays

These results demonstrate the cytotoxicity profiles of GFP transfected MGH-U1 cell lines which are similar to those previously described for non-transfected lines(63;84;150). These results were useful when comparing with the explant cytotoxicity experiments.

4.3.2 Classical MDR drugs

The early experiments with Epirubicin and Mitomycin confirmed that it was possible to apply a cytotoxic agent to the colonies. The tumour colonies retained their MDR properties, and could recover and continue growing after the toxic insult. However, imaging of the colonies by confocal and SEM microscopy showed that the majority were not forming 3 dimensional structures, but rather appeared to be spreading out as a monolayer on the explant surface. This may also explain why the colonies did not show significantly greater survival than monolayer cultures after exposure to the

cytotoxic agent. Similar results were noted for Mitomycin C and MeGLA when the early experiment protocol was used for exposure to drug.

In the later experiments with exposure 24 hours after cell seeding, the MDR differential response was maintained, with parental colonies susceptible to lower doses than resistant colonies. These experiments showed survival of the colony at a dose up to 400x the IC>50 for monolayers. The technique of early drug exposure to the seeded cell pellet was therefore suggested by this observation, and lead to the adoption of this protocol as the standard for other experiments.

The dose responses seen in the splay graphs for Epirubicin and Mitomycin C suggest that the tumour colonies are behaving in a similar manner to *in vivo* bladder tumours. Doses for both these drugs clinically (1mg/ml) are of the same order as those survivable by the tumour colonies, in particular by the resistant cells(26). Further experiments with multiple replicates would be needed to further investigate the variability in this response.

4.3.3 Estramustine

The results for Estramustine showed satisfactory dose response splay graphs for both parental and resistant colonies. The colonies were destroyed at the highest dose of 500μg/ml, but were able to survive the dose at 100μg/ml, still well above the IC>50 for monolayers (22-42μg/ml). This illustrates that the colonies are different to monolayers in their dose response. However, the number of replicates in these experiments was not enough to draw definite conclusions on this finding, and further work would be required to substantiate these results. Estramustine has not as yet been used as an intravesical drug, and therefore it is not possible to make clinical comparisons.

4.3.4 MeGLA

The experiments with MeGLA on parental tumour colonies showed that a clinically relevant high concentration (1mg/ml) of drug could be applied, and still observe growth of the colony after exposure. In comparison the resistant colony was destroyed with no recovery. Again this is a reflection of the variability in colony behaviour seen in the model, and further replicates would be required to investigate this. It could be postulated that this variability may in fact represent the *in vivo* situation more closely. Clinically, bladder tumours in different hosts have considerable differences in response, and the reasons for this are multi-factorial, but include MDR(5).

4.3.5 MeGLA in Albumin

These experiments confirmed that the quenching effects of protein on MeGLA are maintained, and emphasise how the apparent cytotoxic effects on monolayers become much less pronounced in this more realistic model. It also has potential implications for the use of MeGLA as an intravesical agent after TURBT, as any instillation in the immediate post-operative period would have to contend with levels of serum in the irrigant(150).

4.3.6 Indole-3-Carbinol

The IC>50 for a 1 hour exposure to I-3-C on parental monolayers was 200μg/ml. The Parental MGH-U1 colonies increased in relative area at doses below the IC<50 for monolayers, i.e. at 1 and 10μg/ml, but did not survive at 100μg/ml. However, the single colony used in this experiment precludes any meaningful conclusion related to this finding. It could be speculated though that perhaps in this individual colony the I-3-C had better penetration into the cells or the washing process after exposure was inefficient.

In contrast the MMC-MGH-U1 cells continued to increase area of colony at 100μg/ml, but were destroyed at the highest dose. Compared to the genotoxic drugs there does not appear to be any large differential in the survivable dose compared to monolayers. However, the small number of colonies involved in these experiments does not allow any proper conclusion to be drawn. These results would need to be substantiated in further dose-ranging, multiple replicate experiments.

4.4 Limitations of the Model.

There were limitations to the system, some more significant than others. There was the inevitable problem of yeast and other fungal infections probably because serial imaging necessitated daily removal of cultures from the incubator to a distantly located confocal microscope. This was the reason why cultures did not last longer than about 14 days. Several suggestions have been put forward to overcome this problem. Particular care should be taken when extracting the rat bladder, by using as aseptic a technique as possible. Ideally the confocal microscope would be located in close proximity to the incubator, and to allow petri dish lid removal it would ideally be placed in a laminar flow hood. Unfortunately the practicalities of funding a £150,000 microscope, computer and laser could not be overcome in our laboratory. Owning and running one's own confocal microscope would also allow daily examination of colonies, not interrupted by other users, weekends and public holidays.

The combination of human and animal tissue is theoretically not ideal, but the more practical solution given the difficulty in obtaining a regular supply of fresh human tissue and the remit of producing a rational series of experiments using a standardised technique. Criticism has also been received regarding the use of the MGH-U1 cell line,

in a model of superficial bladder cancer, when it was originally derived from an invasive tumour, and has the properties of a high grade invasive cell line. The MGH-U1 cell line has been extensively studied and characterized in our laboratories, with the production of two resistant cell lines. Thus, the pragmatic answer is that this cell line was available and familiar. "In any model, compromises have to be made to achieve utility" (quote, Dr Alan Cooper). Alternatives might have included the RT112 or RT4 cell lines, which potentially have more superficial characteristics.

There was some variability in the size of the tumour colonies produced, and their exact location on the explant surface could not always be accurately predicted, despite the technique described, which used a constant volume and number of cells in the centrifuged pellet. However, as it was possible to follow each explant tumour over time, this difficulty was overcome. In effect each explant acts as its own control. The method of fluorescence analysis was not of high accuracy, because of difficulties in calibration and the way in which the computer software interpreted the data. There was also some background fluorescence to be taken into account and condensation on the petri dish lid varied from day to day. This is the reason why estimates of cytotoxicity were by measurement of the change in area of a colony. It is believed that this gave a more accurate reflection of the effects of an applied drug on the residual viable biomass.

However, even the area measurement suffered from intra-observer error. Figure 4.1 shows a schematic diagram to explain one possible reason for this. The confocal system takes several "slices" through the colony and reconstructs these as a single image, with a maximum depth of 166μm. Thus it is possible to take two different measurements from the same colony giving different areas. In practice this was not a problem, because

the colonies were not generally much larger than the depth limit, and it was also possible to set the microscope to record a similar section by examining the previous image of the colony and setting the petri dish on the microscope in the same orientation.

Fig.4.1 Diagram showing possible reason for variability in area measurement of the explant colony. Transverse views on left, top view right.

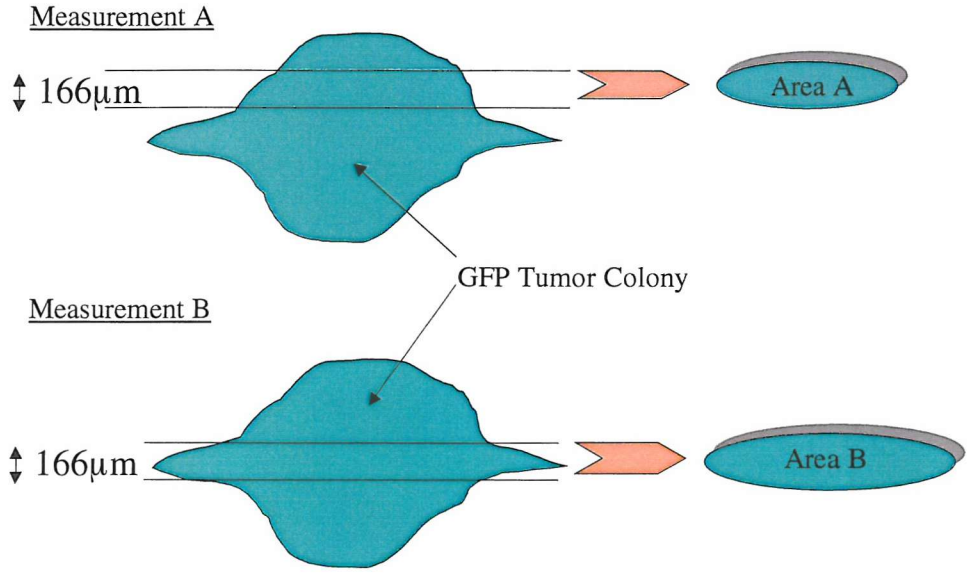

Thus, area B > area A, despite no actual change in the explant colony

In a study of patients undergoing cystectomy, Mitomycin C, for example, was able to penetrate to a depth of up to 2000µm into the muscularis propria, with a semi-logarithmic decline in tissue concentration with greater depth. Median concentration at the urothelium-lamina propria border was 5.6µg/ml, 2.7µg/ml in the lamina propria and 0.9µg/ml in the muscularis. The concentration at the urothelial-lamina propria border was 35 times the urine concentration of MMC. Interestingly tissue levels in superficial tumours were 2 to 3 times higher than in normal tissues(176). This has relevance to the

model in terms of explaining why the tumour colonies were able to survive a high dose of drug.

A schematic diagram is shown in figure 4.2 illustrating the proposed progress of the explant colony. It is hypothesised that the 3-dimensional multicellular nature of the cell pellet gives protection to centrally located cells from a high dose of drug that cause cell death of the outer layers. The central cells are then able to continue growing on the explant surface. The diagram explains how this then results in an increase in colony area, when viewed from above. It also suggests that the actual biomass may be unchanged. It is also possible that the cells were migrating on the urothelial surface as well as proliferating. The actual residual biomass of cells could be measured by, for example, weighing the explants and skirts, although it is likely that very accurate measurements

Fig.4.2 Diagram showing the progress of an explant colony in transverse section.

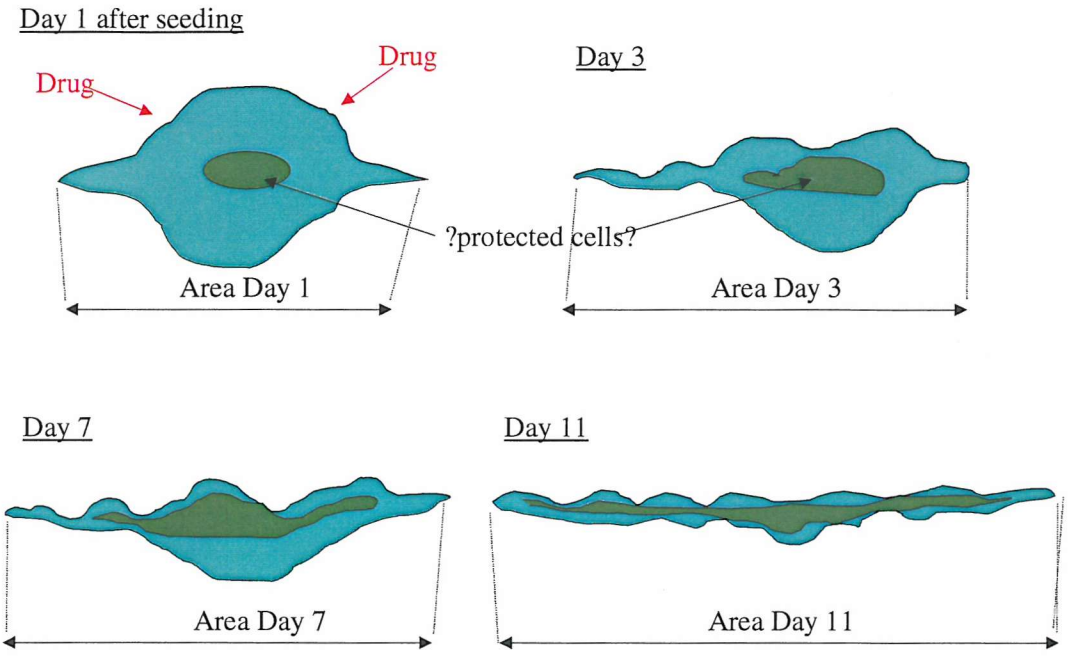

Thus, protected central cells survive, and spread out over the explant surface, increasing the colony area.

would be required to pick up the tiny differences in weight. The structure of the tumour colony might also have been verifiable by H&E sections, but as previously mentioned these were not successful. Another alternative might be to perform ELISA or FACS studies on the absolute amount of GFP expressing cells in the explant or skirt, as used in a recent study of GFP transfected cells in an animal model(162).

The control colonies also caused some difficulty with the model. The results showed that whilst some controls grew well, others either deteriorated or showed very little growth. This is illustrated in the results section with the average areas of control colonies at various time points after seeding. There is an initial growth period up to 3 to 4 days, but then only slow growth in a plateau period. This might be explained by the presence of a super-confluent skirt of MGH-U1 cells surrounding the explant on the petri dish surface, and causing a combination of medium depletion and paracrine growth inhibition. In colonies exposed to a high concentration of drug, this effect is overcome by destruction of the skirt, enabling the explant colony to continue growing. This hypothesis is illustrated schematically in the figure below. Frequent trips to the distantly located microscope may also have affected the colonies. It would be of interest to compare the behaviour of an explant colony with and without a surrounding MGH-U1 skirt. A recent study also suggested caution in the use of GFP as a tumour marker, as its expression is adversely affected by hypoxia(24). This may have been another possible reason why fluorescence of the colonies was variable. The inconsistency of controls meant that it was not possible to make a comparison with those exposed to drug, as would be the case with a microtitre plate experiment.

Fig.4.3 Schematic diagram showing the proposed behaviour of a control compared to a colony exposed to a high drug concentration.

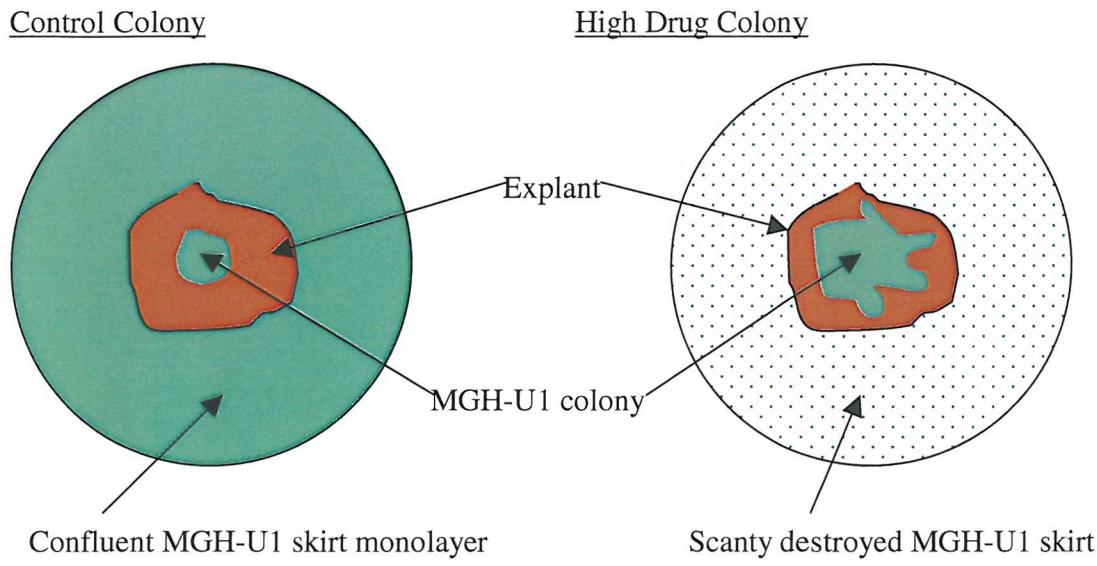

The technique is more time-consuming than colourimetric assays on monolayer cell lines and hence smaller data sets can be collected in a certain time period, albeit in a more realistic fashion. It was not usually possible to have more than 10 explant colonies running synchronously, because of the time it takes to image each colony on the confocal microscope, which is about 15 to 20 minutes per colony. For example, 3 replicates per dose level would allow 3 study doses, per run, as well as a control. Since each run of experiments would last a total of about 3 weeks, and taking into account the high infection rates, a 6 month period might yield about 50 to 60 colony experiments. If these were all dedicated to a single drug study, then this would be quite adequate for assessment. As with animal experiments, there is also a learning curve to be taken into account for anyone wishing to initiate the model.

The issue of consistency has been addressed with regard to the control colonies, but there is also the issue of reproducibility in the drug experiments. With the benefit of hindsight there is no doubt that this work attempted to investigate too many different agents, with not enough replicates for each dose level. This was a mistake and it would clearly have been better to have concentrated on one drug for the same number of explants. Ideally each concentration of drug would have been to several explants, similar to a 96 well plate experiment, where each explant colony is like the well of the plate, in order to provide a measure of consistency.

If this model were to be used as part of the investigation of a potential chemotherapeutic drug then ideally it would be with initial dose ranging studies. Then once a dose ranging experiment has been performed it would then be possible to use a single high dose of drug to expose to several explant colonies in order to measure consistency. If the model were to come to its full potential in a well-equipped laboratory with dedicated staff then of course some of the time and consistency problems would be overcome.

4.5 Advantages of the model.

The clearest advantage of the model is its ability to allow high concentrations of drug to be tested on cell colonies, in some cases hundreds of times more than the IC>50 for monolayers. The model in this sense is more realistic and clinically applicable, and indeed this was the original aim of this work. The model is specifically designed to mimic the events of intravesical chemotherapy, and this it has achieved in terms of short-term cytotoxic effects.

The unique feature of this model is its ability to follow the same colony over several days. To perform a similar time-sequence using a microtitre plate would involve

using separate wells for each time point, and assuming that those cells destroyed by MTT in an early part of the experiment would have gone on to behave similarly to those assayed at a later point. The sequence of images obtained from a single explant colony are amenable to quantitative analysis, as described above, and measurement of the area forms a relatively simple method for assessing biomass. The images themselves are of interest, especially when they are viewed with appropriate computer software as a time-lapse film.

Whilst the explants are more time-consuming than monolayer experiments, they are still potentially a faster and better rationalised method of assessing the behaviour of a 3-dimensional tumour than a full animal model.

4.6 Suggestions for future work.

The fundamental question to be answered is whether the advantages outweigh the problems of the model. There is not a clear answer to this, as some of the issues of consistency and reproducibility remain to be answered.

In terms of further development of the model, the first step would be to transfect a variety of different cell lines, including RT112 and RT4, which are potentially of a more "superficial" nature. The different cell lines could then be compared in the model and the most suitable for investigation of superficial disease identified. It would also be useful to obtain H&E sections of the tumour explants, and certainly a dedicated laboratory microtome, rather than the standard hospital pathology service, would help in this respect. Indeed, as previously mentioned a group working with the model in Newcastle has reproduced this need.

In an ideal setting the laboratory would have a dedicated confocal microscope to avoid some of the problems of moving explants to a distantly located facility. This problem can be partly overcome by using HEPES buffered medium for transporting the explants. In a dedicated confocal microscope within incubator conditions it might also be possible to obtain true time-lapse films of the colonies growth and response to investigational agents.

Many other suggestions have been mentioned in the text above in relation to the problems encountered, but of most interest would be alternative methods for verifying the residual biomass, such as weight, ELISA or FACS sorting. It would then be possible to answer the question of whether the area of the colony measured represents true growth.

4.7. Conclusions.

The explant GFP MGH-U1 colony model is a potential method of assessing drugs used in intravesical therapy of superficial bladder cancer, at clinically relevant concentrations, for. It has limitations, and advantages compared to alternative models, but would form a useful adjunct in the assessment of any new drug. Below is a summary of the general steps needed to set up the model.

1. Establish GFP transfectants of the chosen urothelial tumour cell line by application of a suitable kit, and purify transfectants by flow cytometry, or antibiotic selection. Establish in culture and freeze samples for future use.
2. Obtain explants from rat bladders and glue to the petri dish. Establish in culture and confirm viability by demonstration of urothelial skirts.
3. Passage a flask of transfected cells, and centrifuge the resulting cell suspension to create a cell pellet. Pour off the supernatant.
4. Remove the medium from a 3 to 5 day old explant
5. Apply 5µl of cell pellet to the explant by creating a central depression with the pipette tip and incubate for 1 hour without medium. Carefully re-apply medium at the end of this period, and replace in the incubator.
6. Image the resulting tumour colony by fluorescent confocal microscopy within 6 to 12 hours, as a baseline for further imaging
7. Remove medium and apply an investigational agent to the culture for a set time period of 1 to 2 hours.
8. Image again after 12 to 24 hours and at daily intervals thereafter.

Appendix I: Bladder Cancer TNM Staging.

Primary Tumour.

Tx: Primary tumour cannot be assessed
T0: No evidence of primary tumour
Tis: Pre-invasive carcinoma-in-situ: "flat tumour"
Ta: Papillary non-invasive carcinoma
T1: Tumour invades subepithelial connective tissue
T2: Tumour invades muscle
pT2a: Tumour invades deep muscle (inner half)
pT2b: Tumour invades deep muscle (outer half)
T3: Tumour invades perivesical tissue
pT3a: Microscopically
pT3b: Macroscopically (extravesical mass)
T4: Tumour invades any of the following: prostate, uterus, vagina, pelvic and abdominal wall
T4a: Tumour invades prostate, uterus, or vagina
T4b: Tumour invades pelvic wall or abdominal wall

(Note: The suffix "m" should be added to indicate multiple lesions. The suffix "is" may be added to any T to indicate the presence of associated carcinoma-in-situ.)

Regional Lymph Nodes.

Nx: Regional lymph nodes cannot be assessed
N0: No regional lymph node metastasis
N1: Metastasis in a single lymph node, 2cm or less in greatest dimension
N2: Metastasis in a single lymph node, more than 2cm but not more than 5cm in greatest dimension; or multiple lymph nodes, none more than 5cm in greatest dimension
N3: Metastasis in a lymph node more than 5cm in greatest dimension

(Note: Regional lymph nodes are those within the true pelvis; all others are distant lymph nodes)

Distant Metastasis.

Mx: Distant metastasis cannot be assessed
M0: No distant metastasis
M1: Distant Metastasis

Appendix II: Confocal Microscopy

Confocal microscopes differ from conventional fluorescence microscopes in their ability to image with true three-dimensional resolution. Most images produced by light microscopy consist of superimposed structures, often producing complex optical patterns, which can be difficult to interpret. Such problems are exacerbated in fluorescence microscopy when auto-fluorescent or fluorochrome-labelled structures are overlapping or adjacent to each other. These difficulties are caused because the conventional fluorescence microscope collects light, not only from the focal plane, but also from above and below the focal plane.

The confocal microscope circumvents this problem by ensuring that only the fraction of light from the focal plane is detected. This is achieved by employing a point light source, which produces a small and geometrically well defined light spot in the focal plane. Emitted fluorescent light from the focal plane is collected by the objective lens and sent back through the optical path into a beam splitter, which then directs it to the detector. Both the light source and the detector are equipped with a small pinhole placed within the optical path. Such an arrangement is said to be geometrically conjugated with respect to the focal plane and leads to different points of convergence of the light beam. Light originating from the focal plane converges by definition within the pinhole, whereas light from out of focus planes converges by either in front or behind and is therefore excluded. Thus the blur and haze from fluorescent structures outside the focal plane which plagues conventional fluorescence microscopy is removed. The resulting confocal images are always in focus and are in fact, optical sections of the object.

These optical sections are influenced not only by the numerical aperture of the objective but also by the diameter of the pinholes. As the detector pinhole is made wider, the thickness of the optical section increases until the resulting image approaches that produced by conventional fluorescence microscopy. The optical resolution is also effected by the wavelength of light used.

Diagram showing the optical principle of the confocal microscope

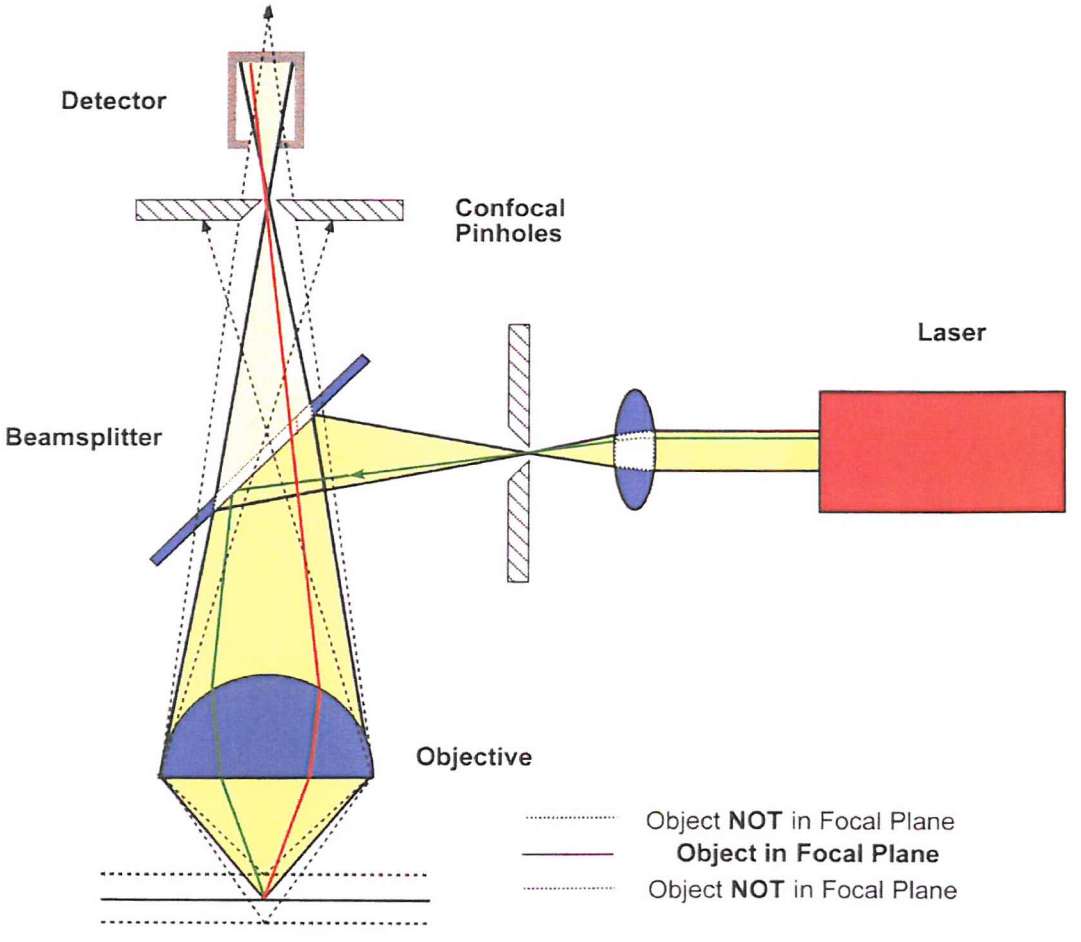

Development

Marvin Minsky laid down the principles of the confocal microscope in a design in 1955 for the study of neural networks in the living brain, a patent for which was issued in 1957. Egger and Petran succeeded in producing the first optical images from a confocal

microscope 10 years later, but their prototype had too many technical problems. The first convincing demonstration of confocal imaging was by Brakenhoff *et al* in 1978(13).

Contemporary confocal microscopy uses high tolerance optical lenses, detectors of high sensitivity, versatile fluorescent markers and powerful lasers producing coherent light of a wavelength appropriate to the chosen fluorochrome. The first instrument incorporating all of these features was produced by Van der Voort *et al* in 1985(166), but used a moving stage to scan the object, rather than moving the beam. Some designs have used a fixed stage and moving beam controlled by moveable mirrors to scan the object, hence avoiding the potential perturbation of the specimen which occurs with a moving stage system(179).

The advantages of the confocal microscope over the conventional microscope may be summarised as follows.

1. Light rays outside the focal plane will not be recorded.
2. True three-dimensional data can be recorded.
3. Recording of such three dimensional data does not require sectioning of the object under study,
4. Scanning in the x/y direction as well as the z direction together with three-dimensional reconstruction allows viewing of the object from all sides.
5. The presence of a small illuminating light spot in the focal plane minimises stray light.
6. Many confocal slices can be superimposed, thus giving an extended image which can only be acquired in conventional microscopy by reducing the aperture and thus sacrificing resolution.

7. Quantitative measurements are no longer focus and operator dependent, as all intensities until below and above the specimen in focus are used for analysis.

The resolution of the confocal microscope is still limited by the wavelength of light and numerical aperture of the objective lens. However, as the confocal light path uses two times the image of a diffraction limited point the confocal microscope has 1.4 fold improved resolution over the conventional set-up(114).

The optical pathway shown in illustration 1.3 demonstrates the geometry involved in the formation of just a single image spot. In order to produce a two dimensional image it is necessary to move this spot in consecutive lines until a square has been scanned. The typical confocal microscope operating in such a fashion contains the following elements.

1. A laser light source allowing selection of suitable wavelengths
2. A scan unit for moving the illuminating beam across the object.
3. Detectors to record the photons coming from the object.
4. A central processing unit to control the hardware, and a data storage unit for storage and manipulation of data.
5. A high quality research microscope to which the scanning unit is attached.

The ability of confocal microscopy to undertake three-dimensional analysis of cell structures has been widely used in the biological and medical sciences. Neurones, axons and dendrites can be easily visualised three dimensionally by impregnating the cell with silver. Complex intracellular structures such as the cytoskeleton can also be visualised and reconstructed using fluorescence labelling techniques.

Within oncology, confocal microscopy can be used to reconstruct cancer tissue morphology, and study deviations from normal tissue structure. Within the nucleus

confocal microscopy can be used with techniques such as in situ hybridisation and immunofluorescence to study the spatial organisation of the nucleus, particularly chromosomal domains at interphase or in dividing nuclei.

Epifluorescence has become one of the most commonly used microscopic techniques in contemporary biological research, particularly with the advent of immunofluorescence (immunological probes which can be conjugated to fluorochromes) and the exquisite chemical specificity of antibodies as a basis for staining. Fluorescent probes have also been developed for intracellular calcium concentration, pH and membrane potential. Confocal microscopy overcomes the problem of the background "glow" associated with signals from structures above or below the plane of focus, and avoids the necessity of cutting of sections. The added benefit of greater optical resolution means that confocal microscopy has now become the imaging modality of choice in fluorescence light microscopy(173).

Appendix II: Fluorescence Activated Cell Sorting.

Flow cytometry is a light based technique for accumulating data from individual cells in suspension. Individual cells in a fluid stream are passed across a beam of intense light and the reflected or fluorescent light from each cell is measured and used to provide cumulative data on various cellular characteristics. Large numbers of cells can be treated with fluorescent agents and "flowed" in this fashion and the data can be used for cell sorting and for estimating cellular parameters such as nucleic acid content, pH, membrane potential and enzyme activity. In addition, the conjugation of fluorescent dyes to ligands and antibodies has enabled extensive studies to be performed on cell membrane, cytoplasmic and nuclear determinants.

Although there are many different flow cytometers, they all rely on fluidics to enable accurate placement of the cells in single file within the fluid stream, and to ensure that the fluid column containing the cells accurately intersects the illuminating beam.

The production of a tightly focused column of fluid within the flow cytometer depends upon the design of the flow chamber. These chambers utilise principles of laminar flow with viscous drag, hydrodynamic focusing and turbulent boundary drag to create the appropriate column of fluid and cells.

Laminar flow is a phenomenon whereby the speed of fluid flow within such a flow chamber is manipulated to ensure that contained particles are accurately placed at the centre of the fluid column. Fluid entering the flow chamber initially travels at the same speed across the entire width of the fluid column. However, as the fluid progresses through the chamber, the viscous drag at the walls slows the outer layers of liquid, causing the speed of flow to vary across the fluid column. Speed of flow is greatest at the

centre of the column, and slowest at the periphery.

Hydrodynamic focusing utilises the laminar flow created by the flow chamber to accurately place the cells within the column of fluid. The velocity gradient of the laminar flow system causes particles to be drawn to the centre of the column, and thus cells in suspension will be drawn into and retained within the centre of the fluid column for as long as the stable parabola is maintained. The distance from the chamber inlet to the point of formation of the stable parabola is some 50 times the channel diameter, and is known as the inlet length.

Turbulent boundary flow utilises a tapering chamber with a narrow exit orifice. Back pressure from the orifice results in sample turbulence, and, when combined with the viscous drag from the boundary of the chamber, creates a velocity parabola in a shorter distance than required in the laminar flow system.

"Sheath" fluid is provided from a sheath fluid reservoir, whilst sample fluid is usually injected directly into the centre of the flow chamber.

A combination of these principles is utilised in the design of flow chambers for the flow cytometer, with the end result that cells are accurately located at the centre of a well defined fluid column.

Flow cytometers use light as their source of excitation. This light is provided by a laser or arc lamp, and must be intense in order to adequately illuminate the cells, which pass through the light beam extremely quickly. The Becton-Dickinson FACScan utilises an argon-ion laser. Laser (Light Amplification by Stimulated Emission of Radiation) creates a coherent, plane polarised, intense and narrow beam of light at specific wavelengths.

A typical laser consists of a resonator, at either end of which are mirrors forming an optical container within which is located the plasma tube. This tube contains a gas at a preset pressure, which fluoresces during application of a current, emitting light in all directions. The current raises the electrons of the gas atoms into a higher energy orbit, from which they spontaneously decay to the base state, producing light, the wavelength of which is dependent upon the energy difference between the high and low orbit states of the electrons. Photons of light emerging from the ends of the plasma tube are reflected by the mirrors back into the tube. When these photons strike an atom in an excited state, a second photon is produced which is of the same wavelength and phase as the stimulating photon, and which travels in the same direction along the plasma tube. These photons in turn stimulate the production of further photons and a chain reaction ensues, producing light amplification, the magnitude of which is proportional to the length of the plasma tube, and is controlled by the current.

At each end of the plasma tube are windows, set at a specific angle called "Brewster's angle". Flat windows would prevent efficient lasing by reflecting too much light. Brewsters angle minimises reflections within the plasma tube and renders the light plane-polarised.

A total of 95-99% of the light produced in the plasma tube is required to be reflected back through the Brewsters windows in order to maintain lasing. The front mirror is therefore specifically designed to permit only 1-5% of the laser light to escape.

The laser light produced is of specific wavelengths determined by the energy levels of the orbits achieved by the electrons. A particular wavelength can be selected by the use of specific mirror coatings, or by the placement of a prism in the laser beam in front

of the reflector. Rotating this prism can alter the wavelength of light reflected back into the plasma tube, and therefore alter the wavelength of emitted light.

Re-emitted or scattered light must be collected by the flow cytometer for analysis. The forward collection lens gathers light from 1 to 20 degrees off the axis of the laser beam, whilst a second lens collects light scattered at right angles to the beam. Both the forward and side scattered light passes through collection lenses before being measured. In addition the side scattered light is passed through a series of mirrors and filters designed to split the light up into different wavelengths to enable measurement of different kinds of fluorescent light. This is achieved by dichroic mirrors, placed at 45 degrees to the beam of light. The first mirror in the optical path of the side scattered light is a 500 nm long pass dichroic filter, reflecting wavelengths less than 500 nm (the 488 nm scattered laser light) towards the right angle scatter detector. Light of a longer wavelength passes onto a second mirror, a 560 nm short pass dichroic filter, which reflects wavelengths of greater than 560 nm towards the red fluorescence detector, and through a filter centred at 585 nm, with a 42 nm half-peak band pass. The shorter wavelengths of 500 to 560 nm pass on to the green fluorescence detector via a 530 nm filter with a 30 nm half-peak bandpass.

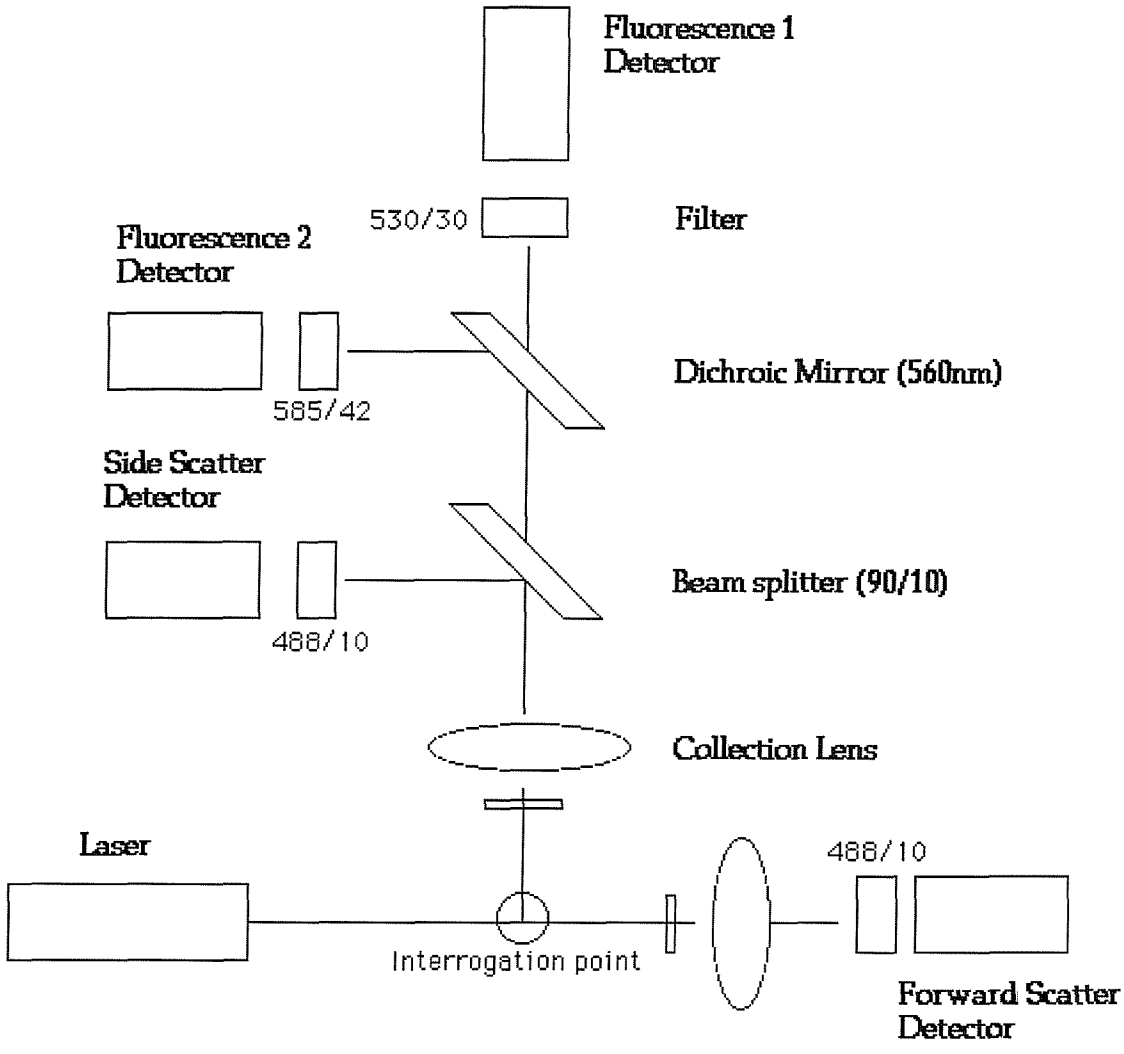

Flow cytometers use either PIN diodes or photomultiplier tubes to detect light. The Becton-Dickinson FACScan uses photomultiplier tubes, which rely on photosensitive electron tubes to convert light impulses into electronic signals.

The electrical impulses generated by the photomultiplier tubes are fed into a filtering pre-amplifier, which converts the raw electronic data into a smoothed voltage pulse of between 0 and 10 V. The amplitude of this pulse is proportional to the number of

photons reaching the photodetector, and the shape of the pulse is determined by the size and speed of the particle, as well as the width of the illuminating beam and the distribution of the fluorochrome within the particle.

The preamplifier output will contain high frequency background "noise" which needs to be filtered out prior to further processing of the signal. This is achieved by using a system threshold, so that further processing only takes place when the input voltage rises above a preset value. The threshold value is usually set on a single parameter, which then triggers all the other measuring circuits. Forward scatter is usually selected as the system trigger pulse, as use of fluorescence as a trigger might result in negative cells not being detected or measured.

The preamplifier pulse output is generally too fast for the measurement and display circuits to keep up with the flow of data. The pulse processing circuitry therefore provides an analogue voltage memory of the signal that is held for long enough to allow the further processing to take place. These sample-and-hold circuits generally hold their voltage output for a fixed period of time, generally about 15 to 120μsec, and are triggered when the signal voltage rises above the preset threshold. During the period that the sample-and-hold circuits are functioning, the system is refractory to the measurement of further pulses. This is known as the system dead time, and events occurring during this period pass undetected. This has more relevance to sorting than analysis, as cells undetected during analysis tend to be taken at random from all cell populations, whilst cells undetected during sorting may compromise the purity of the sorted sample.

The pulse processing modes allow different measurements to be made from the same signal. Pulse width is related to the size of the particle or area of fluorescent staining, and

is composed of the width of the illuminating beam plus the width of the particle (minus the small triggering and de-triggering widths).

Signals can be processed directly or after passage through a logarithmic amplifier. Such logarithmic amplification amplifies weak signals and compresses large signals. Such a process also increases the dynamic range of the system, allowing both weak and strong signals to be displayed on the same scale.

Spectral overlap of two fluorochromes can also be corrected during signal processing. Such spectral overlap produces a small signal from one fluorochrome at the detector intended to measure a second fluorochrome and vice versa. Electronic circuitry can be used to electronically subtract the proportion of the fluorescence due to spectral overlap from each pulse.

References

1. Abol-Enein H, El-Mekresh M, El-Baz M, and Ghoneim MA. Neoadjuvant Chemotherapy in Treatment of Invasive Transitional Bladder Cancer. A Controlled Prospective Randomized Study. Br J Urol 1997;80:191.

2. Ahlering, T. E., Dubeau, L., and Jones, P. A. A New in Vivo Model to Study Invasion and Metastasis of Human Bladder Carcinoma. Cancer Res 1987;47(24 Pt 1):6660-5.

3. Akaza, H., Crabtree, W. N., Matheny, R. B., Jr., and Soloway, M. S. Chemoimmunotherapy of Implanted Murine Bladder Cancer. Urology 1983;21(3):273-6.

4. Alexander, A. A., Liu, J. B., McCue, P., Gomella, L. G., Ross, R. P., and Lattime, E. C. Intravesical Growth of Murine Bladder Tumors Assessed by Transrectal Ultrasound. J Urol 1993;150(2 Pt 1):525-8.

5. Ali-El-Dein, B., Nabeeh, A., El Baz, M., Shamaa, S., and Ashamallah, A. Single-Dose Versus Multiple Instillations of Epirubicin As Prophylaxis for Recurrence After Transurethral Resection of PTa and PT1 Transitional-Cell Bladder Tumours: a Prospective, Randomized Controlled Study [See Comments]. Br J Urol 1997;79(5):731-5.

6. Alley MC, Scudiero DA, Monks A, Hursey ML, Czerwiniski MJ, Fine DL, Abbot BJ, Mayo JG, Shoemaker RH, and Boyd MR. Feasibility of Drug Screening With Panels of Human Tumour Cell Lines Using a Microculture Tetrazolium Assay. Cancer Res 1988;48:589-601.

7. Armstrong B and Doll R. Bladder Cancer Mortality in England and Wales in Relation to Cigarette Smoking and Saccharine Consumption. Br J Prev Soc Med 1974;28:233.

8. Begin ME, Das UN, Ells G, and Horrobin DF. Selective Killing of Human Cancer Cells by Polyunsaturated Fatty Acids. Prostaglandins Leuko.Med. 1985;19(2):177-86.

9. Begin ME, Ells G, Das UN, and Horrobin DF. Differential Killing of Human Carcinoma Cells Supplemented With N-3 and N-6 Polyunsaturated Fatty Acids. J.Natl Cancer Inst. 1986;77(5):1053-62.

10. Begin ME, Ells G, and Horrobin DF. Polyunsaturated Fatty Acid-Induced Cytotoxicity Against Tumour Cells and Its Relationship to Lipid Peroxidation. J.Natl Cancer Inst. 1988;80:188-94.

11. Blandy JP, England HR, Evans SJ, Hope-Stone HF, Mair GM, Mantell BS, Oliver RT, Paris AM, and Risdon RA. T3 Bladder Cancer - the Case for Salvage Cystectomy. Br J Urol 1980;52:506-10.

12. Blum RH and Carter SK. Adriamycin, a New Anticancer Drug With Significant Clinical Activity. Annals of Internal Medicine 1974;80:249-59.

13. Brakenhoff GJ., van der Voort HT, van Spronsen EA, and Nanninga N. 3-Dimensional Imaging of Biological Structures by High Resolution Confocal Scanning Laser Microscopy. Scanning Micrsocopy 1978;2:33-40.

14. Cabral F, Sobel ME, and Gottesman MM. Topoisomerase II Mutations That Confer the Multidrug Resistance Phenotype on Human Cancer Cells. Cell 1980;20:29-36.

15. Carlsson J and Nederman T. Tumour Spheroid Technology in Cancer Therapy Research. Eur J Clin Oncol 1989;25:1127-33.

16. Carroll P. Urothelial carcinoma, cancers of the bladder, ureter and renal pelvis. Tanagho EA and McAninch JW. Smiths General Urology. London: Prentice Hall International; 2000. pp.355-77.

17. Case RAM, Hosker ME, McDonald DB, and et al. Tumors of the Urinary Bladder in Workmen Engaged in the Manufacture and Use of Certain Dyestuff Intermediates in the British Chemical Industry Part1: The Role of Aniline, Benzidine, Alpha-Naphthylamine and Beta-Naphthylamine. Br J Ind Med 1954;11:75.

18. Chin J, Kadhim S, Garcia B, Kim YS, and Karlik S. Magnetic Resonance Imaging for Detecting and Treatment Monitoring of Orthotopic Murine Bladder Tumor Implants. J Urol 1991;145(6):1297-301.

19. Clifford SC, Neal DE, and Lunec J. Alterations in Expression of the Multidrug Resistance-Associated Protein (MRP) Gene in High-Grade Transitional Cell Carcinoma of the Bladder. Br J Cancer 1996;73:659-66.

20. Cole SPC. Rapid Chemosensitivity Testing of Human Lung Tumour Cells Using the MTT Assay. Cancer Chemother.Pharmacol. 1986;17:259-63.

21. Cole SPC, Bhardwaj G, Gerlach JH, Mackie JE, Grant CE, Almquist KC, Stewart AJ, Kurz EU, Duncan AMV, and Deeley RG. Overexpression of a Transporter Gene in a Multidrug-Resistant Human Lung Cancer Cell Line. Science 1992;258:1650-4.

22. Colver GB, Inglis JA, and McVittie E. Dermatitis Due to Intravesical Mitomycin C: A Delayed-Type Hypersensitivity Reaction? British Journal of Dermatology 1990;122:217.

23. Cooper, A. J., Hayes, M. C., Duffy, P. M., Davies, C. L., and Smart, C. J. Multidrug Resistance Evaluation by Confocal Microscopy in Primary Urothelial Cancer Explant Colonies. Cytotechnology 1996;19(3):181-6.

24. Coralli C, Cemazar M, Kanthou C, Tozer GM, and Dachs GU. Limitations of the Reporter Green Fluorescent Protein Under Simulated Tumor Conditions. Cancer Res 2001;61(12):4784-90.

25. Crook TJ, Hall IS, Solomon LZ, Bass PS, Cooper AJ, and Birch BRP. Intravesical Meglumine Gamma Linolenic Acid. Phase I Tolerability Studies in Patients Undergoing Cystectomy. UroOncology 2000;1:39-43.

26. Crook, T. J., Hall, I. S., Solomon, L. Z., Birch, B. R., and Cooper, A. J. A Model of Superficial Bladder Cancer Using Fluorescent Tumour Cells in an Organ-Culture System. BJU Int 2000;86(7):886-93.

27. D.J.Weaver, B.A-L.Barrett, G.Ross jr, and E.H.Adelstein. Transitional Explant Reduction Assay - a New in Vitro Testing System for Intravesical Chemotherapy. J Urol 1986;135:386-91.

28. Dalton JT, Wientjes MG, and Au JLS. Effects of Bladder Resorption on Pharmacokinetic Data Analysis. J Pharmacokinet Biopharm 1994;22:183-205.

29. Dangles, V., Lazar, V., Validire, P., Richon, S., Wertheimer, M., Laville, V., Janneau, J. L., Barrois, M., Bovin, C., Poynard, T., Vallancien, G., and Bellet, D. Gene Expression Profiles of Bladder Cancers: Evidence for a Striking Effect of in Vitro Cell Models on Gene Patterns. Br J Cancer 2002;86(8):1283-9.

30. Das UN, Huang YS, Begin ME, Ells G, and Horrobin DF. Uptake and Distribution of Cis-Unsaturated Fatty Acids and Their Effects on Free-Radical Generation in Normal and Tumour Cells *in Vitro*. Free Radic.Biol.Med. 1987;3(1):9-14.

31. Defuria MD, Bracken RB, and Johnson DE. Phase I-II Study of Mitomycin C Topical Therapy for Low Grade, Low Stage Transitional Cell Carcinoma of the Bladder: An Interim Report. Cancer Treatment Reports 1980;64:225.

32. Dickinson AJ, Fox SB, and Persad RA. Quantification of Angiogenesis As an Independent Predictor of Prognosis in Invasive Bladder Carcinomas. Br J Urol 1994;74:762-4.

33. Dinney, C. P., Fishbeck, R., Singh, R. K., Eve, B., Pathak, S., Brown, N., Xie, B., Fan, D., Bucana, C. D., Fidler, I. J., and . Isolation and Characterization of Metastatic Variants From Human Transitional Cell Carcinoma Passaged by Orthotopic Implantation in Athymic Nude Mice. J Urol 1995;154(4):1532-8.

34. Douglas WHJ, McAteer JA, Dell'Orco RT, and Phelps D. Visualisation of Cellular Aggregates Cultured on a Three-Dimensional Collagen Sponge Matrix. In Vitro 1980;16:306-12.

35. Droller, MJ . Molecular Markers in the diagnosis of bladder cancer; 1-5-2000.

36. Duffy PM, Hayes MC, Gatrell SKE, Cooper A, and Smart CJ. Determination and Reversal of Resistance to Epirubicin Chemotherapy. A Confocal Imaging Study. Br J Urol 1996;77:824-9.

37. Dunning WF, Curtis MR, and Mann ME. The Effect of Added Dietary Tryptophan on the Occurrence of 2-Acetylaminofluorene Induced Liver and Bladder Cancer in Rats. Cancer Res 1950;10:454.

38. Dyer, C. UK Hearing Sets Number of Cancer Patients to Sue Tobacco Companies. BMJ 1998;317:1614-.

39. Eijstein A, Knonagel H, and Hotz E. Reduced Bladder Capacity in Patients Receiving Intravesical Chemoprophylaxis With Mitomycin C. Br J Urol 1990;66:386.

40. Endicott JA and Ling V. The Biochemistry of P-Glycoprotein Mediated Multidrug Resistance. Annu Rev Biochem 1989;58:137-71.

41. Engel, RM . History of the CystoscopeAUA: American Urological Association Conference; 2000.

42. Erlichman C, Vidgen D, and Wu A. Cytotoxicity of Cisplatin and Cisdiamine-1, 1-Cyclobutane Dicarboxylate in MGH-U1 Cells Grown As Monolayers, Spheroids, and Xenografts. J.Natl Cancer Inst. 1985;75:499.

43. Erlichman, C. and Tannock, I. F. Growth and Characterization of Multicellular Tumor Spheroids of Human Bladder Carcinoma Origin. In Vitro Cell Dev.Biol 1986;22(8):449-56.

44. Erturk E, Cohen SM, and Bryan GT. Urinary Bladder Carcinogenicity of N-(4-(5-Nitro-2-Furyl)-2-Thiazolyl) Formamide in Female Swiss Mice. Cancer Res 1970;30:1309.

45. Evans DR, Irwin RJ, Havre PA, Bouchard JG, Kato T, and Prout GR. The Activity of the Pyrimidine Biosynthetic Pathway in MGH-U1 Transitional Carcinoma Cells Grown in Tissue Culture. J Urol 1977;117:712-9.

46. Fearon KCH, Falconer JS, Ross JA, Carter DC, Hunter JO, and Reynolds PD. An Open Label Phase I/II Dose Escalation Study of the Treatment of Pancreatic Cancer Using Lithium Gammalinolenate. Anticancer Research 1996;16:867-74.

47. Franks, C. R., Turner, D. R., Bishop, D., and Perkins, F. T. Growth Characteristics of a Human Bladder Tumour Subcutaneously Implanted in Immune Deficient Mice. Clin Oncol 1976;2(1):25-32.

48. Freiha FS. Treatment Options for Patients With Invasive Bladder Cancer With Special Reference to Bladder Substitution With the Stanford Pouch. Monographs in Urology 1990;11:34.

49. Freshney RI, Paul J, and Kane IM. Assay of Anti-Cancer Drugs in Tissue Culture: Conditions Affecting Their Ability to Incorporate 3H-Leucine After Drug Treatment. Br J Cancer 1975;31:89-99.

50. Freshney, RI, Culture of animal cells. 3rd ed. New York: Wiley-Liss; 1994.

51. Ghersi D, Stewart LA, and Parmar MKB. Does Neoadjuvant Cisplatin-Based Chemotherapy Improve the Survival of Patients With Locally Advanced Bladder Cancer: a Meta-Analysis of Individual Patient Data From Randomised Clinical Trials.". Br J Urol 1995;75:206-13.

52. Goffinet DR, Schneider MJ, and Glatstein EJ. Bladder Cancer: Results of Radiation Therapy in 384 Patients. Radiology 1975;117:149.

53. Goldstein LJ, Crist W, Brodeur GM, Lieber M, and Cossman J. Expression of Multidrug Resistance Gene in Human Cancers. J.Natl Cancer Inst. 1989;81:116-24.

54. Gospodarowitz MK, Hawkins NV, and Rawlings GA. Radical Radiotherapy for Muscle Invasive Transitional Cell Carcinoma of the Bladder: Failure Analysis. J Urol 1989;142:1448.

55. Gottesman MM. How Cancer Cells Evade Chemotherapy. Cancer Res 1993;53:747-54.

56. Gottesman MM and Pastan I. Biochemistry of Multidrug Resistance Mediated by the Multidrug Transporter. Annu Rev Biochem 1993;62:385-427.

57. Gratzner HG, Leif RC, Ingram DJ, and Castro A. The Use of Antibody Specific for Bromodeoxyuridine for the Immunofluorescent Determination of DNA Replication in Single Cells and Chromosomes. Exp Cell Res 1975;95:88-94.

58. Greven KM, Solin LJ, and Hanks GE. Prognostic Factors in Patients With Bladder Carcinoma Treated With Definitive Radiotherapy. Cancer 1990;65:908.

59. Griffiths TRL; Neal DE. Transitional cell carcinoma of the bladder. Mundy AR, Fitzpatrick JM, Neal DE, and George NJR. Scientific Basis of Urology. Oxford: Isis Medical Media; 1999.

60. Gubin AN, Reddy B, Njoroge JM, and Miller JL. Long-Term, Stable Expression of Green Fluorescent Protein in Mammalian Cells. Biochemical and Biophysical research Communications 1997;236:347-50.

61. Harney J, Murphy DM, Jones M, and Mothersill C. Expression of P53 in Urothelial Cell Cultures From Tumour-Bearing and Tumour-Free Patients. Br J Cancer 1995;71(1):25-9.

62. Harris, N. M., Crook, T. J., Dyer, J. P., Solomon, L. Z., Bass, P., Cooper, A. J., and Birch, B. R. Intravesical Meglumine Gamma-Linolenic Acid in Superficial Bladder Cancer: an Efficacy Study. Eur Urol 2002;42(1):39-42.

63. Hayes MC, Birch BR, Cooper AJ, and Primrose JN. Cellular Resistance to Mitomycin C Is Associated With Overexpression of MDR-1 in a Urothelial Cancer Cell Line (MGH-U1). BJU Int. 2001;87(3):245-50.

64. Herman C, Vegt P, Debruyne F, Vooijs G, and Ramaekers F. Squamous and Transitional Elements in Rat Bladder Carcinomas Induced by N-Butyl-N-(4-Hydroxybutyl) Nitrosamine (BBN). M.J.Pathol 1985;120:419.

65. Hermanek P and Sobin LH, UICC-International Union against Cancer TNM classification of Malignant tumors. 4th ed. Heidelberg: Springer-Verlag; 1987.

66. Herr, H. W., Schwalb, D. M., Zhang, Z. F., Sogani, P. C., Fair, W. R., Whitmore, W. F., Jr., and Oettgen, H. F. Intravesical Bacillus Calmette-Guerin Therapy Prevents Tumor Progression and Death From Superficial Bladder Cancer: Ten-Year Follow- Up of a Prospective Randomized Trial. J Clin.Oncol 1995;13(6):1404-8.

67. Herring, HT. An Effective Treatment of Vesical Haemorrhage When Caused by Papillomatous Growths. British Medical Journal 29-7-1899;263-5.

68. Herring, HT. The Treatment of Vesical Papilloma by Injections. British Medical Journal 28-11-1903;2:1398-9.

69. Hicks RM, Wakefield J, and Chowaniec J. Evaluation of a New Model to Detect Bladder Carcinogens or Co-Carcinogens; Results Obtained With Saccharin, Cyclamate and Cyclophosphamide. Chem Biol Interact. 1975;11(3):225-33.

70. Hicks RM and Wakefield J.St.J. Rapid Induction of Bladder Cancer in Rats With N-Methyl-Nitrosurea. I.History.Chem.Biol.Interact. 1972;5:139.

71. Highley MS, Van Oosterom AT, Maes RA, and De Bruijn EA. Intravesical Drug Delivery. Clin Pharmacokinet 1999;37(1):59-73.

72. Hodges GM, Hicks RM, and Spacey GD. Scanning Electron Microscopy of Cell-Surface Changes in Methylnitrosurea (MNU)-Treated Rat Bladders in Vivo and in Vitro. Differentiation 1976;6(3):143-50.

73. Holden HT; Lichter W; Sigel MM. Quantitative methods for measuring cell growth and death. Kruse PF Jr and Patterson MK Jr. Tissue culture methods and applications. New York: Academic Press; 1973. pp.408-12.

74. Hoover R and Cole P. Population Trends in Cigarette Smoking and Bladder Cancer. Am J Epidemiology 1971;94:409.

75. Hoover RN and Strasser PH. Artificial Sweeteners and Human Bladder Cancer. Preliminary Results. Lancet 1980;1(8173):837-40.

76. Hovey RM, Chu L, and Balazs M. Genetic Alterations in Primary Bladder Cancers and Their Metastases. Cancer Res 1998;58:3555-60.

77. Hruban RH, van der Riet P, Erozan YS, and Sidransky D. Brief Report: Molecular Biology and the Early Detection of Carcinoma of the Bladder-the Case of Hubert H. Humphrey. New England Journal of Medicine 1994;330:1276.

78. Hudes G. Estramustine Based Chemotherapy. Seminars in Urologic Oncology 1997;15(1):13-9.

79. Hueper WC. Aniline Tumours of the Bladder. Arch Pathol 1938;25:858.

80. Ibrahiem, E. H., Nigam, V. N., Brailovsky, C. A., Madarnas, P., and Elhilali, M. Orthotopic Implantation of Primary N-[4-(5-Nitro-2-Furyl)-2- Thiazolyl]Formamide-Induced Bladder Cancer

in Bladder Submucosa: an Animal Model for Bladder Cancer Study. Cancer Res 1983;43(2):617-22.

81. Inaba M, Fujikara R, Tsukagoshi S, and Sukurai Y. Restored *in Vitro* Sensitivity of Doxorubicin and Vincristine P388 Leukemia Cells With Reserpine. Biochem Pharmacol 1981;30:2191-4.

82. Iyer VN and Szybaloki W. Mitomycin and Porfiromycin: Chemical Mechanism of Activation and Cross-Linking of DNA. Science 1964;145:55-8.

83. Jenkins BJ, Caulfield MJ, and Fowler CG. Reappraisal of the Role of Radical Radiotherapy and Salvage Cystectomy in the Treatment of Invasive (T2, T3) Bladder Cancer. Br J Urol 1988;62:343.

84. Jennings A, Solomon LZ, Sharpe P, Hayes M, Cooper A, and Birch B. Estramustine Reversal of Resistance to Intravesical Epirubicin Chemotherapy. European Urology 1999;35:327-35.

85. Jewett HJ and Strong GH. Infiltrating Carcinoma of the Bladder: Relation of Depth of Penetration of Bladder Wall to Invasiveness and Vascular Invasion. J Urol 1946;60:435.

86. Jocham D; Staehler G; Shaussy C. Integral dye-laser irradiation of photosensitised bladder tumours with the aid of a light scattering medium. Clayton Symposium: Porphyrin localisation and treatment of tumours.Alan R Liss, Inc.; 1984. p.249.

87. Johnson CD, Puntis M, Davidson N, Todd S, and Bryce R. Randomized, Dose-Finding Phase III Study of Lithium Gamolenate in Patients With Advanced Pancreatic Adenocarcinoma. Br J Surg 2001;88(5):662-8.

88. Johnson MD, Bryan GT, and Reznikoff CA. Serial Cultivation of Normal Bladder Epithelial Cells in Vitro. J Urol 1985;133(6):1076-81.

89. Jones HC and Swinney J. Jones, HC. & Swinney, J. 1961, "Thiotepa in the Treatment of Tumours of the Bladder." *Lancet,* Vol. 2, Pp. 615. Lancet 1961;2:615.

90. Jones, D, On diseases of the Bladder and Prostate, and Obscure affections of the urinary organs. 1st ed. London: Simpkin, Marshall & Co.; 1883.

91. Josefson, D. Tobacco Companies in US to Pay Smoker $22m (£13.8m) . BMJ 2000;320:957-.

92. Kaltenbach JP, Kaltenbach MH, and Lyons WB. Nigrosin As a Dye for Differentiating Live and Dead Ascites Cells. Exp.Cell Res. 1958;15:112-7.

93. Knowles MA. The Genetics of Transitional Cell Carcinoma: Progress and Potential Clinical Application. BJU Int. 1999;84:412-27.

94. Knowles MA, Jani H, Hicks RM, and Berry RJ. N-Methyl-N-Nitrosourea Induces Dysplasia and Cell Surface Markers of Neoplasia in Long-Term Rat Bladder Organ Cultures. Carcinogenesis 1985;6(7):1047-54.

95. Knuchel, R., Feichtinger, J., Recktenwald, A., Hollweg, H. G., Franke, P., Jakse, G., Rammal, E., and Hofstadter, F. Interactions Between Bladder Tumor Cells As Tumor Spheroids From the Cell Line J82 and Human Endothelial Cells in Vitro. J Urol 1988;139(3):640-5.

96. Kunze E and Chowaniec J. Pathology of Tumours in Laboratory Animals. Tumours of the Rat. Tumours of the Urinary Bladder. IARC Sci Publ 1990;99:345-97.

97. Lamm, D. L., Blumenstein, B. A., Crawford, E. D., Montie, J. E., Scardino, P., Grossman, H. B., Stanisic, T. H., Smith, J. A., Jr., Sullivan, J., and Sarosdy, M. F. A Randomized Trial of Intravesical Doxorubicin and Immunotherapy With Bacille Calmette-Guerin for Transitional-Cell Carcinoma of the Bladder. N.Engl.J Med 1991;325(17):1205-9.

98. Lilienfield AM. The Relationship of Bladder Cancer to Smoking. Am J Public Health 1964;54:1864.

99. Lown JW, Anthracycline and anthracenedione-based anticancer agents.Elsevier; 1988.

100. Lutzeyer W, Rubben H, and Dahm H. Prognostic Parameters in Superficial Bladder Cancer: An Analysis of 315 Cases. J Urol 1982;127:250-2.

101. Masters JRW, Hepburn PJ, Walker L, Highman WJ, Trejdosiewicz LK, Povey S, Parkar M, Hill BT, Riddle PR, and Franks LM. Tissue Culture of Transitional Cell Carcinoma: Characterization of Twenty-Two Human Urothelial Cell Lines. Cancer Res 1986;46:3630-6.

102. Masters JRW, Vesey SG, and Mumm CF. C-Myc Oncoprotein Levels in Bladder Cancer. Urology Research 1988;16:341.

103. MatheG, Amiel JL, Schawarzenberg L, Schneider M, Cattan, Schlumberger JR, Hayat M, and De Vassal F. Active Immunotherapy for Acute Lymphoblastic Leukaemia. Lancet 1969;1(7597):697-9.

104. McKeehan WL, Hamilton WG, and Ham RG. Improved Medium for Clonal Growth of Human Diploid Cells at Low Concentrations of Serum Protein. In Vitro 1977;13:399-416.

105. Messing EM. Clinical Implications of the Expression of Epidermal Growth Factor Receptors in Human Transitional Cell Carcinoma. Cancer Res 1990;50:2530.

106. Messing EM; Catalona W. Urothelial tumours of the Urinary Tract. Walsh PC, Retik AB, Vaughan ED, and Wein AJ. Campbells Urology. Philadelphia: WB Saunders; 1998.

107. Messing EM, Young TB, and Hunt VB. Comparison of Bladder Cancer Outcome in Men Undergoing Hematuria Home Screening Versus Those With Standard Clinical Presentations. Urology 1995;45:387.

108. Montie JE, Straffon RA, and Stewart BH. Radical Cystectomy Without Radiation Therapy for Carcinoma of the Bladder. J Urol 1984;131:477.

109. Morales A, Eidinger D, and Bruce AW. Intracavitary Bacillus Calmette-Guerin in the Treatment of Superficial Bladder Tumors. J Urol 1976;116:180.

110. Mossman T. Rapid Colorimetric Assay for Cellular Growth and Survival: Application to Proliferation and Cytotoxicity Assays. J.Immunological Methods 1983;65:55-63.

111. Muller M, MeijerC, Zaman GJR, Borst P, Scheper RJ, Mulder NH, de Vries EGE, and Jansen PLM. Overexpression of the Gene Encoding the Multidrug Resistance-Associated Protein Results in Increased ATP-Dependent Glutathione S-Conjugate Transport. Proc Natl Acad Sci USA 1994;91:13033-7.

112. Murphy, G. P., Sandberg, A. A., Pontes, J. E., Ochi, H., Yoshida, M., and Williams, P. D. A Murine Model for Bladder Cancer. Prog.Clin Biol Res 1984;162A:177-200.

113. Murphy, LJT and Ernest Desnos, The History of Urology. 1st ed.Charles C Thomas, Springfield, Illinois.; 1972.

114. Neri, LM., Martelli AM, Previati M, and Capitani S. From Two Dimensional to Three Dimensional Analysis by Confocal Microscopy. Liver 1992;12:268-79.

115. Nicholson LJ and Jani H. Effects of Sodium Cyclamate and Sodium Saccharin on Focus Induction in Explant Cultures of Rat Bladder. Int J Cancer 1988;42:295-8.

116. Nielsen HV and Thybo E. Epodyl Treatment of Bladder Tumours. Scand J Urol Nephrol 1979;13:59-63.

117. Nissenkorn I, Herrod H, and Soloway MS. Side Effects Associated With Intravesical Mitomycin C. J Urol 1981;126:596.

118. Oshinsky GS, Chen Y, Jarrett T, Anderson AE, and Weiss GH. A Model of Bladder Tumour Xenografts in the Nude Rat. J Urol 1995;154:1925-9.

119. Pagano F, Bassi P, and Galetti TP. Results of Contemporary Radical Cystectomy for Invasive Bladder Cancer: A Clinicopathological Study With an Emphasis on the Inadequacy of the Tumor, Nodes and Metastases Classification. J Urol 1992;145:45.

120. Parada LF, Tabin CJ, Shih C, and Weinberg RA. Human EJ Bladder Carcinoma Oncogene Is Homologue of Harvey Sarcoma Virus Ras Gene. Nature 1982;297(5866):474-8.

121. Pauli BU, Anderson SN, Memoli VA, and Kuettner KE. Development of an in Vitro and in Vivo Epithelial Tumor Model for the Study of Invasion. Cancer Res 1980;40(12):4571-80.

122. Plosker GL and Faulds D. Epirubicin: a Review of Its Pharmacodynamic and Pharmacokinetic Properties, and Therapeutic Use in Cancer Chemotherapy. *Drugs* 45(5): 788-856. Drugs 1993;45(5):788-856.

123. Pode D, Alon Y, Horowitz AT, Vlodavsky I, and Biran S. The Mechanism of Human Bladder Tumor Implantation in an in Vitro Model. J Urol 1986;136(2):482-6.

124. Potter, J. M., Quigley, M., Pengelly, A. W., Fawcett, D. P., and Malone, P. R. The Role of Urine Cytology in the Assessment of Lower Urinary Tract Symptoms. BJU Int 1999;84(1):30-1.

125. Pritchett TR, Wang JK, and Jones PA. Mesenchymal-Epithelial Interactions Between Normal and Transformed Human Bladder Cells. Cancer Res 1989;49(10):2750-4.

126. Prout GR, Barton BA, Griffin PP, and Friedel G. Treated History of Non Invasive Grade 1 Transitional Cell Carcinoma. J Urol 1992;148:1413.

127. Prout GR, Koontz WW Jr, and Coombes LJ. Long Term Fate of 90 Patients With Superficial Bladder Cancer Randomly Assigned to Receive or Not to Receive Thiotepa. J Urol 1983;130:677.

128. Pycha, A., Mian, C., Hofbauer, J., Haitel, A., Wiener, H., and Marberger, M. Does Topical Instillation Therapy Influence Chromosomal Aberrations in Superficial Bladder Cancer? J Urol 1998;159(1):265-9.

129. Raghavan D; Debruyne F; Herr H; Jocham D; Kakizoe T; Okajima E; Sandberg A; Tannock I. Experimental models of bladder cancer: A critical review. Developments in bladder cancer.Alan R Liss, Inc.; 1986. pp.171-208.

130. Rao JY, Hemstreet GP, and Hurst RE. Alterations in Phenotypic Biochemical Markers in Bladder Epithelium During Tumorigenesis. Proc Natl Acad Sci USA 1993;90:8287.

131. Ratliff, T. L., Shapiro, A., and Catalona, W. J. Inhibition of Murine Bladder Tumor Growth by Bacille Calmette-Guerin: Lack of a Role of Natural Killer Cells. Clin Immunol.Immunopathol. 1986;41(1):108-15.

132. Rebel JM, Thijssen CD, Vermey M, Zwarthoff EC, and van der Kwast TH. Modulation of Intra-Epithelial Expansion of Human T24 Bladder-Carcinoma Cells in Murine Urothelium by Growth Factors and Extra-Cellular-Matrix Components. Int J Cancer 1995;60(5):707-11.

133. Reedy EA and Heatfield BM. Histomorphometry and Cell Kinetics of Normal Human Bladder Mucosa in Vitro. Urol Res 1987;15(6):321-7.

134. Reznikoff CA, Belair CD, Yeagar TR, Savelieva E, Blelloch, RH, Puthenveet-til, JA, and Cuthill, S. A Molecular Genetic Model of Human Bladder Cancer Pathogenesis. Seminars in Oncology 1996;23:571-84.

135. Reznikoff CA, Gilchrist KW, Norback DH, Cummings KB, Erturk E, and Bryan GT. Altered Growth Patterns in Vitro of Human Papillary Transitional Carcinoma Cells. American Journal of Pathology 1983;111(3):263-72.

136. Riddle PR, Khan O, Fitzpatrick JM, and Oliver RT. Prognostic Factors Influencing Survival of Patients Receiving Intravesical Epodyl. J Urol 1982;127(3):430-2.

137. Rotin, D., Steele-Norwood, D., Grinstein, S., and Tannock, I. Requirement of the Na+/H+ Exchanger for Tumor Growth. Cancer Res 1989;49(1):205-11.

138. Rotman B and Papermaster BW. Membrane Properties of Living Mammalian Cells As Studied by Enzymatic Hydrolysis of Fluorogenic Esters. Proc Natl Acad Sci USA 1966;55:134-41.

139. Samma S, Uemera H, and Tabata S. Rapid Induction of Carcinoma in Situ in Dog Urinary Bladder by Sequential Treatment With N-Methyl-N-Nitrosurea and N-Butyl-N-(4-Hyrodxybutyl)-Nitrosamine. Gann 1984;75:385.

140. Sangeetha SP and Das UN. Gamma-Linolenic Acid and Eicosapentanoic Acid Potentiate the Cytotoxicity of Anti-Cancer Drugs on Human Cervical Carcinoma Cells *in Vitro*. Med.Sci.Res. 1993;21:457-9.

141. Scheper RJ, Broxteman HJ, Scheffer GL, Kaaijk P, Dalton WS, van Heijningen THM, van Kalken CK, Slovak ML, de Vries EGE, van der Valk P, Meijer CJLM, and Oinedo HM. Overexpression of a 110 KD Vesicular Protein in Non-P-Glycoprotein Mediated Multidrug-Resistance. Cancer Res 1993;3:1475-9.

142. Shin, KY, Kong G, Kim WS, Lee TY, Woo YN, and Lee JD. Overexpression of Cyclin D1 Correlates With Early Recurrence in Superficial Bladder Cancers. Br J Cancer 1997;75:1788-92.

143. Sidransky D and Messing EM. Molecular Genetics and Biochemical Mechanisms in Bladder Cancer. Urological Clinics of North America 1992;19:629.

144. Skinner DG, Daniels JR, and Russell CA. The Role of Adjuvant Chemotherapy Following Cystectomy for Invasive Bladder Cancer. A Prospective Comparative Trial. J Urol 1991;145:459.

145. Smith CD, Zilfou JT, and Zhang X. Modulation of P-Glycoprotein Binding and Modulation of MDR Phenotype by Estramustine. Cancer 1995;75:2597-604.

146. Solomon LZ, Birch BRP, and Cooper AJ. Water As a Tumoricidal Agent in Bladder Cancer. European Urology 1998;34:500-4.

147. Solomon LZ; Harris N; Crook TJ; Sharpe P; Davies CL; Birch BRP; Cooper AJ. Combination intravesical chemotherapy for superficial bladder cancer: synergism between MeGLA, mitomycin C and epirubicin: Cytotoxicity and cellular proliferation assays. Eur J Cancer . 2000.
Ref Type: In Press

148. Solomon LZ, Jennings AM, Foley SJ, Birch BRP, and Cooper AJ. Bladder Cancer Recurrence by Implantation of Exfoliated Cells: Is Gamma-Linolenic Acid an Effective Tumoricidal Agent? British Journal of Urology 1998;82:122-6.

149. Solomon LZ, Jennings AM, Hayes MC, Bass PS, Birch BRP, and Cooper AJ. Is Gamma-Linolenic Acid an Effective Intravesical Agent for Superficial Bladder Cancer? In Vitro Cytotoxicity and in Vivo Tolerance Studies. Urology Research 1997;26:11-5.

150. Solomon LZ, Jennings AM, Sharpe P, Cooper AJ, and Birch BRP. Intravesical Chemotherapy With Gamma Linolenic Acid Becomes a Realistic Prospect in Serum-Free Applications: in Vitro Cytotoxicity and Systemic Absorption Studies. The Journal of Urology 1998;160:1-4.

151. Soloway MS. Intravesical and Systemic Chemotherapy in the Management of Superficial Bladder Cancer. Urological Clinics of North America 1984;11:623-5.

152. Soloway MS, Martino C, Hyatt C, and Marrone JC. Immunogenicity of FANFT-Induced Bladder Cancer. Nat Cancer Inst Monogr 1978;49:293.

153. Soule, S. E., Miller, K. D., Porcu, P., Ansari, R., Fata, F., McClean, J. W., Zon, R., Sledge, G. W., and Einhorn, L. H. Combined Anti-Microtubule Therapy: a Phase II Study of Weekly Docetaxel Plus Estramustine in Patients With Metastatic Breast Cancer. Ann.Oncol 2002;13(10):1612-5.

154. Spruck CH, Ohneseit PF, and Gonzales-Zulueta M. Two Molecular Pathways to Transitional Cell Carcinoma of the Bladder. Cancer Res 1994;54:784.

155. Sterle M, Kreft ME, and Batista U. The Effect of Epidermal Growth Factor and Transforming Growth Factor Beta 1 on Proliferation and Differentiation of Urothelial Cells in Urinary Bladder Explant Culture. Biol Cell 1997;89(4):263-71.

156. Sutherland RM. Cell and Microenvironment Interactions in Tumour Microregions: The Multicell Spheroid Model. Science 1988;240:117-84.

157. Takahashi N, Habuchi T, and Kakehi Y. Clonal and Chronological Genetic Analysis of Multifocal Cancers of the Bladder and Upper Urinary Tract. Cancer Res 1998;58:5835-41.

158. Tanaka M, Gee JR, De La Cerda J, Rosser CJ, Zhou JH, Benedict WF, and Grossman HB. Noninvasive Detection of Bladder Cancer in an Orthotopic Murine Model With Green Fluorescence Protein Cytology. J Urol 2003;170(3):975-8.

159. Thompson RA, Campbell EW Jr, and Kramer HC. Late Invasive Recurrence Despite Long-Term Surveillance for Superficial Bladder Cancer. J Urol 1993;149:1010.

160. Thompson, H, Tumours of the Bladder. 1st ed. London: J. & A. Churchill; 1884.

161. Thrasher JB and Crawford ED. Complications of Intravesical Chemotherapy. Urological Clinics of North America 1992;19(3):529-39.

162. Torti SV, Golden-Fleet M, Willingham MC, Ma R, Cline M, Sakimoto Y, and Torti FM. Use of Green Fluorescent Protein to Measure Tumor Growth in an Implanted Bladder Tumor Model. J Urol 2002;167:724-8.

163. Tsuro T, Iida H, Tsukagoshi S, and Sakuri Y. Increased Accumulation of Vincristine and Doxorubicin in Drug Resistant P388 Tumour Cells Following Incubation With Calcium Antagonists and Calmodulin Inhibitors. Cancer Res 1982;42:4730-3.

164. Tucker GC, Delouvee A, Jouanneau J, Gavrilovic J, Moens G, Valles AM, and Thiery JP. Amplification of Invasiveness in Organotypic Cultures After NBT-II Rat Bladder Carcinoma Stimulation With in Vitro Scattering Factors. Invasion Metastasis 1991;11(6):297-309.

165. Twentyman PR, Fox NE, and White DJG. Cyclosporin A and Its Analogues As Modifiers of Doxorubicin and Vincristine Resistance in a Multidrug Resistant Human Cell Line. Br J Cancer 1987;56:55-60.

166. van der Voort HT, Brakenhoff GJ., van Spronsen EA, and Nanninga N. Three-Dimensional Imaging in Fluorescence by Confocal Scanning Microscopy. Journal of Microscopy 1985;153:151-9.

167. Wagner, H. E., Joyce, A. D., Beatrice, K., and Summerhayes, I. C. Ras Induced Lesions in a Heterotopic Mouse Bladder. Oncogene 1990;5(4):557-63.

168. Wajsman Z, Dhafir RA, and Pfeffer M. Studies of Mitomycin C Absorbtion After Intravesical Treatment of Superficial Bladder Tumours. J Urol 1984;132:30.

169. Webb JA. Imaging in Haematuria. Clinical Radiology 1997;52:167-71.

170. Weber JM, Sircar S, and Begin ME. Greater Sensitivity of Human MDR Resistant Cancer Cells to Polyunsaturated Fatty Acids Than Their Non-MDR Counterparts. J.Natl Cancer Inst. 1994;86(8):638-9.

171. Weiss RB, Sarosy G, Clagett-Carr K, Russo M, and Leyland-Jones B. Anthracycline Analogs: The Past, Present and Future. Cancer Chemotherapy and Pharmacology 1986;18:185-97.

172. Wessex Cancer Intelligence Unit. 2000.

173. White, JG., Amos WB, and Fordham M. An Evaluation of Confocal Versus Conventional Imaging of Biological Structures by Fluorescence Light Microscopy. Journal of Cell Biology 1987;105:41-8.

174. Wibe, E., Berg, J. P., Tveit, K. M., Nesland, J. M., and Lunde, S. Multicellular Spheroids Grown Directly From Human Tumour Material. Int J Cancer 1984;34(1):21-6.

175. Wientjes MG, Badalament RA, and Au JLS. Use of Pharmacologic Data and Computer Simulations to Design an Efficacy Trial of Intravesical Mitomycin C Therapy for Superficial Bladder Cancer. Cancer Chemother Pharmacol 1993;32:255-62.

176. Wientjes MG, Badalament RA, Wang RC, Hassan F, and Au JL. Penetration of Mitomycin C in Human Bladder. Cancer Res 1993;53(14):3314-20.

177. Wientjes MG, Dalton JT, Badalament RA, Drago JR, and Au JL. Bladderwall Penetration of Intravesical Mitomycin C in Dogs. Cancer Res 1991;51(16):4347-54.

178. Wijkstrom H, Edsmyr F, and Lundh B. The Value of Preoperative Classification According to the TNM System. European Urology 1984;10:101.

179. Wilke V.1985. Optical Scanning Microscopy-the Laser Scan Microscope. Scanning Micrsocopy 1985;7:88-96.

180. Wishnow KI, Levinson AK, and Johnson DE. Stage B (P2/3/N0) Transitional Cell Carcinoma of the Bladder Highly Curable by Radical Cystectomy. Urology 1992;39:12.

181. Yuhas JM, Li AP, Martinex AO, and Ladman AJ. A Simplified Method for Production of Multicellular Tumour Spheroids (MTS). Cancer Res 1977;37:3639-43.

182. Zawydiwski R and Duncan GR. Spontaneous ^{51}Cr Release by Isolated Rat Hepatocytes. An Indicator of Membrane Damage. In Vitro 1978;14:707-14.

183. Zhou JH, Rosser CJ, Tanaka M, Yang M, Baranov E, Hoffman RM, and Benedict WF. Visualizing Superficial Human Bladder Cancer Cell Growth *in Vivo* by Green Fluorescent Protein Expression. Cancer Gene Therapy 2002;9:681-6.

Index

$^{51}Cr^{3+}$, 61
acridine orange, 84, 86
Actinomycin, 29
analgesics, 25
anthracyclines, 2, 28, 45, 57, 62
Arachidonic acid, 50
Bardenheuer, 22
BCG, 2, 14, 48, 75
Billroth, 20
bladder outflow obstruction, 31
Bozzini, 21
Calmodulin, 30
Carboplatin, 38
carcinogens, 25
carcinoma in situ, 14, 27, 33, 34, 40
carcinoma-in-situ, 30
cell line
  MGH-U1, 58, 59, 60, 62, 65, 69, 79, 114, 129, 191
  T24, 59
chemotherapy, 33, 38, 40, 65
Chopart, 19
Civiale, 20
Colchicine, 29
Colot, 19
Covillard, 19
Cruciferae, 53
CT scanning, 36
Cyclamates, 25
Cyclophosphamide, 25
Cyclosporins, 30
cystectomy, 22
  partial, 21
  total, 22
cystoscope, 21, 42
cystoscopy, 21, 32
Cystoscopy, 21
d'Etchepare, 42
d'Etoilles, 20
Daunorubicin, 44
David Jones, 21
densitometer, 63
Desault, 19
Desormeaux, 21
DMSO, 14, 64, 91, 96
Doxorubicin, 28, 44
electrocautery, 21
Epirubicin, 6, 7, 8, 9, 29, 30, 44, 45, 53, 68, 79, 86, 91, 94, 98, 103, 104, 111, 114, 125, 126, 137, 138, 139, 140, 142, 144, 145, 146, 147, 148, 149, 150, 153, 161, 168, 189, 192, 193
Epodyl, 43
ErbB2, 26
Estramustine, 14, 55, 94, 161
Estramustine Phosphate, 55
Etoposide, 55, 56, 57
Evans Blue, 84, 86
FANFT, 71, 74, 75
Fick, 41
flexible cystoscopy, 32
fluorescein, 14, 61, 84
fluorescein diacetate, 84
Fluorescein diacetate, 61
GFP, 14, 80, 86, 88, 89, 98, 106, 114
GLA, 6, 50, 51, 52, 53
Glutathione S transferases, 30
glutathione S-transferases, 29
grading, 33
Grunfeld, 21
haematuria, 20, 30, 32
Haematuria, 19, 32
Harrison, 22
Henckel, 19
Herbert Herring, 21
Herring, 42
Hildanus, 19
I-3-C, 7, 12, 13, 14, 53, 129, 130, 183, 184, 185, 186
immunotherapy, 2, 36, 47, 75, 76
Indole-3-Carbinol, 14, 53, 91, 182
industrial exposure, 24
intravenous urography, 32
intravesical chemotherapy, 36, 45, 46, 48, 202
J82, 59
Jones, 42
Kanamycin, 80
Le Cat, 19
leukotrienes, 50
Linolenic Acid, 15, 50, 95
lithotomy, 19
Lung Resistance-related Protein, 29
Magnetic resonance imaging, 37, 76
Major Vault Protein, 29
MeGLA, 7, 11, 12, 15, 50, 52, 53, 91, 95, 128, 168, 169, 170, 171, 172, 173, 174, 175, 177, 178, 179, 180, 189, 194, 195
metallo-proteinases, 28
metastases, 31, 36, 37, 74, 77
Methionine, 63
Methotrexate, 38, 75
Methylene blue, 64
Microtitration, 63
Mitomycin, 9, 10, 29, 45, 46, 47, 49, 75, 79, 91, 94, 125, 151, 154, 155, 156, 157, 158, 192, 193
Mitomycin C, 29, 79, 91, 125, 151
MNU, 71

MTT, 7, 15, 64, 82, 83, 90, 91, 125, 126, 127, 128, 130, 193, 203
Multi-Drug Resistance, 28
Multidrug Resistance Protein, 29
myc oncogene, 26
Mycobacterium, 48
NBT-II, 69
Nicod, 20
nitrate of silver, 20
Nitze, 21
nude, 59, 73, 74, 77
oncogenes, 26, 27
p53, 27, 29, 34, 35, 68
Paclitaxel, 55, 57
papillary, 20
Pawlick, 22
perchloride of iron, 20
perineal urethrotomy, 20
Petit, 20
P-glycoprotein, 15, 28
phenothiazines, 30
platinum, 21
PMV, 38
Propidium iodide, 61
Quercetin, 25
Radical cystectomy, 36, 37
Radiotherapy, 36
ras gene, 26
Rehn, 22
Reserpine, 30
Riolan, 19
Riolan Jean, 19
Rubidomycin, 43
Ruysch, 19
saccharin, 25
Sandifort, 19
scids, 73
Segalas, 21
Sir Henry Thompson, 20
smoking, 24
Sonnenburg, 22
Spheroids, 64, 65
Streptomyces, 43, 44, 45
Strychnine, 42
suppressor genes, 26, 27, 34
Taxol, 29
Thiotepa, 42
thymidine, 64
TNF alpha, 76
TNM system, 33
topoisomerase II, 29, 30, 56
Tryptophan, 25
tubulin, 55, 56
TURBT, 15, 40, 177, 192
urethra, 19
urine cytology, 31
verapamil, 30
Vinblastine, 28, 38, 55, 56, 57
Vinca alkaloids, 28
Vincristine, 28
Vitamin E, 51
Warner, 19
water, 107